OPTICAL PROPERTIES OF THIN VACUUM DEPOSITED SEMICONDUCTING FILMS.

BY

ROBIN ERIC DENTON

B.Sc. Hons. (Adelaide)

A THESIS

SUBMITTED FOR THE DEGREE OF

DOCTOR OF PHILOSOPHY

IN THE

DEPARTMENT OF PHYSICS

UNIVERSITY OF ADELAIDE

DECEMBER 1971.

TABLE OF CONTENTS

TABLE OF CONTENTS (cont.)

TABLE OF CONTENTS (cont.)

TABLE OF CONTENTS (cont.)

SUMMARY

The thesis begins with a brief introduction to the problem of determining the optical constants of thin films, with a critical review of the various techniques for determining these parameters in an effort to arrive at a suitable method applicable to the absorption edge of semiconducting films. It is shown that the measurement of normal incidence reflectance and transmittance is potentially the most accurate method.

In Chapter 2 is described a spectrophotometer which was designed to enable the absolute reflectances and transmittances of thin films to be measured with an accuracy of ±0.002. The thicknesses of the films were measured by the method of Fringes of Equal Chromatic Order, and the apparatus and necessary computations for this are also described in this chapter.

The problem in the past with normal incidence reflectance and transmittance measurements lay in the enormous computations necessary to extract the optical constants, since multiple-beam interference effects must be taken into account resulting in complicated equations for the reflectance and transmittance. In Chapter 3 is described a much simplified method for the exact determination of the refractive index and absorption index of thin films from measured normal incidence reflectances and transmittances. The method requires minimal programming and the computing time is at least a factor of 10 faster than previously reported. Because of the periodic nature of the reflectance and transmittance equations, multiple solutions for the optical constants occur, and an analysis of hypothetical films is

made in an effort to determine which of the solutions is correct. An unambiguous choice can only be made if measurements are taken over a wide wavelength range, and it is shown how the behaviour of the calculated solutions under small changes in film thickness enables the thickness to be determined with precision without recourse to its explicit measurement.

A major advantage of normal incidence measurements is that the effects of the surface are minimized. However it is shown that certain behaviour of the calculated solutions is associated with oxide layers or irregularities on the surface of the films. This behaviour is described in Chapter 4, and it is shown how the effects of the surface may be eliminated by considering a two-layer film. If the surface layer is of known refractive index, it is shown how the optical constants of the underlying film and the film and surface-layer thicknesses may be accurately determined from the measured reflectance and transmittance of the system.

The above analyses revealed that a previous worker, in his determination of the optical constants of selenium films, chose incorrect solutions from the multiple values that existed. His choice of the wrong solutions arose primarily from using incorrect film thickness values. In Chapter 5 the optical constants of selenium films are recalculated from his data, and the results are interpreted in terms of a qualitative semiconducting bond model.

One of the most extensively studied semiconductors is germanium, yet the results obtained by various authors for the optical constants of thin films of this material show wide discrepancies. It was appropriate therefore to apply the theory developed in Chapters 3

and 4 to determine accurately the optical constants of germanium films. The results of this investigation are presented in Chapter 6. Amorphous films are considered in greater detail, but films with various degrees of crystalline perfection are investigated for the purpose of comparison. A model for the observed absorption in germanium films is discussed. Ideas for future work conclude the thesis.

DECLARATION

This thesis contains no material which has been accepted for the award of any other degree or diploma in any University and, to the best of the author's knowledge and belief, contains no material previously published or written by another person, except where due reference is made in the text of the thesis.

(R. DENTON)

ACKNOWLEDGEMENTS

The author gratefully acknowledges the following people and organisations for their assistance during the course of this work.

Mr. T. Spurr of the Physics Department workshop for the construction of the spectrophotometer.

Mr. A. Ewart for his valuable technical assistance.

Mr. S. Wells for photographing the diagrams.

Mrs. K. Possingham for typing the thesis.

Dr. D. McCoy and Messrs. R. Goodwin and T. McDonnell for the many thought provoking discussions.

The Radio Research Board Of Australia for financing the project.

The University of Adelaide for the award of a University Research Grant (1968).

The Commonwealth Department of Education And Science for a Post-graduate Award (1969-71).

Finally the author wishes to thank his Supervisor, Dr. S.G. Tomlin, for his guidance and stimulating critical discussions during the course of this work.

CHAPTER 1.

INTRODUCTION

A feature common to all semiconductors is the rapid increase in optical absorption which occurs over a small energy range when the absorbed radiation has an energy roughly equal to the energy gap of the semiconductor. This is called the absorption edge of the material, and is due to the onset of absorption in which electrons are raised from the valence band across the forbidden gap to the conduction band. A study of the position of this edge and any structure it may have will yield information about the energy gap and the properties of those electron states just above it at the conduction band edge and below it at the valence band edge. This type of information is useful as it is these states close to the conduction and valence band edges which determine the electrical properties of the semiconductor. Consequently, measurement and analysis of the absorption edge spectrum of a semiconductor is an important feature in the study of its properties.

1. 1 NOTATION.

The optical properties of a material may be described by its complex refractive index, N. The significance of N is that a plane electromagnetic wave of frequency ν and wavelength λ propogated through the material in the x- direction has the form

$$\Psi = A \exp\{2\pi i\nu(t-Nx/c)\} \qquad 1.1.1$$

c being the velocity of light in free space.

N may be written in real and imaginary parts in the form

$$N = n - ik \qquad 1.1.2$$

where n is called the refractive index and k the absorption index. These two quantities constitute the so-called optical constants of the medium. In terms of n and k, equation 1.1.1 becomes

$$\Psi = A \exp\{-2\pi\nu kx/c\} \exp\{2\pi i\nu(t-nx/c)\}$$

In terms of the wavelength λ

$$\Psi = A \exp\{-2\pi kx/\lambda\} \exp\{2\pi i(ct-nx)/\lambda\} \qquad 1.1.3$$

The first term of equation 1.1.3 represents the attenuation of the amplitude of the electromagnetic wave on passing through the medium. The square of the factor, $\exp(-4\pi kx/\lambda)$, therefore represents the attenuation in intensity of the wave. The factor K defined by the relation

$$K = 4\pi k/\lambda \qquad 1.1.4$$

is termed the absorption coefficient of the material.

Determination of the optical constants over a wide wavelength range may therefore be expected to yield valuable information on absorption processes in materials.

1. 2 MEASUREMENTS ON BULK MATERIALS.

Measurements of the refractive indices of bulk transparent materials present no serious difficulties. The effect on a transmitted light beam by slight surface disorders, for example, from polishing or from surface films, is generally negligible if the beam traverses a total distance in the medium of the order of millimetres.

The study of absorbing materials, particularly where the absorption is large, presents a much more difficult problem. Measurements usually entail examination of light reflected from the specimen surface. Since the depth of penetration of the light wave may well be much less than a visible wavelength, it is apparent that the behaviour exhibited by a specimen depends almost entirely on the state of the surface which may be completely unrepresentative of the state of the interior of the specimen. Polishing usually produces a surface structure (Bielby layer) in which the normal crystal structure of the material is considerably disordered. The presence of a thin film remaining after polishing, or formed in some other way, will also alter the measured values. These problems have been overcome by cleaving the specimen, when possible, and taking measurements of the cleaved surface. The absorption index is usually found from a successive series of measurements on a crystal which is progressively thinned. This procedure often requires specialised grinding and etching techniques.

In addition, if measurements are taken at other than normal incidence, the polarised state of the incident and reflected waves must be known and taken into account. Such measurements are not easily made.

1. 3 USE OF THIN FILMS.

It was thought originally that the optical properties of absorbing bulk materials could be studied through the use of thin vacuum deposited films. The advantages of films are that they can be made much more uniform in thickness and many times thinner than the bulk material, permitting transmission measurements to be made even when the absorption index is large. The whole depth of the film is sampled, minimising the effect of any surface irregularities.

It has been subsequently found that the optical properties of films often depended on the film thickness and method of preparation, and were different from those which had been found for the bulk material. Instead of an aid in the determination of the properties of bulk material, the study of thin films has become a field of research in its own right.

Although vacuum deposited films are easy to prepare for optical measurements the amount of work which has been done on them has not been extensive. This is because the computation involved in calculating n and k is much more laborious than for bulk specimens. Once the film thickness becomes comparable with the wavelength, the effect of multiple beam interference must be included in any reduction of data. Workers in the past have found this problem so formidable that n and k have usually been determined from approximate equations.

1. 4 METHODS OF DETERMINING THE OPTICAL CONSTANTS OF THIN ABSORBING FILMS.

Extensive reviews of various methods of determining the optical

parameters of thin transparent or absorbing films have been given by Rouard and Bousquet (1965) and Abeles (1963). In this section a brief critical summary of the various methods of determining the optical constants of absorbing films is given. Since the present investigation entailed the examination of the absorption edge of thin film semiconductors, a suitable method must enable n and k to be determined over a wide wavelength range; from the transparent region to the moderately high absorbing region.

1. 4. 1 POLARIMETRIC METHODS.

There are a number of variations of this experiment involving either the measurement of the absolute intensity of the reflected components of a plane polarised beam of light, or the relative phases and intensities.

Measurements are carried out at non-normal incidence so that problems arise in measuring accurately the angle and intensities of the reflected components.

Most of the results obtained using polarimetric methods are inconsistent. The granular surface of films as revealed by electron microscopy and the inhomogeneity and the existence of transition layers shown by Bousquet (1957) make it exceptional for the theoretical conditions on which the polarimetric methods are based to exist.

1. 4. 2 SCHOPPER'S METHOD.

Schopper (1952) showed that it was possible to compute n, k and the film thickness, d, as functions of the complex amplitudes of reflectance from the air and substrate sides of the film and

transmittance, using certain approximations. This method is excellent in theory but it involves six measurements, of which three are measurements of phase changes, these being difficult to make accurately.

Only four of the quantities can be measured without ambiquity and with reasonable accuracy.

1. 4. 3 SPECTROPHOTOMETRY AT NON-NORMAL INCIDENCE.

This method involves the measurement of the reflected and transmitted intensities of radiation incident obliquely on the film. As with polarimetric methods the surface of the film will strongly influence the results. Apart from surface irregularities the possibility of anisotropy must also be considered. Schopper (1952) has noted that if thin films produced by thermal evaporation are anisotropic they probably take the form of uniaxial crystals with the optic axis perpendicular to the plane of the film surface. It is assumed here that the deposition occurs at normal incidence, so that there is no privileged direction in the surface of the film. If the film behaves like a uniaxial crystal with its axis normal to the plane, the anisotropy would affect all measurements made at oblique incidence.

On the other hand, anisotropy cannot affect measurements made at normal incidence. Rouard (1956) has stressed that in these circumstances normal incidence methods are clearly superior.

1. 4. 4 PHOTOMETRIC METHODS AT NORMAL INCIDENCE.

There are several variations of this technique.

(1). Measurement of the absolute reflected intensity at normal incidence from the substrate side (R^1) and air side (R) of the film together with the absolute transmission (T).

This method would require an extensive amount of computation. Furthermore in the low absorbing region the two reflected intensities would be nearly equal, resulting in poorly defined curve intersections in the calculation of the optical constants.

(2). Measurement of the absolute reflected intensity at normal incidence from the substrate side and air side of the film together with the film thickness.

Computation for this method would be less extensive than for (1) since the film thickness does not enter into the equations as an unknown parameter. However this method is again unsuitable except in the highly absorbing region. The optical constants, n and k, are determined by plotting n as a function of k for the measured values of R and R^1, the intersection of these two curves giving the solution. In the low absorption region these two curves exhibit near tangential intersections, giving rise to large errors in the calculated quantities for small errors in the measured quantities.

Thus both methods (1) and (2) are unsuitable for the present investigation where we are particularly interested in the absorption edge.

(3). Measurement of the absolute reflected intensity at normal incidence from the air (or substrate) side of the film and measurement

of the absolute transmitted intensity at normal incidence, together with the film thickness.

This method was considered potentially the most accurate. Measurements at normal incidence minimise the effects of surface irregularities and transmission measurements minimise them further still since the whole thickness of the film is involved. Unlike R and R^1, determining n and k from R (or R^1) and T does not suffer from unstable curve intersections in the transparent or low absorption region, except in limited wavelength regions, these regions depending on the thickness of the film.

1. 5 AIMS OF THE PRESENT INVESTIGATION.

The original aim of this investigation was to determine accurately the optical constants of a number of semiconducting films near the fundamental absorption edge, from measurements of the normal incidence reflectance and transmittance of the films. Initially it was proposed to study germanium films as these films can be prepared with various degrees of crystalline perfection.

In Chapter 2 is described the design and construction of apparatus for the measurement of the absolute reflectance and transmittance of thin films. Also in this chapter is described the apparatus and consequent calculations for the determination of film thickness by multiple beam interferometry. Apparatus for the preparation of vacuum deposited germanium films is also described.

The accurate calculation of the optical constants from the measured reflectance, transmittance and thickness of thin films is

then considered. Until now the computation necessary for determining n and k was lengthy and extensive. In Chapter 3 a much simplified method is described where n and k are determined, not from R and T, but from the functions (1+R)/T and (1-R)/T. Although a high speed computer is still required, the programming is minimal and computing time at least a factor of ten less than previously reported.

It soon became apparent that a thorough investigation of the calculation of n and k from R and T was needed. This arose because often several solutions satisfied the reflectance and transmittance equations (1+R)/T and (1-R)/T, and an unambiguous choice of the correct solution could not be made. This investigation is also described in Chapter 3, firstly in relation to hypothetical films so that all the properties of the film are known exactly, and secondly to show how the results from this analysis could be applied to real films. A consequence of this investigation is the development of a method whereby,provided the film is sufficiently thick to exhibit at least one turning point in the reflectance and transmittance curves, the optical constants together with the thickness of the film may be determined with precision.

Other anomalies in the calculated solutions are shown in Chapter 4 to be due to oxide layers and structural irregularities on the surface of the films. In many cases, and in particular germanium, the oxide is transparent in the region of the absorption edge of the underlying film. A technique is developed in this chapter whereby, provided the oxide layer is transparent and its refractive index known, the optical constants of the underlying film and the film

and oxide thicknesses may be accurately determined. The analysis is applicable to any two-layer system provided one layer is transparent and is of known refractive index while the second layer is absorbing over at least a part of the wavelength range of measurements. The two systems: transparent film - absorbing film - substrate and absorbing film - transparent film - substrate are shown to be readily distinguishable. It is also shown that, under certain conditions, surface irregularities may be treated in a similar manner.

There is some doubt reported in the literature as to the accuracy of measuring film thickness by multiple beam interferometry (Rouard and Bousquet, 1965). The analyses given in Chapters 3 and 4 have enabled the thicknesses of the films to be determined without recourse to their explicit measurement. It was found that in the case of selenium and germanium films the measured film thicknesses agreed within the experimental error to those calculated, thus dispelling fears that the measured film thickness may be seriously in error.

The analyses also revealed that previous calculations of the optical constants of selenium films (Campbell, 1968) were incorrect, and in Chapter 5 these quantities are recalculated from the data of Campbell. The results are then briefly discussed.

In Chapter 6 the optical constants of germanium films are presented. Amorphous films are considered in greater detail, but films with various degrees of crystalline perfection are considered for the purpose of comparison. A model to explain the observed

absorption is then presented.

Ideas for future work conclude the thesis.

CHAPTER 2.

EXPERIMENTAL APPARATUS

2. 1 SPECTROPHOTOMETER FOR MEASURING REFLECTANCE AND TRANSMITTANCE.

A spectrophotometer for measuring the transmittance and absolute reflectance of thin films was designed by the author and built in the Physics Department workshop. A photograph of the apparatus is shown in Figure 2.1. A number of types of systems were considered before the present one was designed and most of the systematic errors associated with previous instruments have been eliminated or minimized.

With the existing spectrophotometer (Campbell, 1968) the measurement of reflectance required a calibrated reference mirror, which was tedious to calibrate, and any change in its reflectance between measurements was unknown.

An elaborate spectrophotometer has been built by Bennett and Koehler (1960) which has the advantages that a calibrated mirror is not required, and the light beam position on the detector is not affected by changes in the dispersion of the substrate at different wavelengths. However the positions of the specimen for measuring the reflectance and transmittance require the specimen holder to be mounted in different positions. As the present system was required to be operated under vacuum with the specimen cooled to near liquid air temperatures, if desired, such movement would have been difficult to achieve.

The Strong - type reflectometer (Kuhn and Wilson,1950) appeared to be the most suitable instrument and the present system was designed

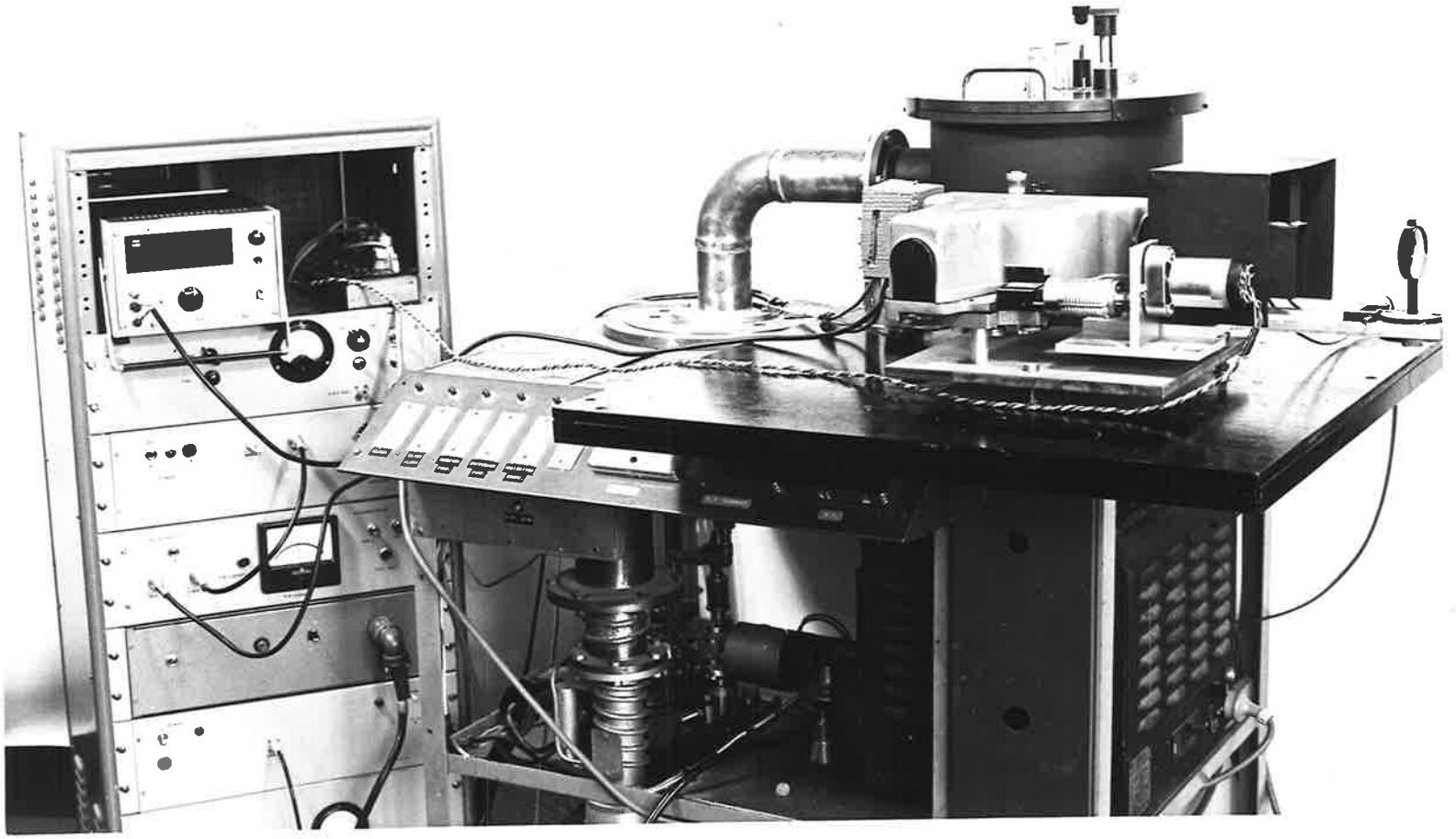

Figure 2.1

on this basis. The disadvantage of this type is that the change in dispersion of the substrate at different wavelengths causes the light beam position on the detector to alter. In the Strong - type reflectometer this was partially compensated for by employing an integrating sphere. The present system was designed so that this error could be eliminated. Only transverse movement of the specimen holder was required which is readily achieved under vacuum.

2. 1. 1 GENERAL DESCRIPTION.

The measurements of reflectance and transmittance were made at near normal incidence, the angle of incidence being about 5° which resulted in a negligible error. Light from a Hilger-Watts prism monochromator was mechanically chopped* and, after reflection or transmission by the specimen, the intensity of the chopped beam was measured by a light-sensitive detector. The square wave signal from the detector was amplified, rectified, smoothed and recorded on a digital voltmeter. The square of the reflectance and transmittance was measured which results in greater accuracy.

2. 1. 2 LIGHT SOURCE.

The light source consisted of a 100 - watt quartz - iodide lamp powered by a 12 volt d.c. regulated supply. A concave mirror was positioned so that the image of the lamp could be focussed on the entrance slit of the monochromator. After an initial warm - up period the intensity of the light source was constant.

* The chopping frequency was 300 Hertz.

2. 1. 3 OPTICAL SYSTEM.

The optical system is shown diagramatically in Figure 2.2. Light from the monochromator, M, was mechanically chopped and passed through adjustable horizontal and vertical slits to limit the spread of the beam. Concave mirrors M1 and M2 focussed the beam onto the plane mirror M3. After reflection from M3, mirrors M4 and M5 focussed the beam onto a light sensitive detector D. The mirror system was enclosed in a vacuum chamber so that experiments could be carried out at low pressures and temperatures if required.

The concave mirrors were housed in milled aluminium blocks. Each block was attached to its support by three spring-loaded positioning screws to a mount to assist in the alignment of the optics. Lateral movement of the blocks was possible, and each mirror mount could be rotated externally via rotating "O" - ring seals. The light beam was positioned on that part of the detector which gave maximum output signal. At each wavelength the beam position could be altered readily, by a slight rotation of mirror M3 or M4, to give maximum output signal from the detector, ensuring the beam fell on the same part of the detector and consequently eliminating the error that arises when the beam position alters due to different dispersion in the substrate at different wavelengths.

For the purpose of measuring reflectance (section 2.1.4), mirror M3 could be rotated externally about a perpendicular axis. This resulted in the same mirror being used for the reference and specimen signals, eliminating (a) the error that could arise due to different reflectivities if two different mirrors were used, and (b) the need

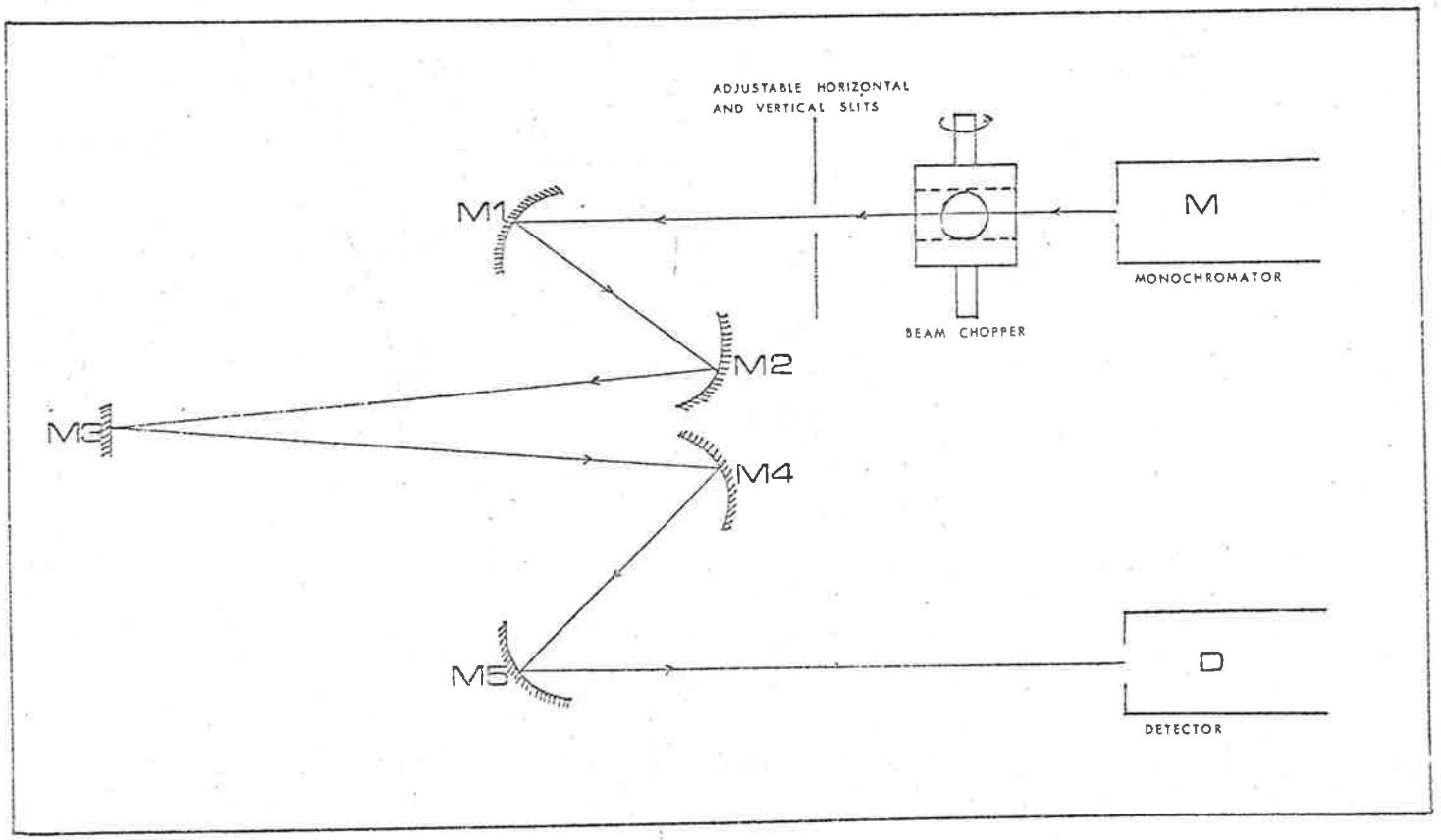

DIAGRAM OF THE OPTICAL SYSTEM

Figure 2.2

to calibrate a reference mirror.

All the mirror mounts were equipped with planetary drive gears connected to worm and wheel gears so that fine adjustments could be made.

2. 1. 4 MEASUREMENTS OF REFLECTANCE AND TRANSMITTANCE.

For measuring reflectance, the reference signal was obtained by allowing the beam to traverse the system as shown in Figure 2.3.a, where the incident beam was reflected by M3. The specimen was then moved into the path of the beam as shown in Figure 2.3.b, and mirror M3 rotated 180° to the position shown, such that the beam was reflected firstly from the specimen, then M3 and again from the specimen, and the corresponding signal recorded.

Let Io be the incident intensity of the light beam and R1, R2, R3, R4, R5, RF the reflectances of mirrors M1, M2, M3, M4, M5 and the film F respectively. The intensity of the reference beam is thus:

Io. R1. R2. R3. R4. R5.

and that of the beam after reflection by the film is

Io. R1. R2. RF. R3. RF. R4. R5

The ratio of the two signals is thus RF^2, the square of the absolute reflectance of the film.

For measuring transmittance, the reference signal was obtained by allowing the beam to traverse the system as shown in Figure 2.3.c, where the incident beam passed through an uncoated half of the substrate, was reflected by M3, and again passed through the

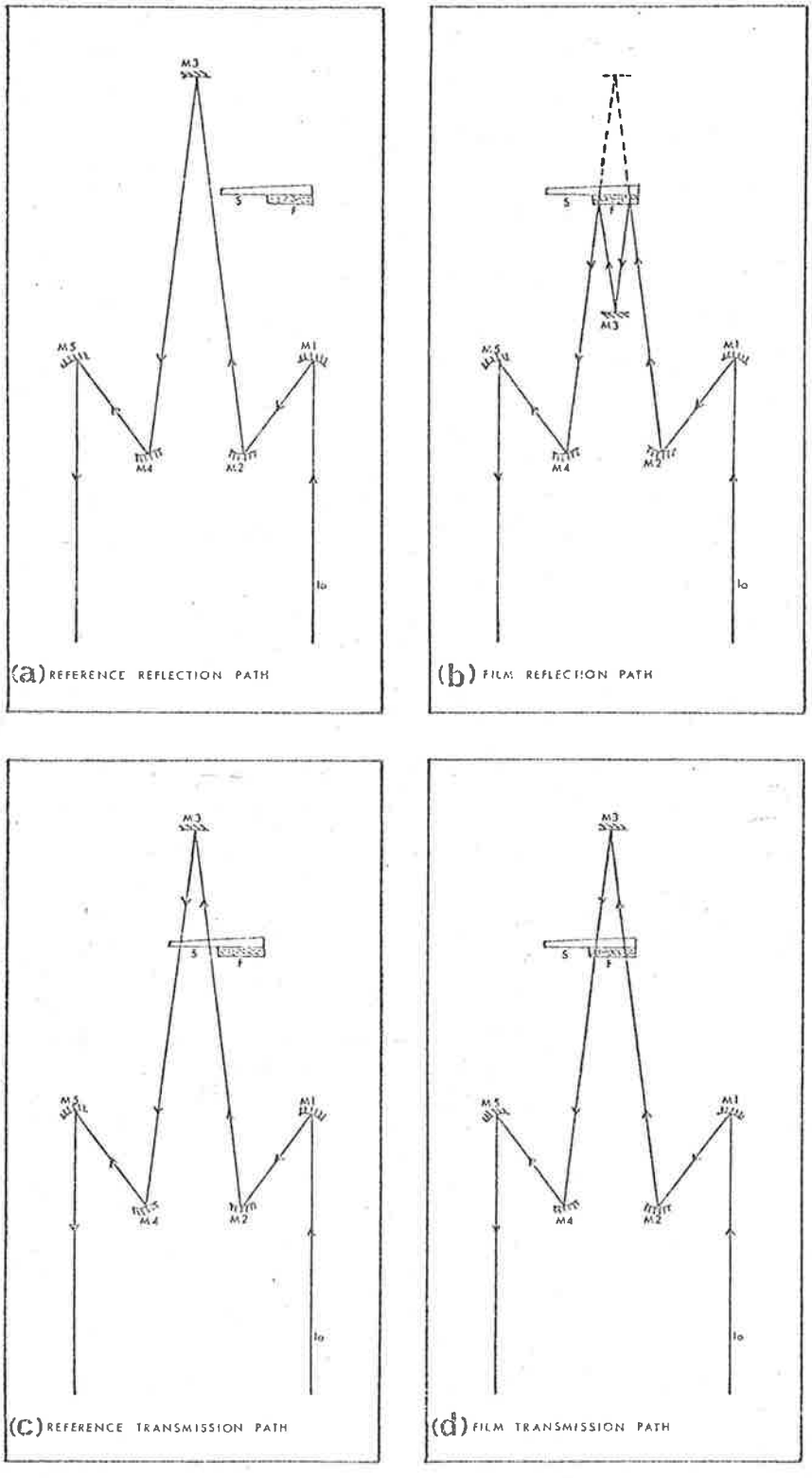
M3
S
F
M5
M1
M4
M2
Io
(a) REFERENCE REFLECTION PATH
(b) FILM REFLECTION PATH
(c) REFERENCE TRANSMISSION PATH
(d) FILM TRANSMISSION PATH

Figure 2.3

uncoated substrate. The specimen was then moved to the position shown in Figure 2.3.d so that the beam passed through the coated half of the substrate, was reflected by M3 and again passed through the coated substrate, and the corresponding signal recorded. If TS and TF are the transmittances of the substrate and film respectively the reference intensity is

Io. R1. R2. TS. R3. TS. R4. R5

and the intensity after transmission through the film and substrate is

Io. R1. R2. TF. TS. R3. TS. TF. R4. R5

The ratio of the two signals thus gives TF^2, the square of the transmittance of the film.

2. 1. 5 SPECIMEN HOLDER.

The copper specimen holder was attached to the lid of the vacuum chamber (see Figure 2.4). The specimen could be moved into the positions shown in Figure 2.3 by means of a rotating seal located in the lid. The tilt of the specimen holder could also be adjusted externally and the lid itself could be rotated with respect to the chamber to assist in the alignment.

A liquid air tank was positioned above the specimen holder, and contact to the holder was achieved by copper bands on either side of a copper block welded to the base of the tank. The sample could then be cooled to near liquid air temperature if desired.

A second liquid air tank was attached to the lid for use as a water vapour trap. For measurements at low temperatures, liquid air was first placed in this tank to remove any water vapour from the

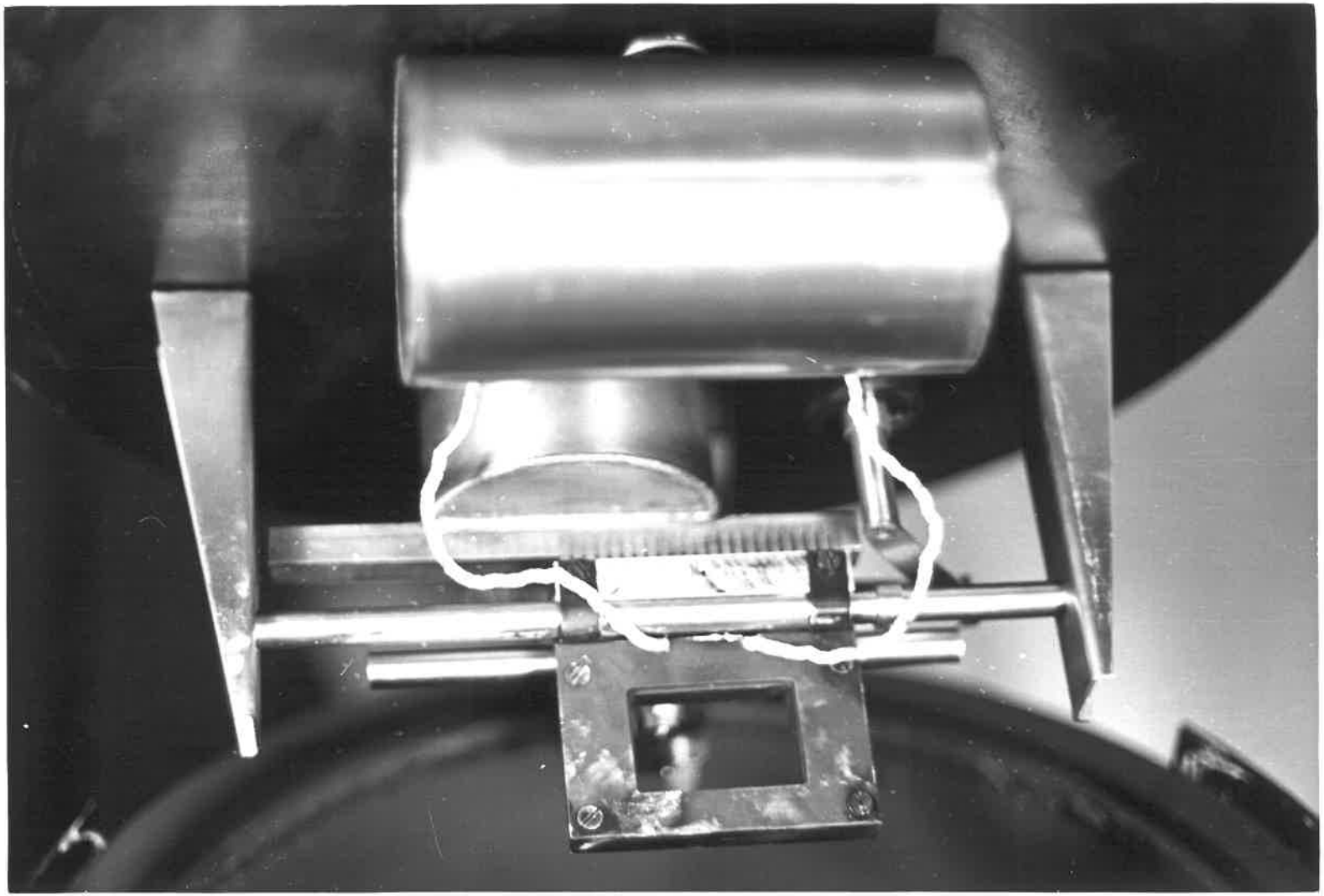

Figure 3.4

evacuated chamber before the specimen was cooled, ensuring no ice film formed on the specimen as it was cooled.

Insulated feed-throughs were welded in the lid to enable electrical measurements to be taken if they were required.

2. 1. 6 REFRACTIVE INDEX OF AND ABSORPTION IN THE SUBSTRATES.

The refractive index of the quartz-homosil substrates was supplied by the manufacturer, and the experimental determination previously carried out in this laboratory (Campbell, loc. cit.) agreed with that supplied by the manufacturer.

Comparison of the transmittances of substrates of different thicknesses showed negligible absorption over the wavelength range 2000Å - 2.4μ. Beyond 2.4μ the homosil quartz gradually became absorbing, with a strong absorption peak at about 3.0μ .

2. 2 BEAM DETECTION.

2. 2. 1 LIGHT - SENSITIVE DETECTORS.

For the wavelength range 5500Å - 2.4μ, a lead sulphide photoconductive cell was used, and for the range 2500Å - 5500Å a Philips 1P28 photomultiplier was used. The germanium films were strongly absorbing before the cross-over point of 5500Å, thus for these films only the lead sulphide cell was required.

The sensitivity of the lead sulphide cell changed with temperature, and as a consequence the signal from it drifted as the ambient temperature altered. This problem was overcome by mounting the cell in an aluminium housing to which was attached a Peltier

battery. Four diodes were mounted in the housing as temperature sensors. The forward bias voltage across the diodes decreases with increasing temperature and this was used as a monitor to control the current through the Peltier battery maintaining the temperature to ±0.05 degrees C. A circuit diagram of the temperature controller and Peltier cell supply is shown in Figure 2.5. If the temperature of the housing was such that the forward voltage across the diodes rose above a predetermined value (set by the variable voltage V1), the comparator would turn transistor T1 on, shutting off the current to the Peltier battery. Likewise if the forward voltage across the diodes fell below the same value, the comparator would turn transistor T1 off, thus allowing current to flow through the battery.

This arrangement had the advantage that the detector could be cooled considerably, thus increasing its sensitivity. The operating temperature was determined by the setting of the variable voltage supply V1.

2. 2. 2 AMPLIFICATION AND RECTIFICATION OF THE BEAM SIGNAL.

A block diagram of the amplifier and rectifier is shown in Figure 2.6. The output impedance of the lead sulphide cell was approximately 10 megohms and consequently a high input impedance amplifier was required. The square wave signal from the detector was capacitively coupled to a bootstrapped voltage follower with an input impedance of the order of 10^{11} ohms. The output of the voltage follower was capacitively coupled to a Fairchild μA709 integrated circuit operational amplifier with fixed gains of 10, 20, and 100.

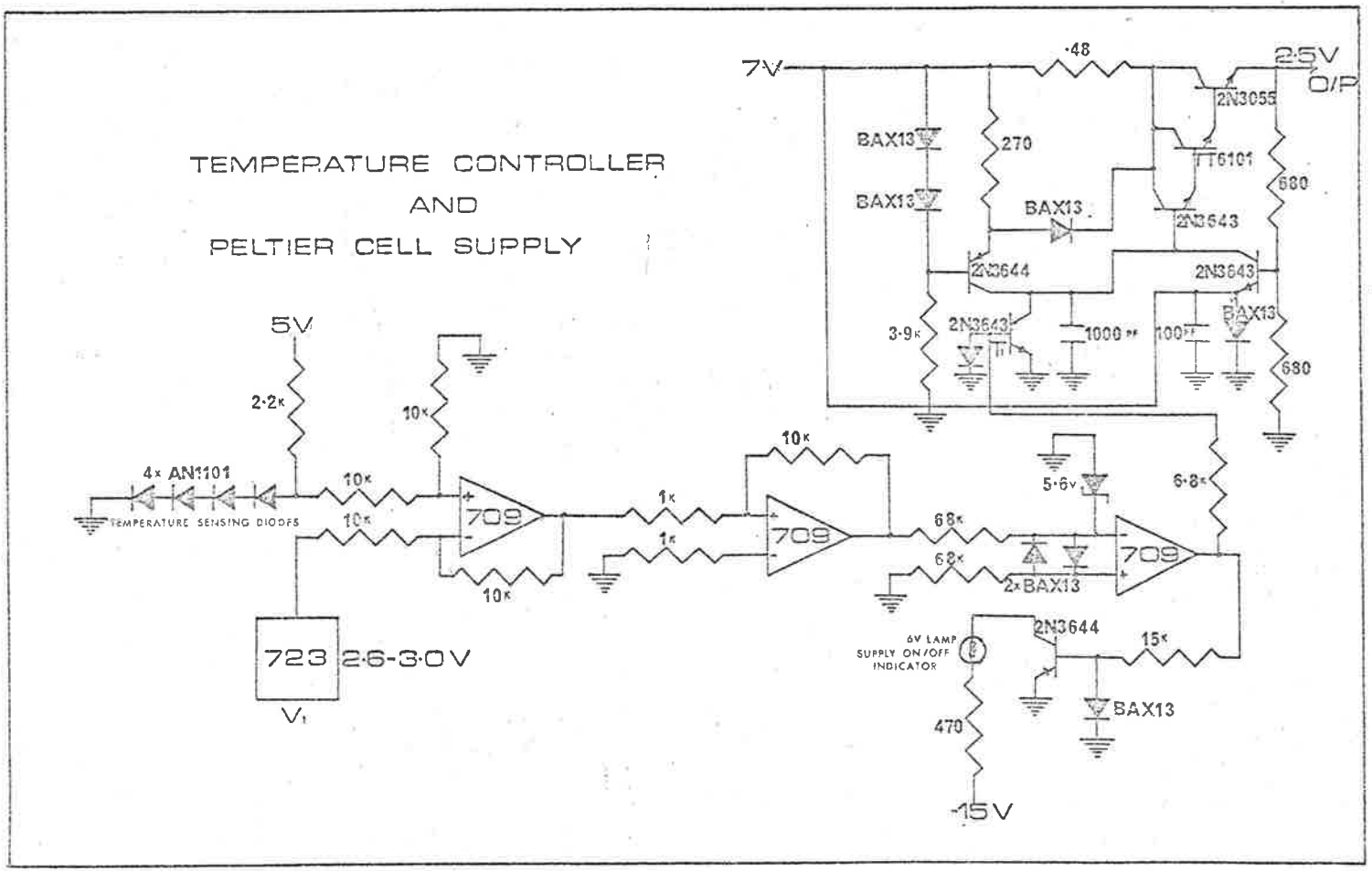
TEMPERATURE CONTROLLER
AND
PELTIER CELL SUPPLY
7V
·48
2·5V
O/P
2N3055
BAX13
BAX13
270
TT6101
680
BAX13
2N3643
2N3644
2N3643
3·9K
2N3643
1000 PF
100PF
BAX13
680
5V
2·2K
10K
4× AN1101
10K
10K
TEMPERATURE SENSING DIODES
709
10K
1K
1K
10K
709
68K
5·6V
6·8K
68K
2×BAX13
709
2N3644
6V LAMP
SUPPLY ON/OFF
INDICATOR
15K
BAX13
470
-15V
723
2·6-3·0V
V1

Figure 2.5

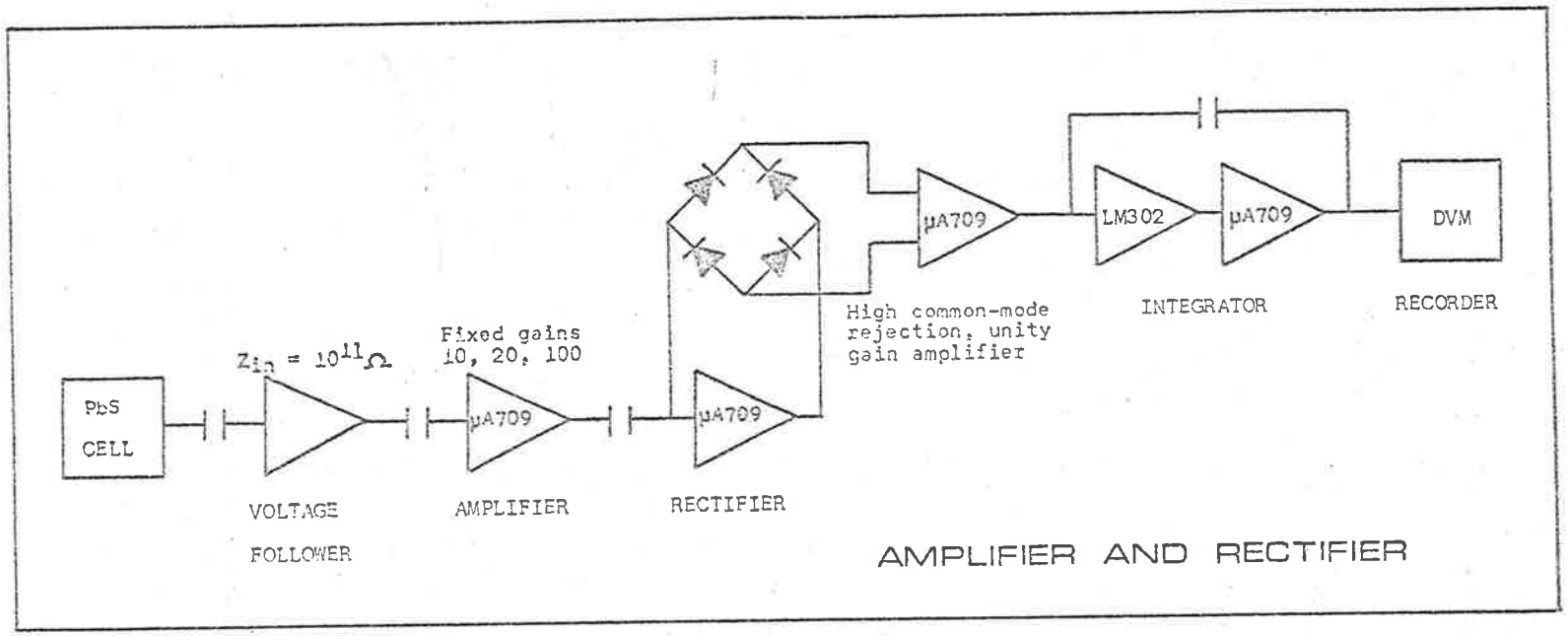
PbS
CELL
$Z_{in} = 10^{11}\Omega$
VOLTAGE
FOLLOWER
Fixed gains
10, 20, 100
μA709
AMPLIFIER
μA709
RECTIFIER
μA709
High common-mode
rejection, unity
gain amplifier
LM302
μA709
INTEGRATOR
DVM
RECORDER
AMPLIFIER AND RECTIFIER

Figure 2.6

The amplified signal was rectified by employing a diode-bridge in the feedback loop of an operational amplifier. The output from the diode-bridge was coupled to a gain 1 operational amplifier designed to give high common-mode rejection. This was required as the output of the bridge floats at a potential of about one volt. This method of rectification reduces non-linearities in the diodes to negligible levels.

The rectified signal was integrated for one second using a capacitor in parallel with the feedback resistor around an operational amplifier, on the front-end of which was a National Instruments LM302 integrated circuit voltage follower to reduce thermal drifts. The smoothed signal was displayed on a digital voltmeter.

The linearity of the amplifier and rectifier was tested by attenuating an input signal by known amounts using a Marconi attenuator, and was found to be better than 1 part in 1000 for input signals from 30μV to 300mV.

After an initial warm-up period, the noise level of the lamp, detector and amplifier was less than 0.5 millivolts.

2. 3 PREPARATION OF FILMS.

2. 3. 1 EVAPORATION OF GERMANIUM.

The germanium films were prepared by evaporation in vacuo. The spectroscopically pure germanium was supplied by New Metals and Chemicals Ltd., England. Germanium lumps were placed in a tungsten conical basket. The evaporation rate was controlled by varying the current flowing through the basket. An electromagnetically operated

shutter was positioned above the source to enable the germanium to be outgassed prior to evaporation onto the substrate.

2. 3. 2 SUBSTRATES.

For the measurement of reflectance and transmittance, the germanium films were deposited on scratch free, optically flat quartz wedges*, prepared to specification by the Scientific and Optical Laboratories of Australia, Adelaide. Each wedge measured 2" x 1½" and was cut in half to form a thick and a thin wedge. The films were deposited on a part of the thicker half. The reason for using wedges was two-fold. Firstly it is difficult and expensive to obtain plane parallel-sided substrates of sufficient accuracy to accurately take account of multiple-beam interference effects within them. Secondly by using wedges, the beam reflected from the back surface passes away from the detector so that the multiple reflections in the substrate do not have to be taken into account, consequently simplifying the reflectance and transmittance equations.

2. 3. 3 SUBSTRATE CLEANING.

An extremely clean surfaced substrate is necessary in order to obtain a pin-hole free film and to ensure that the film will adhere to it. The following cleaning procedure was found to be sufficient.

The substrates were first cleaned in warm concentrated chromic acid solution, and then washed in clean chromic acid solution at 80°C until the acid formed an even film over the substrate. They were subsequently rinsed in doubly distilled water, dried in a stream of

* The wedge angle was 3°.

dry air and finally placed in the dark space between two electrodes in a vacuum chamber and ion bombarded for three to five minutes.

The chromic acid solution was prepared by dissolving chromic oxide in water (approximately 100 gms. of chromic oxide in 100 ml. of water) and adding concentrated sulphuric acid. At first a white precipitate formed. Further sulphuric acid was added until the precipitate dissolved.

To remove germanium films, the substrates were washed in aqua regia.

2. 3. 4 PUMPING UNIT.

The pumping unit consisted of a 6" oil diffusion pump and a single-stage rotary backing pump. A phosphorous pentoxide vapour trap was inserted between the diffusion and backing pumps to remove water vapour, and a liquid air trap was mounted between the diffusion pump and chamber to improve the evaporating pressure and to prevent contamination of the evaporating equipment by oil vapour. The pressure during evaporation was less than 10^{-5} torr.

2. 3. 5 SUBSTRATE SUPPORT AND OVEN.

The substrates had to be maintained at temperatures between room temperature and 700°C. It will be shown in the next chapter that the uniformity of the films is an important factor in the accurate determination of the optical constants of them. It was therefore necessary to rotate the substrate during evaporation in order to obtain a more uniform film. A diagram of the substrate

support and oven is shown in Figure 2.7.

The oven consisted of a silica cylinder about which was wound molybdenum heating wire. A stainless steel jacket was inserted inside the cylinder to prevent contamination from the oven, and a water-cooled copper jacket was mounted around the oven. The substrate support was constructed of stainless steel, and the shaft of the support could be adjusted to enable the distance from the source to the substrate to be varied. The support was milled to receive the wedges which were held in place by tungsten clips.

The substrates were heated by radiation from the oven, the temperature of which was controlled by the heating current. After about two hours the substrate reached the temperature of the oven. The oven temperature was measured as a function of the heating current with a chromel-alumel thermocouple, so that if a particular temperature was desired, the appropriate heating current could be determined. With this arrangement the temperature was accurate to within about 10% which was sufficient for the present purpose. The rotation of the substrate was obtained by direct drive from a small electric motor mounted above the oven. The motor was shielded from the high temperature of the oven by a thick copper disc bolted to the water-cooled jacket.

2. 4 MEASUREMENT AND CALCULATION OF FILM THICKNESS.

The method of Fringes of Equal Chromatic Order (FECO) viewed in reflection (Tolansky, 1960) was used for the measurement of film thickness. A review of the available techniques and the arguments for using this method have been given by Campbell (1967) and by McCoy

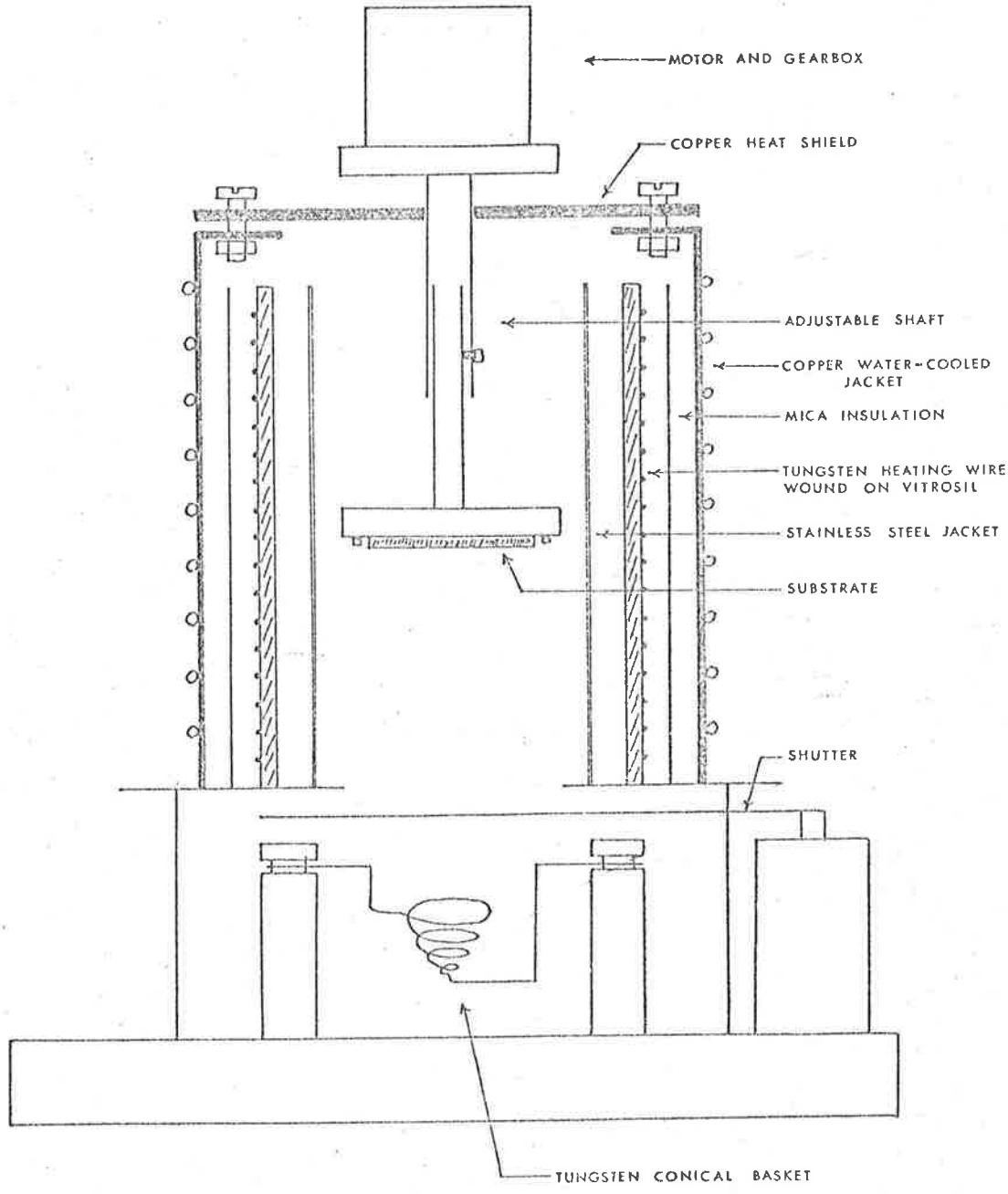

OVEN AND SUBSTRATE HOLDER

Figure 2.7

(1966).

The apparatus for measuring film thickness was built in this laboratory (McCoy, loc. cit.) and will only be briefly described here.

2. 4. 1 OPTICAL SYSTEM FOR MEASURING THE WAVELENGTHS OF THE INTERFERENCE ORDERS.

The optical system is shown schematically in Figure 2.8. The light from a carbon arc lamp was collimated by a system of lenses and was incident on a half-reflecting half-transmitting mirror. The light reflected from the film was collected and focussed onto the entrance slit of a spectrometer. The wavelength could be measured to the nearest 1Å.

2. 4. 2 HIGH REFLECTANCE COATINGS.

For well defined interference fringes, a high reflectance silver coating is necessary. A scratch-free optical flat, used as a reference surface, was coated with a silver layer with a reflectance of approximately 95% each time a thickness measurement was made.

The germanium films were prepared with a sharp step, and an opaque silver layer was deposited over this when thickness measurements were made. Tolansky has shown that a thin silver layer accurately contours the surface over which it is evaporated.

The reference surface was clamped over the coated film to form a Fabry-Perot interferometer. The existence of a step causes the fringes of equal chromatic order to be displaced. Measurement of

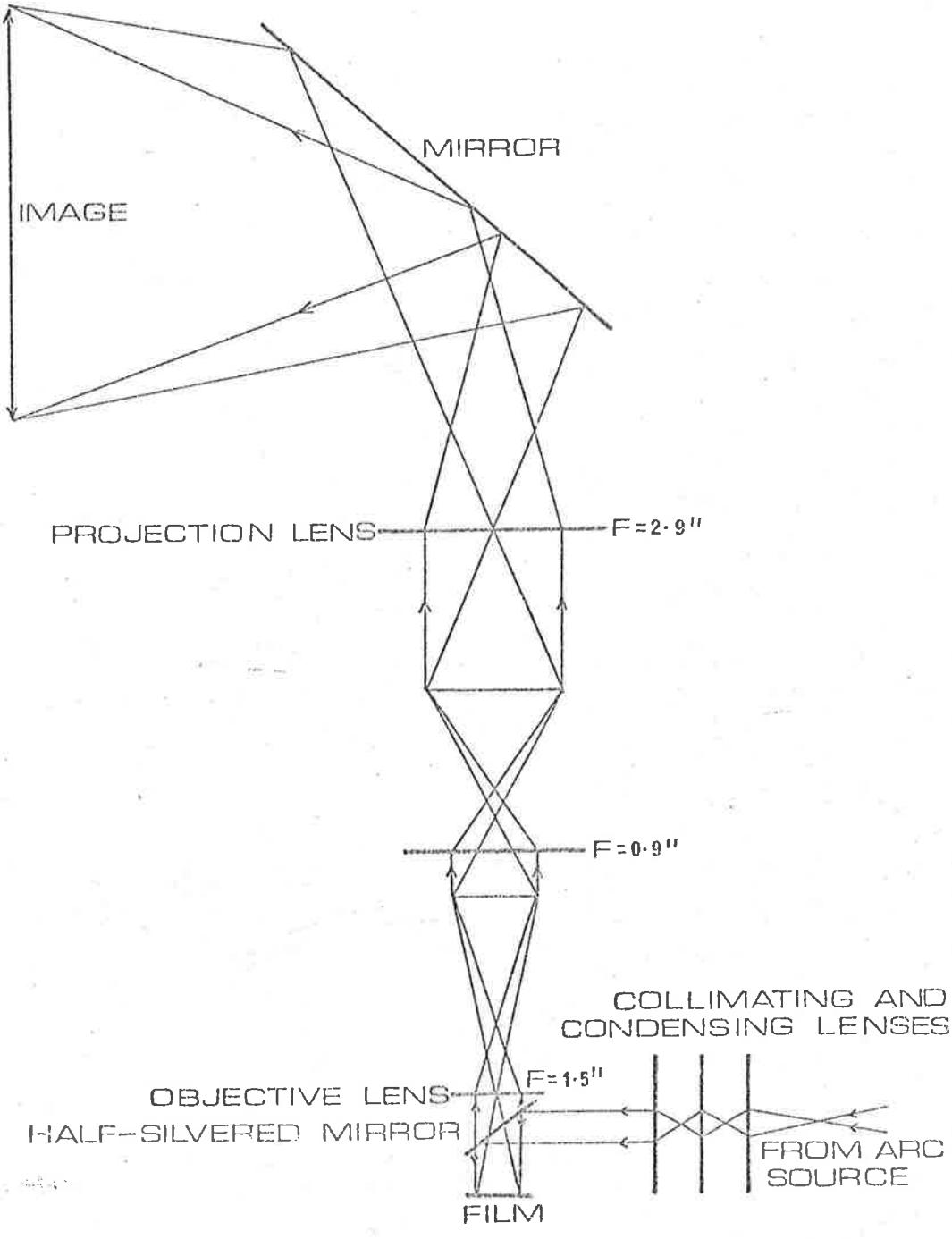

OPTICAL SYSTEM FOR MEASURING FILM THICKNESS

Figure 2.8

the wavelengths of the fringes before and after the step provides a method of accurately determining the height of the step, i.e. the geometrical film thickness.

2. 4. 3 CALCULATION OF FILM THICKNESS.

The thickness of each film was determined at several points across the film, and the average film thickness together with an estimate of the non-uniformity of the film calculated. The calculation procedure used is described in detail by McCoy (loc. cit.) and Campbell (loc. cit.). The problem with the technique of FECO is to account for phase changes on reflection. When the fringe system is viewed in reflection, only the phase effects of the overcoating silver layer need be considered.

From the derivation of the Airy equation which includes phase changes on reflection, the condition for a minimum in the reflected intensity is given to a high degree of accuracy by (Bennett, 1964):

$$N\lambda = 2nt - (\lambda/2\pi)\{\beta_1(\lambda) + \beta_2(\lambda)\} \qquad 2.4.1$$

where N is an integer, n is the refractive index of the material between the two reflecting surfaces which form the Fabry-Perot interferometer, t is the geometrical separation of the plates and $\beta_1(\lambda)$ and $\beta_2(\lambda)$ are the absolute phase changes on reflection at the two reflecting surfaces.

For adjacent fringes at λ_1 and λ_2 $(\lambda_1>\lambda_2)$, the Nth. minimum in the reflected fringe system is given by (Bennett, 1964)

$$N+1 = \lambda_2/(\lambda_1-\lambda_2) \qquad 2.4.2$$

For the fringe pattern on each side of the step, the equations

$$N\lambda = 2t - (\lambda/2\pi)\{\beta_1(\lambda) + \beta_2(\lambda)\} \qquad 2.4.3$$

$$N\lambda' = 2(t+\delta t) - (\lambda'/2\pi)\{\beta_1(\lambda') + \beta_2(\lambda')\} \qquad 2.4.4$$

follow from equation 2.4.1 where λ and λ' are the wavelengths of corresponding minima and n for air is taken as 1.

For high reflectance films deposited simultaneously in vacuo, the phase change on reflection at the two reflecting surfaces will be very nearly the same. Then, to a good approximation,

$$\beta_1(\lambda) = \beta_2(\lambda) = \beta(\lambda)$$

Bennett (loc. cit.) has shown that $\beta(\lambda)$ for silver films is a slowly varying function of λ and may be approximated to a straight line of the form

$$\beta(\lambda) = \pi(c+d\lambda) \qquad 2.4.5$$

Hence

$$N\lambda = 2t - c\lambda - d\lambda^2 \qquad 2.4.6$$

A plot of $N\lambda$ against λ is no longer linear, but is modified by the term in λ^2. McCoy (loc. cit.) and Campbell (loc. cit.) have shown that if a straight line is fitted through the $(\lambda, N\lambda)$ points, the maximum deviation from the parabolic fit over the visible range is less than $\pm 25\text{Å}$ and is independent of both N and δt.

For a linear fit through the $(\lambda, N\lambda)$ points, the most convenient equations for each set of points are

$$N_i\lambda_i = m\lambda_i + c \qquad 2.4.7$$

$$N_j\lambda_j = m\lambda_j + c + \delta t \qquad 2.4.8$$

where N_i is the integer closest to the value given by equation 2.4.3. The two lines of slope m are required to be parallel and the parameters are calculated by minimising the standard deviation of

each set of points from the corresponding straight line. Using these equations, the film thickness is calculated as one of the parameters.

Campbell (loc. cit.) and McCoy (loc. cit.) have programmed the computer to calculate the average film thickness from the measurements at a number of points across the film, together with an estimate of the non-uniformity of the film calculated from the standard deviation of the thickness at each point from the average thickness. They have shown that, at least for carbon and selenium films, the uniformity of the film is generally the limiting factor in the accuracy of the calculations.

CHAPTER 3.

CALCULATION OF THE OPTICAL CONSTANTS OF A THIN ABSORBING SINGLE - LAYER FILM.

3. 1 INTRODUCTION.

The equations for the reflectance, R, and transmittance, T, of light at normal incidence on a thin absorbing film on a transparent substrate are complicated, and the exact solution for the refractive index, n, and absorption index, k, from them involves extensive computation (McCoy, 1966; Campbell, 1968). Consideration of the expressions for (1 + R)/T and (1 - R)/T resulted in simpler equations which were more readily solved.

A program has been written for a digital computer to calculate n and k from measured values of R and T, and uses a calculation procedure suitable for data from any thin film. The program has been used to calculate the optical constants of germanium films, selenium films and carbon films. The solutions from the data for the carbon films agree exactly with those calculated by McCoy (loc. cit.).

In the calculation of the optical constants, multiple solutions can occur, and the solutions for the refractive index are markedly affected by small changes in film thickness. The behaviour of the solutions under such changes is discussed, and the results of this investigation show that the choice of the correct solutions depends critically on film thickness, and use can be made of this in determining accurately the optical film thickness.

3. 2 THE EQUATIONS FOR THE OPTICAL CONSTANTS.

3. 2. 1 REFLECTANCE AND TRANSMITTANCE EQUATIONS.

The equations for the reflectance and transmittance of a single absorbing film on a transparent substrate are (Heavens, 1955)

$$R = \frac{(g_1^2+h_1^2)\exp(2\alpha_1) + (g_2^2+h_2^2)\exp(-2\alpha_1) + A\cos 2\gamma_1 + B\sin 2\gamma_1}{\exp(2\alpha_1) + (g_1^2+h_1^2)(g_2^2+h_2^2)\exp(-2\alpha_1) + C\cos 2\gamma_1 + D\sin 2\gamma_1} \qquad 3.2.1$$

$$T = \left(\frac{n_2}{n_0}\right) \frac{\{(1+g_1)^2 + h_1^2\}\{(1+g_2)^2 + h_2^2\}}{\exp(2\alpha_1) + (g_1^2+h_1^2)(g_2^2+h_2^2)\exp(-2\alpha_1) + C\cos 2\gamma_1 + D\sin 2\gamma_1} \qquad 3.2.2$$

where

$$g_1 = \frac{n_0^2 - n_1^2 - k_1^2}{(n_0+n_1)^2 + k_1^2} \qquad g_2 = \frac{n_1^2 - n_2^2 + k_1^2}{(n_1+n_2)^2 + k_1^2}$$

$$h_1 = \frac{2n_0k_1}{(n_0+n_1)^2 + k_1^2} \qquad h_2 = \frac{-2n_2k_1}{(n_1+n_2)^2 + k_1^2}$$

$$A = 2(g_1g_2 + h_1h_2) \qquad B = 2(g_1h_2 - g_2h_1)$$

$$C = 2(g_1g_2 - h_1h_2) \qquad D = 2(g_1h_2 + g_2h_1)$$

$$\alpha_1 = 2\pi k_1d_1/\lambda \qquad \gamma_1 = 2\pi n_1d_1/\lambda$$

and

n_0 is the refractive index of the surrounding medium ($n_0 = 1$ for air).

n_1 is the refractive index of the film.

n_2 is the refractive index of the substrate.

k_1 is the absorption index of the film.

d_1 is the thickness of the film.

λ is the wavelength of the incident light.

3. 2. 2 CORRECTED TRANSMITTANCE EQUATION.

Equation 3.2.2 for the transmittance is the expression for the intensity transmitted into the medium of refractive index n_2. This equation has to be corrected for the case of a substrate of finite thickness where the transmitted intensity passes through the substrate and is measured in the medium of refractive index n_0. For the wedge-shaped substrates used, the beam reflected from the back face of the substrate passed out of the substrate away from the incident beam and hence produced no multiple beam effect in the substrate. The transmittance of the half of the wedge with the film deposited on it was compared to that of the blank half.

From the diagram below, if I_0 is the incident intensity, then the reference intensity I_R is given by

$$I_R = I_0 t^2$$

where t is the transmission coefficient of the substrate-air interface.

The specimen intensity I_S is

$$I_S = I_0 Tt$$

where T is the transmittance given by equation 3.2.2. Thus the measured transmittance ratio Γ is

$$\Gamma = \frac{I_S}{I_R} = \frac{T}{t}$$

i.e.
$$\Gamma = \frac{(n_2+n_0)^2}{4n_2n_0}.T \qquad 3.2.3$$

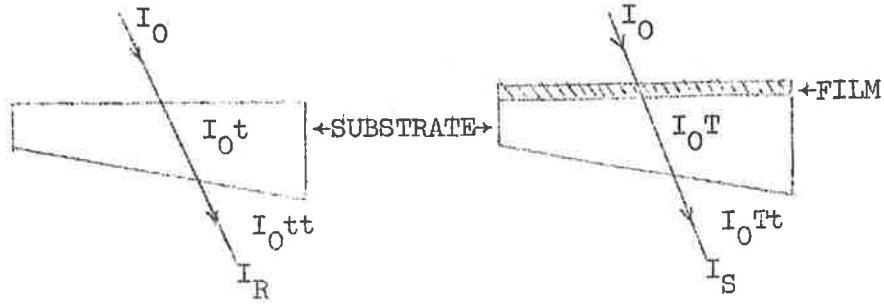

3. 3 SOLUTION OF THE REFLECTANCE AND TRANSMITTANCE EQUATIONS.

Equations 3.2.1 and 3.2.2 cannot be separated to give explicit expressions for n_1 and k_1, the alternative is to solve the equations graphically. Bennett and Booty (1966) used a trial and error process in which n_1 and k_1 were altered in increments and the values of n_1 and k_1 stored for which the computed values of R and T were nearest to the measured values. Smaller increments were then used for n_1 and k_1 and the process repeated until the measured and calculated values of R and T were within the desired degree of accuracy. This process has a number of disadvantages. Firstly, approximate solutions to the equations have to be inserted as the starting point for the calculation, these being obtained from the bulk material. Secondly, McCoy (loc. cit.) has found the number of computations involved in finding a solution to the equations can become excessive under certain conditions. Thirdly, the equations often had more than one solution, either of which was acceptable at the wavelength at which the calculation was made. Alternatively no solution may exist and this

possibility was not taken into account. Fourthly, in the paper quoted there was no estimate of the error in the solutions arising from experimental errors.

Nilsson (1968) recognised the existence of multiple solutions and attempted to solve the reflectance and transmittance equations in the following manner: The equations for R and T were rewritten in the implicit forms:

$$F(R, n_1, k_1) = 0$$

$$G(T, n_1, k_1) = 0$$

Approximate values of n_1 and k_1 gave certain values of F and G. Through the corresponding points in the F, n_1, k_1 and G, n_1, k_1 system, tangent planes were laid. The common point of those planes in the plane $F = G = 0$ was then taken as a second approximation, and the process repeated until the equation system was satisfied.

However again with this method only one solution was determined, although it should be possible to calculate the other solutions using appropriate initial values of n_1 and k_1. Nilsson gave an ad hoc method for determining the initial values of n_1 and k_1 under certain conditions. He admitted that over some spectral regions the results obtained by this method were uncertain. No estimate of the error in the solutions was given although he realised that the error depended on the curve intersections.

McCoy (loc. cit.) and Campbell (loc. cit.) solved the equations graphically with the aid of a digital computer. This was achieved by allowing n_1 to take a range of values, and for each n_1, calculating the values of k_1 which satisfied the experimentally determined

values of reflectance and transmittance. These loci of constant reflectance and constant transmittance were plotted as n_1 against k_1, the solutions for n_1 and k_1 being the points of intersection of the two loci. The large number of types of curve intersections which could occur necessitated extensive programming and required considerable computing time, but nevertheless exact solutions were obtained, and all the solutions in a given range of n_1 were determined. An estimate of the error in the solution at each wavelength was also calculated, involving the numerical differentiation of the reflectance and transmittance equations.

3.4 THE EQUATIONS (1+R)/T AND (1-R)/T.

The denominators of the right-hand sides of equations 3.2.1 and 3.2.2 are identical except for the factor n_0 in equation 3.2.2. By considering the expressions (1+R)/T and (1-R)/T, the following simpler equations can be derived (Tomlin, 1968):

$$\frac{1+R}{T} = \frac{1}{4n_0n_2(n_1^2+k_1^2)}\Big[(n_0^2+n_1^2+k_1^2)\{(n_1^2+n_2^2+k_1^2)\cosh 2\alpha_1 + 2n_1n_2\sinh 2\alpha_1\} + (n_0^2-n_1^2-k_1^2)\{(n_1^2-n_2^2+k_1^2)\cos 2\gamma_1 - 2n_2k_1\sin 2\gamma_1\}\Big] \qquad 3.4.1$$

$$\frac{1-R}{T} = \frac{1}{2n_2(n_1^2+k_1^2)}\Big[n_1\{(n_1^2+n_2^2+k_1^2)\sinh 2\alpha_1 + 2n_1n_2\cosh 2\alpha_1\} + k_1\{(n_1^2-n_2^2+k_1^2)\sin 2\gamma_1 + 2n_2k_1\cos 2\gamma_1\}\Big] \qquad 3.4.2$$

For the wedge-shaped substrates used, the measured quantities are R and Γ. Thus from equations 3.2.3, 3.4.1 and 3.4.2:

$$\frac{1+R}{\Gamma} = \frac{1}{(n_1^2+k_1^2)(n_0+n_2)^2}\Big\{(n_0^2+n_1^2+k_1^2)\{(n_1^2+n_2^2+k_1^2)\cosh 2\alpha_1 + 2n_1n_2\sinh 2\alpha_1\} + (n_0^2-n_1^2-k_1^2)\{(n_1^2-n_2^2+k_1^2)\cos 2\gamma_1 - 2n_2k_1\sin 2\gamma_1\}\Big\} \qquad 3.4.3$$

$$\frac{1-R}{\Gamma} = \frac{2n_0}{(n_1^2+k_1^2)(n_0+n_2)^2}\Big\{n_1\{(n_1^2+n_2^2+k_1^2)\sinh 2\alpha_1 + 2n_1n_2\cosh 2\alpha_1\} + k_1\{(n_1^2-n_2^2+k_1^2)\sin 2\gamma_1 + 2n_2k_1\cos 2\gamma_1\}\Big\} \qquad 3.4.4$$

3.5 SOLUTION OF THE EQUATIONS (1+R)/Γ AND (1-R)/Γ FOR n_1 AND k_1.

Equations 3.4.3 and 3.4.4 again cannot be separated to give explicit expressions for n_1 and k_1. They have been solved in a similar manner to that described in section 3.3 by Campbell, with less extensive computation due to a decrease in the number of modes of curve intersections. The behaviour of these equations is much simpler than for R and T (orΓ) as can be seen in Figure 3.1 where normalised contour curves of R, T, (1+R)/T and (1-R)/T, are plotted as functions of n_1 and k_1 for $n_2 = 1.5$ and $d_1/\lambda = 0.4$. By plotting curves of constant (1±R)/T(orΓ) in the first quadrant of the n_1-k_1 plane for a series of values of d_1/λ, it was found that equations 3.4.3 and 3.4.4 were single-valued in k_1 for a given n_1. Since equation 3.4.4 is readily differentiated with respect to k_1, the solutions to the equations may be determined as follows:

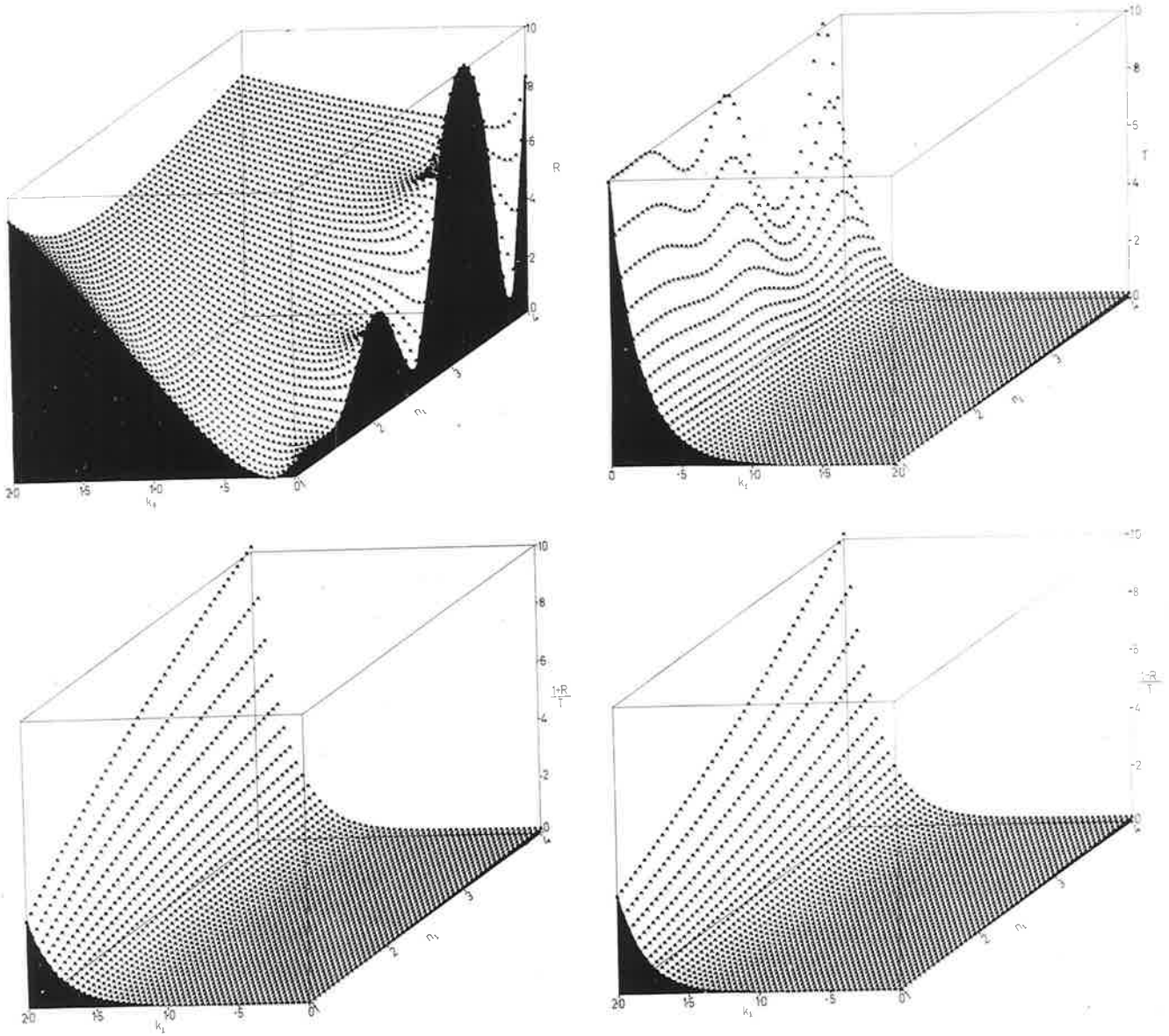

Figure 3.1

Rewriting equations 3.4.3 and 3.4.4

$$(n_0^2+n_1^2+k_1^2)\{(n_1^2+n_2^2+k_1^2)\cosh 2\alpha_1 + 2n_1n_2\sinh 2\alpha_1\}$$
$$+ (n_0^2-n_1^2-k_1^2)\{(n_1^2-n_2^2+k_1^2)\cos 2\gamma_1 - 2n_2k_1\sin 2\gamma_1\}$$
$$- (n_1^2+k_1^2)(n_0+n_2)^2\left(\frac{1+R}{T}\right) = 0 \qquad 3.5.1$$

$$2n_0n_1\{(n_1^2+n_2^2+k_1^2)\sinh 2\alpha_1 + 2n_1n_2\cosh 2\alpha_1\}$$
$$+ 2n_0k_1\{(n_1^2-n_2^2+k_1^2)\sin 2\gamma_1 + 2n_2k_1\cos 2\gamma_1\}$$
$$- (n_1^2+k_1^2)(n_0+n_2)^2\left(\frac{1-R}{T}\right) = 0 \qquad 3.5.2$$

Let

$f_1(n_1,k_1)$ = left-hand side of equation 3.5.1

$f_2(n_1,k_1)$ = left-hand side of equation 3.5.2

The solution is thus that (n_1,k_1) for which

$$f_1(n_1,k_1) = f_2(n_1,k_1) = 0$$

For a given n_1, equation 3.5.2 can be solved for k_1 using Newton's method (see for example, National Physical Laboratory, 1961). If $k_1^{(0)}$ is an approximate solution of equation 3.5.2 for a given n_1, a better approximation is given by

$$k_1^{(1)} = k_1^{(0)} - f_2(n_1,k_1^{(0)})/f_2'(n_1,k_1^{(0)})$$

where

$$f_2'(n_1,k_1) = \frac{\partial f_2(n_1,k_1)}{\partial k_1}$$

$$= 2n_0\{2n_1(k_1+2n_2\gamma_1)\sinh 2\alpha_1 + 2\gamma_1(n_1^2+n_2^2+k_1^2)\cosh 2\alpha_1$$
$$+ (n_1^2-n_2^2+3k_1^2)\sin 2\gamma_1 + 4n_2k_1\{\cos 2\gamma_1 - (n_0+n_2)^2(\tfrac{1-R}{T})\}\}$$

For the present investigation it was sufficient to set $k_1^{(0)}$ to zero.

Thus by successive approximations, i.e.

$$k_1^{(n)} = k_1^{(n-1)} - \frac{f_2(n_1,k_1^{(n-1)})}{f_2'(n_1,k_1^{(n-1)})}$$

k_1 can be found to any preset limit, for a given n_1.
For the present investigation the limit was such that $f_2(n_1,k_1)$ was within 0.0001 of zero.

3. 5. 1 CALCULATION OF n_1 AND k_1.

n_1 and k_1 which satisfy both equations 3.5.1 and 3.5.2 may be determined as follows: n_1 is set to a lower limit and the value of k_1 which satisfies equation 3.5.2 is calculated as described above. The set value of n_1 and calculated k_1 are substituted in the equation for $f_1(n_1,k_1)$. If $f_1(n_1,k_1) = 0$, then this (n_1,k_1) satisfies both equations 3.5.1 and 3.5.2 and hence constitutes a solution.

If $f_1(n_1,k_1) \neq 0$ these values of n_1,k_1 and $f_1(n_1,k_1)$ are stored in the computer, an increment is added to n_1, and the process repeated. The sign of the new value of $f_1(n_1,k_1)$ is compared with that of the stored value, and if identical, the stored values of n_1,k_1 and $f_1(n_1,k_1)$ are rejected and the new values stored. A further increment is added to n_1 and the procedure continued until a change of sign occurs between corresponding values of $f_1(n_1,k_1)$, which then implies that a solution exists between these two values of n_1. This can be seen from Figure 3.2.a where $f_1(n_1,k_1)$ is plotted as a function of n_1 for a given d_1/λ and $\frac{1-R}{T}$.

Let $n_1^{(1)}$ and $n_1^{(2)}$ be the values of n_1 corresponding to the values of $f_1(n_1,k_1)$ between which there occurred a change of sign.

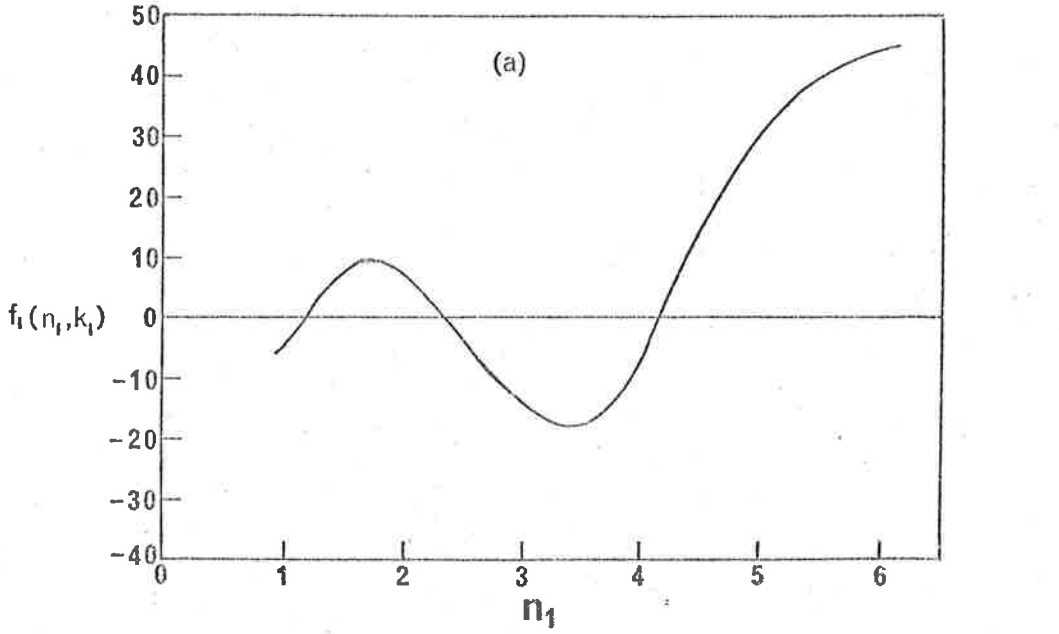
(a)
50
40
30
20
10
0
-10
-20
-30
-40
0
1
2
3
4
5
6
$f_i(n_i,k_i)$
n_1

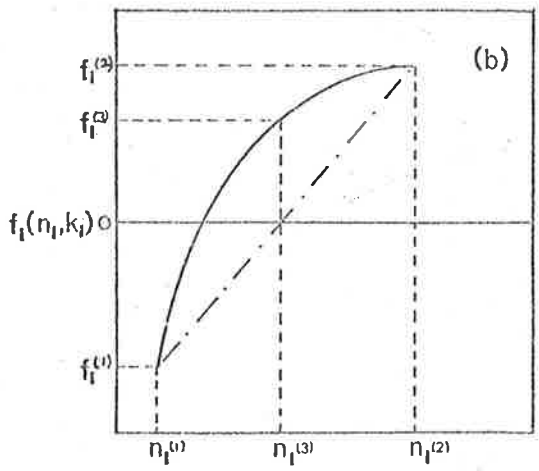
(b)
$f_i^{(3)}$
$f_i^{(2)}$
$f_i(n_i,k_i)$ o
$f_i^{(1)}$
$n_i^{(1)}$
$n_i^{(3)}$
$n_i^{(2)}$

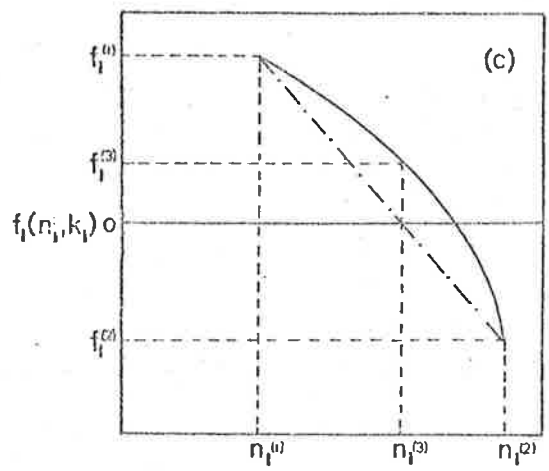
(c)
$f_i^{(1)}$
$f_i^{(3)}$
$f_i(n_i,k_i)$ o
$f_i^{(2)}$
$n_i^{(1)}$
$n_i^{(3)}$
$n_i^{(2)}$

Figure 3.2

Let $f_1^{(1)} = f_1(n_1^{(1)}, k_1)$ and $f_1^{(2)} = f_1(n_1^{(2)}, k_1)$. There are two cases to consider corresponding to $f_1^{(1)}$ being negative or positive. Consider the case where $f_1^{(1)}$ is negative. An approximation to n_1 can be found by linear interpolation between $n_1^{(1)}$ and $n_1^{(2)}$.

From Figures 3.2.b and 3.2.c, an approximate solution is $n_1^{(3)}$ where, from similar triangles,

$$n_1^{(3)} = n_1^{(2)} - \frac{\{n_1^{(2)} - n_1^{(1)}\} f_1^{(2)}}{f_1^{(2)} - f_1^{(1)}} \qquad 3.5.3$$

k_1 is calculated as before for this new value of n_1, and the corresponding $f_1^{(3)} = f_1(n_1^{(3)}, k_1)$ calculated. If $f_1^{(3)} < 0$ then $f_1^{(1)}$ and $n_1^{(1)}$ are replaced by $f_1^{(3)}$ and $n_1^{(3)}$ and equation 3.5.3 again applied. If $f_1^{(3)} > 0$, then $f_1^{(2)}$ and $n_1^{(2)}$ are replaced by $f_1^{(3)}$ and $n_1^{(3)}$ and equation 3.5.3 again applied. By continuing this process until some preset limit (e.g. $|f_1^{(3)}| < 0.001$), the values $n_1^{(3)}$ and corresponding k_1 are good approximations to the correct solutions.

For the case where $f_1^{(1)}$ is initially positive, the procedure and equations are identical to the above if $(n_1^{(1)}, f_1^{(1)})$ and $(n_1^{(2)}, f_1^{(2)})$ are interchanged. Thus n_1 and k_1 can be found to any required degree of accuracy by imposing appropriate limits.

Although for a given n_1, there is only one positive k_1 which satisfies equation 3.5.2, there may exist more than one set of n_1 and k_1 which satisfy both equations 3.5.1 and 3.5.2. Consequently, further increments must be added to n_1, until some preset limit is reached, to determine all possible solutions.

3. 6 CALCULATION OF THE ERROR IN THE SOLUTION.

Along with each value of n_1 and k_1 calculated, an estimate of the maximum error in each, due to errors in R,Γ,d_1 and n_2, was evaluated as follows:

We may write $(1+R)/\Gamma$ and $(1-R)/\Gamma$ in the functional form

$$(1+R)/\Gamma = F(n_1,k_1,d_1,n_2) \qquad 3.6.1$$

$$(1-R)/\Gamma = G(n_1,k_1,d_1,n_2) \qquad 3.6.2$$

Taking total derivatives

$$dF = \frac{\partial F}{\partial n_1}\,dn_1 + \frac{\partial F}{\partial k_1}\,dk_1 + \frac{\partial F}{\partial d_1}\,dd_1 + \frac{\partial F}{\partial n_2}\,dn_2 \qquad 3.6.3$$

$$dG = \frac{\partial G}{\partial n_1}\,dn_1 + \frac{\partial G}{\partial k_1}\,dk_1 + \frac{\partial G}{\partial d_1}\,dd_1 + \frac{\partial G}{\partial n_2}\,dn_2 \qquad 3.6.4$$

From equations 3.6.3 and 3.6.4

$$dk_1 = \frac{1}{J}\left(dG.\frac{\partial F}{\partial n_1} - dF.\frac{\partial G}{\partial n_1} + \left\{\frac{\partial G}{\partial n_1}.\frac{\partial F}{\partial d_1} - \frac{\partial F}{\partial n_1}.\frac{\partial G}{\partial d_1}\right\}dd_1 + \left\{\frac{\partial G}{\partial n_1}.\frac{\partial F}{\partial n_2} - \frac{\partial F}{\partial n_1}.\frac{\partial G}{\partial n_2}\right\}dn_2 \right) \qquad 3.6.5$$

$$dn_1 = \frac{1}{J}\left(dF.\frac{\partial G}{\partial k_1} - dG.\frac{\partial F}{\partial k_1} + \left\{\frac{\partial F}{\partial k_1}.\frac{\partial G}{\partial d_1} - \frac{\partial G}{\partial k_1}.\frac{\partial F}{\partial d_1}\right\}dd_1 + \left\{\frac{\partial F}{\partial k_1}.\frac{\partial G}{\partial n_2} - \frac{\partial G}{\partial k_1}.\frac{\partial F}{\partial n_2}\right\}dn_2 \right) \qquad 3.6.6$$

where

$$J = \frac{\partial G}{\partial k_1}.\frac{\partial F}{\partial n_1} - \frac{\partial G}{\partial n_1}.\frac{\partial F}{\partial k_1} \qquad 3.6.7$$

Although explicit expressions for n_1 and k_1 cannot be found, they may be written in the functional form

$$n_1 = n_1(F,G,d_1,n_2) \qquad 3.6.8$$

$$k_1 = k_1(F,G,d_1,n_2) \qquad 3.6.9$$

Similarly

$$dn_1 = \frac{\partial n_1}{\partial F}.dF + \frac{\partial n_1}{\partial G}.dG + \frac{\partial n_1}{\partial d_1}.dd_1 + \frac{\partial n_1}{\partial n_2}.dn_2 \qquad 3.6.10$$

$$dk_1 = \frac{\partial k_1}{\partial F}.dF + \frac{\partial k_1}{\partial G}.dG + \frac{\partial k_1}{\partial d}.dd_1 + \frac{\partial k_1}{\partial n_2}.dn_2 \qquad 3.6.11$$

Equating coefficients of equations 3.6.5 and 3.6.6 with those of equations 3.6.10 and 3.6.11

$$\frac{\partial n_1}{\partial F} = \frac{1}{J}\frac{\partial G}{\partial k_1} \qquad 3.6.12$$

$$\frac{\partial n_1}{\partial G} = -\frac{1}{J}\frac{\partial F}{\partial k_1} \qquad 3.6.13$$

$$\frac{\partial n_1}{\partial d_1} = \frac{1}{J}\left(\frac{\partial F}{\partial k_1}.\frac{\partial G}{\partial d_1} - \frac{\partial G}{\partial k_1}.\frac{\partial F}{\partial d_1}\right) \qquad 3.6.14$$

$$\frac{\partial n_1}{\partial n_2} = \frac{1}{J}\left(\frac{\partial F}{\partial k_1}.\frac{\partial G}{\partial n_2} - \frac{\partial G}{\partial k_1}.\frac{\partial F}{\partial n_2}\right) \qquad 3.6.15$$

$$\frac{\partial k_1}{\partial F} = -\frac{1}{J}\frac{\partial G}{\partial n_1} \qquad 3.6.16$$

$$\frac{\partial k_1}{\partial G} = \frac{1}{J}\frac{\partial F}{\partial n_1} \qquad 3.6.17$$

$$\frac{\partial k_1}{\partial d_1} = \frac{1}{J}\left(\frac{\partial G}{\partial n_1}.\frac{\partial F}{\partial d_1} - \frac{\partial F}{\partial n_1}.\frac{\partial G}{\partial d_1}\right) \qquad 3.6.18$$

$$\frac{\partial k_1}{\partial n_2} = \frac{1}{J}\left(\frac{\partial G}{\partial n_1}.\frac{\partial F}{\partial n_2} - \frac{\partial F}{\partial n_1}.\frac{\partial G}{\partial n_2}\right) \qquad 3.6.19$$

Hence an estimate of the maximum error in n_1 and k_1 is given by

$$\Delta n_1 = \left|\frac{\partial n_1}{\partial F}.\Delta F\right| + \left|\frac{\partial n_1}{\partial G}.\Delta G\right| + \left|\frac{\partial n_1}{\partial d_1}.\Delta d_1\right| + \left|\frac{\partial n_1}{\partial n_2}.\Delta n_2\right| \qquad 3.6.20$$

$$\Delta k_1 = \left|\frac{\partial k_1}{\partial F}.\Delta F\right| + \left|\frac{\partial k_1}{\partial G}.\Delta G\right| + \left|\frac{\partial k_1}{\partial d_1}.\Delta d_1\right| + \left|\frac{\partial k_1}{\partial n_2}.\Delta n_2\right| \qquad 3.6.21$$

where the partial derivatives of n_1 and k_1 are given by equations 3.6.12 to 3.6.19; ΔF and ΔG are found from the experimental errors in R and Γ, Δd_1 is the estimate of the error in the film thickness, and Δn_2 is the error in n_2. The partial derivatives of F and G are given in Appendix A. These first order formulae are valid provided J is not too small.

3. 7 THE EFFECTS OF FILM THICKNESS ON THE CALCULATION OF n_1 AND k_1.

The effects of variations in film thickness on the calculated values of n_1 considered in this section are for the situation where $n_1 > n_0, n_2$. This is generally the case for a semiconducting film supported on a transparent substrate. It will be shown that an underestimate or overestimate of the film thickness produces quite distinct results.

Although not considered in this thesis, the cases $n_0 < n_1 < n_2$ and $n_1 < n_0$ give different behaviour but again underestimates or overestimates of the film thickness produce quite distinct results.

3. 7. 1 THE HYPOTHETICAL FILM.

In order to determine the behaviour of the optical constants of a film under small changes in film thickness, a hypothetical film was formulated so that its properties were known exactly. The film was assumed to have properties approximating those of germanium.

The refractive index, n_1, was set equal to 4.0 over the wavelength range $0.5\mu - 2.5\mu$

The absorption index varied as $0.25/\lambda$ (λ in μ)

Film thickness was set equal to 2000Å.

The reflectance and transmittance for this film were calculated using equations 3.2.1 and 3.2.2 (corrected using equation 3.2.3). The reflectance and transmittance curves are shown in Figure 3.3.a; and, when compared with those obtained for a germanium film, 1800Å thick, (Figure 3.3.b) it can been seen that the hypothetical film is not far different from the real situation.

3. 7. 2 CALCULATION OF n_1 AND k_1 FOR THE HYPOTHETICAL FILM.

The calculated reflectance and transmittance for the hypothetical film were used as data for the calculation of n_1 and k_1 using the method described above. The calculated n_1 - curve is shown in Figure 3.4.a. In various parts of the wavelength range, multiple solutions exist, although at each point the exact value of 4.0 is a solution. Some solutions are close together and an iterative process, as used by Bennett and Booty (1966), assuming initially bulk values may readily converge to an incorrect solution.

The incorrect solutions are seen to form loops intersecting the correct curve. The number and position of these loops depends on the film thickness. As the thickness increases, more loops appear. If the film is very thin no such loops will appear and only the correct solutions will be determined. This situation will be discussed later.

3. 7. 3 FILM THICKNESS TOO LARGE.

Using the same reflectance and transmittance data as in 3.7.2, n_1 and k_1 were calculated assuming a film thickness of 2100Å instead

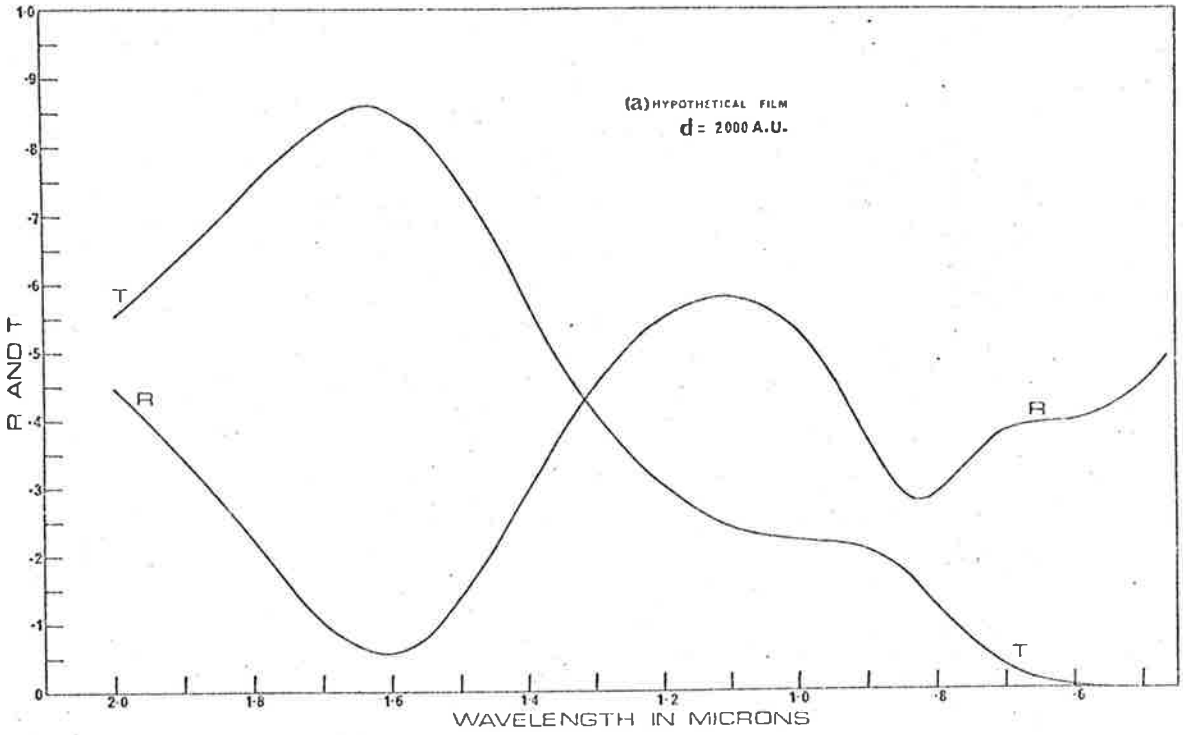
(a) HYPOTHETICAL FILM
d = 2000 A.U.
T
R
R
T
R AND T
WAVELENGTH IN MICRONS

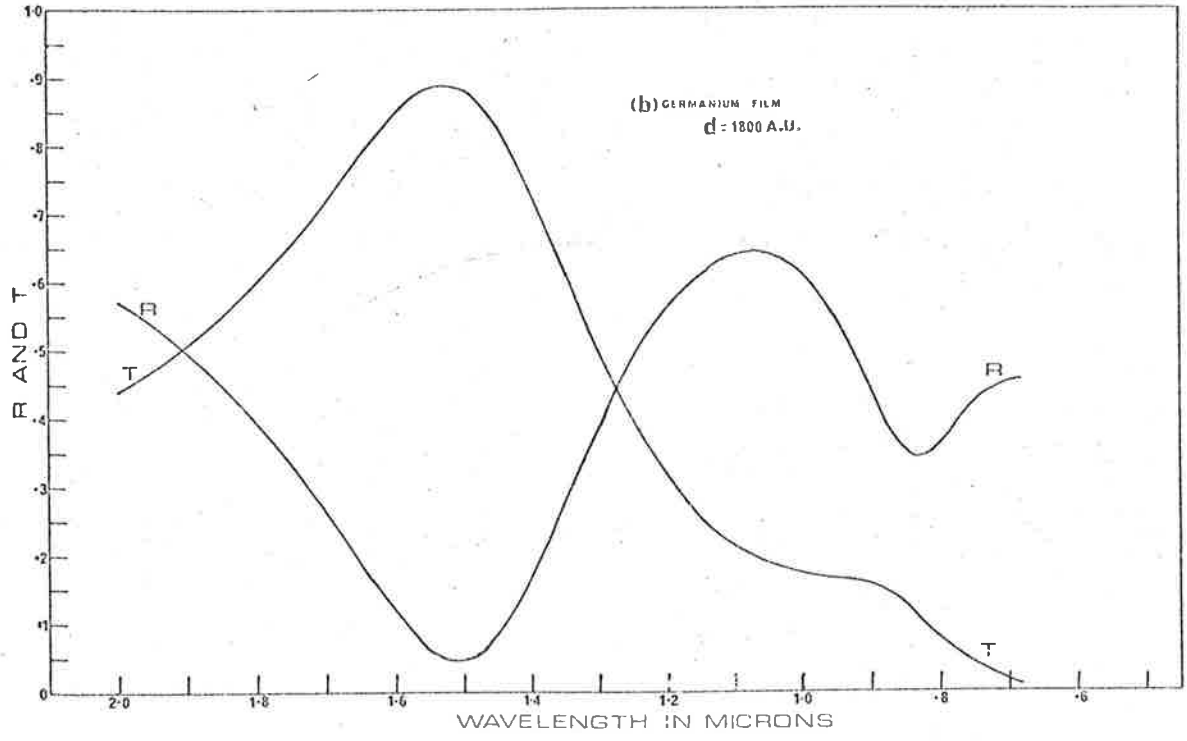
(b) GERMANIUM FILM
d = 1800 A.U.
R
T
R
T
R AND T
WAVELENGTH IN MICRONS

Figure 3.3

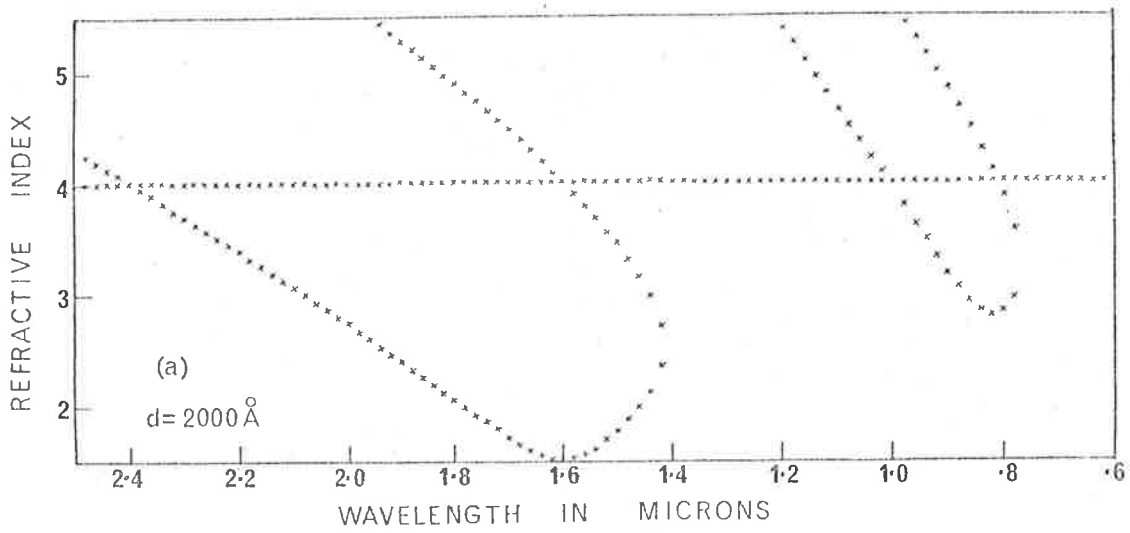
REFRACTIVE INDEX
5
4
3
2
(a)
d= 2000 Å
2·4
2·2
2·0
1·8
1·6
1·4
1·2
1·0
·8
·6
WAVELENGTH IN MICRONS

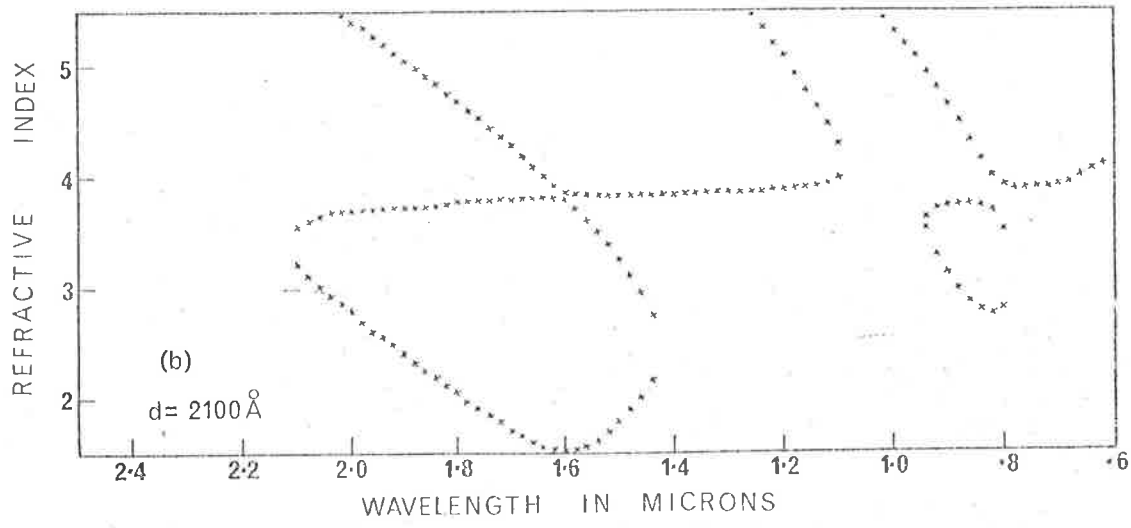
REFRACTIVE INDEX
5
4
3
2
(b)
d= 2100 Å
2·4
2·2
2·0
1·8
1·6
1·4
1·2
1·0
·8
·6
WAVELENGTH IN MICRONS

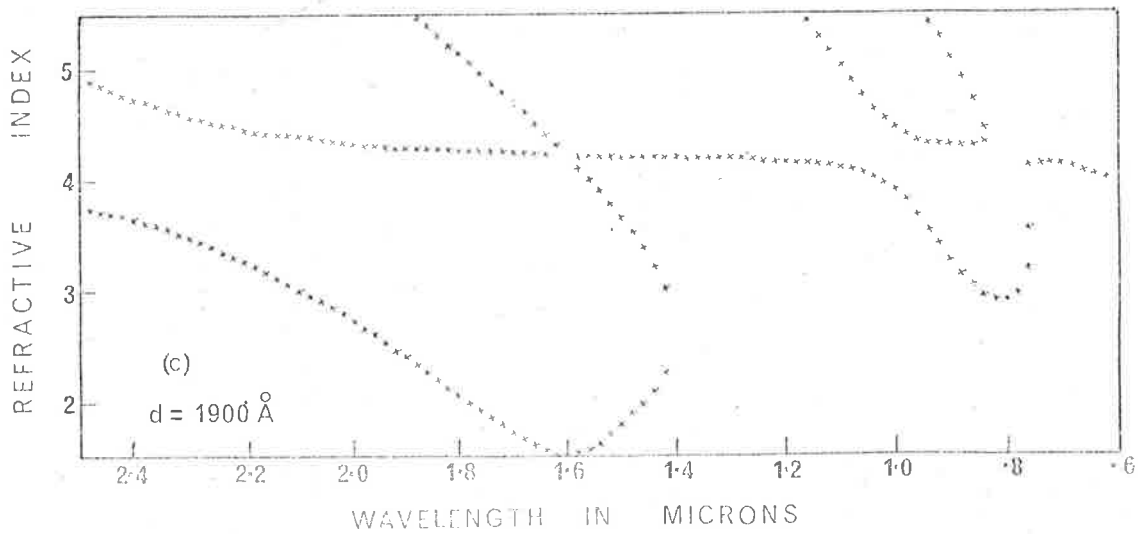
REFRACTIVE INDEX
5
4
3
2
(c)
d = 1900 Å
2·4
2·2
2·0
1·8
1·6
1·4
1·2
1·0
·8
·6
WAVELENGTH IN MICRONS

Figure 3.4

of the correct value of 2000Å. The calculated n_1 - curve is shown in Figure 3.4.b. In some wavelength regions no solutions for n_1 were found, and a continuous dispersion curve cannot be drawn. Parts of the correct curve have shifted down and merged with the lower parts of the loops to form isolated islands.

3. 7. 4 FILM THICKNESS TOO SMALL.

Again using the same reflectance and transmittance data as above, n_1 and k_1 were calculated assuming a film thickness of 1900Å. The calculated n_1 - curve is shown in Figure 3.4.c. Although a continuous dispersion curve can be drawn, it is vastly incorrect. Various regions of the correct solutions have shifted up to form loops with parts of the incorrect solutions. The remaining regions have shifted down and merged with the incorrect solutions to form a continuous dispersion curve with the appearance of valleys. This curve is also multi-valued at some points.

3. 7. 5 EFFECT ON PREVIOUS WORK.

Campbell (loc. cit.), in his calculations of the optical constants of selenium films, found that use of the measured film thickness produced curves similar to that shown in Figure 3.4.b. He recognised this as being related to too large a value for the film thickness being used in calculations. He accordingly reduced the film thickness but failed to recognise the behaviour of an underestimate in the film thickness, and curves similar to that shown in Figure 3.4.c were assumed correct. Thus all the refractive index and absorption

curves calculated by him are incorrect.

The reason why the measured film thickness corresponded to the situation of an overestimate in this quantity will be considered in Chapter 4. The optical constants of selenium films were recalculated from the data of Campbell and the results of this are presented in Chapter 5.

3. 7. 6 ACCURATE DETERMINATION OF THE OPTICAL FILM THICKNESS.

The behaviour of the refractive index solutions as a function of wavelength is quite distinct for film thicknesses which are either too small or too large. This characteristic behaviour is readily detected for film thickness variations as small as 0.5%. Hence adjustments can be made to the film thickness until the correct behaviour occurs, thus giving the correct optical constants together with an accurate value of the optical film thickness.

3. 7. 7 EFFECTS OF ERRORS IN R AND T ON THE CALCULATED FILM THICKNESS.

From our calculations on hypothetical films it was apparent that obtaining the correct behaviour for the refractive index solutions was very critical on the choice of the correct film thickness. Before any conclusions could be drawn as to the absolute accuracy of the film thickness determined by this method it was necessary to determine the sensitivity of obtaining the correct refractive index behaviour to errors in R and T.

This was most suitably determined from the use of the hypothetical films. The calculated reflectances and transmittances for hypothetical

films of varying thicknesses were altered in the four following ways:

(1).	R + 0.003	T + 0.003
(2).	R - 0.003	T - 0.003
(3).	R + 0.003	T - 0.003
(4).	R - 0.003	T - 0.003

Cases (1) and (2) did not affect the calculated film thickness to any detectable extent. For case (3) the film thickness had to be reduced by 0.5% while in case (4) it had to be increased by 0.5%.

Provided one has a uniform film of sufficient thickness to enable the above method to be used, and provided that R and T can be measured to about ± 0.003, then the optical thickness of the film may be determined with considerable precision.

3. 7. 8 VERY THIN FILMS.

If the thickness of the film is less than the order of 500Å, maxima and minima in the R and T curves are no longer apparent in the wavelength range of measurements. For such films multiple solutions do not occur. Variations in film thickness for these films therefore do not exhibit the behaviour discussed above, and the method described in section 3.7.6 cannot be used to determine the film thickness.

In order to be certain that the film thickness is correct, and correspondingly the optical constants, it is preferable to use films thick enough to exhibit multiple solutions. For germanium this corresponds to 600Å or greater. From the discussion of surface layers in the next chapter, the existence of multiple solutions provides

valuable information, and enhances the desirability to use sufficiently thick films such that multiple solutions occur.

3. 8 APPROXIMATE FILM THICKNESS.

If two consecutive turning points of the $(1+R)/T$ vs. λ curve exists in the infra-red (i.e. away from the absorption edge), and the long-wavelength refractive index is known, an approximate value for the film thickness may be found as follows:

In the infra-red, $k_1 \simeq 0$, hence, from equation 3.4.3

$$\frac{1+R}{T} = \frac{1}{n_1^2(n_0+n_2)^2}\{(n_1^2+1)(n_1^2+n_2^2) - (n_1^2-1)(n_1^2-n_2^2)\cos 2\gamma_1\}$$

$$\frac{\partial\{(1+R)/T\}}{\partial\lambda} = \frac{-4\pi d_1}{\lambda^2 n_2 n_1 (n_0+n_2)^2}(n_1^2-1)(n_1^2-n_2^2)\sin 2\gamma_1$$

Turning points occur when

$$\frac{\partial\{(1+R)/T\}}{\partial\lambda} = 0$$

i.e. when

$$\sin 2\gamma_1 = 0$$

Now $\gamma_1 = 2\pi n_1 d_1/\lambda$, hence turning points occur when

$$4\pi n_1 d_1/\lambda = m\pi, \text{ m an integer}$$

i.e. $$d_1 = \frac{m\lambda_{T.P.}}{4n_1} \qquad 3.7.1$$

Let m correspond to the turning point at wavelength λ_1, then (m+1) corresponds to the consecutive turning point at wavelength λ_2.

Hence

$$d_1 = \frac{m\lambda_1}{4n_1} = \frac{(m+1)\lambda_2}{4n_1} \qquad 3.7.2$$

Therefore

$$m\lambda_1 = (m+1)\lambda_2$$

$$m = \frac{\lambda_2}{\lambda_1-\lambda_2} \qquad 3.7.3$$

Substituting in equation 3.7.2

$$d_1 = \frac{\lambda_1\lambda_2}{4n_1(\lambda_1-\lambda_2)} \qquad 3.7.4$$

where λ_1 and λ_2 are the wavelengths of consecutive turning points in the infra-red, and n_1 is the long-wavelength refractive index.

3. 9 DETERMINATION OF THE OPTICAL CONSTANTS FROM THE MEASURED TRANSMITTANCE AND REFLECTANCE FROM THE BACK SURFACE.

An alternative method of determining the optical constants of a thin film deposited on a transparent substrate is from the transmittance and reflectance from the back surface where the incident beam passes through the substrate and is reflected by the film.

The reflectance from the back surface is given by (Heavens, loc. cit.):

$$R^1 = \frac{(g_2^2+h_2^2)\exp(2\alpha_1) + (g_1^2+h_1^2)\exp(-2\alpha_1) + A\cos 2\gamma_1 - B\sin 2\gamma_1}{\exp(2\alpha_1) + (g_1^2+h_1^2)(g_2^2+h_2^2)\exp(-2\alpha_1) + C\cos 2\gamma_1 + D\sin 2\gamma_1} \quad \dagger$$

where the symbols have the same meaning as in section 3.2.1. Following the method of Tomlin (loc. cit.), much simpler equations can be derived by considering the expressions $(1\pm R^1)/T$.

---

† There is an incorrect sign in the numerator of the formula given by Heavens.

$$\frac{1\pm R^1}{T} = \left(\frac{n_0}{n_2}\right)\left[\{1 \pm (g_2^2+h_2^2)\}\{\exp(2\alpha_1) \pm (g_1^2+h_1^2)\exp(-2\alpha_1)\} + (C\pm A)\cos 2\gamma_1 + (D\pm B)\sin 2\gamma_1\right] \Big/ \{(1+g_1)^2 + h_1^2\}\{(1+g_2)^2 + h_2^2\}$$

$$C \pm A = 4g_1g_2 \quad \text{or} \quad -4h_1h_2$$

$$D \pm B = 4g_1h_2 \quad \text{or} \quad 4g_2h_1$$

$$(1+g_1)^2 + h_1^2 = \frac{4n_0^2}{(n_0+n_1)^2 + k_1^2}$$

$$(1+g_2)^2 + h_2^2 = \frac{4(n_1^2+n_1n_2+k_1^2)^2 + 4n_2^2k_1^2}{\{(n_1+n_2)^2 + k_1^2\}^2}$$

$$g_1^2+h_1^2 = \frac{(n_0-n_1)^2 + k_1^2}{\{(n_0+n_1)^2 + k_1^2\}}$$

$$1\pm(g_2^2+h_2^2) = \frac{2(n_1^2+n_2^2+k_1^2)}{(n_1+n_2)^2 + k_1^2} \quad \text{or} \quad \frac{4n_1n_2}{(n_1+n_2)^2 + k_1^2}$$

$$\exp(2\alpha_1) \pm (g_1^2+h_1^2)\exp(-2\alpha_1) = \frac{\{(n_0+n_1)^2 + k_1^2\}\exp(2\alpha_1) \pm \{(n_0-n_1)^2 + k_1^2\}\exp(2\alpha_1)}{(n_0+n_1)^2 + k_1^2}$$

Substituting the above in the equations for $(1\pm R^1)/T$ and simplifying we obtain

$$\frac{1+R^1}{T} = \frac{1}{4n_0n_2(n_1^2+k_1^2)}\Big[(n_1^2+n_2^2+k_1^2)\{(n_0^2+n_1^2+k_1^2)\cosh 2\alpha_1 + 2n_0n_1\sinh 2\alpha_1\} + (n_1^2-n_2^2+k_1^2)\{(n_0^2-n_1^2-k_1^2)\cos 2\gamma_1 + 2n_0k_1\sin 2\gamma_1\}\Big] \qquad 3.8.1$$

$$\frac{1-R^1}{T} = \frac{1}{2n_0(n_1^2+k_1^2)} \left[n_1\{(n_0^2+n_1^2+k_1^2)\sinh 2\alpha_1 + 2n_0n_1\cosh 2\alpha_1\} \right.$$
$$\left. + k_1\{(n_1^2-n_0^2+k_1^2)\sin 2\gamma_1 + 2n_0k_1\cos 2\gamma_1\} \right] \qquad 3.8.2$$

For the wedge-shaped substrates used:

$$\frac{1+R^1}{\Gamma} = \frac{1}{(n_1^2+k_1^2)(n_2+n_0)^2} \left[(n_1^2+n_2^2+k_1^2)\{(n_0^2+n_1^2+k_1^2)\cosh 2\alpha_1 \right.$$
$$+ 2n_0n_1\sinh 2\alpha_1\}$$
$$\left. + (n_1^2-n_2^2+k_1^2)\{(n_0^2-n_1^2-k_1^2)\cos 2\gamma_1 + 2n_0k_1\sin 2\gamma_1\} \right] \qquad 3.8.3$$

$$\frac{1-R^1}{\Gamma} = \frac{2n_2}{(n_1^2+k_1^2)(n_2+n_0)^2} \left[n_1\{(n_0^2+n_1^2+k_1^2)\sinh 2\alpha_1 \right.$$
$$+ 2n_0n_1\cosh 2\alpha_1\}$$
$$\left. + k_1\{(n_1^2-n_0^2+k_1^2)\sin 2\gamma_1 + 2n_0k_1\cos 2\gamma_1\} \right] \qquad 3.8.4$$

The method of solving equations 3.8.3 and 3.8.4 is identical to that employed for solving equations 3.4.3 and 3.4.4. The multiple solutions that occur are slightly different in magnitude to those obtained from equations 3.4.3 and 3.4.4, with the exception of the correct solutions which are identical. The effects of film thickness are identical to those discussed in section 3.7.

3.10 ALTERNATIVE DERIVATION OF THE EQUATIONS FOR $(1\pm R)/T$ AND $(1\pm R^1)/T$.

A simpler derivation of the equations $(1\pm R)/T$ and $(1\pm R^1)/T$ can be achieved by considering the formulae for R, R^1 and T given by

Abeles (1963) which are written in a different form to those given by Heavens (loc. cit.). This derivation is given in Appendix B. We have retained the nomenclature of Heavens in this chapter for consistency with the two-layer equations considered in the next chapter.

CHAPTER 4.

SURFACE LAYERS ON THIN FILMS

4. 1 INTRODUCTION.

Although accurate measurements were taken of the thicknesses of the selenium films, it was found that the measured value used in the calculation of n and k, corresponded to the situation of too large a film thickness being used. This behaviour was also apparent with the germanium films which were deposited on hot substrates.

Electron microscope examinations of the surface of vitreous selenium films (Campbell, 1968) did not indicate any definite surface roughness which would cause some scattering of the incident beam. However macroscopic undulations did exist which would mean that the beam transmitted through the film traversed different thicknesses of the film.

In the present investigation of germanium films, such undulations were reduced considerably due to the use of a rotating substrate during the evaporation of the films. Thus the non-uniformity of the films did not appear to explain the necessity to reduce the measured film thickness.

Campbell has also suggested that overcoating layers may give a measured thickness value less than the geometrical height of the step in the film due to the tendency of the overcoating material to migrate towards the uncoated portion of the substrate. Thus the presence of the overcoating silver layer in the measurement of the film thickness is unlikely to result in an overestimate of its thickness.

The second problem encountered was the non-closure of the refractive index curve over parts of the wavelength range. By closure is meant the removal of the island or valley type appearances of the calculated solutions as was discussed in the previous chapter, and the production of a smooth single-valued dispersion curve. This is demonstrated in Figure 4.1 where the refractive index is plotted for a selenium film, and a germanium film deposited on a 350°C substrate. When the film thickness was adjusted to give the correct behaviour in the long wavelength region, then the short wavelength region behaviour corresponded to that of too small a value of film thickness. Likewise when the thickness was increased such that correct behaviour was obtained in the short wavelength region, the long wavelength region exhibited the behaviour of too large a value of thickness. No film thickness existed which would close the curve over the entire wavelength range.

Both of these problems were solved by considering the existence of a thin oxide layer, or some other layer, on the surface of the film. Potter (1964) in his calculations of the optical constants of germanium corrected for an oxide layer 50Å thick. Dash (1954) has shown that at least a monolayer and probably more is formed very quickly on an amorphous or crystalline film of germanium. Recent work by a number of authors in surface state science support the findings of Dash (see for example, Henzler, 1971). Thus evidence exists which indicates that such oxide layers do exist for germanium. A search of the literature did not reveal any work on whether oxide layers also formed on selenium. However, postulating the existence

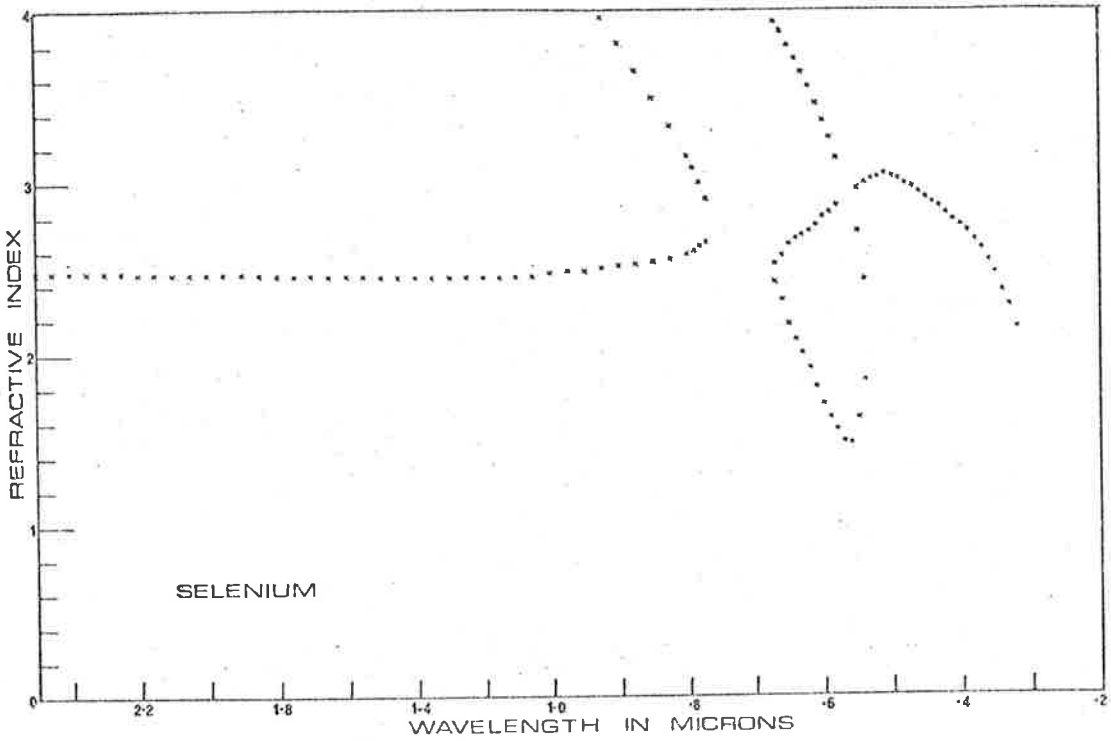
REFRACTIVE INDEX
SELENIUM
WAVELENGTH IN MICRONS

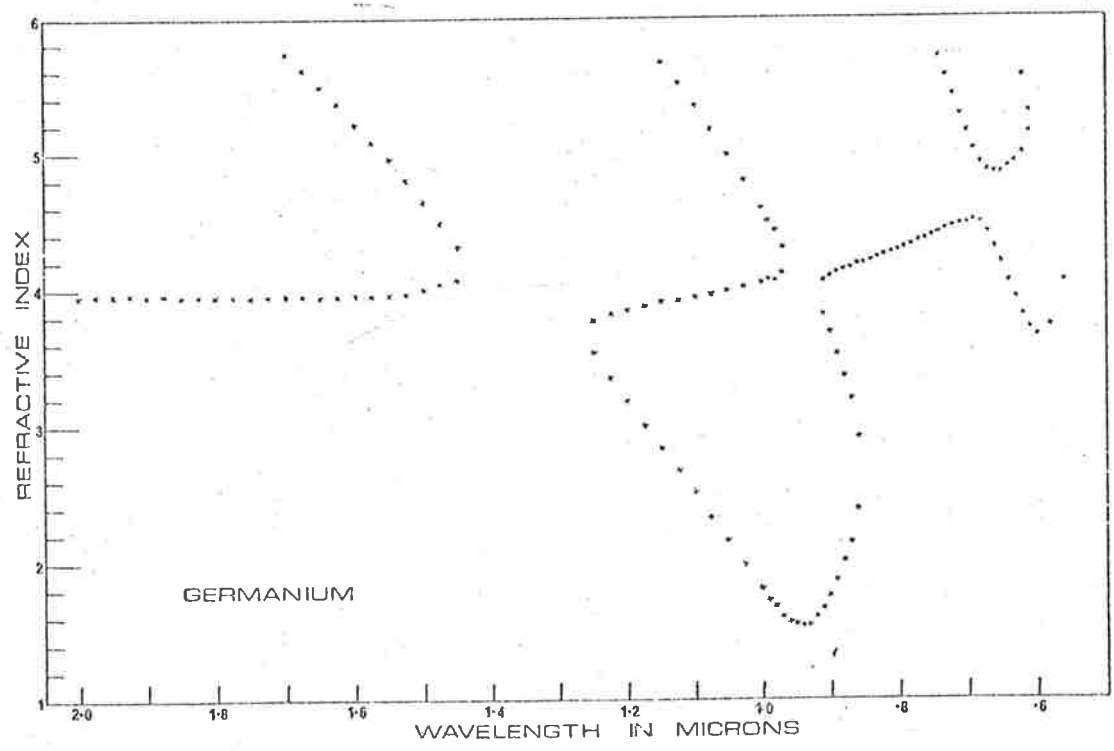
REFRACTIVE INDEX
GERMANIUM
WAVELENGTH IN MICRONS

Figure 4.1

of such a layer solved both problems mentioned above and is good evidence that selenium oxide, or a compound of selenium with a similar refractive index, does form on the surface of selenium films.

Papazian (1956) has found that the oxide formed on germanium is usually hexagonal GeO_2 which he found had a strong absorption band at 2450Å. Garino - Canina (1958, 1959) and Cohen and Smith (1958) found similar results. Thus in the wavelength range of the present measurements, the germanium oxide layer is non-absorbing.

The oxide of selenium was also assumed to be transparent over the wavelength range of measurements. A literature survey did not reveal any previous optical absorption measurements on this compound. The error introduced by possible absorption in the oxide layer not being accounted for would be very small since this layer is very thin.

Thus the problem reduced to considering the system: transparent-film - absorbing film - transparent substrate. Although we are concerned primarily with germanium and selenium and their corresponding oxides, the analyses presented in this chapter are applicable to any such system. The system: absorbing film - transparent film -- transparent substrate is also considered (for reasons discussed in section 4.11) and it will be shown that the two systems may be readily differentiated. We then proceed to solve the two-layer system where the refractive index of the transparent layer is known. Provided the system is thick enough to exhibit at least one turning point in the reflectance and transmittance curves, it is shown how the optical constants of the absorbing film together with the thicknesses of both the absorbing and transparent layers may be accurately

determined from the measurement of the reflectance and transmittance of the system.

4. 2 REFLECTANCE AND TRANSMITTANCE EQUATIONS FOR A TWO - LAYER FILM.

Consider the system shown in Figure 4.2 where

n_0 is the refractive index of air.

$n_1 - ik_1$ is the complex refractive index of the first layer of thickness d_1.

$n_2 - ik_2$ is the complex refractive index of the second layer of thickness d_2.

$n_3 - ik_3$ is the complex refractive index of the substrate.

From Heavens (1955):

$$g_1 = \frac{n_0^2 - n_1^2 - k_1^2}{(n_0+n_1)^2 + k_1^2} \qquad h_1 = \frac{2n_0k_1}{(n_0+n_1)^2 + k_1^2}$$

$$g_2 = \frac{n_1^2 - n_2^2 + k_1^2 - k_2^2}{(n_1+n_2)^2 + (k_1+k_2)^2} \qquad h_2 = \frac{2(n_1k_2 - n_2k_1)}{(n_1+n_2)^2 + (k_1+k_2)^2}$$

$$p_2 = e^{\alpha_1}\cos\gamma_1 \qquad q_2 = e^{\alpha_1}\sin\gamma_1$$

$$t_2 = e^{-\alpha_1}(g_2\cos\gamma_1 + h_2\sin\gamma_1) \qquad u_2 = e^{-\alpha_1}(h_2\cos\gamma_1 - g_2\sin\gamma_1)$$

$$\alpha_1 = 2\pi k_1 d_1/\lambda \qquad \gamma_1 = 2\pi n_1 d_1/\lambda$$

$$p_{12} = p_2 + g_1t_2 - h_1u_2 \qquad q_{12} = q_2 + h_1t_2 + g_1u_2$$

$$t_{12} = t_2 + g_1p_2 - h_1q_2 \qquad u_{12} = u_2 + h_1p_2 + g_1q_2$$

$$g_3 = \frac{n_2^2 - n_3^2 + k_2^2 - k_3^2}{(n_2+n_3)^2 + (k_2+k_3)^2} \qquad h_3 = \frac{2(n_2k_3 - n_3k_2)}{(n_2+n_3)^2 + (k_2+k_3)^2}$$

$$\alpha_2 = 2\pi k_2 d_2/\lambda \qquad \gamma_2 = 2\pi n_2 d_2/\lambda$$

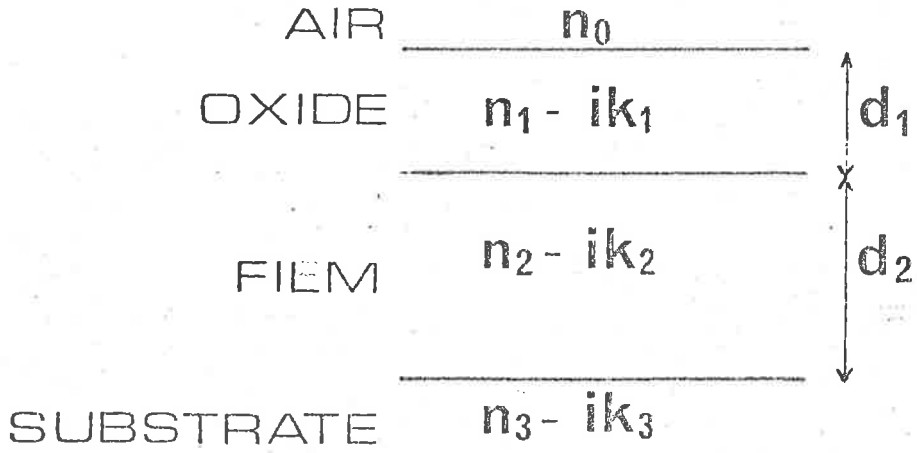

TWO-LAYER SYSTEM

Figure 4.2

$$p_3 = e^{\alpha_2}\cos\gamma_2 \qquad q_3 = e^{\alpha_2}\sin\gamma_2$$

$$t_3 = e^{-\alpha_2}(g_3\cos\gamma_2 + h_3\sin\gamma_2) \qquad u_3 = e^{-\alpha_2}(h_3\cos\gamma_2 - g_3\sin\gamma_2)$$

$$r_2 = e^{\alpha_1}(g_2\cos\gamma_1 - h_2\sin\gamma_1) \qquad s_2 = e^{\alpha_1}(h_2\cos\gamma_1 + g_2\sin\gamma_1)$$

$$v_2 = e^{-\alpha_1}\cos\gamma_1 \qquad w_2 = -e^{-\alpha_1}\sin\gamma_1$$

$$r_{12} = r_2 + g_1v_2 - h_1w_2 \qquad s_{12} = s_2 + h_1v_2 + g_1w_2$$

$$v_{12} = v_2 + g_1r_2 - h_1s_2 \qquad w_{12} = w_2 + h_1r_2 + g_1s_2$$

$$p_{13} = p_{12}p_3 - q_{12}q_3 + r_{12}t_3 - s_{12}u_3$$

$$q_{13} = q_{12}p_3 + p_{12}q_3 + s_{12}t_3 + r_{12}u_3$$

$$t_{13} = t_{12}p_3 - u_{12}q_3 + v_{12}t_3 - w_{12}u_3$$

$$u_{13} = u_{12}p_3 + t_{12}q_3 + w_{12}t_3 + v_{12}u_3$$

$$l_{13} = (1+g_1)(1+g_2)(1+g_3) - h_2h_3(1+g_1) - h_3h_1(1+g_2) - h_1h_2(1+g_3)$$

$$m_{13} = h_1(1+g_2)(1+g_3) + h_2(1+g_3)(1+g_1) + h_3(1+g_1)(1+g_2) - h_1h_2h_3$$

Then the reflectance and transmittance of the double-layer system are given by

$$R = \frac{t_{13}^2 + u_{13}^2}{p_{13}^2 + q_{13}^2} \qquad 4.2.1$$

$$T = \frac{n_3}{n_0}\,\frac{l_{13}^2 + m_{13}^2}{p_{13}^2 + q_{13}^2} \qquad 4.2.2$$

As in the single-layer case, if a wedge-shaped transparent substrate is used, the measured transmittance ratio, Γ, is related to T by

$$\Gamma = \frac{(n_3+n_0)^2}{4n_3n_0} \cdot T \qquad 4.2.3$$

4. 3 THE HYPOTHETICAL FILMS.

As in the discussion of the effects of film thickness in section 3.7, the two-layer system was best analysed by considering, first of all, hypothetical films. The transparent and absorbing films had the following properties:

Transparent film refractive index = 2.0

Absorbing film refractive index = 4.0

Absorbing film absorption index = $0.25/\lambda^3$ (λ in μ)

Transparent substrate refractive index = 1.45

The properties of the absorbing film approximate those of germanium and the refractive index of the transparent layer approximates that of germanium dioxide.

The two systems mentioned above are designated thus:

System 1 : Transparent film - absorbing film - transparent substrate

System 2 : Absorbing film - transparent film - transparent substrate

The reflectances and transmittances of both systems for various transparent and absorbing film thicknesses were calculated from equations 4.2.1 and 4.2.2. The reflectance and transmittance curves so obtained are shown in Figure 4.3 for System 1 and Figure 4.4 for System 2. It can be seen that the transparent layer has the greater influence in System 1 where the most significant differences occur in the short wavelength region of the reflectance curves, particularly with the thicker absorbing films, and become more pronounced as the transparent layer thickness is increased. The transparent layer has a lesser influence on System 2, particularly in the short wavelength region.

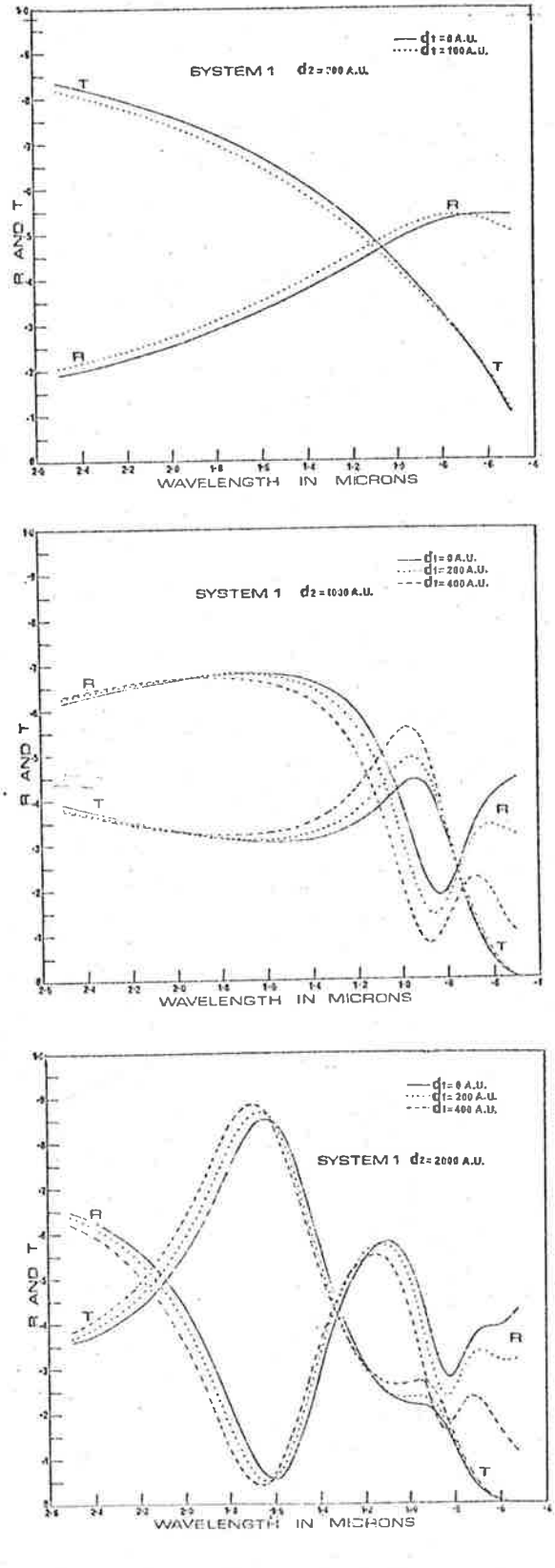
SYSTEM 1
R AND T
WAVELENGTH IN MICRONS
SYSTEM 1
R AND T
WAVELENGTH IN MICRONS
SYSTEM 1
R AND T
WAVELENGTH IN MICRONS

Figure 4.3

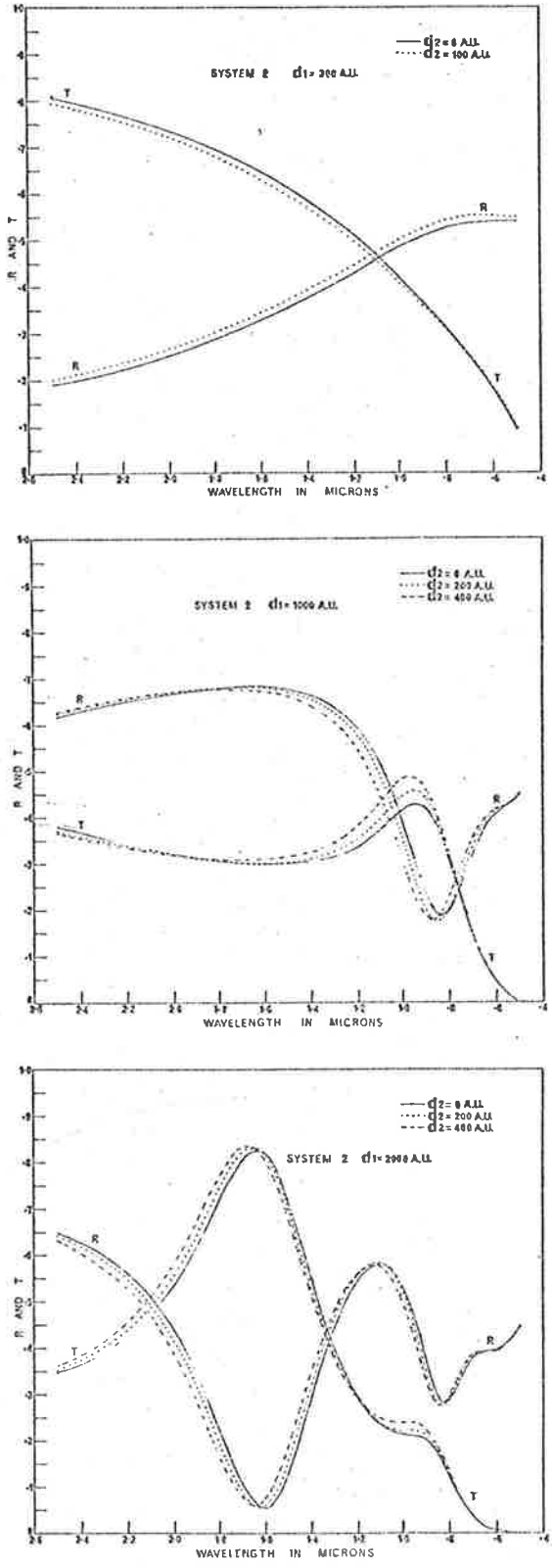
SYSTEM 2
WAVELENGTH IN MICRONS
R AND T
SYSTEM 2
WAVELENGTH IN MICRONS
R AND T
SYSTEM 2
WAVELENGTH IN MICRONS
R AND T

Figure 4.4

4. 4 EFFECT OF USING THE SINGLE - LAYER EQUATIONS.

4. 4. 1 SYSTEM 1.

Consider a hypothetical film with absorbing layer thickness 2000Å and transparent layer thickness 50Å. If the single-layer equations are now used to determine the refractive index and absorption index for the above film assuming a thickness of 2050Å, which would be the value obtained if the thickness was measured directly, the solutions for the refractive index so obtained are shown in Figure 4.5.a. One can see that this is the behaviour exhibited when too large a film thickness is used in the calculation. When the film thickness is reduced to 2015Å, the refractive index curve shown in Figure 4.5.b is obtained. With the exception of the short wavelength region, where there is a fall in the refractive index, the values obtained are negligibly different from the exact value of 4.0.

Thus a transparent oxide layer will explain the need to reduce the measured film thickness in order to obtain the correct behaviour.

Consider now the case where the absorbing film thickness is 2000Å but the transparent layer is 200Å thick. Figure 4.6.a shows the calculated refractive index solutions when a thickness of 2200Å is used in the single-layer equations. When the thickness is reduced to 2050Å the curve shown in Figure 4.6.b is obtained. The curve is closed in the long wavelength region, but not in the short wavelength region, and no adjustment of the film thickness will give a curve which is closed over the entire wavelength range. In the figure shown, the short wavelength region has the appearance of too small a value for the film thickness. If the thickness is increased so that

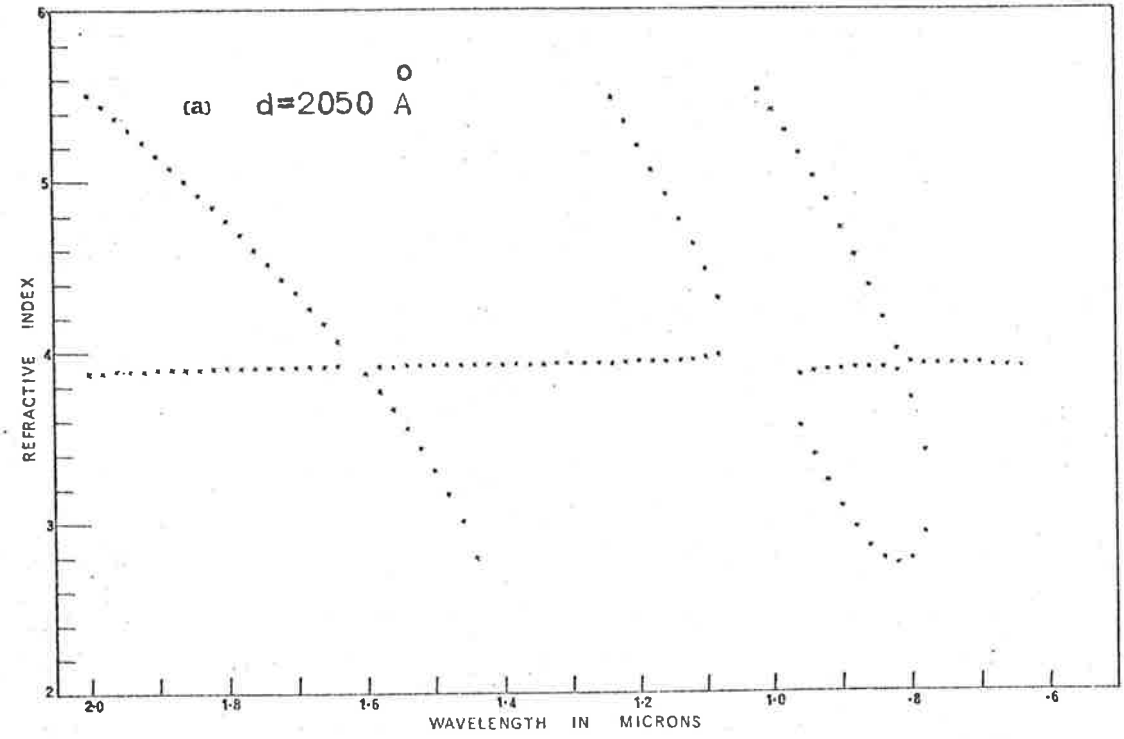
(a) d=2050 Å
REFRACTIVE INDEX
6
5
4
3
2
2·0
1·8
1·6
1·4
1·2
1·0
·8
·6
WAVELENGTH IN MICRONS

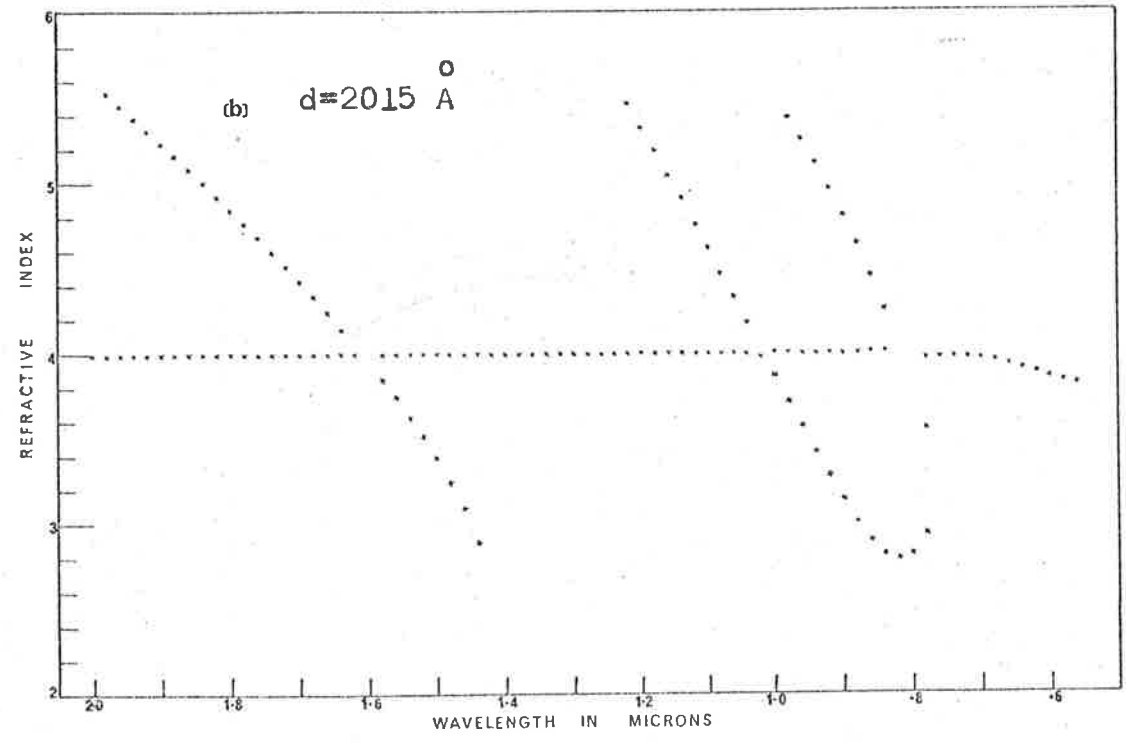
(b) d=2015 Å
REFRACTIVE INDEX
6
5
4
3
2
2·0
1·8
1·6
1·4
1·2
1·0
·8
·6
WAVELENGTH IN MICRONS

Figure 4.5

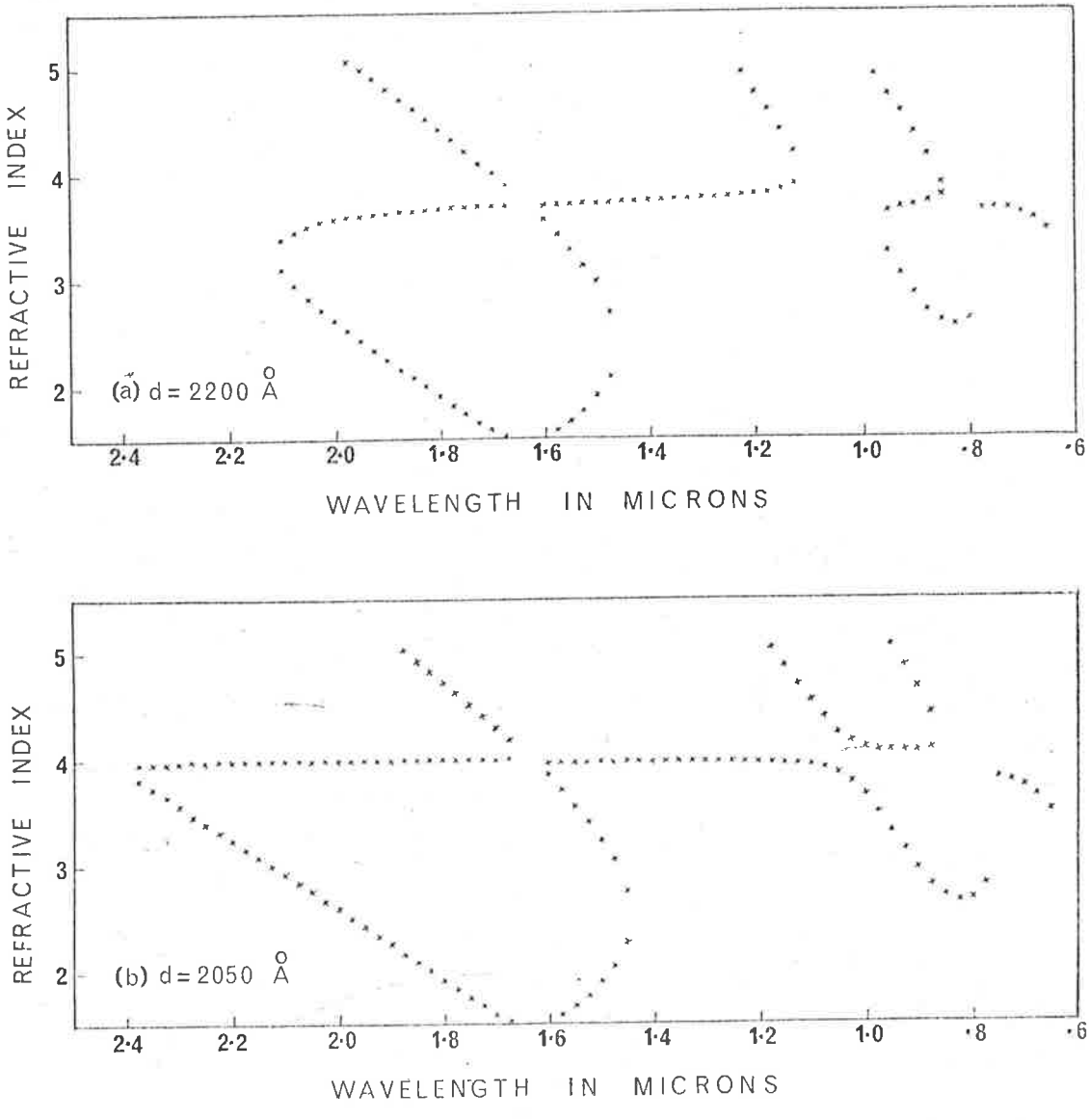

Effect of using the single-layer equations for a 2000 A.U. film with an oxide layer 200 A.U. thick.

Figure 4.6

closure occurs in the short wavelength region then the long wavelength region has the appearance of too large a film thickness.

The effect of a transparent oxide layer on a hypothetical film with optical constants approximating those of selenium showed identical behaviour, except that the effects were more pronounced. This is due to the refractive index of selenium oxide (1.76) being comparable to that of selenium (2.45) whereas the refractive index of germanium oxide is 2.0 while that of germanium is 4.0.

Thus the presence of a transparent oxide layer on the surface of the film will produce both the problems discussed in section 4.1.

4. 4. 2 SYSTEM 2.

For the case where the absorbing layer is 2000Å thick and the transparent layer 50Å thick, the effect of using the single-layer equations assuming a thickness of 2050Å is similar to that for System 1. That is the refractive index solutions have the appearance of too large a value of film thickness being used in the calculations. If the thickness is reduced to 2015Å then, as with System 1, the solutions are negligibly different from the value 4.0, except in the short wavelength region where there is a slight rise in the refractive index (compared to a fall in System 1).

For the case where the thickness of the absorbing layer is 2000Å but that of the transparent layer is 200Å, the film thickness again appears too large if the single-layer equations are used assuming a thickness of 2200Å, (Figure 4.7.a). If the thickness is reduced to 2050Å, the refractive index solutions shown in Figure 4.7.b are

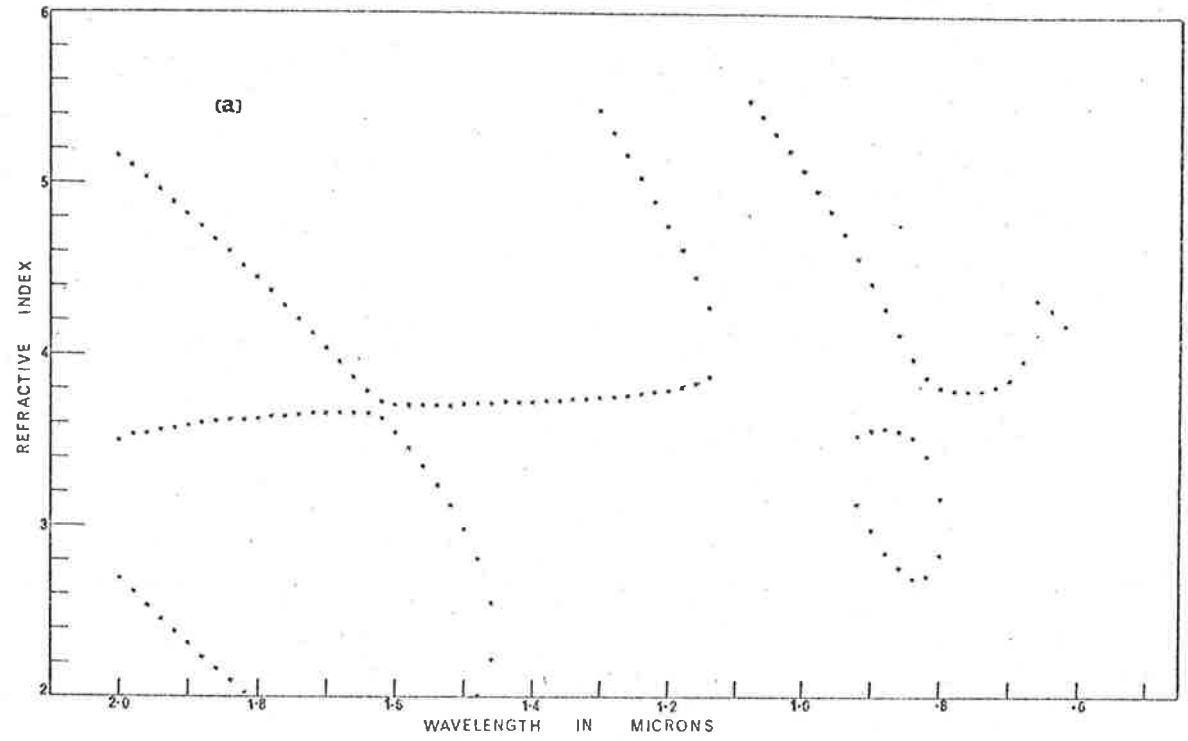
(a)
REFRACTIVE INDEX
6
5
4
3
2
2·0
1·8
1·5
1·4
1·2
1·0
·8
·6
WAVELENGTH IN MICRONS

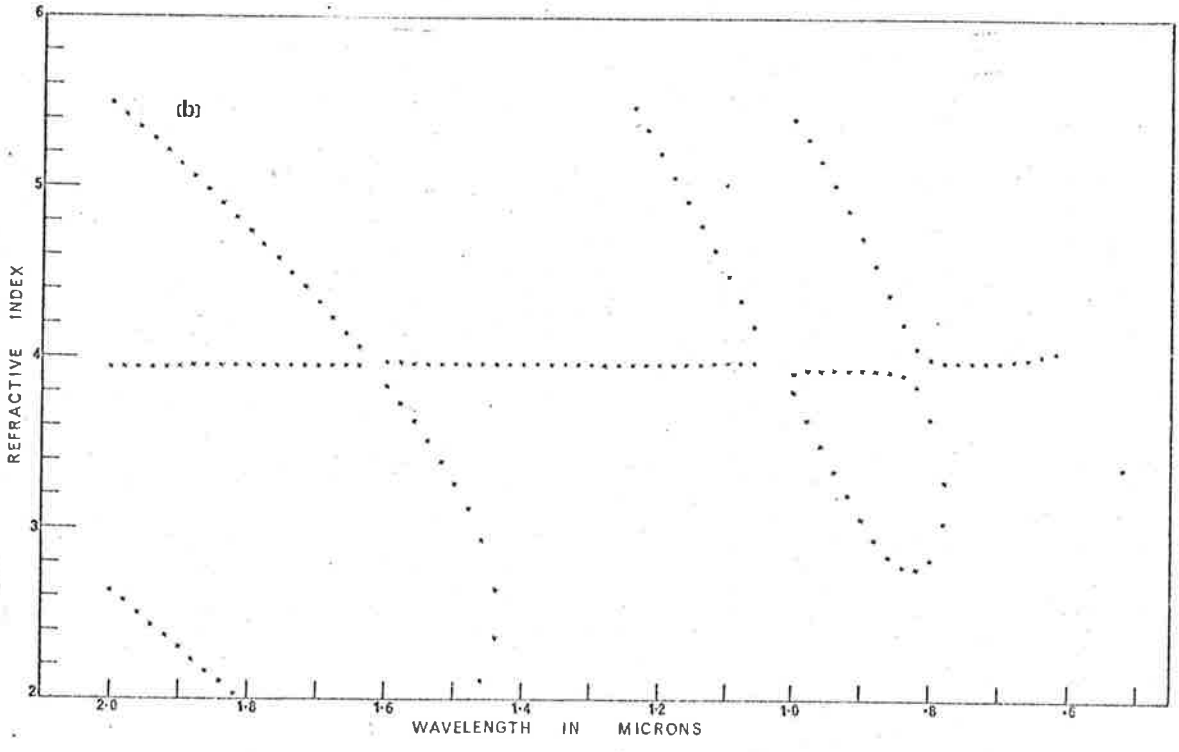
(b)
REFRACTIVE INDEX
6
5
4
3
2
2·0
1·8
1·6
1·4
1·2
1·0
·8
·6
WAVELENGTH IN MICRONS

Figure 4.7

obtained. The curve is closed in the long wavelength region while the short wavelength region has the island type appearance characteristic of using too large a value of film thickness. If the thickness is reduced to give closure in the short wavelength region, the long wavelength region has the appearance of too small a value of film thickness being used in the calculations.

That is, the behaviour is just the opposite to that for System 1. Thus, for moderate transparent layer thicknesses it is possible to distinguish between the two systems.

System 1 characterised the behaviour observed for the selenium and germanium films. For very thin oxide layers, the results obtained using the single-layer equations are negligibly different from the correct values of the absorbing film, provided the total film thickness is reduced in order to obtain a closed refractive index curve. For moderate oxide thicknesses the use of the single-layer equations no longer produces accurate results. It was therefore necessary to attempt to solve the two-layer equations.

4. 5 SOLVING THE TWO - LAYER EQUATIONS.

Equations 4.2.1 and 4.2.2 can be solved for the refractive index of the absorbing film, the absorption index of the absorbing film and the transparent and absorbing film thicknesses, from the measured values of R and T and given the refractive indices of the transparent layer and substrate.

Consider System 1 where n_1 is the refractive index of the transparent layer of thickness d_1, n_2 and k_2 are the refractive and

absorption indices of the absorbing film of thickness d_2.

From equations 4.2.1 and 4.2.2

$$\frac{1+R}{T} = \frac{n_0}{n_3}\frac{(p_{13}^2 + q_{13}^2 + t_{13}^2 + u_{13}^2)}{(l_{13}^2 + m_{13}^2)} \qquad 4.2.3$$

$$\frac{1-R}{T} = \frac{n_0}{n_3}\frac{(p_{13}^2 + q_{13}^2 - t_{13}^2 - u_{13}^2)}{(l_{13}^2 + m_{13}^2)} \qquad 4.2.4$$

As with the single-layer equations, these two functions are single-valued in k_2 given the other parameters. If we define the following functions:

$$F_1(n_2,k_2) = n_0(p_{13}^2+q_{13}^2+t_{13}^2+u_{13}^2) - n_3(l_{13}^2+m_{13}^2)\{(1+R)/T\}$$

$$F_2(n_2,k_2) = n_0(p_{13}^2+q_{13}^2-t_{13}^2-u_{13}^2) - n_3(l_{13}^2+m_{13}^2)\{(1-R)/T\}$$

then the solutions are those n_2 and k_2 which satisfy

$$F_1(n_2,k_2) = F_2(n_2,k_2) = 0$$

simultaneously, given the other parameters.

$F_2(n_2,k_2)$ is no longer readily differentiable with respect to k_2 as was the corresponding function in the single-layer case. For a given n_2 there is only one k_2 which satisfies $F_2(n_2,k_2) = 0$. Consequentially for a given n_2, k_2 which satisfies $F_2(n_2,k_2) = 0$ was found by allowing k_2 to start from some preset value and incrementing it until a change of sign occurred in $F_2(n_2,k_2)$. An iterative interpolation was then used to find the intersection point.

The set value of n_2 and calculated k_2 were then substituted into the equation $F_1(n_2,k_2)$. n_2 was then incremented and the process repeated until a change of sign occurred in $F_1(n_2,k_2)$, and again an

iterative interpolation was used to determine the intersection point. Further increments were added to n_2, until some upper limit was reached, to determine all the possible solutions.

The above method was used to calculate n_2 and k_2 for the hypothetical film with transparent and absorbing layer thicknesses of 400Å and 2000Å respectively. The results for n_2 are shown in Figure 4.8. At each wavelength the correct solution (4.0) was found, and again multiple solutions occurred as with the single-layer film. It was also found that only the correct values of the two film thicknesses would result in closure of the refractive index curve over the entire wavelength range.

For System 2, where n_1 and k_1 are the refractive and absorption indices of the absorbing film of thickness d_1 and n_2 is the refractive index of the transparent film of thickness d_2; given the other parameters, n_1 and k_1 may be found in exactly the same manner as was n_2 and k_2 for System 1. Again only the correct values of the two film thicknesses would result in complete closure of the refractive index curve.

4. 6 APPLICATION TO REAL FILMS.

In practice it is not possible to measure explicitly both the transparent and absorbing film thicknesses and one therefore has two equations, $(1\pm R)/T$, and three unknowns, the absorbing film refractive and absorption indices and either d_1 or d_2 (the total film thickness, d_1+d_2, may be measured explicitly). However the refractive index curve will not close unless accurate values of d_1 and d_2 are used, and

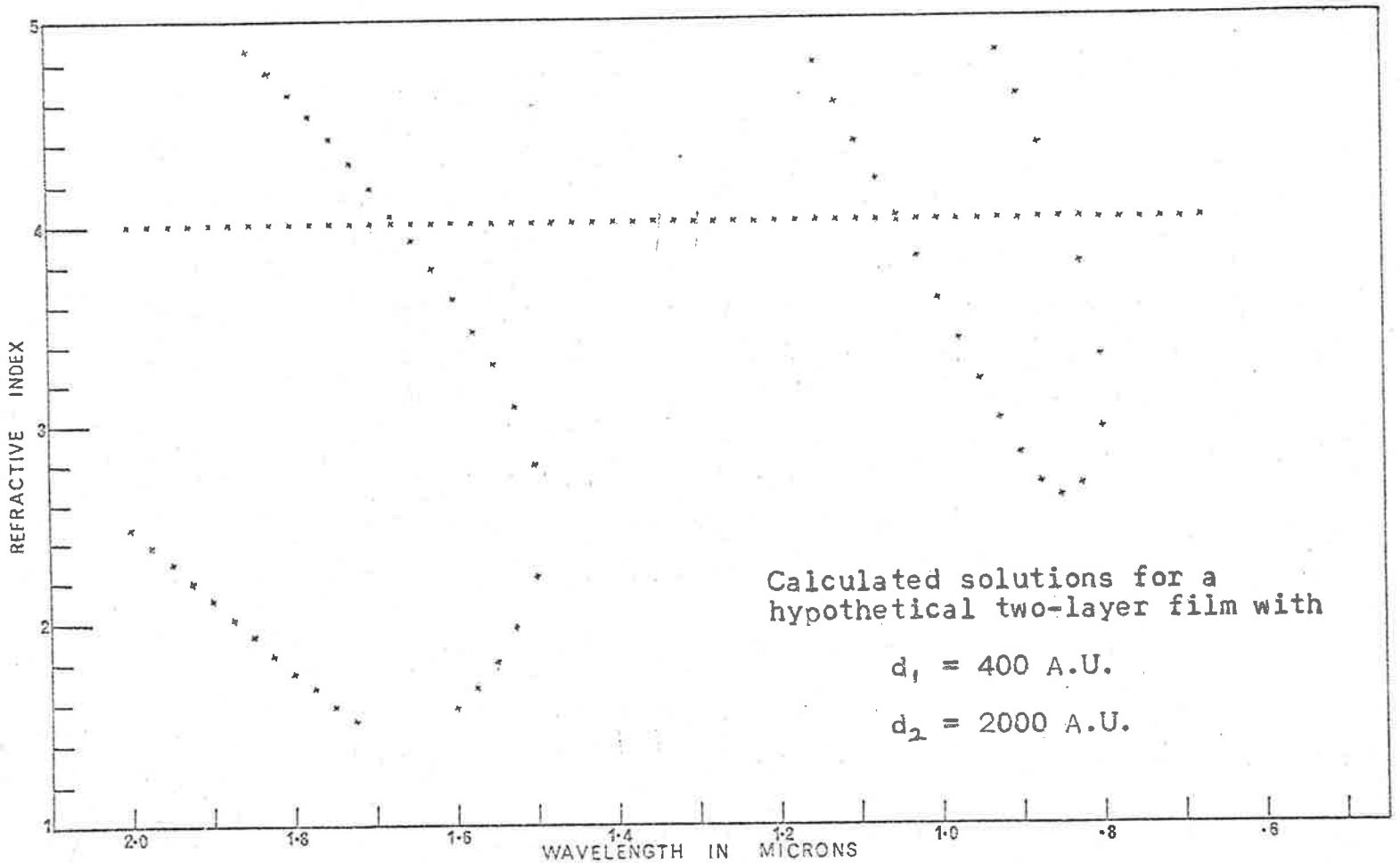
REFRACTIVE INDEX
5
4
3
2
1
2·0
1·8
1·6
1·4
1·2
1·0
·8
·6
WAVELENGTH IN MICRONS
Calculated solutions for a
hypothetical two-layer film with
d_1 = 400 A.U.
d_2 = 2000 A.U.

Figure 4.8

this fact may be used to determine both d_1 and d_2. If the total film thickness is known exactly, then d_1 and d_2 may be altered, such that d_1+d_2 remains constant, until closure occurs, thus giving the optical constants of the absorbing film together with the transparent film thickness and absorbing film thickness.

It is not even necessary to know d_1+d_2 exactly. An approximate value for d_1 and d_2 may be estimated from the solutions obtained from the single-layer equations. That thickness which gives closure in the long wavelength region is slightly greater than the absorbing film thickness, and the extent of the non-closure gives a good indication of the transparent layer thickness. These values may then be substituted in the two-layer equations and adjusted within small limits until closure of the refractive index curve occurs. The method adopted here was to increase the transparent layer thickness to close up the short wavelength region, while at the same time reducing the absorbing layer thickness to retain closure in the long wavelength region. After some experience complete closure could be achieved in about four or five steps.

4. 6. 1 EXAMPLES FOR GERMANIUM AND SELENIUM.

As mentioned earlier, the behaviour of the germanium and selenium films were characterised by System 1. The refractive index curves for the selenium and germanium films discussed in section 4.1, obtained from the double layer equations (System 1) are shown in Figure 4.9. The values of absorbing film and oxide layer thicknesses required to give closure of the curves are shown on the figures

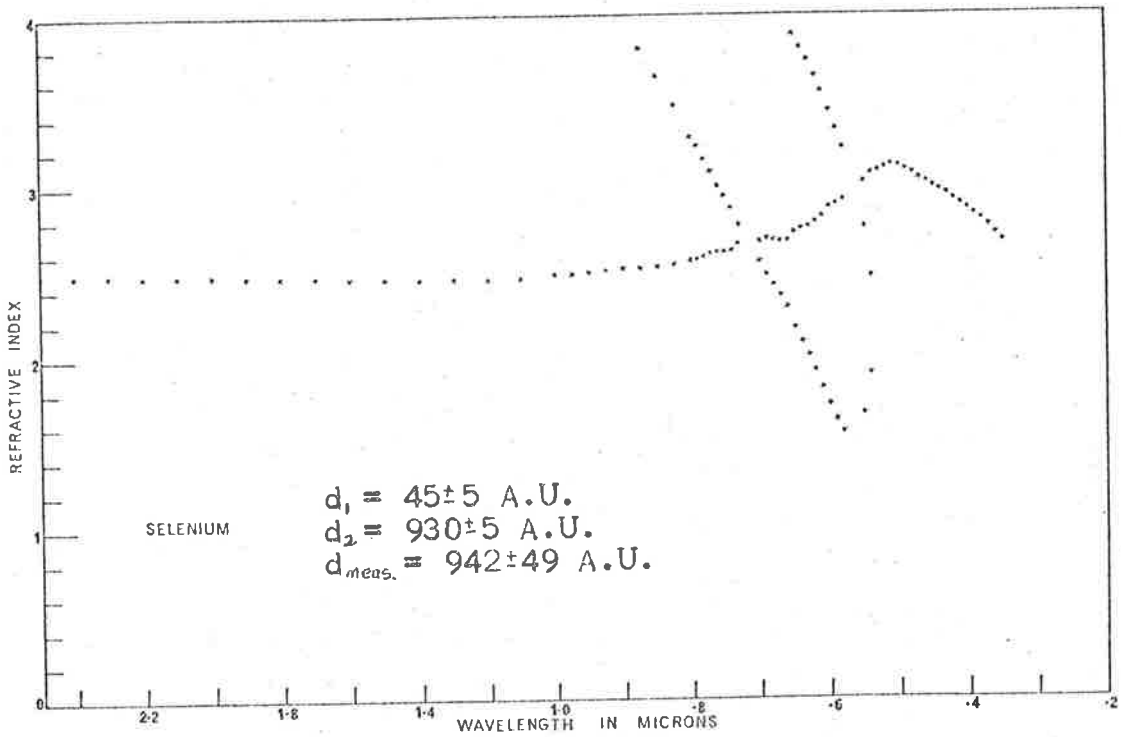
REFRACTIVE INDEX
SELENIUM
d_1 = 45±5 A.U.
d_2 = 930±5 A.U.
$d_{meas.}$ = 942±49 A.U.
WAVELENGTH IN MICRONS

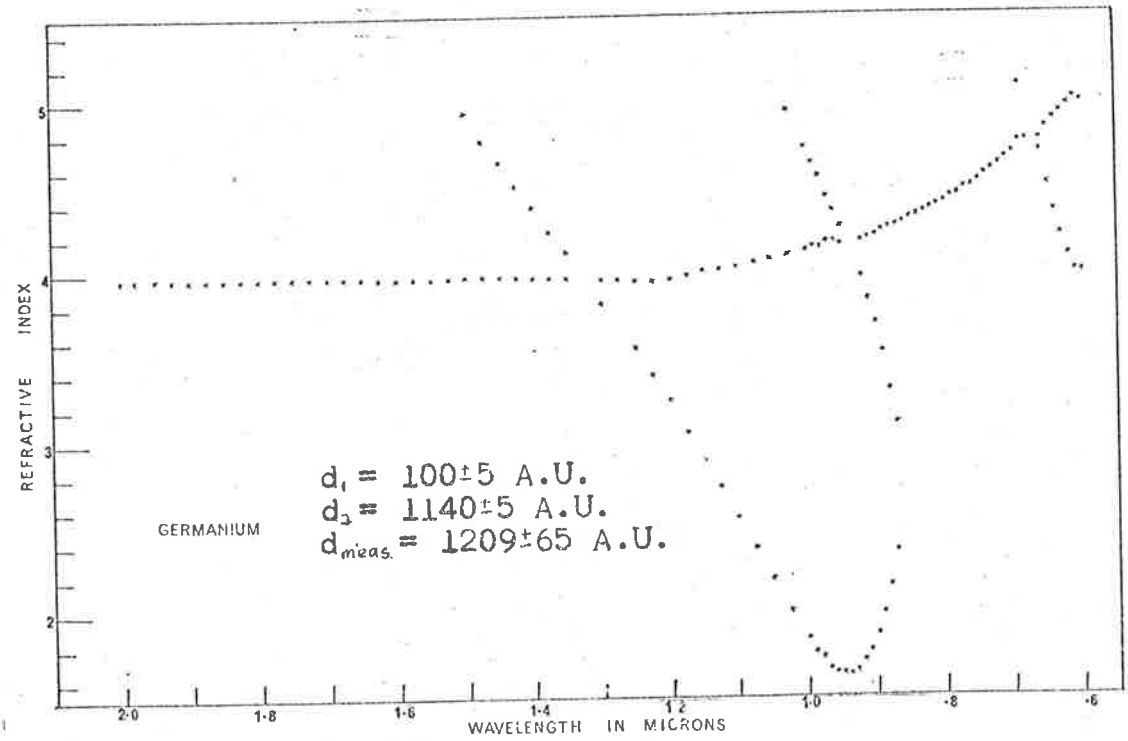
REFRACTIVE INDEX
GERMANIUM
d_1 = 100±5 A.U.
d_2 = 1140±5 A.U.
$d_{meas.}$ = 1209±65 A.U.
WAVELENGTH IN MICRONS

Figure 4.9

together with the measured total thicknesses.

It can be seen that the inclusion of an oxide layer enables closure to be achieved over the entire wavelength range. Also the calculated total film thicknesses are in agreement, within experimental error, with the measured values.

4. 6. 2 EFFECT OF ERRORS IN R AND T ON THE CALCULATED FILM AND SURFACE - LAYER THICKNESSES.

From our calculations on hypothetical films and germanium films, the closure of the refractive index curves appeared to be very sensitive functions of film and surface-layer thicknesses. As with the single-layer calculations in the previous chapter, it was necessary to determine the effects of errors in R and T on the calculated thicknesses.

This was again most suitably determined from the use of hypothetical films. The calculated reflectances and transmittances for films of varying thicknesses were altered in the four following ways:

(1)	R + 0.003	T + 0.003
(2)	R - 0.003	T - 0.003
(3)	R + 0.003	T - 0.003
(4)	R - 0.003	T + 0.003

Cases (1) and (2) did not affect the film or surface-layer thicknesses. For case (3) the film thickness had to be reduced by 0.5% while in case (4) it had to be increased by 0.5%, in both cases the surface layer thickness remaining unaltered.

4. 7 EXPLICIT EXPRESSIONS FOR (1±R)/T.

One drawback in solving the double-layer equations is the relatively large computing time required, being about twenty times that required for the single-layer equations. This increase in time is brought about largely by having to increment k, for a given n, until it satisfies $F_2(n,k) = 0$ instead of using Newton's method as in the single-layer case.

Following the success of explicit expressions for (1±R)/T for the single-layer film which afforded a large reduction in computing time, Tomlin (1971) has derived explicit expressions for (1±R)/T for two absorbing layers on an absorbing substrate. From Tomlin we have:

$$\frac{1 + R}{T} = \frac{(n_0^2+n_1^2+k_1^2)F_1 + (n_0^2-n_1^2-k_1^2)F_2}{16n_0n_3(n_1^2+k_1^2)(n_2^2+k_2^2)} \qquad 4.7.1$$

where

$$\begin{aligned} F_1 = {} & \{(n_1+n_2)^2 + (k_1+k_2)^2\}\{A\cosh 2(\alpha_1+\alpha_2) + B\sinh 2(\alpha_1+\alpha_2)\} \\ & + \{(n_1-n_2)^2 + (k_1-k_2)^2\}\{A\cosh 2(\alpha_1-\alpha_2) - B\sinh 2(\alpha_1-\alpha_2)\} \\ & + 2(n_1^2-n_2^2+k_1^2-k_2^2)\cosh 2\alpha_1(C\cos 2\gamma_2 + D\sin 2\gamma_2) \\ & + 4(n_1k_2-n_2k_1)\sinh 2\alpha_1(C\sin 2\gamma_2 - D\cos 2\gamma_2) \end{aligned}$$

$$\begin{aligned} F_2 = {} & \{(n_1+n_2)^2 + (k_1+k_2)^2\}\{C\cos 2(\gamma_1+\gamma_2) + D\sin 2(\gamma_1+\gamma_2)\} \\ & + \{(n_1-n_2)^2 + (k_1-k_2)^2\}\{C\cos 2(\gamma_1-\gamma_2) - D\sin 2(\gamma_1-\gamma_2)\} \\ & + 2(n_1^2-n_2^2+k_1^2-k_2^2)\cos 2\gamma_1(A\cosh 2\alpha_2 + B\sinh 2\alpha_2) \\ & + 4(n_1k_2-n_2k_1)\sin 2\gamma_1(A\sinh 2\alpha_2 + B\cosh 2\alpha_2) \end{aligned}$$

and

$$A = n_2^2 + n_3^2 + k_2^2 + k_3^2 \qquad B = 2(n_2n_3 + k_2k_3)$$

$$C = n_2^2 - n_3^2 + k_2^2 - k_3^2 \qquad D = 2(n_2k_3 - n_3k_2)$$

$$\frac{1-R}{T} = \frac{n_1G_1 + k_1G_2}{8n_3(n_1^2+k_1^2)(n_2^2+k_2^2)} \qquad 4.7.2$$

where

$$\begin{aligned} G_1 &= \{(n_1+n_2)^2 + (k_1+k_2)^2\}\{A\ \sinh 2(\alpha_1+\alpha_2) + B\ \cosh 2(\alpha_1+\alpha_2)\} \\ &+ \{(n_1-n_2)^2 + (k_1-k_2)^2\}\{A\ \sinh 2(\alpha_1-\alpha_2) - B\ \cosh 2(\alpha_1-\alpha_2)\} \\ &+ 2(n_1^2-n_2^2+k_1^2-k_2^2)\sinh 2\alpha_1(C\ \cos 2\gamma_2 + D\ \sin 2\gamma_2) \\ &+ 4(n_1k_2-n_2k_1)\cosh 2\alpha_1(C\ \sin 2\gamma_2 - D\ \cos 2\gamma_2) \end{aligned}$$

$$\begin{aligned} G_2 &= \{(n_1+n_2)^2 + (k_1+k_2)^2\}\{C\ \sin 2(\gamma_1+\gamma_2) - D\ \cos 2(\gamma_1+\gamma_2)\} \\ &+ \{(n_1-n_2)^2 + (k_1-k_2)^2\}\{C\ \sin 2(\gamma_1-\gamma_2) + D\ \cos 2(\gamma_1-\gamma_2)\} \\ &+ 2(n_1^2-n_2^2+k_1^2-k_2^2)\sin 2\gamma_1(A\ \cosh 2\alpha_2 + B\ \sinh 2\alpha_2) \\ &- 4(n_1k_2-n_2k_1)\cos 2\gamma_1(A\ \sinh 2\alpha_2 + B\ \cosh 2\alpha_2) \end{aligned}$$

The symbols have their meaning given in section 4.2.

4. 7. 1 EXACT EXPRESSIONS FOR THE CASE $k_1 = k_3 = 0$. SYSTEM 1.

For the case where the first layer and substrate are transparent, the following expressions can be derived from equations 4.7.1 and 4.7.2:

$$\frac{1+R}{T} = \frac{(n_0^2+n_1^2)F_{11} + (n_0^2-n_1^2)F_{21}}{16n_0n_3n_1^2(n_2^2+k_2^2)} \qquad 4.7.3$$

where

$$\begin{aligned} F_{11} &= 2(n_1^2+n_2^2+k_2^2)\{(n_2^2+n_3^2+k_2^2)\cosh 2\alpha_2 + 2n_2n_3\sinh 2\alpha_2\} \\ &+ 2(n_1^2-n_2^2-k_2^2)\{(n_2^2-n_3^2+k_2^2)\cos 2\gamma_2 - 2n_3k_2\sin 2\gamma_2\} \end{aligned}$$

$$\begin{aligned} F_{21} &= \{(n_1+n_2)^2 + k_2^2\}\{(n_2^2-n_3^2+k_2^2)\cos 2(\gamma_1+\gamma_2) - 2n_3k_2\sin 2(\gamma_1+\gamma_2)\} \\ &+ \{(n_1-n_2)^2 + k_2^2\}\{(n_2^2-n_3^2+k_2^2)\cos 2(\gamma_1-\gamma_2) + 2n_3k_2\sin 2(\gamma_1-\gamma_2)\} \end{aligned}$$

$$+ 2(n_1^2-n_2^2-k_2^2)\cos 2\gamma_1\{(n_2^2+n_3^2+k_2^2)\cosh 2\alpha_2 + 2n_2n_3\sinh 2\alpha_2\}$$
$$+ 4n_1k_2\sin 2\gamma_1\{(n_2^2+n_3^2+k_2^2)\sinh 2\alpha_2 + 2n_2n_3\cosh 2\alpha_2\}$$

$$\frac{1-R}{T} = \frac{1}{2n_3(n_2^2+k_2^2)}\Big[n_2\{(n_2^2+n_3^2+k_2^2)\sinh 2\alpha_2 + 2n_2n_3\cosh 2\alpha_2\} + k_2\{(n_2^2-n_3^2+k_2^2)\sin 2\gamma_2 + 2n_3k_2\cos 2\gamma_2\}\Big] \qquad 4.7.4$$

Equation 4.7.4 is identical to the equation for a single film on a transparent substrate, and is thus readily differentiated with respect to k_2. Consequentially the method for solving the two-layer equations, where the first layer is transparent and is of known refractive index, is identical to that employed for the single-layer equations. For a given n_2, k_2 may be solved by Newton's method from equation 4.7.4 instead of the incremental method discussed in section 4.5. This resulted in a reduction of computing time by a factor of ten.

4. 7. 2 EXACT EXPRESSIONS FOR THE CASE $k_2 = k_3 = 0$. SYSTEM 2.

From equations 4.7.1 and 4.7.2 for the case $k_2 = k_3 = 0$ we obtain:

$$\frac{1+R}{T} = \frac{(n_0^2+n_1^2+k_1^2)F_{12} + (n_0^2-n_1^2-k_1^2)F_{22}}{8n_0n_2^2n_3(n_1^2+k_1^2)} \qquad 4.7.5$$

where

$$F_{12} = (n_2^2+n_3^2)(n_1^2+n_2^2+k_1^2)\cosh 2\alpha_1 + 4n_2n_3\sinh 2\alpha_1$$
$$+ (n_2^2-n_3^2)\{(n_1^2-n_2^2+k_1^2)\cosh 2\alpha_1\cos 2\gamma_2 - 2n_2k_1\sinh 2\alpha_1\sin 2\gamma_2\}$$

$$F_{22} = (n_2^2-n_3^2)\{(n_1^2+n_2^2+k_1^2)\cos 2\gamma_1 \cos 2\gamma_2 - 2n_1n_2\sin 2\gamma_1 \sin 2\gamma_2\}$$
$$+ (n_2^2+n_3^2)(n_1^2-n_2^2+k_1^2)\cos 2\gamma_1 - 4n_2^2n_3k_1\sin 2\gamma_1$$

$$\frac{1-R}{T} = \frac{n_1G_{12} + k_1G_{22}}{4n_3n_2^2(n_1^2+k_1^2)} \qquad 4.7.6$$

where

$$G_{12} = (n_1^2+n_2^2+k_1^2)(n_2^2+n_3^2)\sinh 2\alpha_1 + 4n_1n_2^2n_3\cosh 2\alpha_1$$
$$+ (n_2^2-n_3^2)\{(n_1^2-n_2^2+k_1^2)\sinh 2\alpha_1 \cos 2\gamma_2 - 2n_2k_1\cosh 2\alpha_1 \sin 2\gamma_2\}$$

$$G_{22} = (n_2^2-n_3^2)\{(n_1^2+n_2^2+k_1^2)\sin 2\gamma_1 \cos 2\gamma_2 + 2n_1n_2\cos 2\gamma_1 \sin 2\gamma_2\}$$
$$+ (n_1^2-n_2^2+k_1^2)(n_2^2+n_3^2)\sin 2\gamma_1 + 4n_2^2n_3k_1\cos 2\gamma_1$$

Although not as simple as equation 4.7.4, equation 4.7.6 may again be readily differentiated with respect to k_1. Thus the method for solving the two-layer equations, where the second layer is transparent and is of known refractive index, is the same as for the previous case with a consequent reduction in computing time.

4. 7. 3 ERROR ANALYSIS FOR THE CASE $k_1 = k_3 = 0$. SYSTEM 1.

Since the two-layer equations (System 1) had to be employed for the selenium and germanium films, it was desirable to calculate the errors in the calculated refractive index and absorption index solutions due to errors in the other parameters. The method is identical to that employed for the single-layer equations. It was found that the error in the substrate refractive index contributed a negligible amount to the total error in the calculated solutions. Thus this variable was eliminated and was replaced by the oxide thickness. The errors in the absorbing film and oxide film thicknesses

were estimated from the accuracy with which the refractive index curve could be closed over the entire wavelength range. The error in the oxide layer refractive index was assumed to be zero. The partial derivatives for the two-layer equations (System 1) are given in Appendix C.

4. 8 USE OF THE SINGLE-LAYER EQUATIONS FOR A TWO-LAYER FILM.

In general there is no single-layer film equivalent to a two-layer film, even if both layers are transparent. However for the special case where one of the layers is very thin, as is generally the case for oxide layers, then in the transparent region it can be shown that the single-layer equations may be used provided the total film thickness is reduced.

We define a very thin film as one whose thickness is such that

$$\gamma < 0.1$$

The two-layer equations, for the case $k_1 = k_2 = k_3 = 0$, then become:

$$\frac{1 + R}{T} = \frac{F}{16 n_0 n_3 n_1^2 n_2^2} \qquad 4.8.1$$

where

$$F = (n_0^2+n_1^2)\{2(n_1^2+n_2^2)(n_2^2+n_3^2) + 2(n_1^2-n_2^2)(n_2^2-n_3^2)\cos 2\gamma_2\}$$
$$+ (n_0^2-n_1^2)\{(n_2^2-n_3^2)\{(n_1+n_2)^2\cos 2(\gamma_1+\gamma_2) + (n_1-n_2)^2\cos 2(\gamma_1-\gamma_2)\}$$
$$+ 2(n_1^2-n_2^2)(n_2^2+n_3^2)\cos 2\gamma_1\}$$

4. 8. 1 SYSTEM 1 : 1st. LAYER VERY THIN.

For a single film with refractive index n_2 and thickness d_2 on a substrate with refractive index n_3, then

$$\frac{1+R}{T} = \frac{1}{4n_0n_3n_2^2}\{(n_0^2+n_2^2)(n_2^2+n_3^2) + (n_0^2-n_2^2)(n_2^2-n_3^2)\cos 2\gamma_2\} \qquad 4.8.2$$

If γ_2 is increased to $\gamma_2 + \gamma_0$ with $\gamma_0 \ll 1$ then

$$\frac{1+R}{T} = \frac{1}{4n_0n_3n_2^2}\{(n_0^2+n_2^2)(n_2^2+n_3^2) + (n_0^2-n_2^2)(n_2^2-n_3^2)\cos 2(\gamma_2+\gamma_0)\}$$

$$\simeq \frac{1}{4n_0n_3n_2^2}\{(n_0^2+n_2^2)(n_2^2+n_3^2) + (n_0^2-n_2^2)(n_2^2-n_3^2)(\cos 2\gamma_2 - 2\gamma_0 \sin 2\gamma_2)\} \qquad 4.8.3$$

From equation 4.8.1 with $\gamma_1 \ll 1$ we have

$$F \simeq 2(n_0^2+n_1^2)\{(n_1^2+n_2^2)(n_2^2+n_3^2) + (n_1^2-n_2^2)(n_2^2-n_3^2)\cos 2\gamma_2\}$$
$$+ (n_0^2-n_1^2)\{(n_1+n_2)^2(n_2^2-n_3^2)(\cos 2\gamma_2 - 2\gamma_1 \sin 2\gamma_2)$$
$$+ (n_1-n_2)^2(n_2^2-n_3^2)(\cos 2\gamma_2 + 2\gamma_1 \sin 2\gamma_2)$$
$$+ 2(n_1^2-n_2^2)(n_2^2+n_3^2)\}$$

i.e.

$$F \simeq 4n_1^2(n_0^2+n_2^2)(n_2^2+n_3^2) + 4n_1^2(n_0^2-n_2^2)(n_2^2-n_3^2)\cos 2\gamma_2$$
$$- 4n_1n_2(n_0^2-n_1^2)(n_2^2-n_3^2)2\gamma_1 \sin 2\gamma_2$$

Hence

$$\frac{1+R}{T} \simeq \frac{1}{4n_0n_3n_2^2}\{(n_2^2+n_3^2)(n_0^2+n_2^2) + (n_0^2-n_2^2)(n_2^2-n_3^2)\cos 2\gamma_2$$
$$- 2\gamma_1 \frac{n_2}{n_1}(n_0^2-n_1^2)(n_2^2-n_3^2)\sin 2\gamma_2\} \qquad 4.8.4$$

Comparing equation 4.8.4 with equation 4.8.3, the condition for equivalence becomes

$$\frac{\gamma_0}{\gamma_1} = \frac{n_2}{n_1}\frac{(n_0^2-n_1^2)}{(n_0^2-n_2^2)}$$

i.e.

$$\frac{d_0}{d_1} = \frac{(n_0^2-n_1^2)}{(n_0^2-n_2^2)}$$

where d_0 is the equivalent thickness of the thin first layer (of refractive index n_1 and thickness d_1) if it is considered to have a refractive index n_2.

For example if $n_1 = 2.0$, $n_2 = 4.0$, $d_1 = 100\text{Å}$, $n_0 = 1$, then $d_0 = 20\text{Å}$. That is, the "measured" film thickness has to be reduced by 80Å. This supports the computations in section 4.4 where a reduction in total film thickness gave a closed refractive index curve in the infra-red.

4. 8. 2 SYSTEM 2 : VERY THIN SECOND LAYER.

For a single film of refractive index n_1 and thickness d_1 on a substrate with refractive index n_3.

$$\frac{1+R}{T} = \frac{1}{4n_0n_3n_1^2}\{(n_0^2+n_1^2)(n_1^2+n_3^2) + (n_0^2-n_1^2)(n_1^2-n_3^2)\cos 2\gamma_1\}$$

If γ_1 is increased to $\gamma_1 + \gamma_0$ with $\gamma_0 \ll 1$, then

$$\frac{1+R}{T} \simeq \frac{1}{4n_0n_3n_1^2}\{(n_0^2+n_1^2)(n_1^2+n_3^2) + (n_0^2-n_1^2)(n_1^2-n_3^2)(\cos 2\gamma_1 - 2\gamma_0 \sin 2\gamma_1)\}$$

4.8.5

From equation 4.8.1 with $\gamma_2 << 1$ we have

$$\frac{1+R}{T} \simeq \frac{1}{4n_0n_3n_1^2}\{(n_0^2+n_1^2)(n_1^2+n_3^2) + (n_0^2-n_1^2)(n_1^2-n_3^2)\cos 2\gamma_1 - \frac{n_1}{n_2}(n_0^2-n_1^2)(n_2^2-n_3^2)2\gamma_2 \sin 2\gamma_1\} \qquad 4.8.6$$

Comparing equation 4.8.6 with equation 4.8.5 the condition for equivalence is

$$\frac{\gamma_0}{\gamma_2} = \frac{n_1}{n_2}\frac{(n_2^2-n_3^2)}{(n_1^2-n_3^2)}$$

i.e.

$$\frac{d_0}{d_2} = \frac{(n_2^2-n_3^2)}{(n_1^2-n_3^2)}$$

where d_0 is the equivalent thickness of the thin layer if it is considered to have refractive index n_1.

For example, if $n_1 = 4.0$, $n_2 = 2.0$, $d_2 = 100\text{Å}$, $n_3 = 1.5$, then $d_0 = 15\text{Å}$. That is, the "measured" film thickness would have to be reduced by 85Å if the single-layer equations were used, which is again in agreement with the computations.

It is also worth noting that if the refractive index of the very thin layer was greater than that of the thick layer, then for both systems the total film thickness would have to be increased to allow the use of the single-layer equations. This also shows that the surface layers on the germanium and selenium films have a refractive index less than that of the germanium or selenium respectively, in agreement with the original assumptions as to the nature of these layers.

4. 9 CHOICE OF INCORRECT REFRACTIVE INDEX FOR THE 1st. LAYER.

Provided the first layer is very thin and transparent, it will be shown that an incorrect choice of its refractive index will only result in a difference in its calculated thickness, and will not affect the results of the underlying film.

For the case of a very thin 1st. layer, i.e. $\gamma_1 << 1$, $\alpha_1 << 1$, Tomlin (1971) has derived the following expressions from equations 4.7.1 and 4.7.2.

$$\frac{1+R}{T} = \frac{F}{4n_0n_3(n_2^2+k_2^2)} \qquad 4.9.1$$

where

$$\begin{aligned} F = {} & (n_0^2+n_2^2+k_2^2)\{(n_2^2+n_3^2+k_2^2+k_3^2)\cosh 2\alpha_2 \\ & \qquad + 2(n_2n_3+k_2k_3)\sinh 2\alpha_2\} \\ & + (n_0^2-n_2^2-k_2^2)\{(n_2^2-n_3^2+k_2^2-k_3^2)\cos 2\gamma_2 + 2(n_2k_3-n_3k_2)\sin 2\gamma_2\} \\ & + 2t_1\Big[\{k_2(n_0^2-n_1^2+k_1^2) + 2n_1n_2k_1\}\{(n_2^2+n_3^2+k_2^2+k_3^2)\sinh 2\alpha_2 \\ & \qquad + 2(n_2n_3+k_2k_3)\cosh 2\alpha_2\} \\ & - \{n_2(n_0^2-n_1^2+k_1^2) - 2n_1k_1k_2\}\{(n_2^2-n_3^2+k_2^2-k_3^2)\sin 2\gamma_2 \\ & \qquad - 2(n_2k_3-n_3k_2)\cos 2\gamma_2\}\Big] \end{aligned}$$

$$\frac{1-R}{T} = \frac{G}{2n_3(n_2^2+k_2^2)} \qquad 4.9.2$$

where

$$\begin{aligned} G = {} & n_2\{(n_2^2+n_3^2+k_2^2+k_3^2)\sinh 2\alpha_2 + 2(n_2n_3+k_2k_3)\cosh 2\alpha_2\} \\ & + k_2\{(n_2^2-n_3^2+k_2^2-k_3^2)\sin 2\gamma_2 - 2(n_2k_3-n_3k_2)\cos 2\gamma_2\} \\ & + 2n_1k_1t_1\{(n_2^2+n_3^2+k_2^2+k_3^2)\cosh 2\alpha_2 + 2(n_2n_3+k_2k_3)\sinh 2\alpha_2 \\ & \qquad + (n_2^2-n_3^2+k_2^2-k_3^2)\cos 2\gamma_2 + 2(n_2k_3-n_3k_2)\sin 2\gamma_2\} \end{aligned}$$

where

$$t_1 = 2\pi d_1/\lambda$$

It is seen that these equations are those for a single absorbing layer on an absorbing substrate plus the addition of a correction term in t_1.

For the case where $k_1 = k_3 = 0$ (transparent first layer and substrate), the correction term for (1-R)/T becomes zero while that for (1+R)/T becomes:

$$2(n_0^2-n_1^2)t_1\Big[k_2\{(n_2^2+n_3^2+k_2^2)\sinh 2\alpha_2 + 2n_2n_3\cosh 2\alpha_2\} - n_2\{(n_2^2-n_3^2+k_2^2)\sin 2\gamma_2 + 2n_3k_2\cos 2\gamma_2\}\Big] \qquad 4.9.3$$

The expression between the curly brackets is independent of n_1 and d_1.

Therefore to be equivalent to a thin first layer of refractive index n_1' and thickness d_1', the condition for equivalence of (1-R)/T is always met while that for (1+R)/T is, from equation 4.9.3

$$(n_0^2-n_1^2)t_1 = (n_0^2-n_1'^2)t_1'$$

i.e.

$$\frac{t_1}{t_1'} = \frac{d_1}{d_1'} = \frac{n_0^2-n_1'^2}{n_0^2-n_1^2}$$

For example if $n_0 = 1$, $n_1 = 2$, $n_1' = 3$, $d_1 = 100\text{Å}$, then $d_1' = 37\text{Å}$. That is, a very thin first layer of thickness 100Å and refractive index 2.0 has the same effect as a layer 37Å thick with refractive index 3.0.

So provided the first layer is very thin and transparent we may assume an incorrect value for its refractive index and still eliminate its effect when determining the optical properties of the underlying

film using the two-layer equations.

4. 10 MORE THAN ONE VERY THIN LAYER ON THE SURFACE.

We can show that two very thin transparent layers are equivalent to a single transparent layer.

Consider two very thin transparent layers with refractive indices n_1 and n_2 of thicknesses d_1 and d_2 respectively on an absorbing substrate of refractive index n_3 and absorption index k_3.

Equation 4.9.1 with $k_1 = k_2 = 0$ becomes:

$$\frac{1+R}{T} = \frac{1}{4n_0n_3n_2^2}\Big\{(n_0^2+n_2^2)(n_2^2+n_3^2+k_3^2) + (n_0^2-n_2^2)\{(n_2^2-n_3^2-k_3^2)\cos 2\gamma_2 + 2n_2k_3\sin 2\gamma_2\} - 2t_1n_2(n_0^2-n_1^2)\{(n_2^2-n_3^2-k_3^2)\sin 2\gamma_2 - 2n_2k_3\cos 2\gamma_2\}\Big\} \qquad 4.10.1$$

For $\gamma_2 << 1$ equation 4.10.1 becomes

$$\frac{1+R}{T} = \frac{1}{4n_0n_3}\Big\{2(n_0^2+n_3^2+k_3^2) + 2k_3\{(n_0^2-n_2^2)2t_2+(n_0^2-n_1^2)2t_1\} - (n_0^2-n_1^2)(n_2^2-n_3^2-k_3^2)4t_1t_2\Big\}$$

Since $t_1 << 1$ and $t_2 << 1$, we may neglect terms in t_1t_2. Hence

$$\frac{1+R}{T} \quad \frac{1}{4n_0n_3}\Big\{2(n_0^2+n_3^2+k_3^2) + 2k_3\{(n_0^2-n_2^2)2t_2+(n_0^2-n_1^2)2t_1\}\Big\} \qquad 4.10.2$$

For a single very thin transparent film of refractive index n and thickness d on an absorbing substrate with optical constants n_3 and k_3:

$$\frac{1+R}{T} = \frac{1}{4n_0n_3}\{2(n_0^2+n_3^2+k_3^2) + 2k_3(n_0^2-n^2)2t\} \qquad 4.10.3$$

For two very thin transparent layers on an absorbing substrate to be equivalent to a single transparent film on an absorbing substrate, the conditions for (1-R)/T to be equivalent are always met and from equations 4.10.2 and 4.10.3 the conditions for (1+R)/T to be equivalent are thus

$$(n_0^2-n^2)t = (n_0^2-n_2^2)t_2 + (n_0^2-n_1^2)t_1$$

or

$$(n_0^2-n^2)d = (n_0^2-n_2^2)d_2 + (n_0^2-n_1^2)d_1 \qquad 4.10.4$$

e.g. if $d_1 = d_2 = 50\text{Å}$, $n_1 = 2$, $n_2 = 3$, $n_0 = 1$, then

$$(n^2-1)d = 550\text{Å}$$

e.g. if $n = 2$, $d = 183\text{Å}$

$n = 3$, $d = 69\text{Å}$

That is, two very thin non-absorbing layers with refractive indices 2.0 and 3.0 and thickness 50Å each, have the same effect as a single film with refractive index 2.0 and thickness 183Å, or a single film with refractive index 3.0 and thickness 69Å.

4. 11 SURFACE LAYERS ON GERMANIUM FILMS.

The calculated oxide thicknesses on the germanium films were estimated to be accurate to within about ±5Å (assuming the choice of refractive index was correct). Amorphous germanium films and films deposited on room temperature substrates and subsequently annealed showed oxide layer thicknesses less than 10Å, which is of the same order of magnitude as has been previously reported.

However films deposited on substrates at 350°C exhibited apparent oxide layer thicknesses of the order of 100Å, which is much larger

than that found for the other films. One possible explanation for this was that the oxide may have formed on the hot substrate during deposition and not on the top surface of the film. This possibility was precluded since the analyses presented in this chapter showed that the layer was definitely on the surface.

A clue to the answer to this problem was found from the work of Sloope and Tiller (1962) who studied the formation conditions and structure of thin epitaxial germanium films on single-crystal substrates. They found that films deposited on calcium flouride substrates below 300°C and above 550°C were smooth, whereas, between 300°C and 550°C, the films were wrinkled. Although quartz substrates were employed in the present investigation it was possible that a similar effect existed. Electron microscope examinations of the surfaces of the germanium films were therefore undertaken.

4. 11. 1 SURFACE TOPOGRAPHY OF GERMANIUM FILMS.

Surface replicas of germanium films deposited on room temperature substrates, films deposited on room temperature substrates and subsequently annealed, and films deposited on substrates preheated to 350°C, were prepared and studied with the aid of an electron microscope. Figure 4.10.a is a micrograph of the surface of a film deposited on a room temperature substrate, and is also typical of those that were annealed. The surface is generally quite smooth with occassional crater-like depressions. Figure 4.10.b is an electron micrograph of the surface of a film deposited on a substrate which was preheated to 350°C. The surface of the film is seen to be

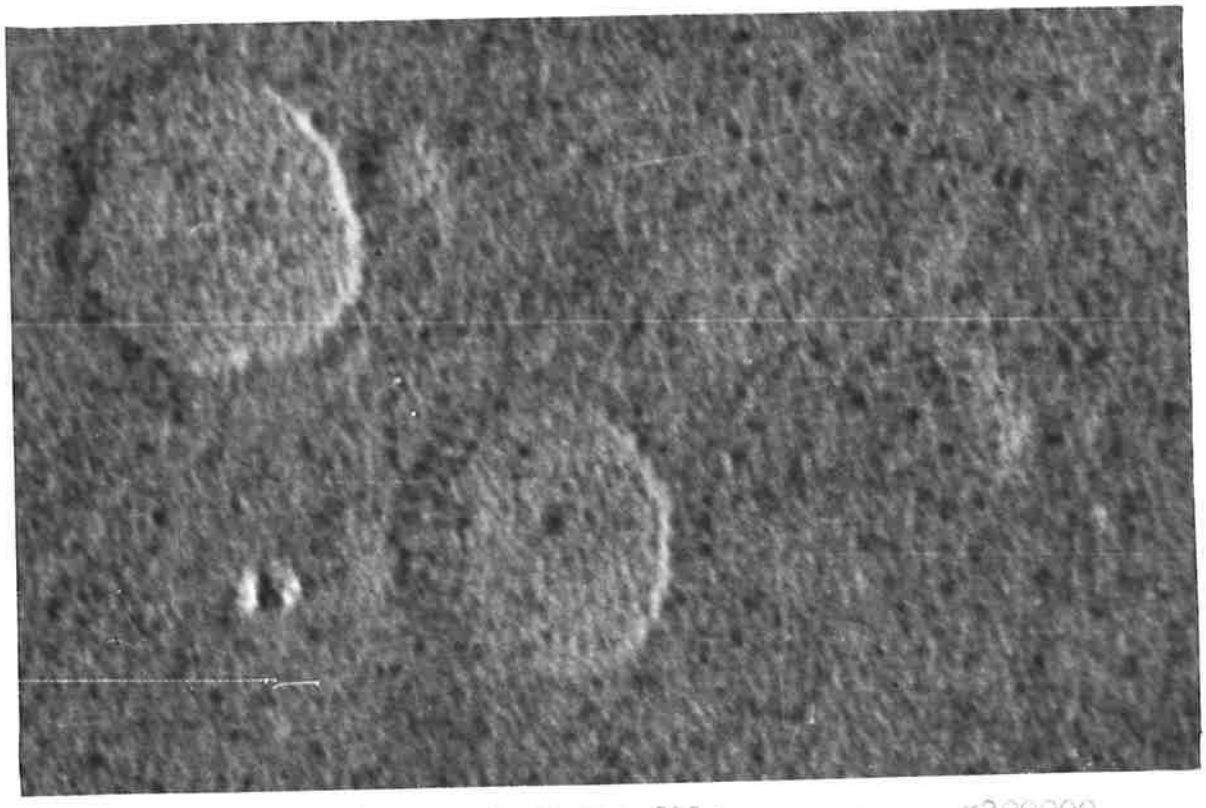

a. Room temperature substrate film x200000

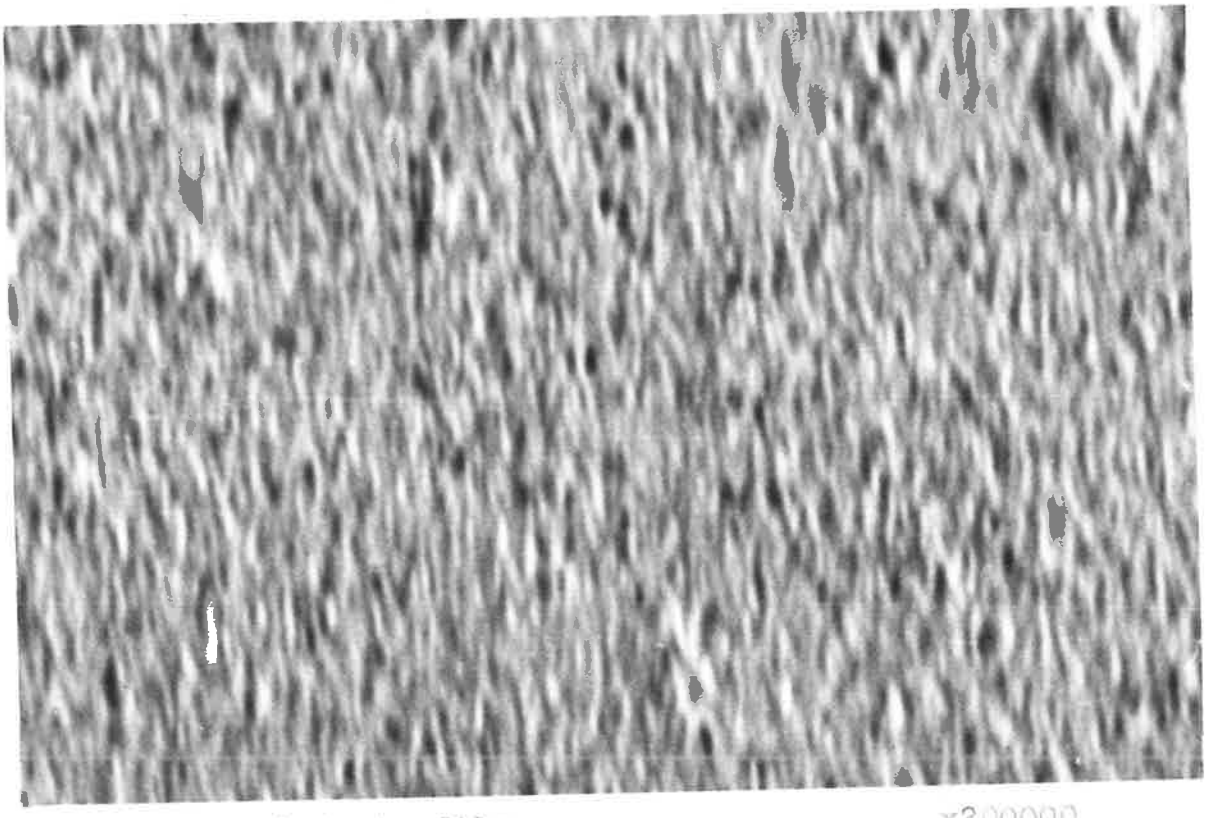

b. 350 C substrate film x200000

Figure 4.10

wrinkled. The wrinkles are of the order of 100Å diameter and 1000Å long. If we consider the surface as being composed of semi-cylinders 100Å in diameter and 1000Å long, then the ratio of the surface of the film compared to that if it was perfectly flat is about 1.6, in excellent agreement with that determined by MacDonald (1967). He investigated the absorption of gases on germanium films deposited on quartz-crystal oscillators and deduced the above ratio for films deposited on 350°C substrates.

4. 11. 2 TREATMENT OF THE SURFACE LAYER.

It is apparent that the large surface layer calculated for the germanium films deposited on 350°C substrates is not germanium oxide, but has arisen from the wrinkled nature of the surface which produces the same effect as an oxide layer. Although not an oxide, we can still treat the surface as a separate layer and we will show that, to a good approximation, it may be treated as transparent so that the analyses presented in this chapter in eliminating the effects of the surface layer on the properties of the underlying film are still valid.

Treating the surface of the film as a separate layer, we may apply Schopper's theory (Schopper, 1951; Heavens, 1955) which has been applied successfully to account for the anomalous optical behaviour observed in very thin metal films. In the simple case the surface layer may be considered as a film consisting of ellipsoidal particles of the same size and axial ratio. The ratio of the average film thickness to that deduced from the mass per unit area on the assumption

of bulk density is γ. If Ne is the observed value of the complex refractive index for such a film (i.e. $Ne = n_e - i\,k_e$ where n_e and k_e are the observed refractive and absorption indices), and N the complex refractive index of the bulk material, then

$$\gamma(Ne^2-1) = \frac{N^2-1}{(N^2-1)f+1} \qquad 4.11.1$$

where f is a function (David's function) of the axial ratio of the ellipsoids whose variation is seen in Figure 4.11.

Thus from equation 4.11.1

$$Ne = \left\{1 + (N^2-1)/\gamma\{(N^2-1)f+1\}\right\}^{\frac{1}{2}} \qquad 4.11.2$$

This was the most convenient form of the equation as the computer was capable of executing complex arithmetic.

Although it was not possible to measure accurately γ and f, they were estimated from the electron micrographs to be of the order of 1.5 for γ and 0.1 for f. Using these values and applying equation 4.11.2 to values of the optical constants approximating those of bulk germanium produced the results shown in Figure 4.12.

It can be seen that the effective refractive index of this layer is less than that of the bulk germanium in agreement with the observed results. The value of n_e in this case is 2.2 which is close to the value which was originally assumed for this layer. The absorption edge of the surface layer is shifted towards shorter wavelengths. For our range of measurements, the inclusion of this absorption in a very thin surface layer did not alter the reflectance and transmittance of the two-layer system outside the experimental

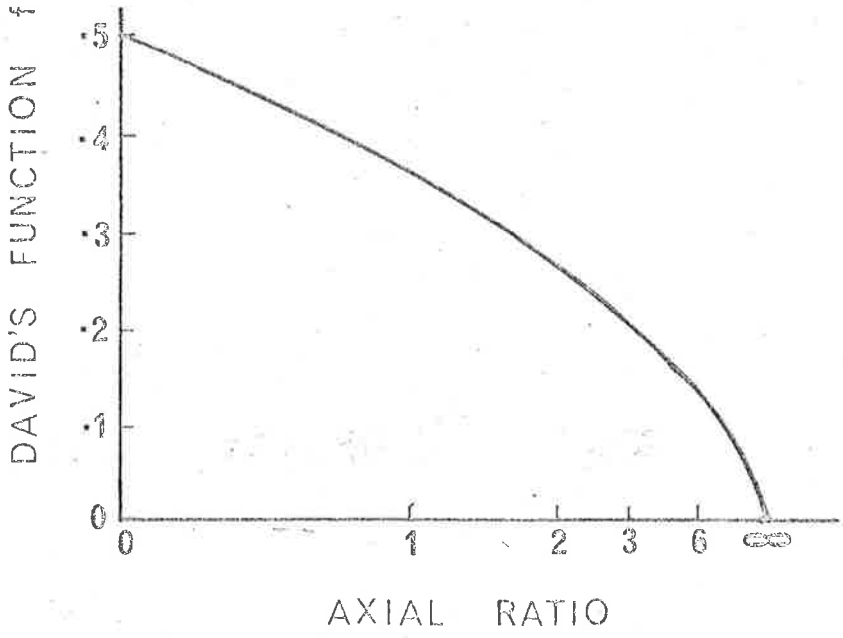

Figure 4.11

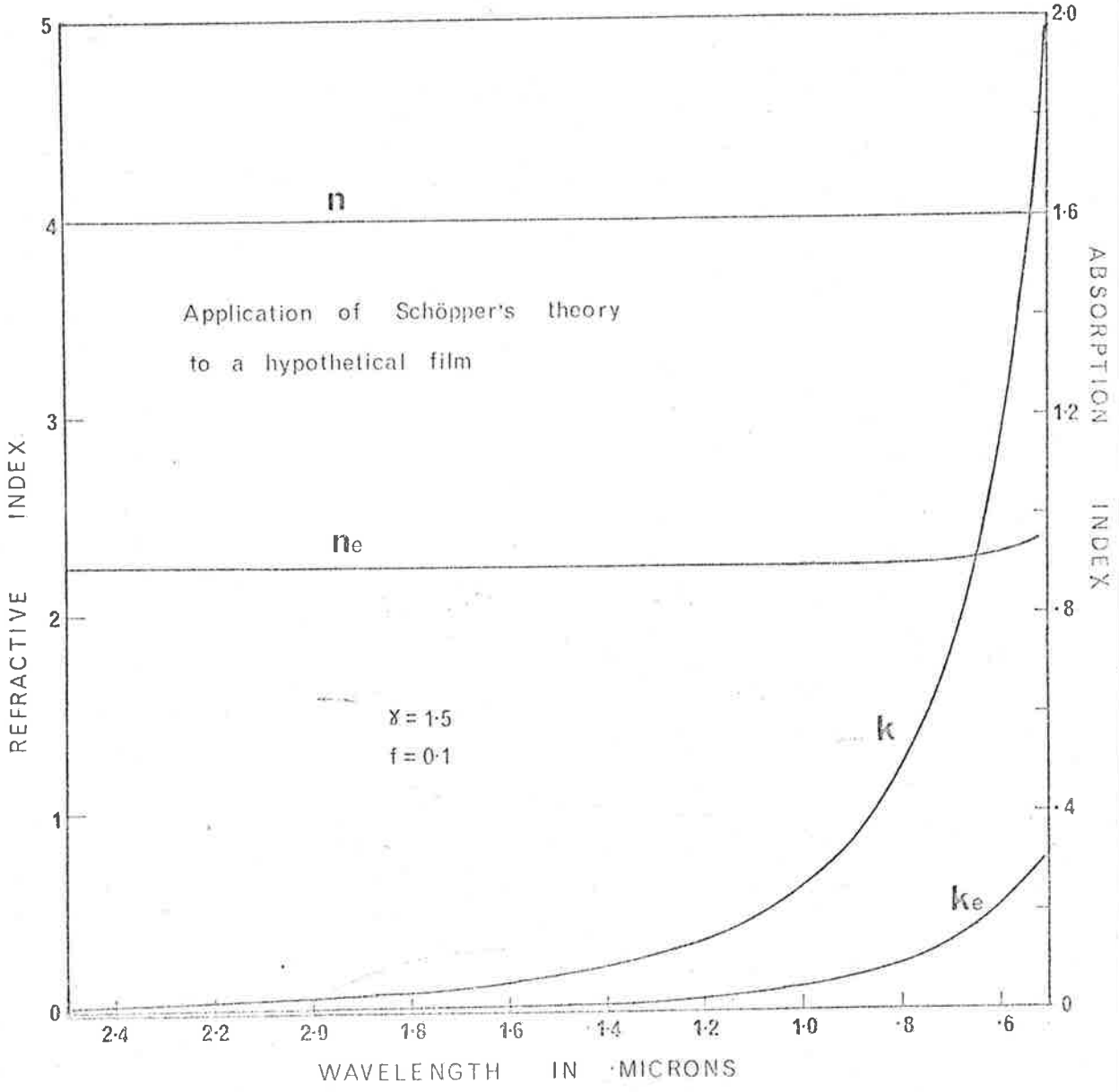
5
4
3
2
1
0
2·0
1·6
1·2
·8
·4
0
n
Application of Schöpper's theory
to a hypothetical film
ne
X = 1·5
f = 0·1
k
ke
REFRACTIVE INDEX
ABSORPTION INDEX
2·4
2·2
2·0
1·8
1·6
1·4
1·2
1·0
·8
·6
WAVELENGTH IN MICRONS

Figure 4.12

errors in these quantities. Thus for the present purpose the surface layer may be considered transparent without introducing a significant error.

Although the treatment of the surface layer given above is simplified, it nevertheless demonstrates why the postulation of a transparent oxide layer on the surface of the germanium films produced excellent closure of the refractive index curves and gave good agreement between the measured and calculated film thicknesses. To a good approximation, therefore, we may treat the surface of the film as a transparent layer with a refractive index of 2.0. We have shown in section 4.9 that an error in the choice of the refractive index of the transparent layer will only result in a difference in its calculated thickness and will not affect the results of the underlying film. Furthermore if germanium oxide is also present on the surface we have shown in section 4.10 that two or more very thin transparent layers on the surface may be treated effectively as a single layer with no measurable effect on the quantities calculated for the underlying film.

4. 12 SURFACE LAYERS ON SELENIUM FILMS.

The calculated surface layer thicknesses for the selenium films varied between 40Å and 125Å, these values being estimated to within about 20% for each film. The large error compared to that determined for the germanium films most probably arises from the non-uniformity of these films as a rotating substrate was not employed during the deposition of the films.

The values obtained appear rather large for an oxide layer, but no other measurements to compare with could be found in the literature. Campbell (1968) reported that there was no significant surface roughness for these films, and that they were generally smooth with isolated crystalline patches. Whether surface irregularities of the order of 40Å - 120Å were present the author was not in a position to determine. If the large apparent oxide layer is in fact due to surface irregularities then the surface may be treated in a similar manner to the surface of the germanium films in the previous section, with the consequent elimination of the effects of the surface on the calculated quantities for the underlying film.

4. 13 CONCLUSIONS.

The existence of surface layers accounts readily for the need to reduce the measured film thickness in order to obtain the correct type of refractive index curve from the single layer equations, and also the non-closure of the refractive index curve when these equations are used. For very thin transparent layers, the results obtained using the single layer equations with reduced film thickness are negligibly different from the exact results. For moderate surface layers it becomes necessary to use the double layer equations in order to obtain a closed refractive index curve.

As with the single-layer equations where one can use the property of closure to obtain an accurate value of the film thickness, so with the two-layer case one can use the property of closure over the entire wavelength range to obtain accurate values of film and

transparent layer thicknesses along with accurate values of the optical constants of the film. The absolute accuracy of the transparent layer thickness is dependent on the accuracy with which its refractive index is known.

The property of closure leads to the possibility that a film may be coated with a thin layer of transparent material of known refractive index. The optical constants of the underlying film and its thickness may then be calculated from the measured reflectance and transmittance of the two-layer system. This method might prove useful for the investigation of the optical properties of substances which are highly reactive in air.

CHAPTER 5.

OPTICAL CONSTANTS OF SELENIUM FILMS.

5. 1 INTRODUCTION.

The calculation of the optical constants of thin vitreous selenium films, from the measured reflectance and transmittance of the films, using exact theory was attempted by Campbell (1968). Inadequate information on the behaviour of the calculation procedure led to incorrect solutions being chosen from the multiple solutions that existed. The reason for the incorrect choice is discussed, and the optical constants of selenium films are recalculated on the basis of the knowledge of the behaviour of the calculation process determined in the previous two chapters. The effects of surface layers are also accounted for. The absorption found in these films is then briefly discussed in terms of a qualitative semi-conducting - bond model.

5. 2 INCORRECT SOLUTIONS.

The argument put forward by Campbell for the selection of his solutions was that at certain wavelengths only one solution for the refractive index n (and absorption index k) existed. This solution must therefore have been the correct solution and consequently the correct dispersion curve must pass through this point. For example, in Figure 5.1 one of his refractive index curves is reproduced. At the wavelength 0.8 μ the only solution found was $n = 1.4$, and it

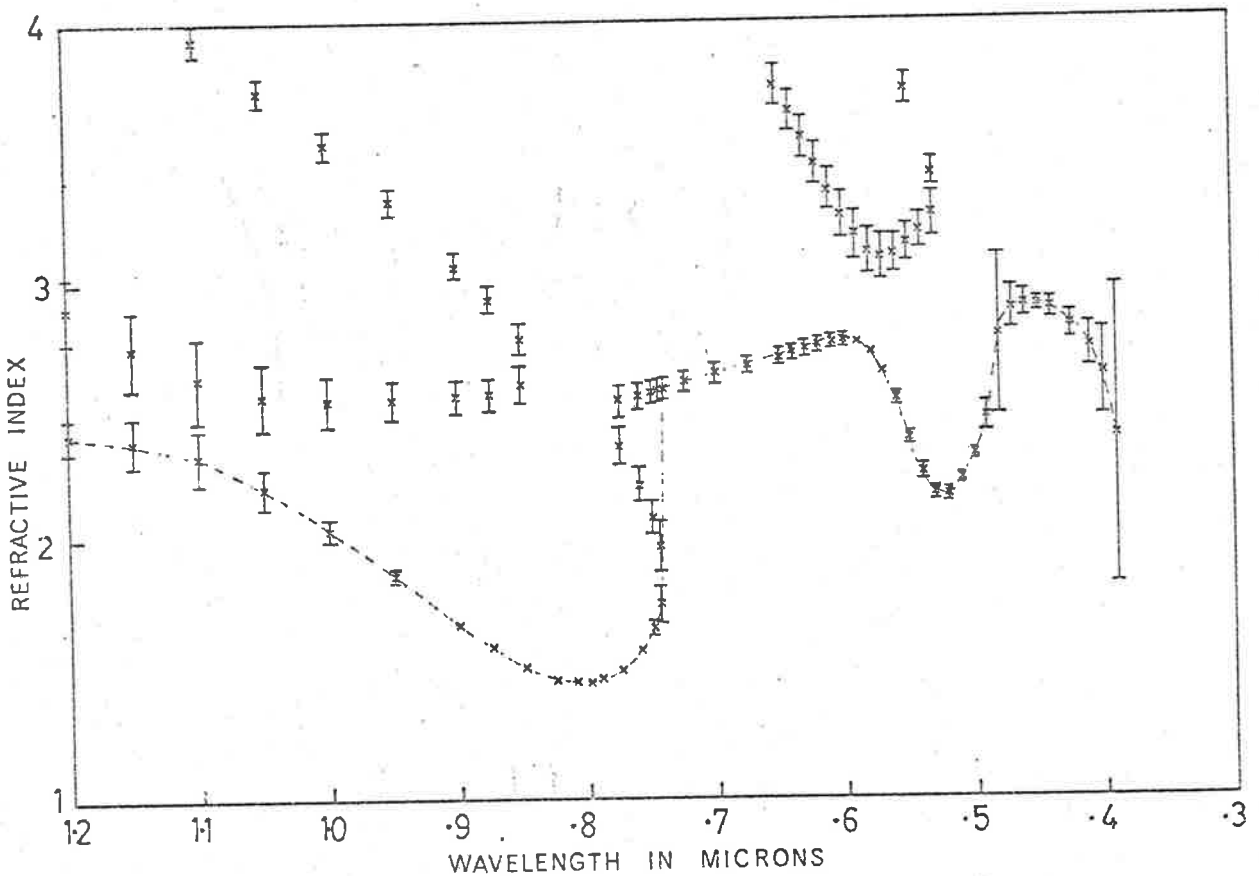
4
3
2
1
REFRACTIVE INDEX
1·2
1·1
1·0
·9
·8
·7
·6
·5
·4
·3
WAVELENGTH IN MICRONS

Figure 5.1

was assumed that the curve must pass through this point and as a result the curve shown as a dashed line was obtained.

It will be shown that, given accurate experimental data, more than one solution does exist at these wavelengths, but their existence may be missed in the calculation method. In the present case the missing of solutions was enhanced by experimental errors in the measured reflectance and transmittance, by the presence of surface layers on the films, and particularly by errors in the film thickness values used in the calculations.

5. 2. 1 MISSING SOLUTIONS.

The reason why some solutions may not be found at particular wavelengths can be clearly demonstrated by considering the calculation for the hypothetical film discussed in section 3.7. The calculated refractive index solutions for this film are shown again in Figure 5.2.

Initially it was found that at wavelength 1.6μ only the solution n = 1.5 was reproduced, the correct solution n = 4.0 being omitted. The reason for this was as follows:

In Figure 5.3.a the right-hand side of equation 3.4.1 (i.e. (1+R)/T) is plotted as a function of n for wavelength 1.5μ (for each n, k was found such that (n,k) satisfied the equation for (1-R)/T). The measured value of the left-hand side of equation 3.4.1 is included. Three solutions exist.

(1). n = 1.76

(2). n = 3.44

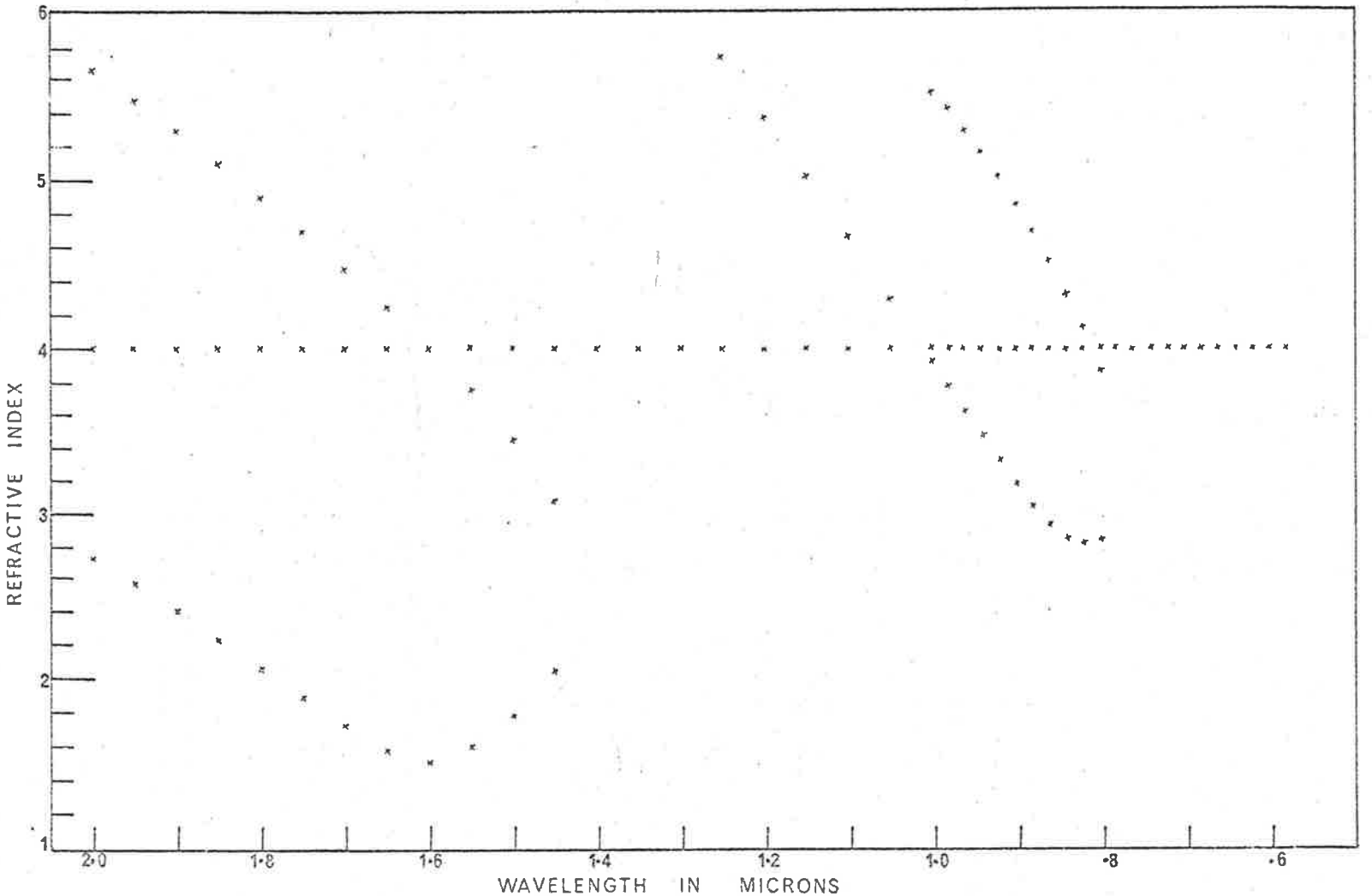
REFRACTIVE INDEX
6
5
4
3
2
1
2·0
1·8
1·6
1·4
1·2
1·0
·8
·6
WAVELENGTH IN MICRONS

Figure 5.2

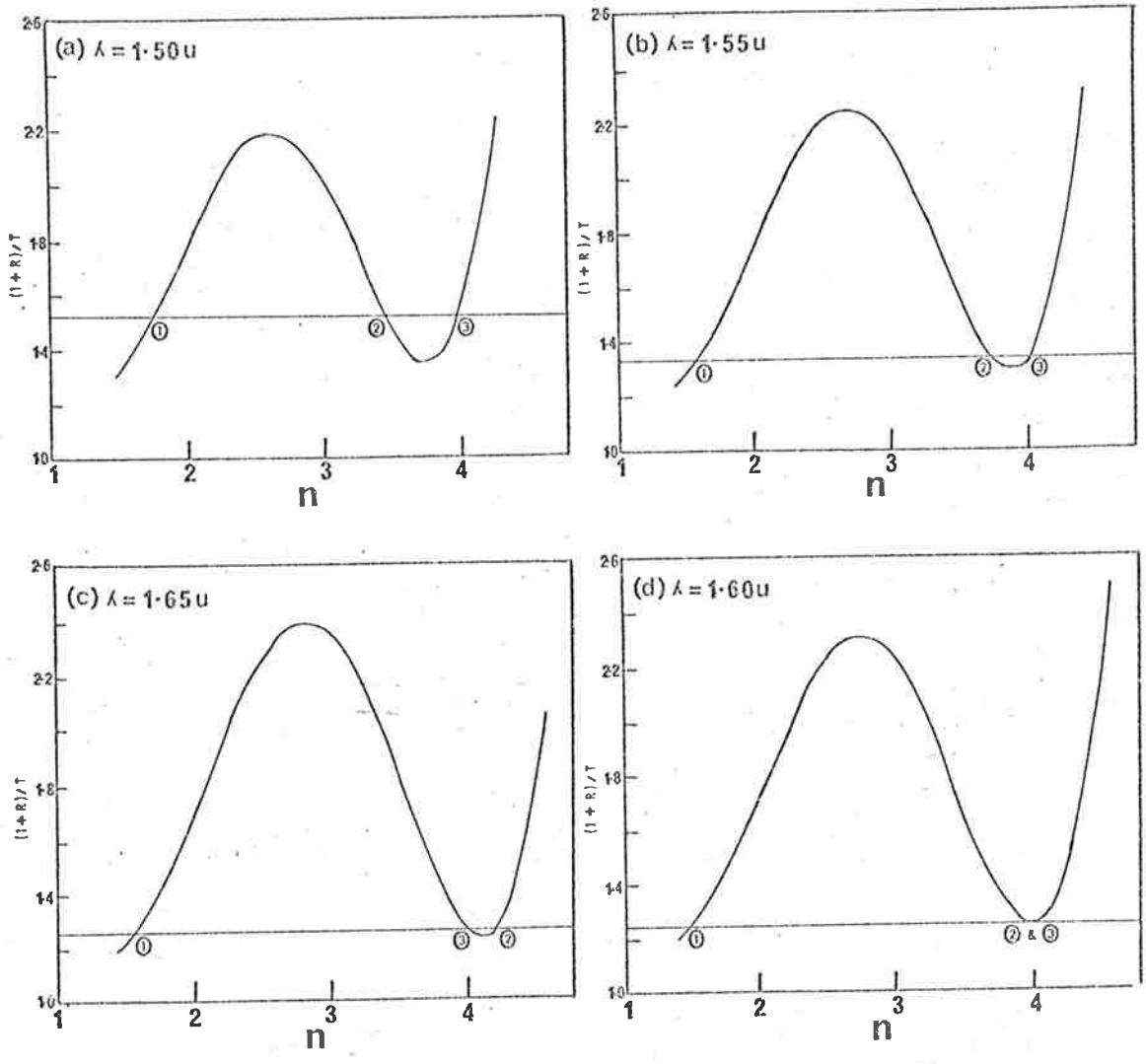

(1+R)/T as a function of n near the critical wavelength.

Figure 5.3

(3). n = 4.00

Figure 5.3.b shows the similar curve for $\lambda = 1.55\mu$.
Solution (2) has moved closer to solution (3).

Figure 5.3.c is the curve for $\lambda = 1.65\mu$.
Solution (2) has now moved to the other side of solution (3).

Figure 5.3.d is the curve for $\lambda = 1.60\mu$. Solution (1) still exists, but solutions (2) and (3) have merged to give two coincident solutions at the correct value of 4.0.

The measured value of (1+R)/T, represented by the straight line parallel to the n-axis, is tangential to the (1+R)/T vs. n curve at this point. It is this solution that was previously missed. Unobtainable accuracy in the experimental data and film thickness is necessary to reproduce this solution. An error of 1 part in 10^4 in the reflectance or transmittance will cause a separation of the tangent at this point from the correct value of the order of 0.01, and any calculation procedure searching for "zeroes" less than this at the particular wavelength of concern will miss the solution. The separation is greatly increased, and exists for a wider wavelength range, if incorrect film thickness values are used. As shown in Chapter 4 the presence of surface layers will also cause this behaviour if one attempts to use the single-layer equations in place of the two-layer equations.

Although Campbell employed a different calculation procedure, a similar effect existed. In his method, loci of constant reflectance and constant transmittance were plotted as n against k, the solutions for n and k being the points of intersection of the loci. A typical

curve is shown in Figure 5.4.a. At the critical wavelengths the loci touch at a point as shown in Figure 5.4.b. It was these points that were missed in his calculations.

5. 3 REFLECTANCE AND TRANSMITTANCE OF SELENIUM FILMS.

The values of R and T for eight vitreous selenium films, measured previously in this laboratory by Campbell, are tabulated in Appendix D. The curves for four of the films are shown in Figure 5.5. Multiple beam interference effects are apparent in all but the thinnest film and become more pronounced as the film thickness increases. The transmittance of the films rapidly falls to zero at short wavelengths, corresponding to the region of strong absorption. These films were still strongly absorbing at 0.25μ.

Campbell suggests that no multiple beam interference effect occurs in film 1. (Figure 5.5.a) as it is near the limiting thickness for which the film is a continuous layer. However the number of maxima and minima observed in the reflectance and transmittance curves depends primarily on the ratio d/λ, the value of d for this film being such that multiple beam effects are not seen for the wavelength range considered. In fact this was the only film for which Campbell obtained results which were in qualitative agreement with those for the bulk material, but he dismissed these results as being meaningless with the suggestion that this film may not be a continuous layer.

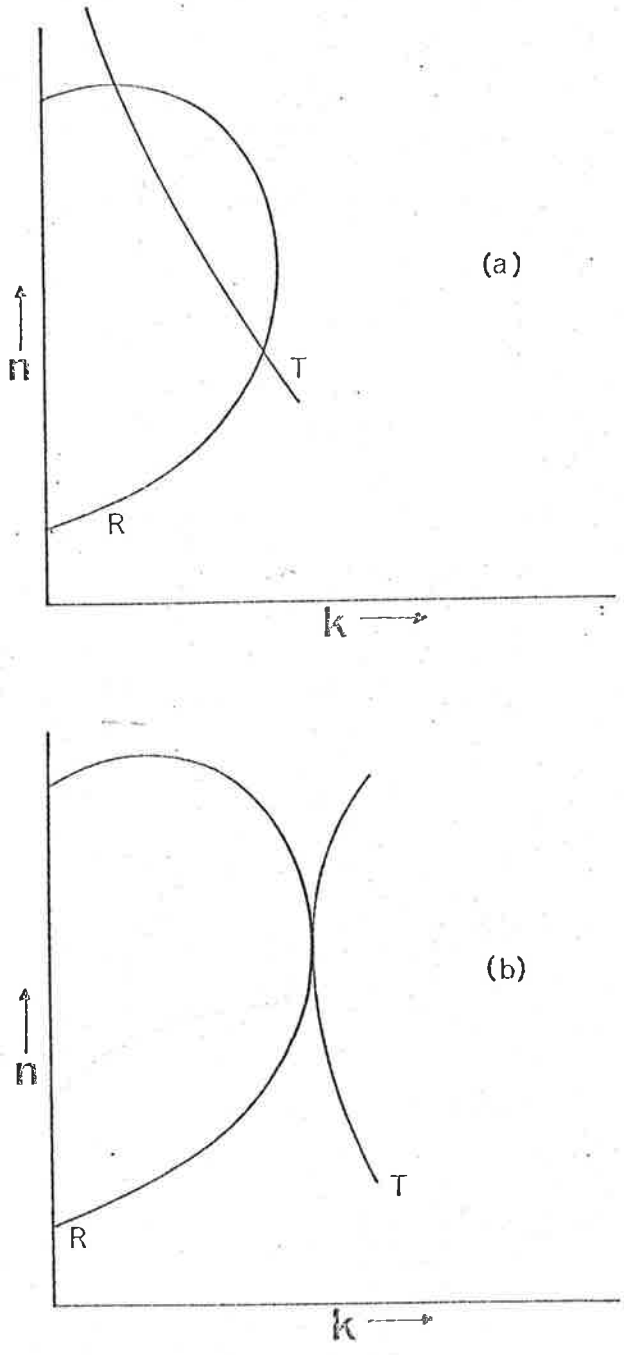

Figure 5.4

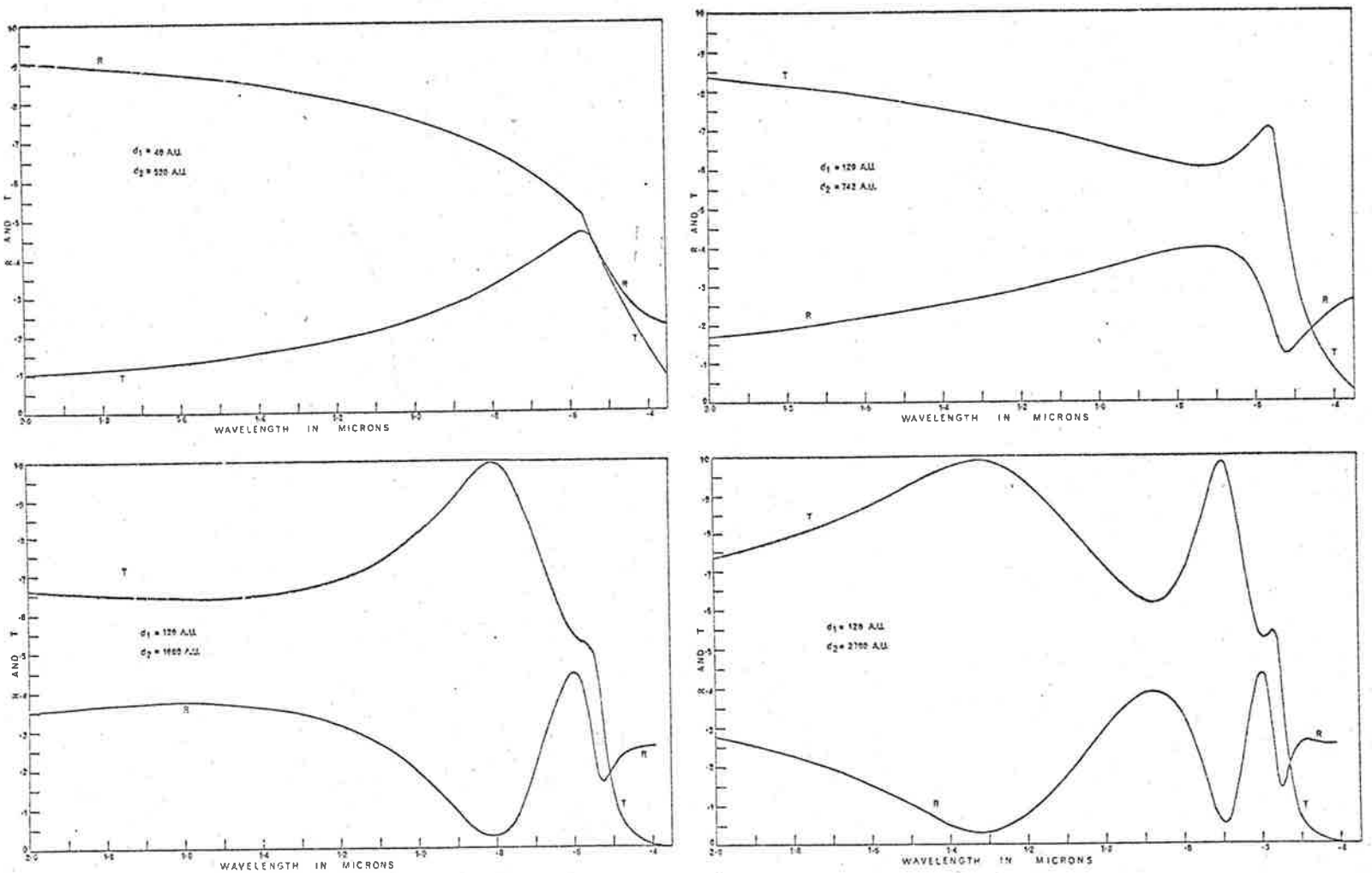
R
T
d_1 = 49 A.U.
d_2 = 520 A.U.
R AND T
WAVELENGTH IN MICRONS
T
R
d_1 = 129 A.U.
d_2 = 742 A.U.
R AND T
WAVELENGTH IN MICRONS
T
R
d_1 = 129 A.U.
d_2 = 1665 A.U.
R AND T
WAVELENGTH IN MICRONS
T
R
d_1 = 129 A.U.
d_2 = 2700 A.U.
R AND T
WAVELENGTH IN MICRONS

Figure 5.5

5. 4 CORRECTED FILM THICKNESS.

Table 5.1 gives the measured values of the thicknesses of the eight films, the values assumed by Campbell, and the film and surface layer thicknesses calculated by the method described in Chapter 4. The surface layer was assumed to be SeO_2 which has a refractive index of 1.76. With the exception of films 2 and 3 the total of the calculated film and oxide thicknesses agree remarkably well with the measured thicknesses. This would indicate that our assumption of the first layer being selenium dioxide is possible, although a wrinkled surface as found for germanium will give a similar effect. As shown in the previous chapter, regardless of the exact nature of the surface layer, provided it is thin and near transparent its effect on the underlying film is still eliminated.

It is possible that the difference in measured and calculated thickness values for films 2 and 3 may be the results of experimental errors. Selenium reacts with silver, and so an inert layer must be deposited over the film before the silver in order to make thickness measurements. Some material may migrate towards part of the substrate not coated with selenium. This would result in a smaller measured film thickness and it is possible that this has occurred with these two films. Alternatively the nature of the surface for these films may be such that our choice of its effective index (1.76) may be too small, resulting in a larger calculated surface layer thickness.

Table 5.1 also gives the accuracy with which the film and surface layer thicknesses could be calculated. The accuracy is generally less than for the germanium films (Chapter 6), probably due to non-uniformit-

ies in the films as a rotating substrate was not employed as in the case of the germanium films.

FILM NUMBER	CAMPBELL'S FILM THICKNESS (Å)	CALC.FILM THICKNESS (Å)	CALC.OXIDE THICKNESS (Å)	TOTAL FILM+ OXIDE (Å)	MEASURED FILM THICKNESS (Å)
1.	538	520±10	40±10	560±20	538±25
2.	724	682±10	125±10	807±20	724±43
3.	781	742±5	120±5	862±10	781±29
4.	942	930±5	45±5	975±10	942±49
5.	1017	1012±5	45±5	1057±10	1089±32
6.	1582	1600±30	120±20	1720±50	1732±26
7.	2380	2500±50	80±20	2580±70	2680±73
8.	2567	2700±50	120±20	2820±70	2867±57

TABLE 5.1

5. 5 REFRACTIVE INDEX OF SELENIUM FILMS.

The calculated refractive index solutions for the eight vitreous selenium films in the range of n = 1 to n = 4 are plotted in Appendix D. The values for one of the films are shown in Figure 5.6. Multiple solutions occur because of the periodic nature of the reflectance and transmittance equations, the periodicity being determined by the parameter γ which is affected by the ratio d/λ. As d increases, more solutions are calculated in a given range of n.

For the thicker films there were small wavelength ranges where

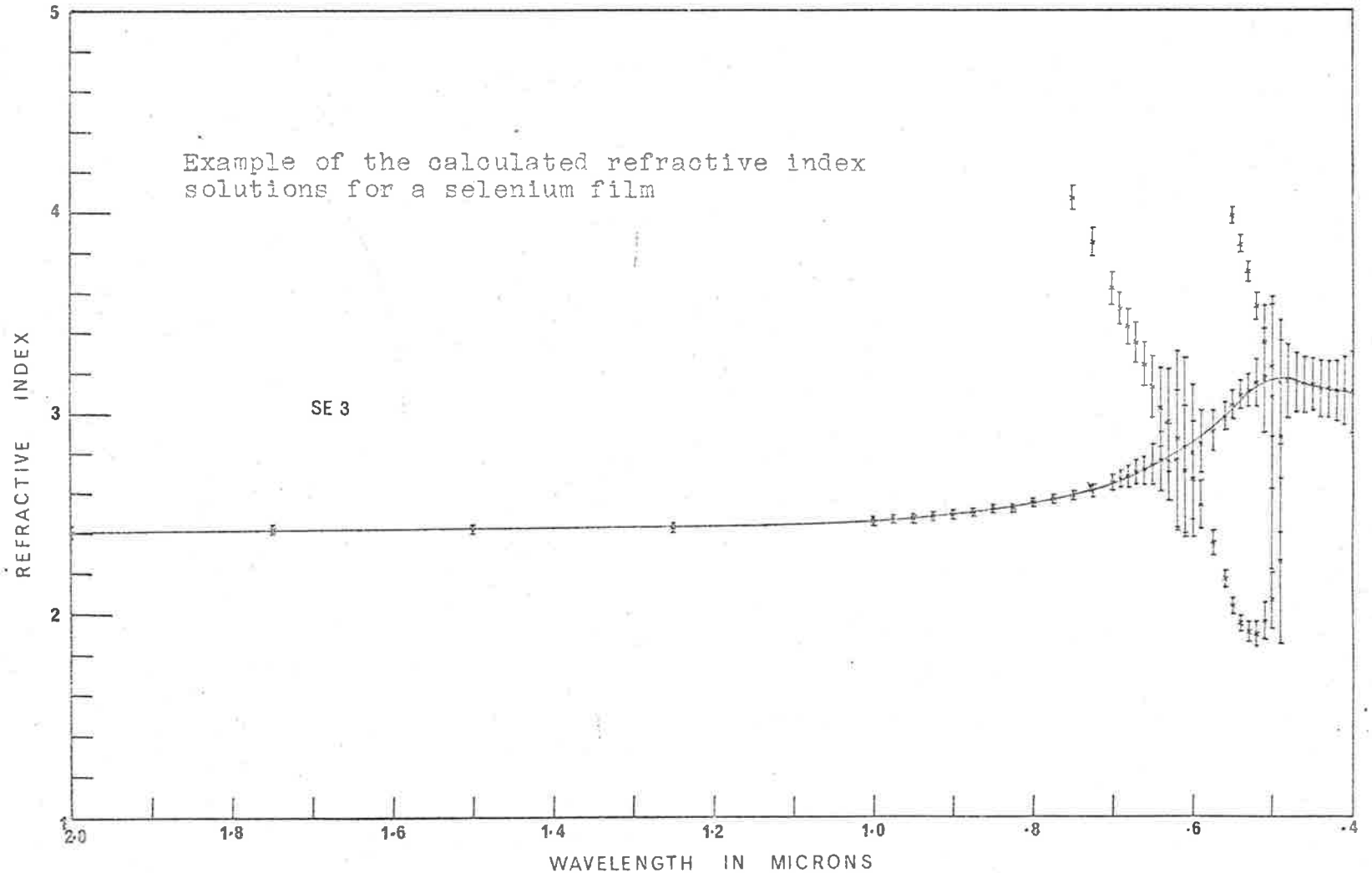
Example of the calculated refractive index solutions for a selenium film
SE 3
REFRACTIVE INDEX
5
4
3
2
2·0
1·8
1·6
1·4
1·2
1·0
·8
·6
·4
WAVELENGTH IN MICRONS

Figure 5.6

the correct values were not found. The reason for this has been discussed in section 5.2. Although these solutions could have been found by searching for the turning points in the (1+R)/T vs. n curve, the increase in computation and corresponding computing time was considered unnecessary since the problem occurred only for small regions in the infra-red where there is little change in the refractive and absorption indices.

5. 5. 1 ERRORS IN THE CALCULATED SOLUTIONS.

The errors in the calculated solutions were determined by the method described in Chapter 4, and are indicated on the curves by vertical bars. The error in R and T was estimated by Campbell to be 0.0025. The errors in the surface layer and film thicknesses were estimated from the accuracy with which the refractive index curve could be closed over the entire wavelength range, and are given in Table 5.1.

Near the regions where the correct curve intersects with the incorrect loops, the calculated errors are seen to be much larger than elsewhere. These regions correspond to the wavelength range where the curve (1+R)/T vs. n is near tangential to the straight line, parallel to the n axis, representing the experimental value of (1+R)/T. In these circumstances a small error in (1+R)/T makes a large error in n. It is possible that the first order formulae for the errors are inadequate in these regions, since the expression for the Jacobian (equation 3.6.7, page 37) tends to zero in these regions. The smoothness of the computed curve suggests that the errors may be

overestimated in these regions.

5. 5. 2 COMPARISON WITH PREVIOUS WORK.

In Figure 5.7 the average refractive index curve for the vitreous selenium films is plotted as a function of wavelength together with the results of Wood (1902) for thin sputtered films and Dowd (1951) which were obtained from the bulk material. There is seen to be close agreement between the present results and those of these authors.

5. 6 ABSORPTION INDEX OF SELENIUM FILMS.

The absorption index curves obtained for the selenium films are plotted in Appendix D. The correct solutions for one of the films, together with the calculated errors in the solutions, are plotted in Figure 5.8. The incorrect solutions, corresponding to the incorrect refractive index values, were in general close to the correct values and are consequently not shown on the graphs.

The large errors associated with certain critical regions in the refractive index curves are not apparent in the absorption index curves. We have found that, although the multiple solutions for the refractive index at a given wavelength may be widely separated, the corresponding absorption index solutions are not widely different. Thus although the calculated errors in n at the critical points may be large, they do not necessarily give rise to large errors in k in these regions.

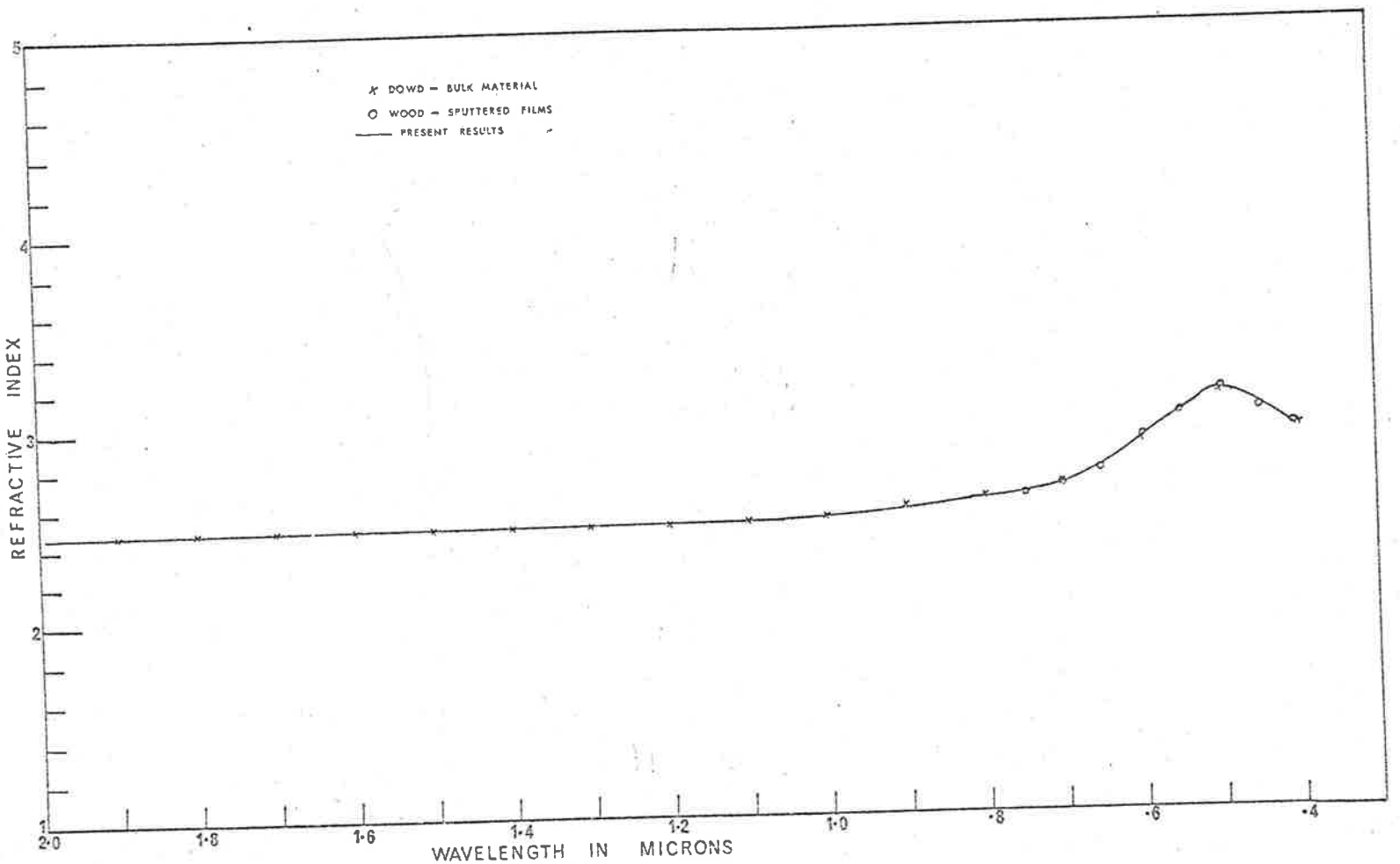
DOWD – BULK MATERIAL
WOOD – SPUTTERED FILMS
PRESENT RESULTS
REFRACTIVE INDEX
5
4
3
2
1
2·0
1·8
1·6
1·4
1·2
1·0
·8
·6
·4
WAVELENGTH IN MICRONS

Figure 5.7

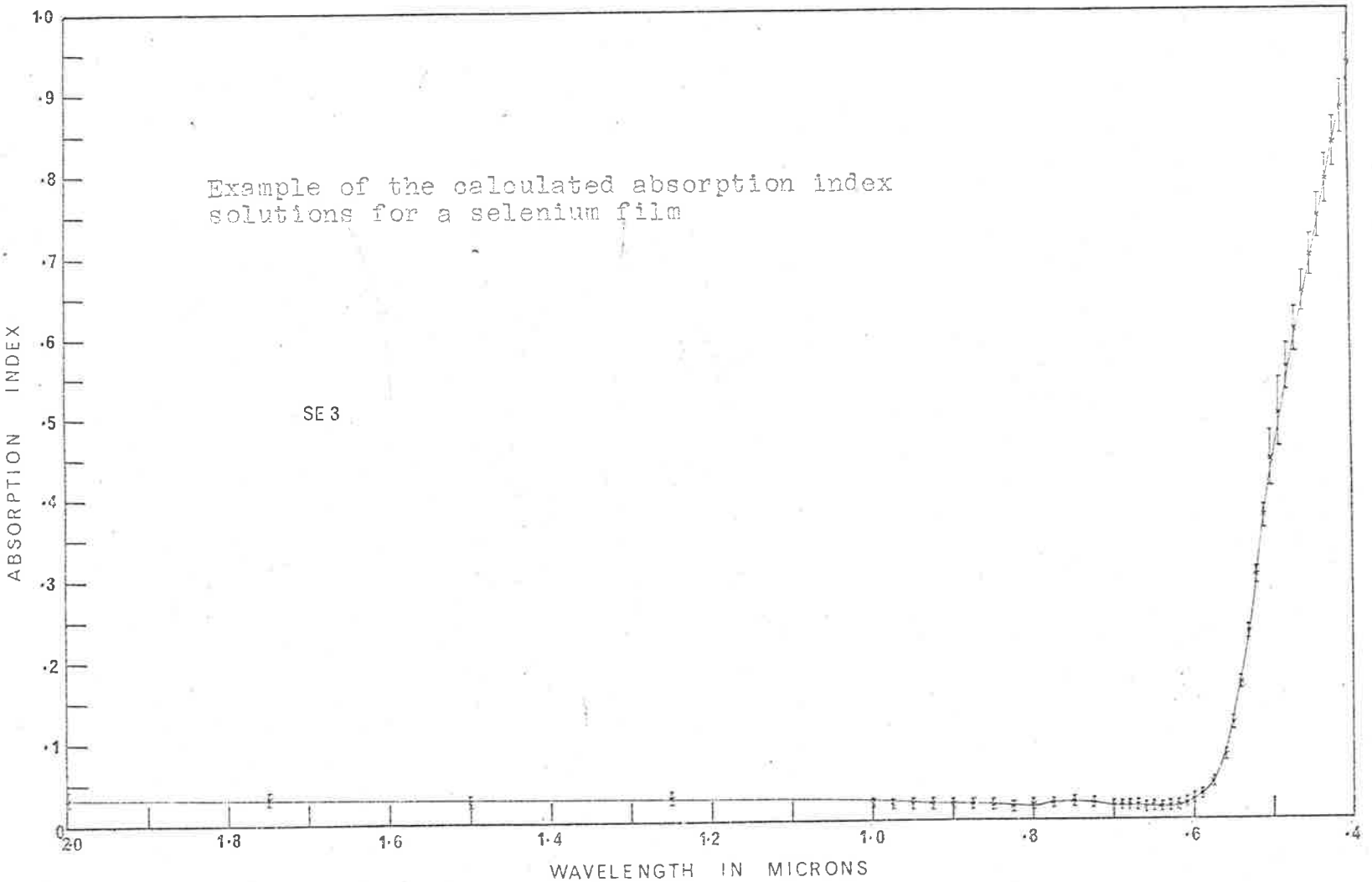
Example of the calculated absorption index solutions for a selenium film
SE 3
ABSORPTION INDEX
1·0
·9
·8
·7
·6
·5
·4
·3
·2
·1
0
2·0
1·8
1·6
1·4
1·2
1·0
·8
·6
·4
WAVELENGTH IN MICRONS

Figure 5.8

5. 7 ABSORPTION COEFFICIENT OF SELENIUM FILMS.

The absorption coefficient, defined by the relation

$$K = 4\pi k/\lambda$$

is plotted as a function of photon energy in Figure 5.9 for a typical selenium film, together with the curve of Seimsen and Fenton (1967) which is representative of previous work. The main difference is in the low energy region where the present films exhibit much stronger absorption than have previously been reported. This result is consistent with the conclusions of Campbell where he has shown that approximate equations are not suitable for the wavelength range where K is not very large, and that important information concerning absorption processes within the films may not be apparent from the approximate optical constants.

5. 8 ABSORPTION IN SELENIUM FILMS.

From the theory of light absorption in semiconductors (see, for example, R.A. Smith in "Semiconductors", 1959) the absorption near the edge may be represented by

$$EnK \propto (E-Eg)^{\beta} \qquad 5.8.1$$

where E is the photon energy, n the refractive index of the material, K the absorption coefficient and Eg the forbidden energy gap. For direct transitions β has the value $\frac{1}{2}$ and for phonon-assisted indirect transitions it has the value 2. For forbidden direct and indirect transitions β has the values 3/2 and 5/2 respectively.

Equation 5.8.1 may be more conveniently written

$$E-Eg \propto (EnK)^{1/\beta} \qquad 5.8.2$$

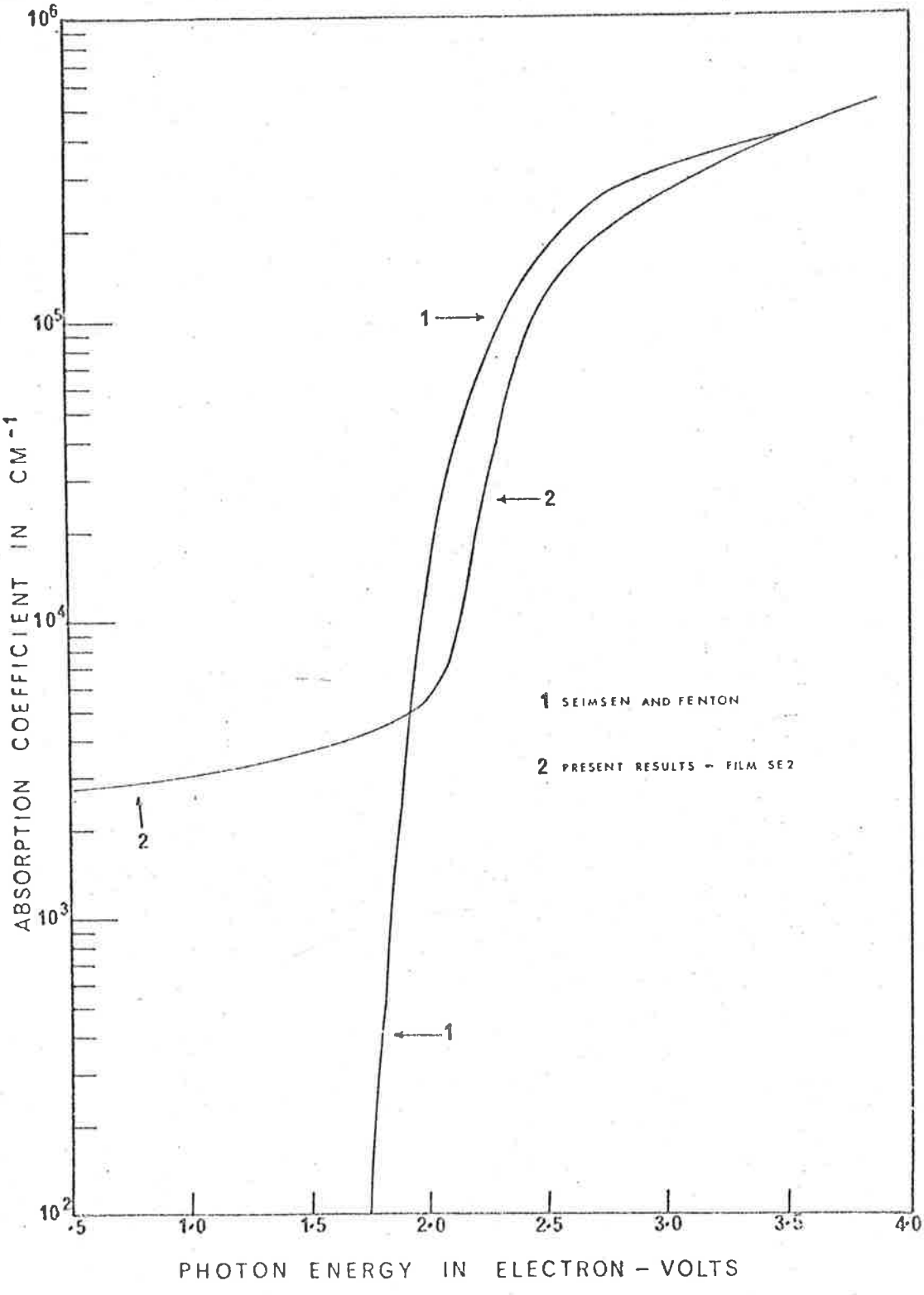
ABSORPTION COEFFICIENT IN CM⁻¹
10⁶
10⁵
10⁴
10³
10²
1
2
1 SEIMSEN AND FENTON
2 PRESENT RESULTS – FILM SE2
·5
1·0
1·5
2·0
2·5
3·0
3·5
4·0
PHOTON ENERGY IN ELECTRON – VOLTS

Figure 5.9

A plot of $(EnK)^{1/\beta}$ vs. E for various values of β would therefore be expected to reveal the absorption mechanisms occurring.

For the selenium films the best value of β was found to be 1.0, and in Figure 5.10, EnK is plotted as a function of photon energy on a linear scale for one of the selenium films. It is seen to consist of two straight lines. This behaviour was typical of all the selenium films, with the extrapolated line intersecting the energy axis between 2.18eV and 2.25eV, and the change in slope of the line occurring between 2.50eV and 2.63eV.

Thus for the selenium films β has the value of 1 which is not representative of any of the above standard transitions. It is recognised that it is doubtful whether selenium can be described by the theory of metallic conduction giving rise to an energy band model. The well defined energy value of the sharp increase in absorption indicates that band structure itself has an application to selenium, which appears to be an argument for an approach to semi-conduction which does not require a periodic lattice.

Mooser and Pearson (1956, 1958, 1960), by a qualitative argument based on the chemical bonding between atoms, deduced an energy level structure for hexagonal selenium. The structure of the hexagonal form consists of spiral chains with the selenium atoms arranged at the corners and in the centre of a hexagon. The chain direction is the c-axis of the crystal. Every third atom in a chain completes one revolution of the spiral. The distance of an atom to the two nearest neighbours in the same chain is 2.32Å and the distance to the four next-nearest neighbours in adjacent chains is 3.46Å.

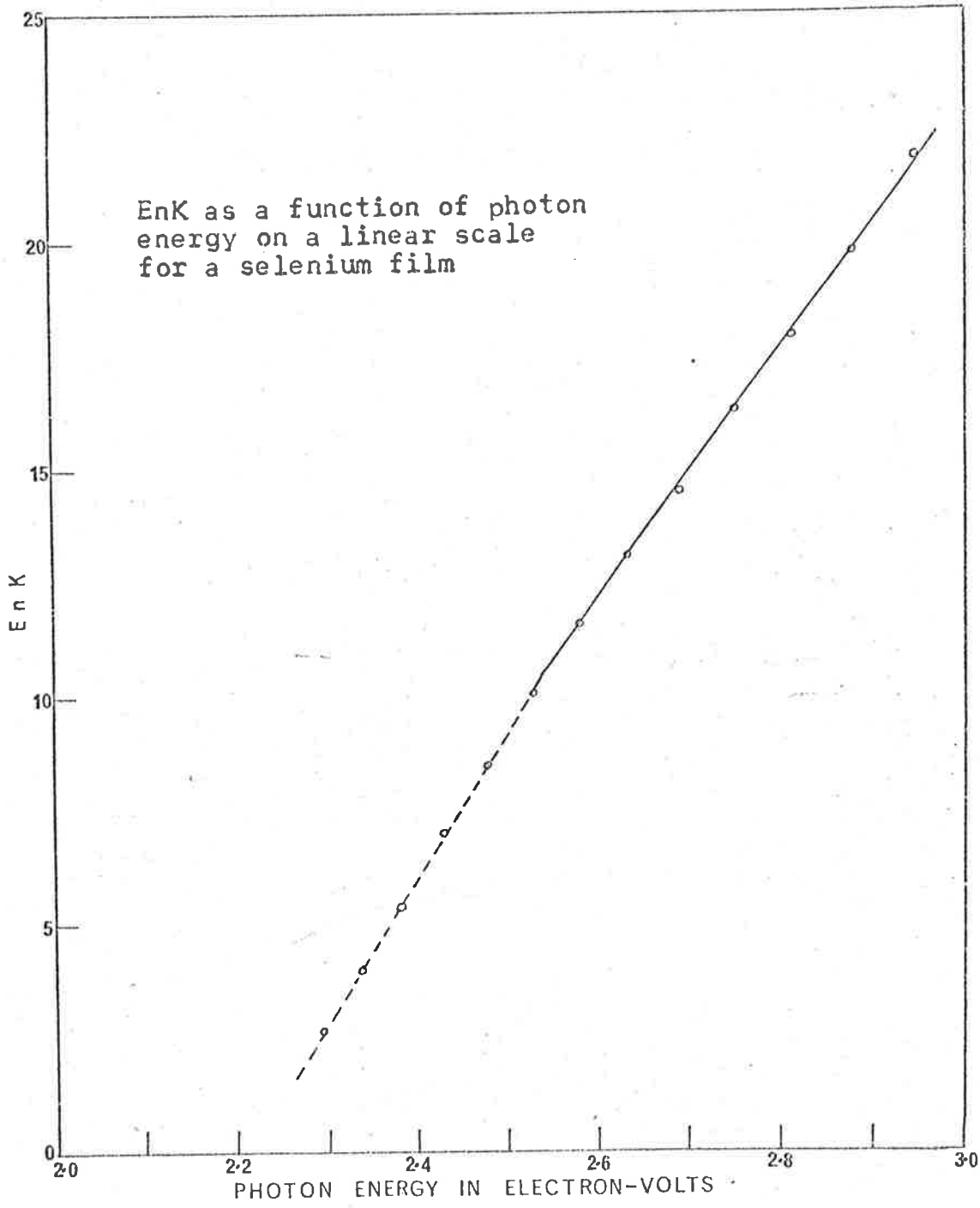
EnK as a function of photon energy on a linear scale for a selenium film
25
20
15
10
5
0
E n K
2·0
2·2
2·4
2·6
2·8
3·0
PHOTON ENERGY IN ELECTRON-VOLTS

Figure 5.10

The spiral chain structure is preserved in the vitreous form but the chains are randomly oriented.

The selenium atom has six outer electrons (s^2p^4) above five completed shells. The bonding between nearest neighbours in the same chain involves the s and p orbitals and leads to allowed and forbidden energy levels. The occurrence of resonating bonds between next-nearest neighbours in adjacent chains suggested that the forbidden gap is bridged by a band of low state density overlapping the valence band. The resonating bond requires that either or both of the unpaired p electrons is promoted to the higher d orbital.

Mooser and Pearson suggest that the overlapping band does not exist in vitreous selenium films because the random arrangement of the chains destroys all resonances. This conclusion was deduced from the increased distance to next-nearest neighbours in vitreous selenium. This, at first sight, appears inconsistent with the present measurements which indicate that considerable long wavelength absorption exists, particularly in the thinner films. However, if the residual long wavelength absorption is plotted as a function of film thickness (Figure 5.11) a definite trend is observed. As the film thickness increases so the residual absorption decreases in an exponential manner.

The chain structure of selenium grows upwards from the substrate with amorphous material separating the chains (Campbell, 1968). As the thickness increases the chain structure becomes better developed. Krebs and Schultze - Gebhardt (1955) have suggested that chains are 100 to 1000 atoms long which represents a length between 230Å and

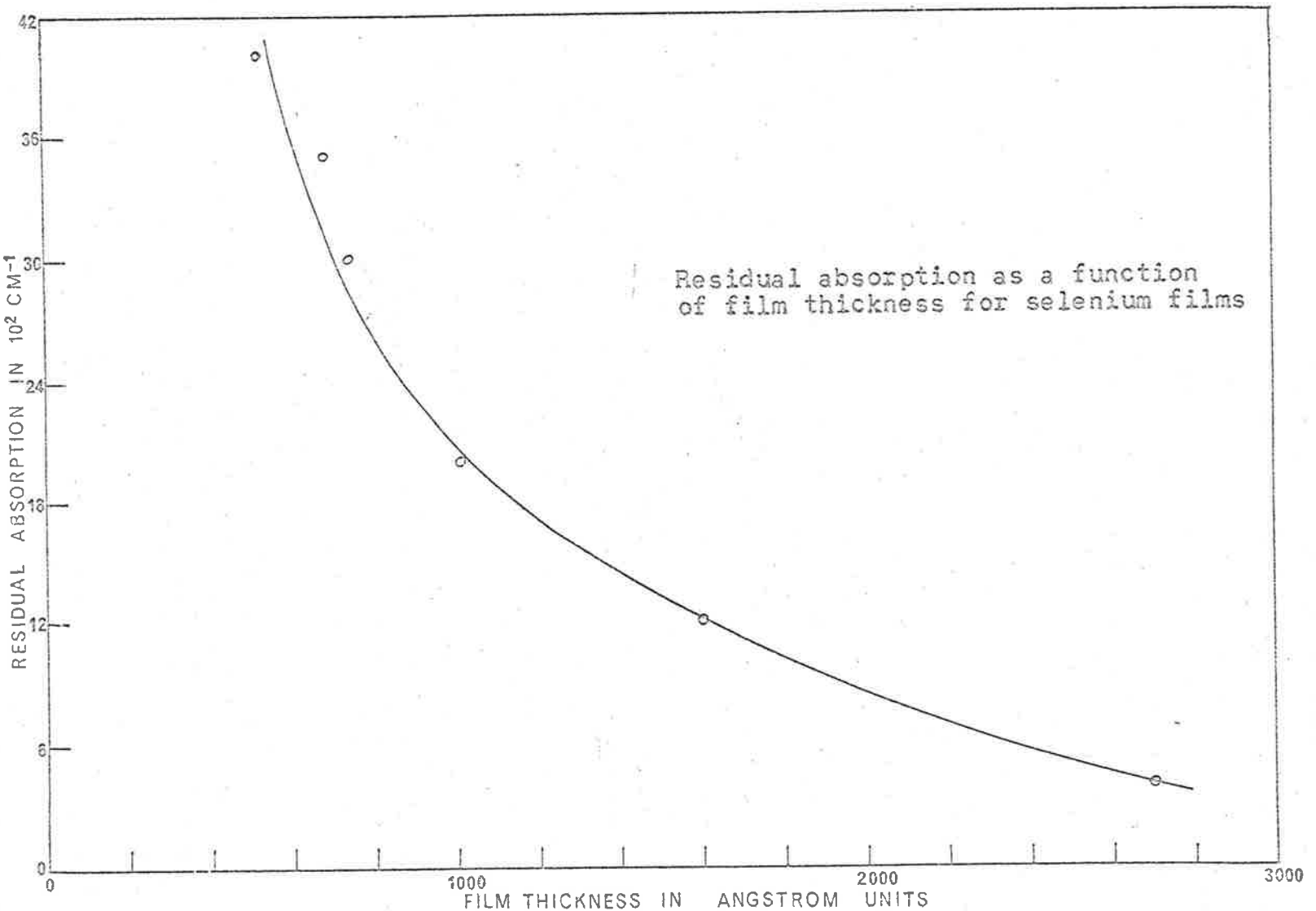
Residual absorption as a function
of film thickness for selenium films
RESIDUAL ABSORPTION IN 10^2 CM^{-1}
42
36
30
24
18
12
6
0
0
1000
2000
3000
FILM THICKNESS IN ANGSTROM UNITS

Figure 5.11

2300Å. For films less than about 1000Å thick most of the chains will be underdeveloped. Open-ended chains will abound in the material, particularly near the film surface. Campbell has attributed the low energy absorption mechanism to the ease with which electrons are excited at the open ends of the chains. As the thickness increases, and the chains become better developed, this absorption mechanism will decrease, in agreement with the present results.

The change in slope of the line in the EnK vs. E curve corresponds to the energy at which photoconductivity in the amorphous films rises sharply (Campbell, loc. cit.). Moss (1959) suggests that the difference in photon energy for absorption and photoconduction arises from potential barriers within the material which results from the basic structure of selenium. It is assumed that within individual chains of selenium atoms carriers may move freely, but that to travel to neighbouring chains it is necessary to cross potential barriers. It is suggested that these barriers are responsible for the difference in photon energy between the rise in absorption and photoconduction. It is also suggested that the barrier height corresponds to the difference in energy between the occurrence of the change in slope of the EnK vs. E curve and the energy at which the extrapolated line intersects the energy axis. For our measurements this is 0.3eV to 0.4eV. From the difference in photon energy levels between equivalent photoconduction and absorption levels, Moss (loc. cit.) estimates the barrier height as $\sim$ 0.6eV. It is suggested that our method affords a more accurate estimate. The change in slope of the EnK vs. E curve is associated with the change in the density of

allowed states when sufficient energy becomes available for the electrons to cross the potential barriers. The position of the change in slope can be determined with reasonable accuracy.

The above qualitative arguments account readily for the observed absorption in thin vitreous selenium films. Until further quantitive analyses are available to determine whether the above mechanism will result in a linear dependence of the absorption with energy, it is not possible to assess further the validity of the model.

CHAPTER 6.

OPTICAL PROPERTIES OF GERMANIUM FILMS.

6. 1 INTRODUCTION.

Considerable discrepancies exist in the published values of the optical constants of germanium films. No doubt, in many cases, accurate measurements have been taken of the reflectance and/or transmittance of these films but, as seen from the discussions in the previous chapters, these measurements must be followed by accurate calculations using exact theory to obtain accurate and meaningful results.

A brief summary of measurements on germanium films up to the present time is given. The results of our measurements and calculations are then presented, and a model to explain the observed absorption in the films is discussed.

6. 2 FORMS OF GERMANIUM FILMS.

Evaporation conditions for obtaining germanium films with varying degrees of crystalline perfection, from highly disordered amorphous films to relatively well-oriented epitaxial films, are well known (Kurov, Vasilev and Kosaganova, 1962, 1963; Kurov, Semiletov and Pinsker, 1957; Donovan and Ashley, 1964).

Films deposited at room temperature on fused quartz substrates are highly disordered and have an apparently amorphous structure, as shown by X-ray powder diffraction measurements on material scraped

from the quartz flats (Donovan and Ashley, loc. cit.).

Films deposited on quartz substrates at 325°C and higher are polycrystalline, while films evaporated onto substrates between 625°C and 725°C are polycrystalline and highly oriented, the principal planes being the (100) and (110) planes as shown by electron diffraction (Donovan and Ashley, loc. cit.).

Films deposited on single-crystal electropolished germanium substrates maintained at 800°C are shown by electron diffraction measurements to be epitaxial. That is, electron diffraction patterns of these films exhibit a spot structure and sharp Kichuchi lines similar to the patterns obtained from electropolished single crystals (Donovan and Ashley, loc. cit.).

Gebbie (1952) found that annealing his films after deposition for several hours at temperatures up to 525°C produced an electron diffraction pattern of fine Debye - Scherrer - Hull rings characteristic of the polycrystalline state.

Cardona and Harbeke (1963) have deposited epitaxial films on cleaved calcium flouride substrates at a temperature of 600°C. Reflection electron diffraction patterns clearly showed their epitaxial behaviour.

For the present investigation, amorphous films were prepared by evaporating germanium onto room temperature quartz substrates. Polycrystalline films were prepared either by evaporation onto quartz substrates at 350°C or by deposition onto room temperature quartz substrates and subsequent annealing at 350°C for several hours. The polycrystalline but highly oriented films were prepared by depositing

germanium onto room temperature quartz substrates and subsequently annealing them at 650°C for several hours.

6. 3 PREVIOUS CALCULATIONS OF THE OPTICAL CONSTANTS OF GERMANIUM FILMS.

Brattain and Briggs (1949) calculated the optical constants of thick polycrystalline films from transmission measurements. In the infra-red region, where the absorption is low, the refractive index was determined from the conditions for transmission maxima and minima. That is,

maximum transmission occurs when $2\,nd = m\,\lambda$

minimum transmission occurs when $2\,nd = \frac{1}{2}(2m+1)\lambda$

where n is the refractive index of the film, λ the wavelength, m the order of interference, and d the thickness of the film which was determined by weighing.

For the absorbing region they used a wedge of germanium deposited on a quartz substrate. The thickness versus distance was determined and then transmission versus distance. Using approximate equations, and neglecting the quartz-air interface, they calculated n and k at several wavelengths. For the highly absorbing region it was assumed that the transmission was an exponential function of the thickness whereby the logarithm of the transmission versus thickness should give a curve which is a straight line with a slope which determines k.

Lukes (1960) has determined n in the wavelength range 3500Å - 2.5μ and k in the region 3500Å - 7800Å from measured values of the reflectance and transmittance. To calculate k they used the method of

Brattain and Briggs, employing films of different thicknesses instead of a wedge-shaped film.

The refractive index was calculated, in the region 3500Å -- 8000Å, from the reflectance using the relation

$$R = \frac{(n_0-n)^2 + k^2}{(n_0+n)^2 + k^2}$$

where n_0 is the refractive index of air. This is the equation for the reflectance from an air - to - metal interface, and is only valid in the highly absorbing region. Greater than 9000Å, k was assumed to be zero and n determined from the transmission maxima and minima.

Grant and Paul (1964) determined n and k for an epitaxial film 250Å thick, in the region 2000Å - 6000Å, from measurements of the normal incidence reflectance and transmittance of the film. The film thickness was measured by infra-red transmissivity. They do not give details of their calculation procedure, only to say n and k were determined from the theoretical expressions for R and T through a Newton - Raphson iteration using a high-speed computer.

Tauc et al (1964, 1966, 1970) calculated the optical constants of amorphous and polycrystalline films for the wavelength range 5000Å - 3μ from measured values of normal incidence reflectance and transmittance. The refractive and absorption indices were determined from the formulae given by Mayer (1950), but no details of the calculation method were given. They found the optical properties of the polycrystalline layers were practically identical to those of single crystals. They also reported significant long wavelength absorption in the films, in agreement with the theoretical predictions

of Gubanov (1965).

Wales, Lovitt and Hill (1967) have determined n and k for amorphous and polycrystalline films in the region 1μ - 5μ. They determined n in a similar manner to Brattain and Briggs. For the absorption index, the observed transmission was compared with that calculated for pairs of n and k until the two agreed. However a large number of such pairs exist and it is difficult to assess the validity of their results.

Donovan, Spicer and Bennett (1969) investigated the absorption in amorphous films. From measurements of reflectance, transmittance and film thickness they calculated the absorption coefficient of the films using an iterative method described by Bennett and Booty (loc. cit.). This method of calculating n and k was shown in Chapter 3 to be doubtful as it may converge on the wrong solutions, particularly where the multiple solutions are close together.

They were particularly interested in determining whether long - wavelength absorption existed in the films as had been reported earlier (Tauc, loc. cit.). They found no evidence for absorption in the infra-red beyond the absorption edge, in agreement with their photoemission experiments.

The results of the above authors are summarized in Figure 6.1. There are seen to be wide variations between the various authors, showing the need for a more accurate and reliable determination of the optical constants of germanium films.

No previous worker has been able to take account of any oxide or surface layers which may form on the surface of the films, nor have

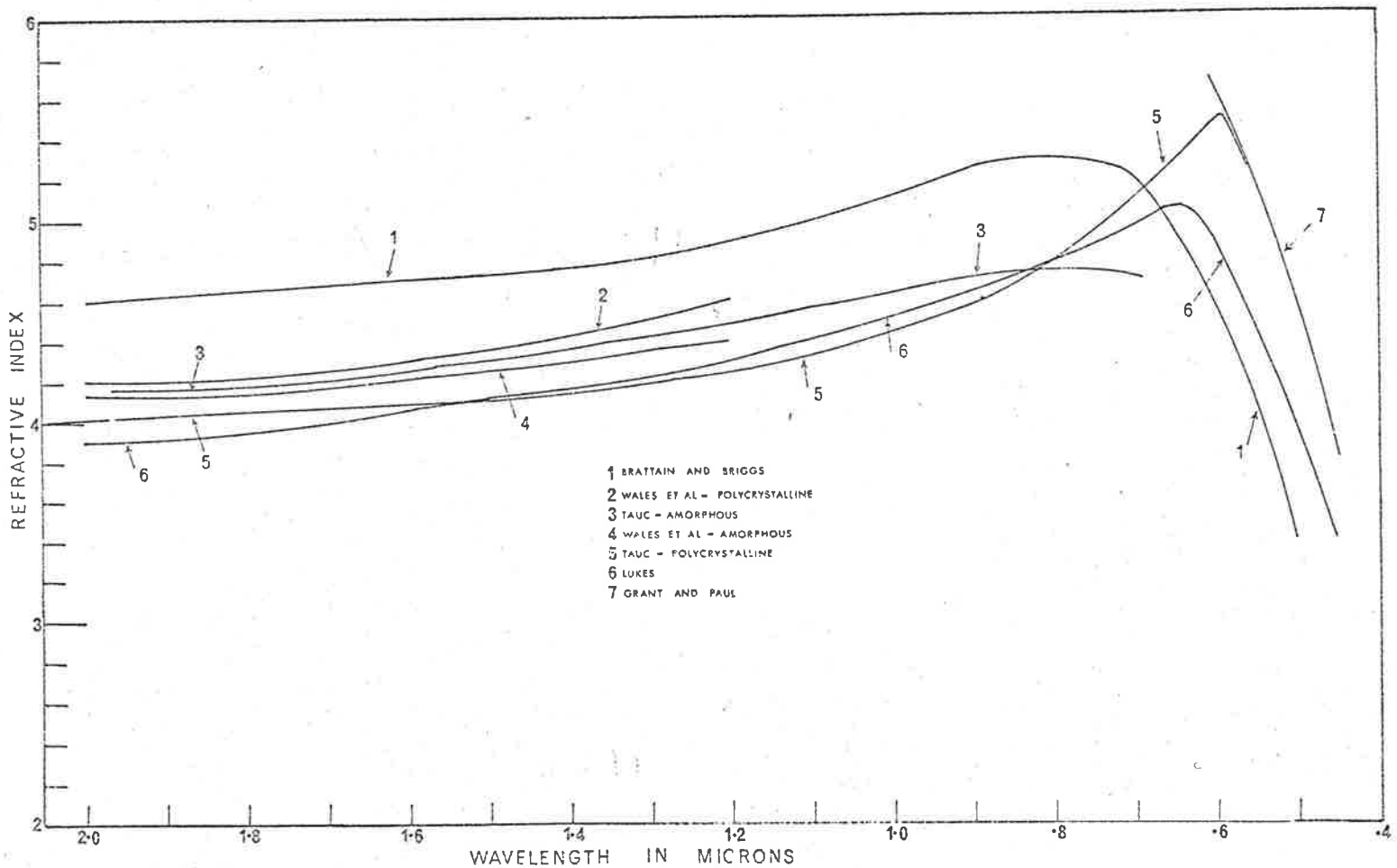
REFRACTIVE INDEX
6
5
4
3
2
2·0
1·8
1·6
1·4
1·2
1·0
·8
·6
·4
WAVELENGTH IN MICRONS
1 BRATTAIN AND BRIGGS
2 WALES ET AL - POLYCRYSTALLINE
3 TAUC - AMORPHOUS
4 WALES ET AL - AMORPHOUS
5 TAUC - POLYCRYSTALLINE
6 LUKES
7 GRANT AND PAUL

Figure 6.1.a

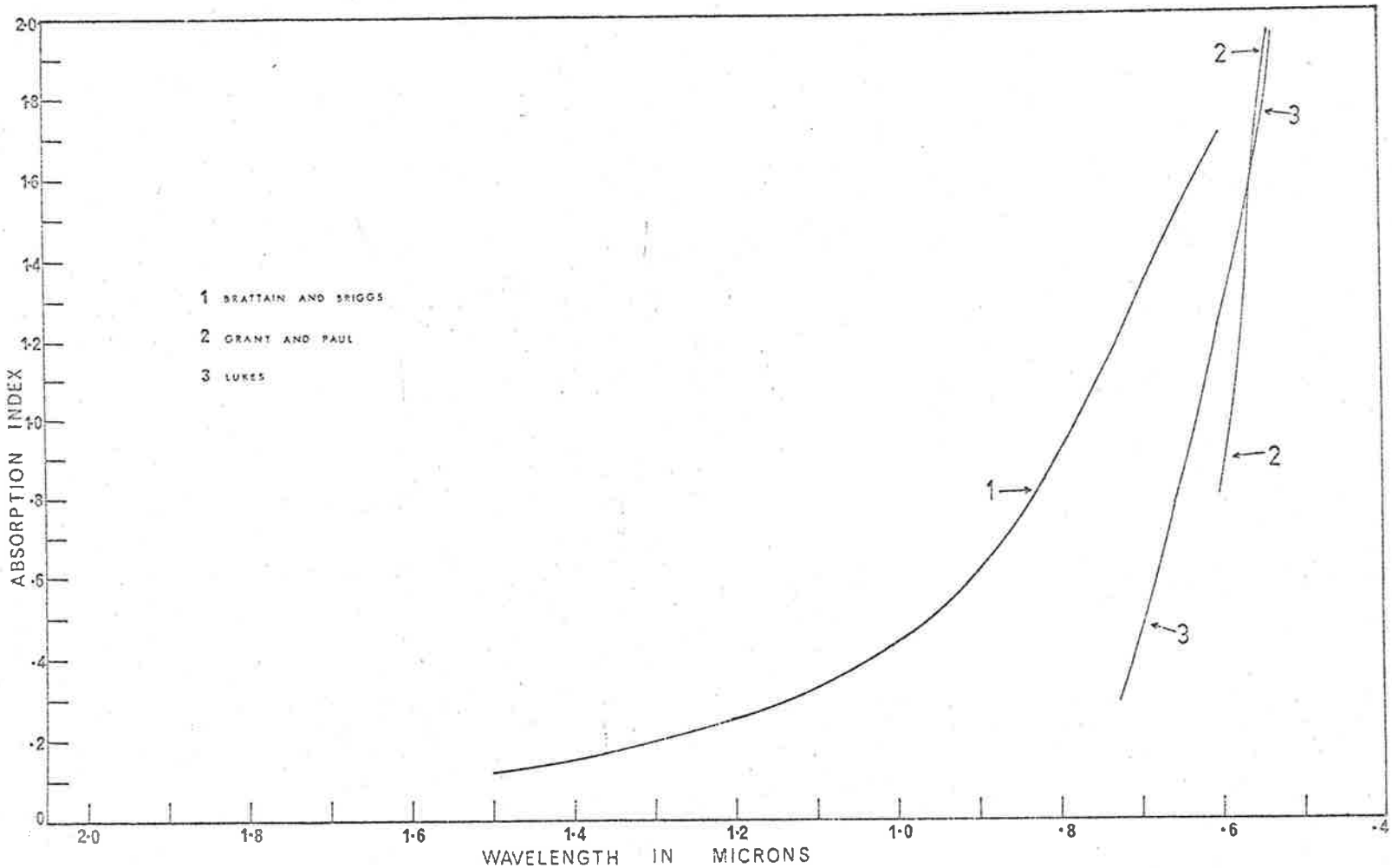
1 BRATTAIN AND BRIGGS
2 GRANT AND PAUL
3 LUKES
ABSORPTION INDEX
2·0
1·8
1·6
1·4
1·2
1·0
·8
·6
·4
·2
0
2·0
1·8
1·6
1·4
1·2
1·0
·8
·6
·4
WAVELENGTH IN MICRONS
1
2
3
2
3
2

Figure 6.1.b

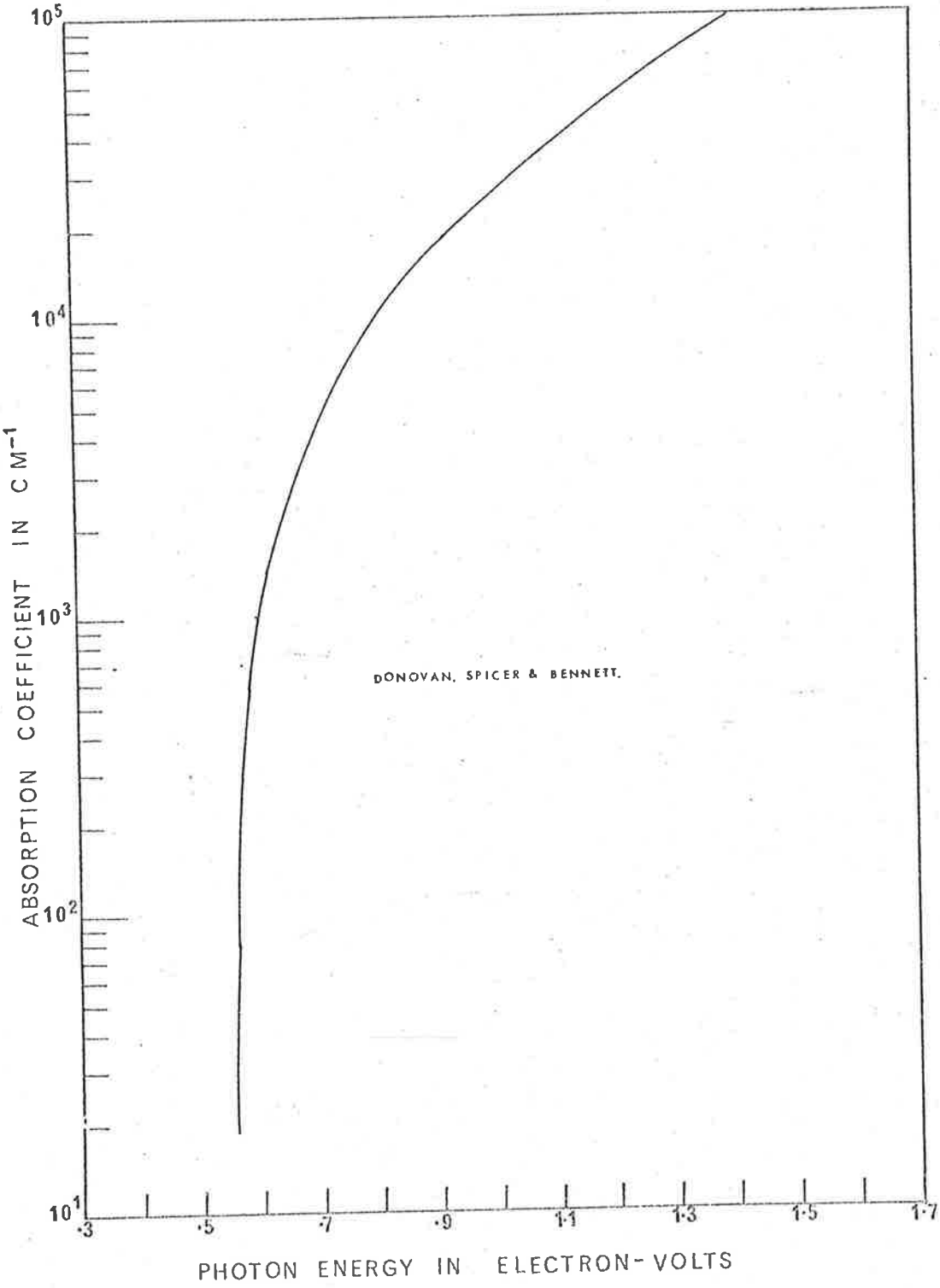
10^5
10^4
10^3
10^2
10^1
ABSORPTION COEFFICIENT IN $C M^{-1}$
DONOVAN, SPICER & BENNETT.
·3
·5
·7
·9
1·1
1·3
1·5
1·7
PHOTON ENERGY IN ELECTRON-VOLTS

Figure 6.1.c

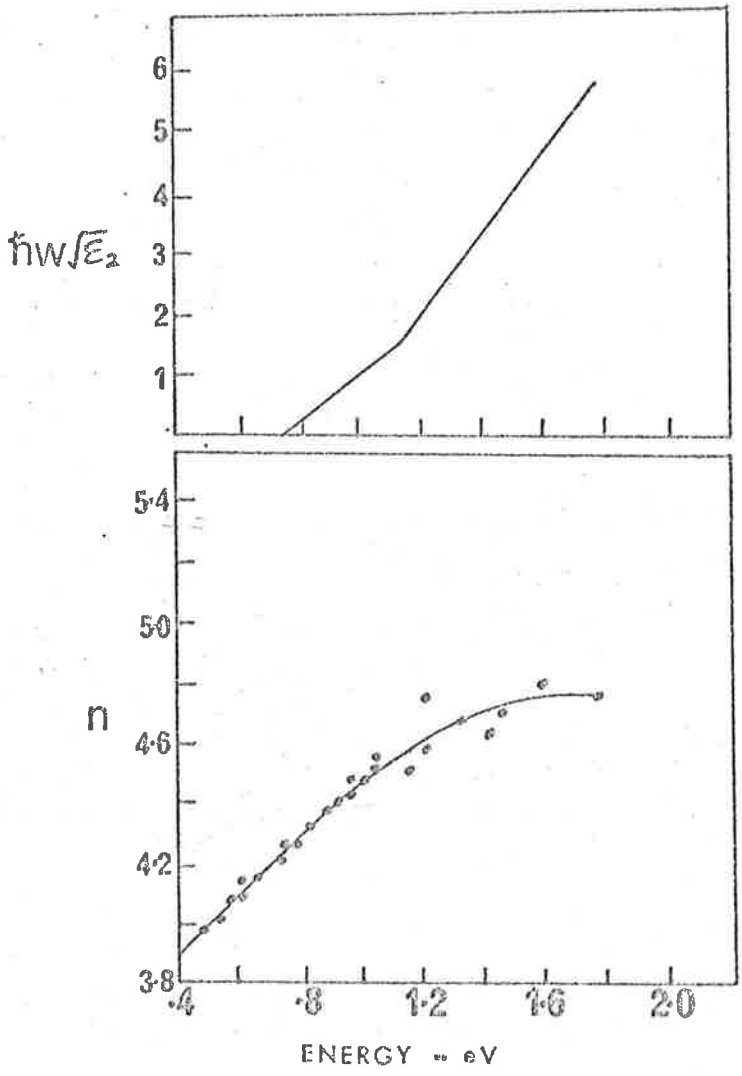

RESULTS OF TAUC

Figure 6.1.d

exact calculations been performed. Potter (1964), in his calculations on single crystals, arbitrarily corrected for an oxide layer 50Å thick.

The results presented below constitute the most accurate determination of the optical constants of germanium films thus far presented.

6. 4 REFLECTANCE AND TRANSMITTANCE OF GERMANIUM FILMS.

The reflectance and transmittance of 12 germanium films, measured with the reflectometer described in Chapter 2, are given in Appendix E. The curves for four of the films are plotted in Figure 6.2. As with the selenium films multiple beam interference effects are apparent, particularly in the thicker films. The estimated errors in the measured values of R and T are ±0.002.

6. 5 CALCULATED FILM AND OXIDE THICKNESSES.

The film and surface layer thicknesses of the germanium films, calculated by the method described in Chapter 4, are tabulated in Table 6.1. The exceptions are the first three films which were too thin for this method to be applicable. Their thicknesses were measured explicitly by the method of fringes of equal chromatic order described in Chapter 2. The thicknesses of some of the thicker films were also measured explicitly, the calculated total thicknesses agreeing well with the measured values. After a few films the practice of measuring the thickness of the thicker films was discontinued.

For many of the films, the closure of the refractive index curve

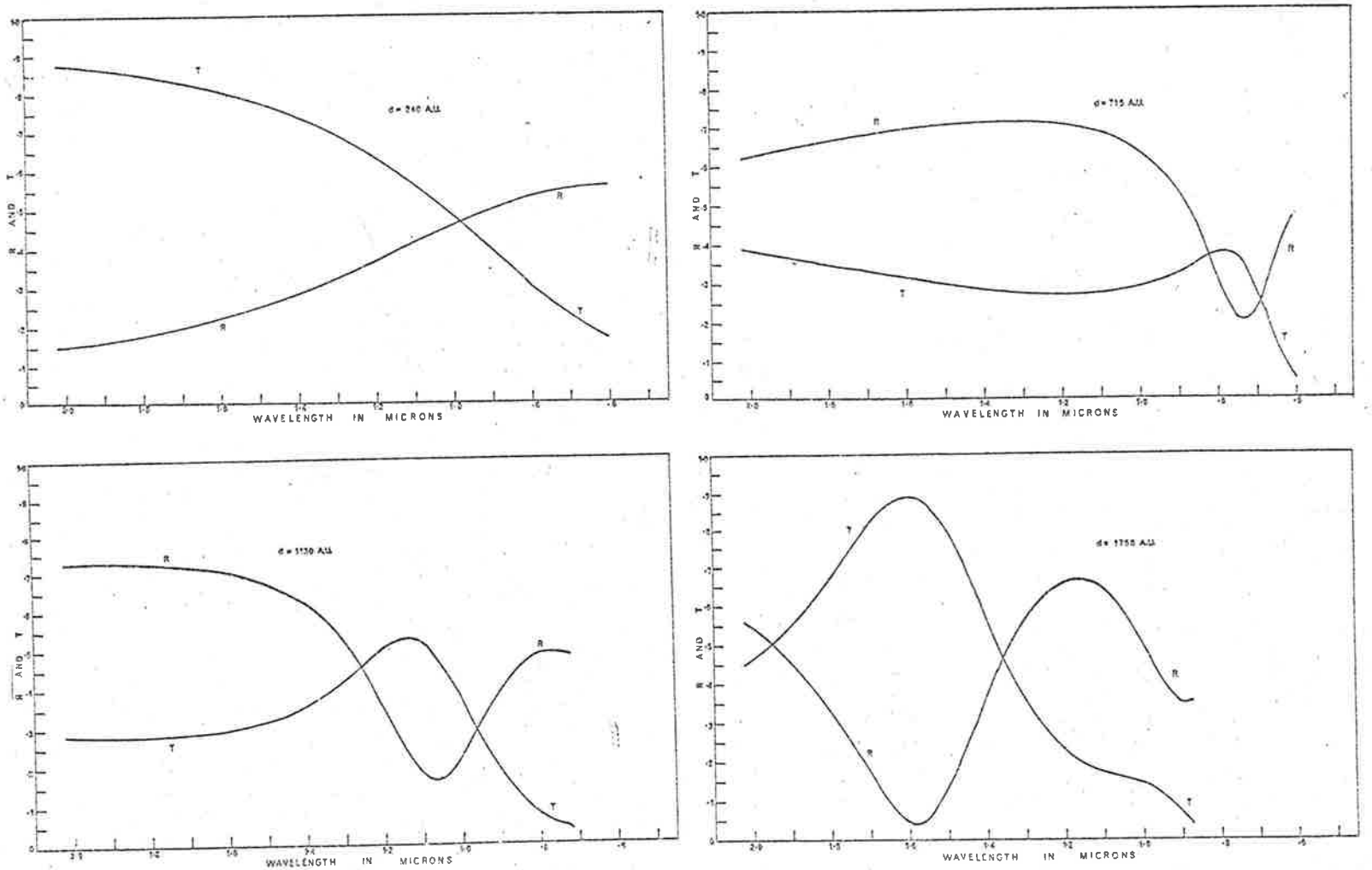

Figure 6.2

was sensitive to about five angstrom units in both film and surface layer thicknesses. This represents about one monolayer of substance which appears strange since the non-uniformity of the films would exceed this value. It is suggested that the calculated thicknesses are accurate averages taken over the area of the light beam on the films.

FILM NO.	EVAPORATION CONDITIONS.	d_1 CALC. (Å)	d_2 CALC. (Å)	(d_1+d_2) CALC. (Å)	MEASURED d (Å)
GE1	Room Temp.Substrate				240±20
GE2	" " "				250±20
GE3	" " "				510±25
GE4	" " "	10±3	997±3	1007±6	1020±23
GE5	" " "	0±2	1098±10	1098±12	
GE6	" " "	0±5	1130±5	1130±10	1147±35
GE7	" " "	0±5	1425±20	1425±25	
GE8	" " "	10±5	1750±20	1760±25	1743±46
GE9	Annealed at 350°C	0±5	915±40	915±45	
GE10	Deposited on 350°C substrate.	155±5	715±5	870±10	895±27
GE11	"	100±5	855±5	955±10	
GE12	Annealed at 650°C	0±5	1072±10	1072±15	

TABLE 6.1.

6. 6 OPTICAL CONSTANTS OF GERMANIUM FILMS.

The calculated refractive and absorption indices for all of the germanium films investigated are plotted in Appendix E. The solutions for one of the films are plotted in Figure 6.3. The behaviour of the solutions are similar to those for selenium. The behaviour of the errors is seen to be similar to those calculated for the selenium films. As with the selenium films only the correct solutions for the absorption index have been plotted.

6. 6. 1 AMORPHOUS FILMS.

Films with thickness greater than about 400Å produced similar results, and the refractive index and absorption index curves for these films are plotted together in Figure 6.4. The small variations from film to film are not surprising since one would expect the optical properties of a film to depend on the structure of the film. In turn, the structure of evaporated films depend on a number of conditions such as substrate temperature during and after evaporation, evaporation rate, partial pressures of the residual gases in the vacuum chamber, source temperature, etc. These conditions change slightly from film to film resulting in small variations in the optical properties of the films.

From these results however, reasonably accurate averages for the refractive and absorption indices can be drawn and are shown in Figure 6.5. These values have been used in the preparation of multilayer thin film interference filters with excellent agreement between predicted and experimental results (Ward, 1971).

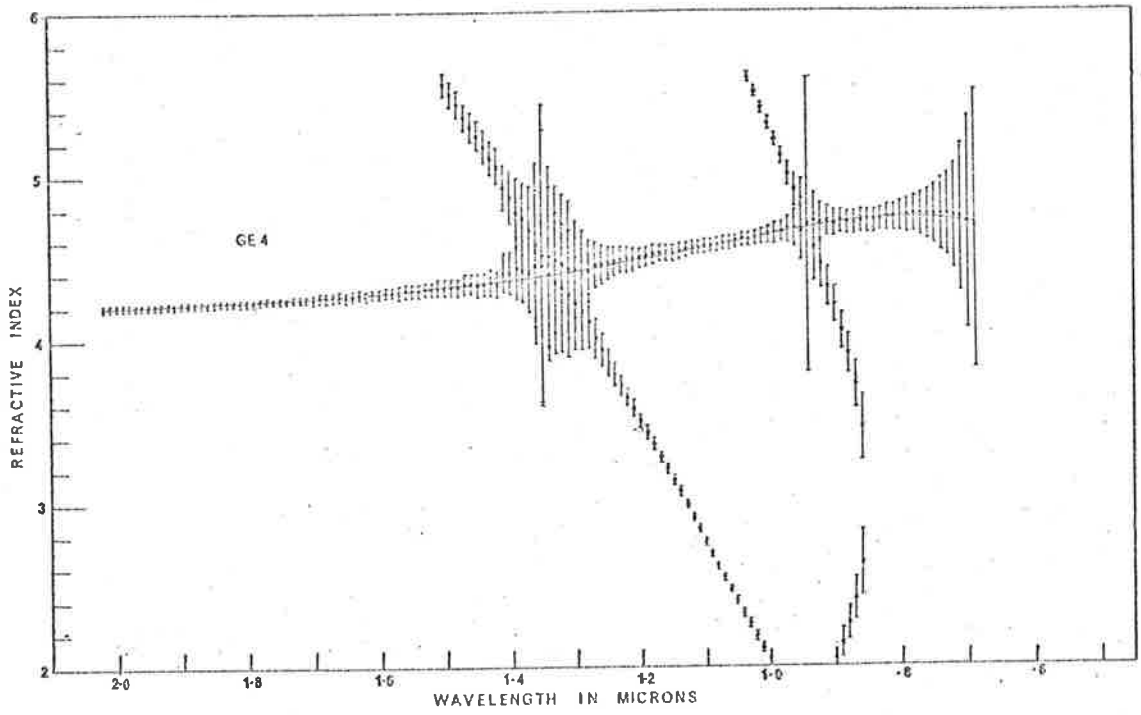

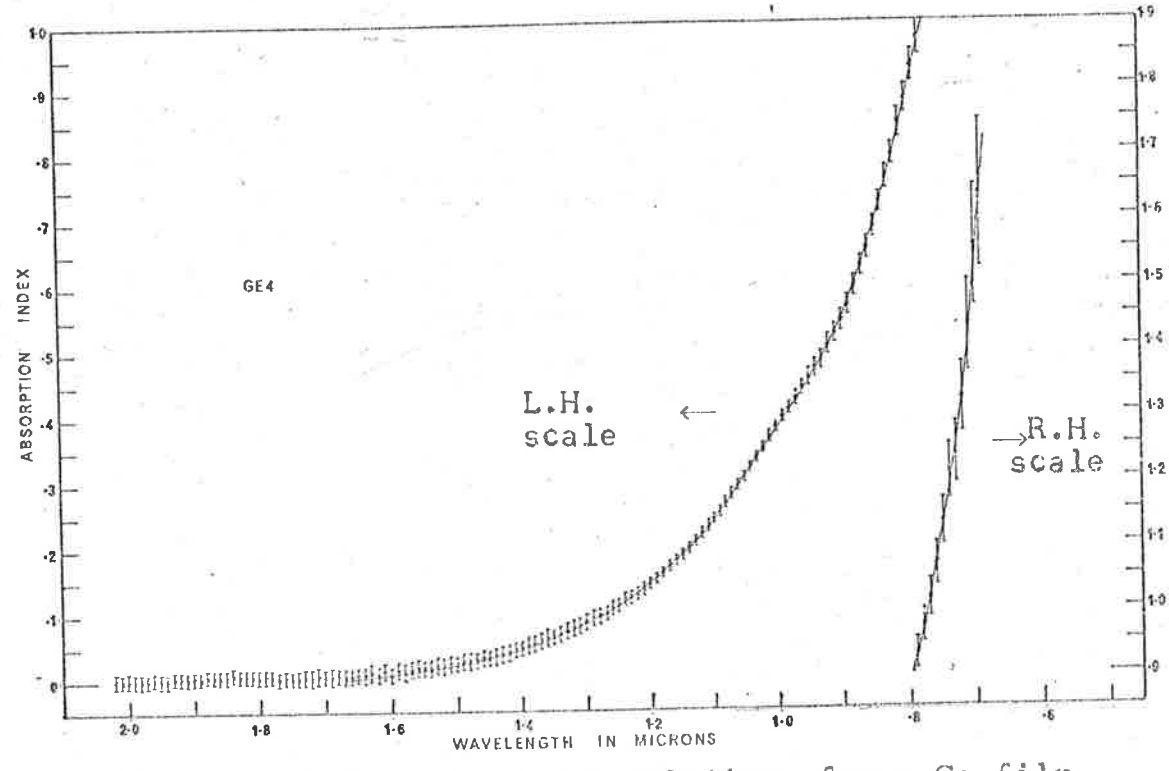

Example of the calculated solutions for a Ge film.
Figure 6.3

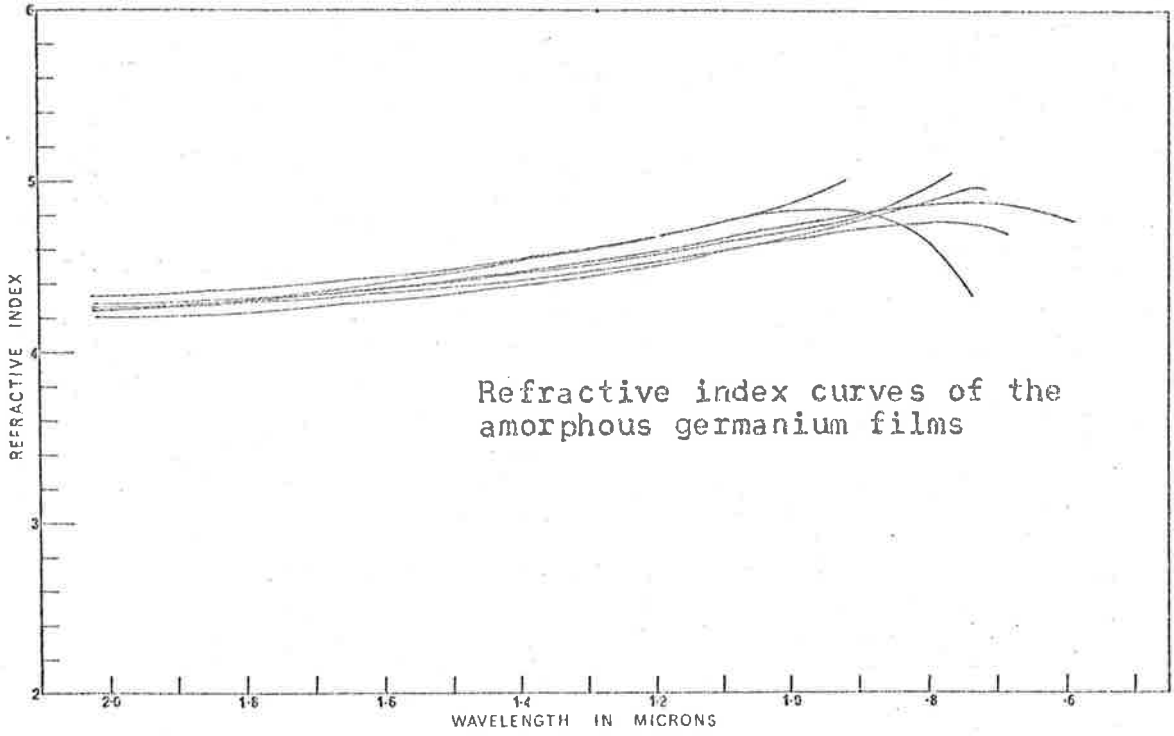

Refractive index curves of the amorphous germanium films

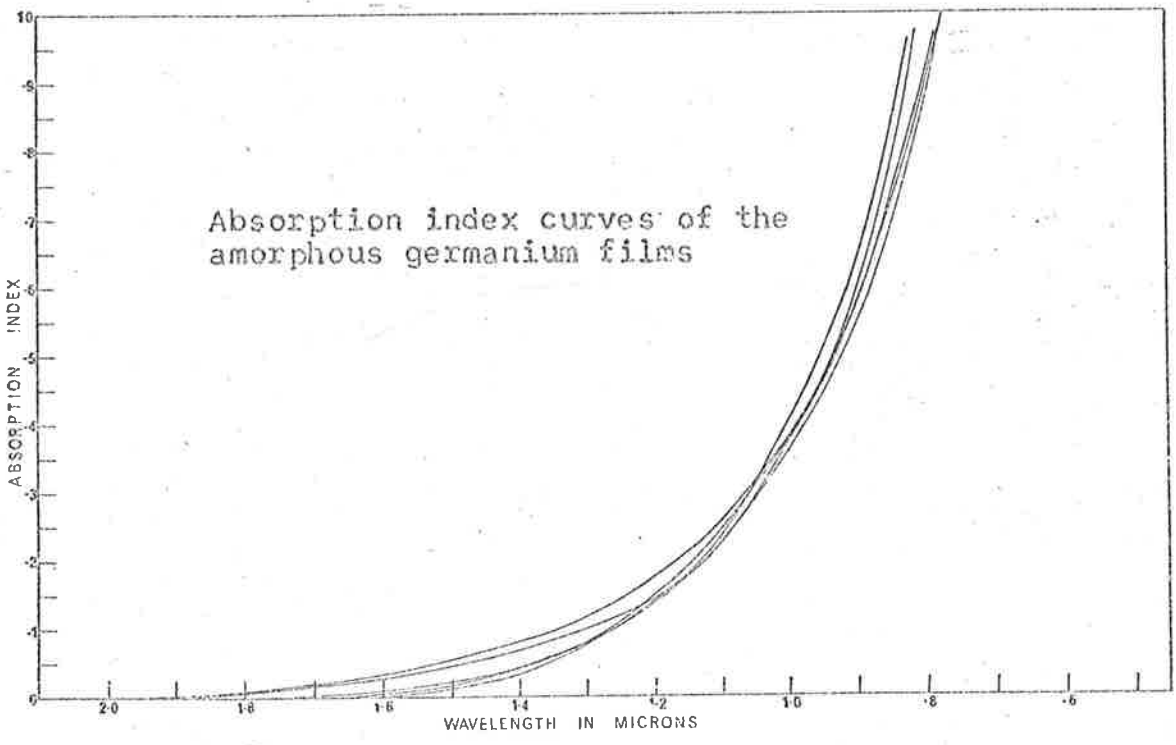

Absorption index curves of the amorphous germanium films

Figure 6.4

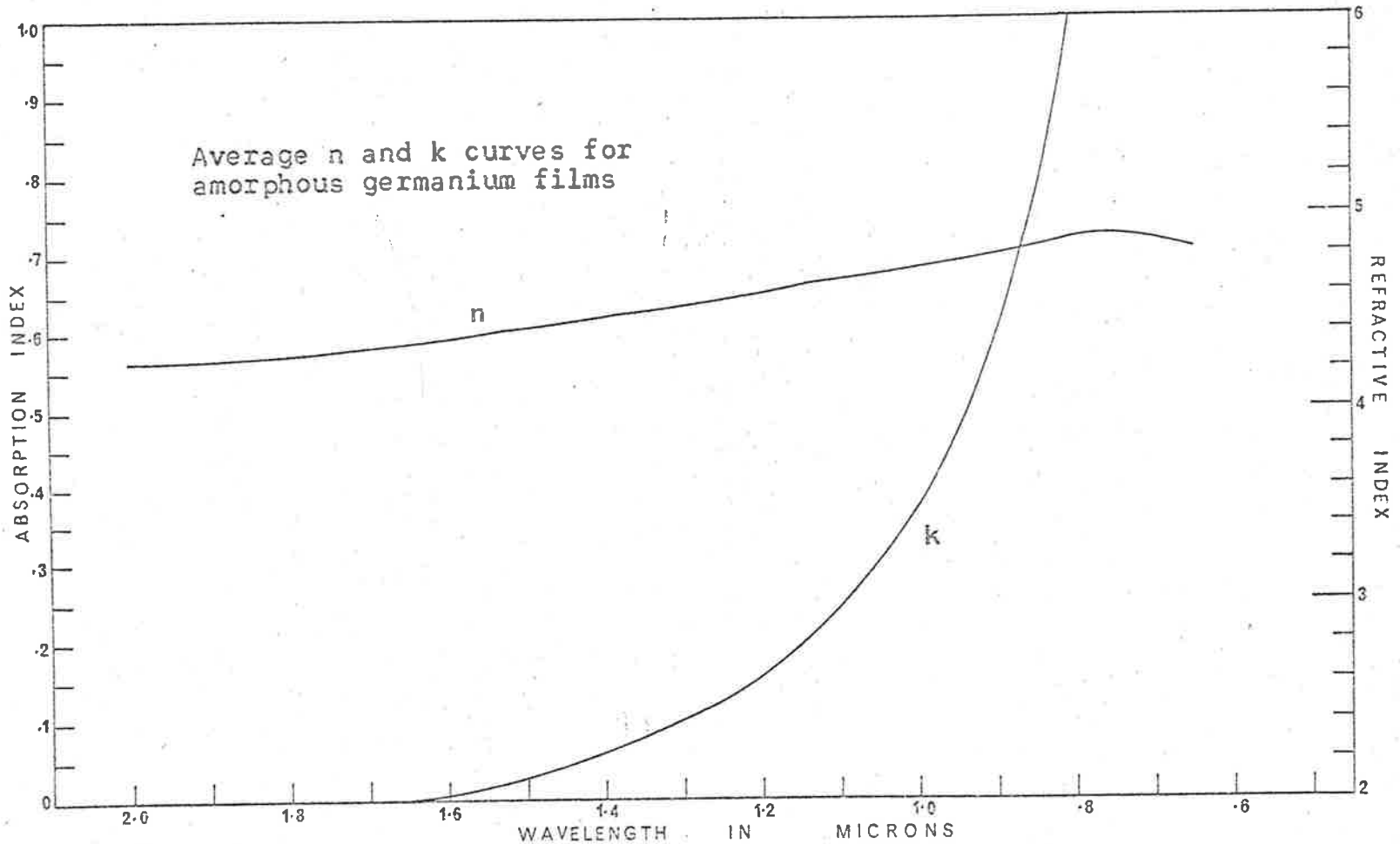
Average n and k curves for
amorphous germanium films
n
k
ABSORPTION INDEX
REFRACTIVE INDEX
WAVELENGTH IN MICRONS
1·0
·9
·8
·7
·6
·5
·4
·3
·2
·1
0
6
5
4
3
2
2·0
1·8
1·6
1·4
1·2
1·0
·8
·6

Figure 6.5

6. 6. 2 VERY THIN AMORPHOUS FILMS.

Films Ge1 (240Å thick) and Ge2 (250Å thick) had a much lower refractive index than the thicker amorphous films, and also exhibited an apparent shift in the absorption edge, the shift being towards the short wavelength end. The optical constants of film Ge1 are compared to those of a thicker film in Figure 6.6. This behaviour is readily explained on the basis of Schopper's theory (section 4.11.2). From equation 4.11.1.

$$N = \left(\{1 + \gamma(N_e^2 - 1)\}(1-f)/\{1 - \gamma f(N_e^2 - 1)\} \right)^{\frac{1}{2}} \qquad 6.6.1$$

For values of $\gamma = 1.02$ and $f = 0.012$, the results of film Ge1 are brought into near agreement with those of the thicker film, as can be seen in Figure 6.6. Considering the simplifications involved, the agreement is excellent.

The small value of f indicates that the major axis of the ellipsoids, parallel to the substrate, is much larger than the minor axis. That is, the film consists of long islands. This picture is consistent with studies of the kinetics of the formation of thin evaporated films (Johnson, 1965), which show that initially some atoms form nuclei on the substrate about which the film grows, at first in the form of islands. These islands grow until eventually the deposition is uniform over the entire substrate. Studies on cadmium sulphide films in this laboratory (Goodwin, 1971) show that for these films the deposition does not become uniform until a thickness of about 300Å. Electron microscope examinations of selenium films by Campbell (loc. cit.) showed that very thin films were discontinuous and consisted of islands.

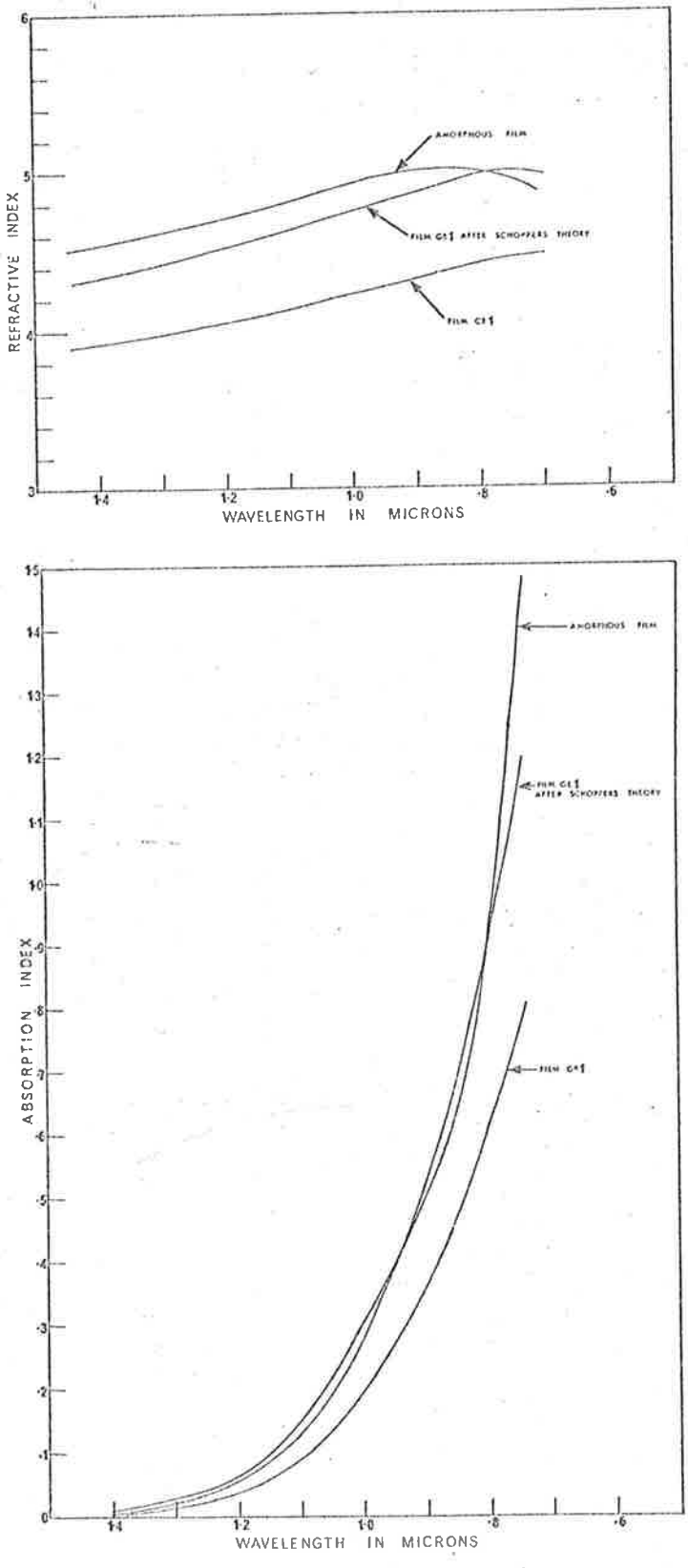

Application of Schopper's theory to a very thin film.

Figure 6.6

Thus the postulation of very thin germanium films consisting of ellipsoids, although simplified by the assumption that they are the same size, is therefore reasonable and in agreement with experimental observations.

6. 6. 3 FILMS ANNEALED AT 350°C AND FILMS DEPOSITED ON SUBSTRATES AT 350°C.

The films deposited on room temperature substrates and subsequently annealed at 350°C for several hours exhibited optical constants similar to those which were not annealed. The optical constants of films deposited on substrates preheated to 350°C showed similar behaviour to the very thin amorphous films; that is, the refractive index was smaller and the absorption edge appeared to have shifted to shorter wavelengths.

It appears that these films have a different structure to those deposited on room temperature substrates, this structure arising in some way from the presence of a hot substrate during the evaporation. We have already seen that the surfaces of these films are wrinkled which is not the case for the other methods of film preparation we have used. There is a need for further experiments on these films before any conclusions can be drawn, particularly in relation to the kinetics of the formation of these films and their subsequent structure.

Apart from this difference, the optical constants of amorphous and polycrystalline films exhibit a similar dependence on wavelength. These results are consistent with the theory of absorption in germanium films to be presented in section 6.7.

6. 6. 4 OPTICAL CONSTANTS OF FILMS ANNEALED AT 650°C.

The optical constants of a germanium film annealed at 650°C are compared to those of an amorphous film in Figure 6.7. The refractive index of the high temperature film is slightly less than that for the amorphous film. There is a significant difference in the absorption indices of the two films. Initially both films show similar behaviour, but at a wavelength of about 1.05μ the high temperature film absorption index departs markedly from that of the amorphous film. The significance of this will be discussed in section 6.7.

6. 7 ABSORPTION PROCESSES IN GERMANIUM FILMS.

The theory of absorption processes in crystalline materials is treated in detail in a number of books (see, for example, Smith in "Wave Mechanics of Crystalline Solids," 1961). A brief treatment is presented and this is then extended to the case of amorphous germanium films.

6. 7. 1 BASIC THEORY.

The interaction between the incident electro-magnetic radiation and the electrons in a semiconducting crystal is described by the Hamiltonian

$$H_{rad} = \frac{e}{m} \underset{\sim}{A} \cdot \underset{\sim}{p} \qquad 6.7.1$$

where $\underset{\sim}{A}$ is the vector potential of the electromagnetic field and $\underset{\sim}{p}$ the momentum operator.

For radiation of wave vector $\underset{\sim}{k}_{rad}$ and angular frequency ω

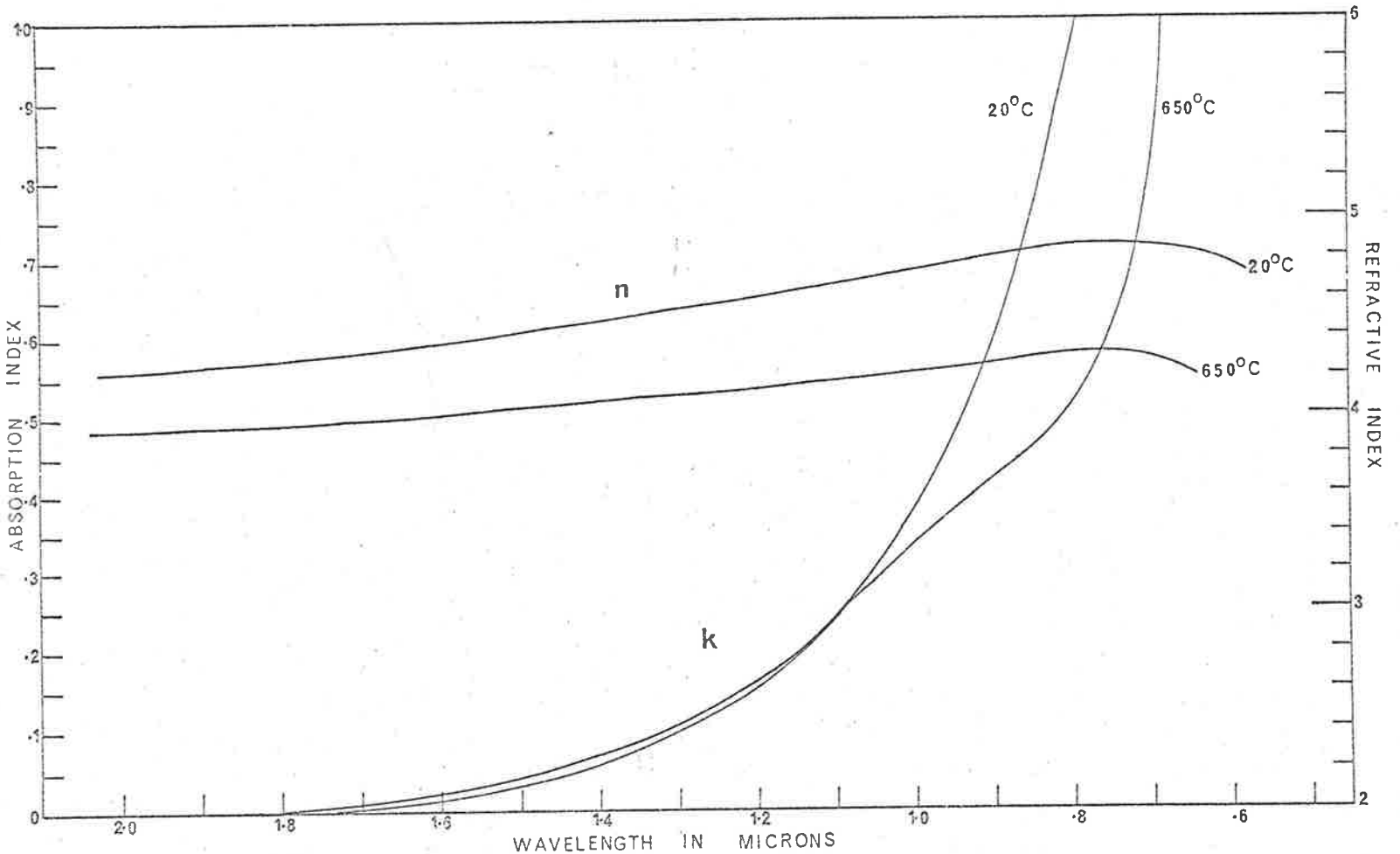
ABSORPTION INDEX
REFRACTIVE INDEX
WAVELENGTH IN MICRONS
20°C
650°C
n
k
20°C
650°C
1·0
·9
·8
·7
·6
·5
·4
·3
·2
·1
0
6
5
4
3
2
2·0
1·8
1·6
1·4
1·2
1·0
·8
·6

Figure 6.7

$$\underset{\sim}{A} = A_0 \underset{\sim}{\alpha} \cos(\omega t - \underset{\sim}{k}_{rad} \cdot \underset{\sim}{r}) \qquad 6.7.2$$

where $\underset{\sim}{\alpha}$ is a unit vector in the direction of polarisation of the radiation.

Equation 6.7.1 may then written

$$H_{rad} = \frac{eA_0}{2m} \left[\exp\{i(\omega t - \underset{\sim}{k}_{rad} \cdot \underset{\sim}{r})\} + \exp\{-i(\omega t - \underset{\sim}{k}_{rad} \cdot \underset{\sim}{r})\} \right] \underset{\sim}{\alpha} \cdot \underset{\sim}{p} \qquad 6.7.3$$

The first and second part of equation 6.7.3 represent the emission and absorption of a photon respectively. Thus the transition probability for absorption may be determined by applying time dependent perturbation theory to the second part. Integrating over a range of frequencies for the incident radiation (random phase approximation) gives

$$W_{if} \propto \left| \langle i | \exp i(\underset{\sim}{k}_{rad} \cdot \underset{\sim}{r}) \underset{\sim}{\alpha} \cdot \underset{\sim}{p} | f \rangle \right|^2 \delta(E_i - E_f - \hbar\omega) \qquad 6.7.4$$

where W_{if} is the transition probability per unit time between the two energy levels E_i and E_f. The total energy of frequency ω absorbed per unit volume per unit time is then

$$P(\omega) = \sum_i \sum_f (E_i - E_f) W_{if} \qquad 6.7.5$$

where the summation is over all initial and final states per unit volume. If $\underset{\sim}{S}$ is the poynting vector, then the absorption coefficient K is given by

$$K = \frac{\hbar\omega P(\omega)}{|\underset{\sim}{S}|}$$

$$= \frac{C}{\hbar\omega n} \sum_i \sum_f \left| \langle i | \exp i(\underset{\sim}{k}_{rad} \cdot \underset{\sim}{r}) \underset{\sim}{\alpha} \cdot \underset{\sim}{p} | f \rangle \right|^2 \delta(E_i - E_f - \hbar\omega) \qquad 6.7.6$$

where C is a constant.

The absorption can therefore be found by summing over all non-zero matrix elements between the initial and final states $\langle i|, \langle f|$, for which the energy is equal to the photon energy $\hbar\omega$.

Tauc (1965) has shown that if the matrix element changes only slightly for all the possible transitions then it may be put in front of the summation and the summation replaced by g(E), where g(E)dE is the number of possible transitions per unit volume in which the transition energy lies in the range E to E+dE. The function g(E) is known as the joint density of states function. Equation 6.7.6 then becomes

$$K(\omega) = \frac{C}{\hbar\omega n} \left|M_{if}\right|^2 g(\omega) \qquad 6.7.7$$

where

$$M_{if} = \langle i|\exp i(\underset{\sim}{k}_{rad}\cdot\underset{\sim}{r})\underset{\sim}{\alpha}\cdot\underset{\sim}{p}|f\rangle$$

6. 7. 2 DIRECT TRANSITIONS.

The matrix element M_{if} may be evaluated as follows:

$$M_{if} = -i\hbar\int_V \psi_i^*\{\exp i(\underset{\sim}{k}_{rad}\cdot\underset{\sim}{r})\underset{\sim}{\alpha}\cdot\nabla\}\psi_f \, dV$$

where ψ_i and ψ_f are the wave functions of the initial and final states respectively. For a periodic lattice these may be written in the familiar Bloch form

$$\psi_n(\underset{\sim}{r},\underset{\sim}{k}) = U_n(\underset{\sim}{r},\underset{\sim}{k})\exp i(\underset{\sim}{k}\cdot\underset{\sim}{r})$$

where $U_n(\underset{\sim}{r},\underset{\sim}{k})$ has the periodicity of the lattice.

Thus

$$M_{if} = -i\hbar\int_V U_i^*(\underset{\sim}{r},\underset{\sim}{k}_i)\exp(-i\underset{\sim}{k}_i\cdot\underset{\sim}{r})\exp\{i(\underset{\sim}{k}_{rad}\cdot\underset{\sim}{r})\underset{\sim}{\alpha}\cdot\nabla\}U_f(\underset{\sim}{r},\underset{\sim}{k}_f)\exp(i\underset{\sim}{k}_f\cdot\underset{\sim}{r}) \, dV$$

where $\underset{\sim}{k}_i$ and $\underset{\sim}{k}_f$ are the wave vectors of the initial and final electron states respectively.

$$M_{if} = -i\hbar\int_V U_i^*\{\underset{\sim}{\alpha}\cdot\nabla U_f + i(\underset{\sim}{\alpha}\cdot\underset{\sim}{k}_f)U_f\}\exp i\{(\underset{\sim}{k}_f + \underset{\sim}{k}_{rad} - \underset{\sim}{k}_i)\cdot\underset{\sim}{r}\}\, dV \qquad 6.7.8$$

Using the periodicity of U_i and U_f

$$M_{if} = -i\hbar\int_{\text{unit cell}} \phi(\underset{\sim}{r},\underset{\sim}{k}_i,\underset{\sim}{k}_f)\, dV \sum_j \exp i(\underset{\sim}{k}_f + \underset{\sim}{k}_{rad} - \underset{\sim}{k}_i)\cdot\underset{\sim}{R}_j \qquad 6.7.9$$

Where $\underset{\sim}{R}_j$ is the vector to the j-th cell.

The summation in equation 6.7.9 may be shown to be zero unless either

$$\underset{\sim}{k}_f + \underset{\sim}{k}_{rad} - \underset{\sim}{k}_i = 0 \quad \text{or} \quad 2\pi\underset{\sim}{b}_n \qquad 6.7.10$$

where $\underset{\sim}{b}_n$ is a reciprocal lattice vector. $\underset{\sim}{k}_{rad}$ is very small for optical wavelengths and therefore the second condition does not apply, thus:

$$\underset{\sim}{k}_i - \underset{\sim}{k}_f = \underset{\sim}{k}_{rad}$$

$$\text{i.e.} \quad \underset{\sim}{k}_i \simeq \underset{\sim}{k}_f \qquad 6.7.11$$

This requirement therefore severely limits the number of initial and final states which can contribute to the absorption for a given energy of separation $\hbar\omega$. Such transitions are known as direct transitions where the wave vector of the electron is conserved during the transition. If E_c is measured up from the bottom of the conduction band and E_v down from the top of the valence band then

$$\hbar\omega = E_g + E_c + E_v \qquad 6.7.12$$

The joint density of states function is given by

$$g(E) = g_c(E_c) + g_v(E_v) \qquad 6.7.13$$

If the energy dependence for the valence and conduction bands can be represented by the usual k^2 approximation near the band edge, then

$$E_c = \frac{\hbar k^2}{2m_c^*} \quad \text{and} \quad E_v = \frac{\hbar k^2}{2m_v^*} \qquad 6.7.14$$

where m_c^* and m_v^* are the effective masses of electrons and holes respectively. Using equation 6.7.14 and the fact that $\underset{\sim}{k}$ before transition is equal to $\underset{\sim}{k}$ after transition, gives

$$g(E) \propto (E - E_g)^{\frac{1}{2}}$$

Hence

$$K(E) \propto \frac{C}{\hbar\omega n} |M_{if}|^2 (E - E_g)^{\frac{1}{2}}$$

i.e.

$$\hbar\omega n K(E) \propto (E - E_g)^{\frac{1}{2}} \qquad 6.7.15$$

6. 7. 3 INDIRECT TRANSITIONS.

In a periodic structure the conditions given by equation 6.7.11 can be relaxed by conserving momentum with an electron-phonon interaction at the same time as the transition. The transition probability is calculated by first considering that the electron makes a vertical transition to a virtual state where the lifetime is short and energy is not conserved. Electron-phonon scattering then takes place so that both energy and momentum are finally conserved. Figure 6.8.b is a diagrammatic representation of the transition.

For these phonon-assisted transitions

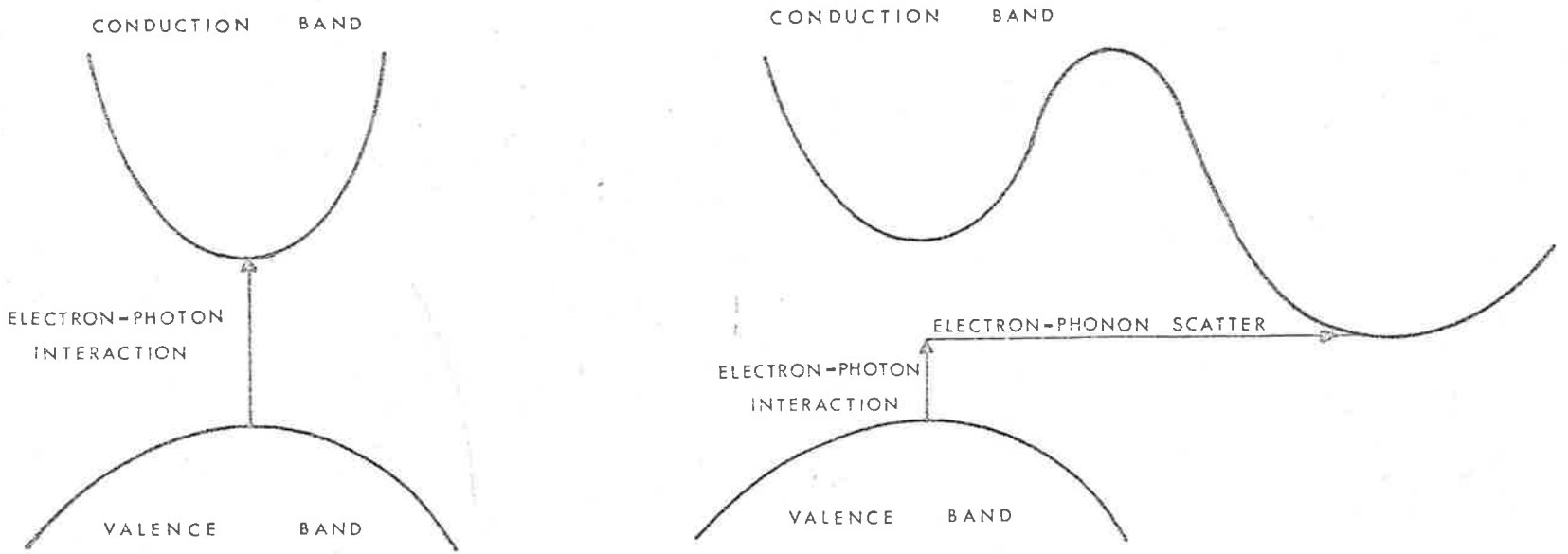

(a) DIRECT TRANSITION

(b) INDIRECT TRANSITION

Figure 6.8

$$g(E) \propto (\hbar\omega - E_g' \pm \hbar\omega_{ph})^2$$

where E_g' is the indirect band-gap and ω_{ph} the phonon frequency. Since $\hbar\omega_{ph}$ is very small, then to a good approximation

$$\hbar\omega nK(E) \propto (E - E_g')^2 \qquad 6.7.16$$

6. 7. 4 ABSORPTION IN CRYSTALLINE GERMANIUM FILMS.

Band structure calculations on crystalline germanium (Herman, 1954, 1955) show that its valence and conduction bands are represented by Figure 6.8.b. From equations 6.7.15 and 6.7.16, the absorption in a crystal may be represented by

$$E - E_g \propto \{\hbar\omega nK(E)\}^\beta$$

where $\beta = 2$ for direct transitions and $\beta = \frac{1}{2}$ for indirect transitions. A plot of $\{\hbar\omega nK(E)\}^\beta$, as a function of photon energy E, for various values of β may therefore be expected to reveal the absorption processes in the material.

For germanium films which had been annealed at 650°C, the value of β was $\frac{1}{2}$ for photon energies from 0.75eV to 1.1eV, and β was 2 for photon energies from 1.1eV to 1.5eV. This can be seen in Figure 6.9 where $\{\hbar\omega nK(E)\}^{\frac{1}{2}}$ and $\{\hbar\omega nK(E)\}^2$ have been plotted against E.

The initial absorption in these films is thus of the form given for indirect transitions, where the minimum in the conduction band and maximum in the valence band correspond to different values of the electron wave vector $\underset{\sim}{k}$. The energy separation between these two points is 0.75eV. The absorption then changes to the form given for direct transitions, where a minimum in the conduction band corresponds

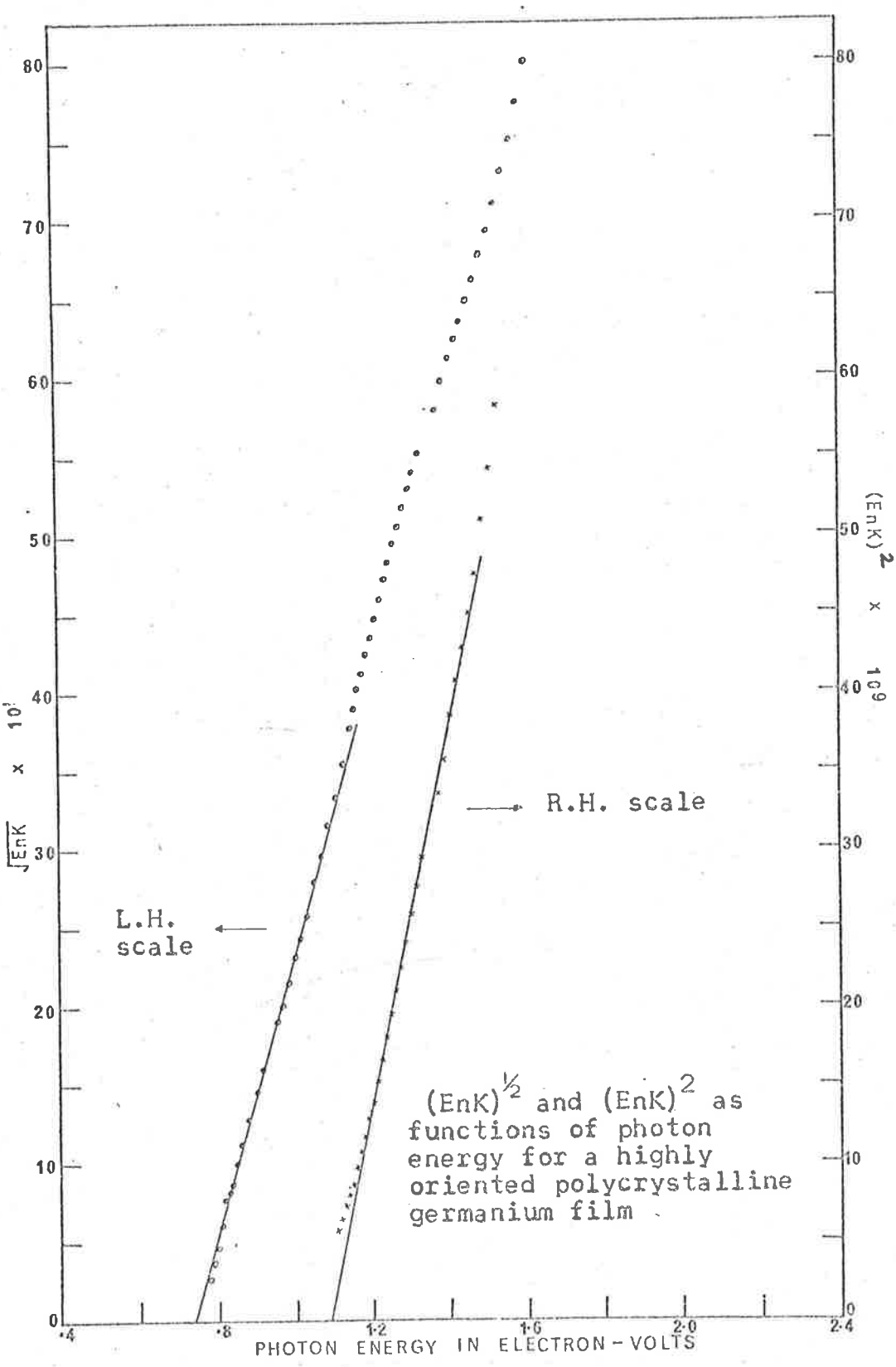
80
70
60
50
40
30
20
10
0
$\sqrt{EnK}$ x 10^1
$(EnK)^2$ x 10^9
R.H. scale
L.H. scale
$(EnK)^{1/2}$ and $(EnK)^2$ as functions of photon energy for a highly oriented polycrystalline germanium film
·4
·8
1·2
1·6
2·0
2·4
PHOTON ENERGY IN ELECTRON-VOLTS

Figure 6.9

to the minimum in the valence band for the same $\underset{\sim}{k}$. The vertical energy gap in this case is about 1.1eV.

Thus the band structure and absorption processes in the highly oriented polycrystalline films are basically unaltered from those found for single crystal germanium. The main difference is in the values of the thresholds for the onset of indirect and direct transitions, those for single crystal germanium being 0.62eV and 0.81eV respectively (Dash and Newman, 1955), compared to 0.75eV and 1.1eV for the films.

6. 7. 5 ABSORPTION IN AMORPHOUS FILMS.

Initially the absorption in the amorphous germanium films follows that of the highly oriented polycrystalline films. That is from 0.72eV to about 1.1eV the absorption follows the form given for indirect transitions. From 1.1eV to about 1.4eV the absorption also follows the same form, as is shown in Figure 6.10 where $\{\hbar\omega nk(E)\}^{\frac{1}{2}}$ has been plotted as a function of E for the amorphous films. It is seen to consist of two straight lines with a change in slope at 1.1eV, and intersecting the energy axis at 0.72eV. This behaviour has also been observed by Tauc (loc. cit.).

Thus either the band structure, or absorption process or both have changed for amorphous germanium. Theoretical calculations on amorphous semiconductors by Gubanov (loc. cit.) indicate that the essential features of the band structure remain unaltered, except for a possible change in the magnitudes of the energy gaps, which would mean that the absorption process has altered.

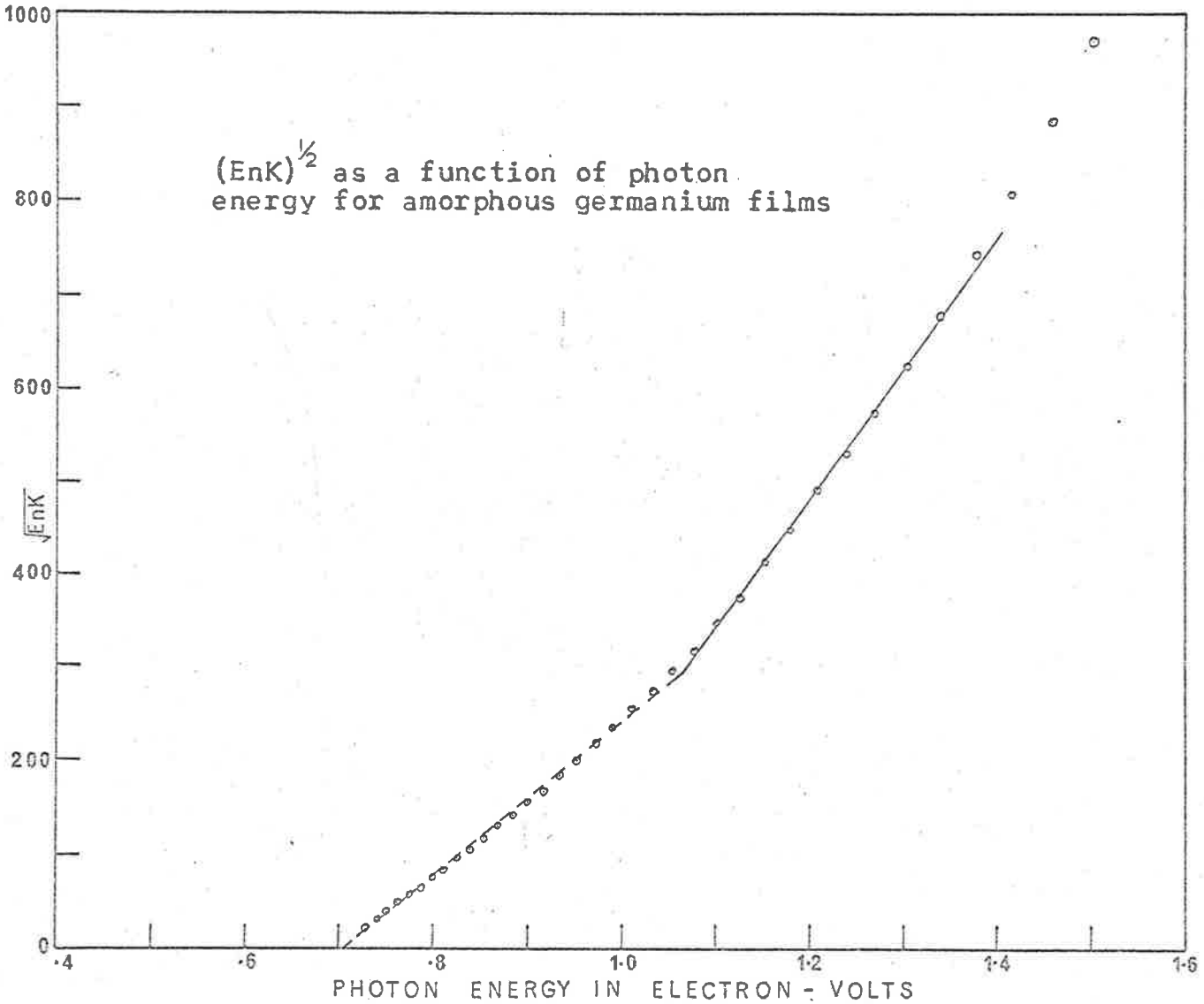
$(EnK)^{1/2}$ as a function of photon energy for amorphous germanium films
1000
800
600
400
200
0
$\sqrt{EnK}$
·4
·6
·8
1·0
1·2
1·4
1·6
PHOTON ENERGY IN ELECTRON - VOLTS

Figure 6.10

The derivation of the joint density of states function, g(E), for direct transitions was evaluated using all initial and final states for which both energy and momentum were conserved. The conservation of momentum given by equation 6.7.11 depends upon the electron wave function being represented by a Bloch wave, and the regular periodicity of the lattice allowing the separation of the integral in equation 6.7.8 into two parts, (1) an integral over the unit cell and (2) the sum over all unit cells in the crystal. In general it may be said that translational invariance would lead to conservation of momentum.

In an amorphous structure where either of both of these conditions do not apply, there would be a relaxation on the condition which makes the matrix element non-zero. The evaluation of g(E) must then be made using all initial and final states which are separated by an energy $\hbar\omega$. Equation 6.7.13 may therefore be replaced by the integral:

$$g(\omega) = \int_0^{\hbar\omega - E_g} g_c(E_c) g_v(E_v)\, dE_v \qquad 6.7.17$$

where

$$E_c = \hbar\omega - E_g - E_v$$

If g_c and g_v are considered to be proportional to $E^{\frac{1}{2}}$, then integrating equation 6.7.17 gives (McCoy, 1965)

$$g(\omega) \propto (\hbar\omega - E_g)^2 \qquad 6.7.18$$

This expression is of the same form as that given for phonon aided indirect transitions, except for the omission of the term $\hbar\omega_{ph}$ for

the phonon energy. Hence

$$\hbar\omega nK(E) \propto (E - E_g)^2 \qquad 6.7.19$$

in agreement with the observed results.

Figure 6.11 is a diagrammatic representation of the transitions which occur in amorphous germanium.

6. 7. 6 LONG WAVELENGTH ABSORPTION IN GERMANIUM FILMS.

Although the calculated errors in the solutions for the absorption index are relatively large in the long wavelength region, it is apparent that the absorption falls to very small values in this region. This result is in agreement with the photoemission experiments of Donovan et al (loc. cit.). Tauc (loc. cit.) on the other hand reported significant long wavelength absorption in the germanium films he investigated. The error analysis used in the present calculations showed that an error of ±0.001 in R and T resulted in an error in the absorption index of about ±0.003. Thus a small error in R or T will result in a significant error in the calculated absorption coefficient in the long wavelength region. It is suggested that the absorption observed by Tauc in this region may have resulted from small errors in the measured reflectance and/or transmittance.

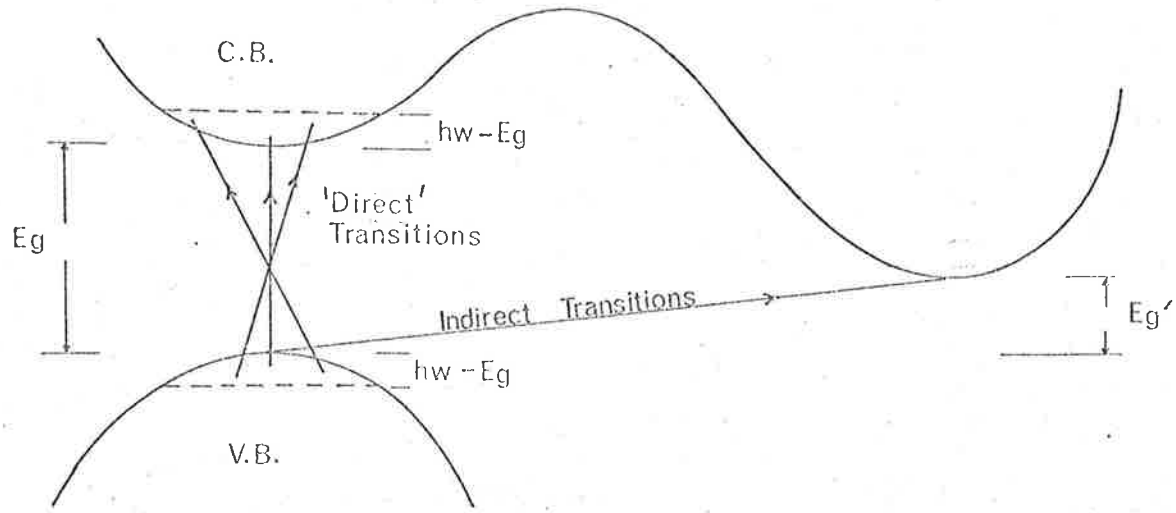

$Eg' = \cdot 72$ eV $Eg = 1 \cdot 1$ eV

Figure 6.11

CHAPTER 7.

CONCLUSIONS.

7. 1 ON THE DETERMINATION OF THE OPTICAL CONSTANTS OF THIN FILMS.

Much of this thesis has been concerned with the calculation of the optical constants of thin films. For the study of the absorption edge of semiconductor films, the measurement of normal incidence reflectance and transmittance is clearly the most reliable method for determining these parameters, as other methods depend critically on the properties of the surface of the film. Even so, this method has not been applied extensively to the study of thin films because of the complicated nature of the reflectance and transmittance equations. Analytical solutions for the refractive index and absorption index are no longer possible and one must resort to numerical methods to calculate these quantities. The situation is further complicated by the occurrence of multiple solutions, and this has probably been the most formidable problem in the past since often an incorrect solution may be mistaken for the correct value.

The numerical solution of the reflectance and transmittance equations itself has in the past presented a major problem because of their complicated behaviour.

We have shown that the functions $(1\pm R)/T$ exhibit a much simpler behaviour, and we have described in detail the calculation of n and k from them. Given R, T and the film thickness d, it is now a simple matter to calculate n and k.

The problem of multiple solutions required careful analysis and

was best examined by considering hypothetical films. We have shown that an unambiguous choice of the correct solution can only be made if measurements are taken over a sufficiently wide wavelength range. We have also seen that the film thickness is a critical parameter and that the behaviour of the calculated solutions under small changes in film thickness is quite distinct for thicknesses which are either too small or too large, leading to a method whereby the film thickness may be calculated along with the optical constants, without recourse to its explicit measurement.

The inability to find a single film thickness which would enable the refractive index curve to be closed over the entire wavelength range, assuming R and T were accurate, was shown to be due to either an oxide layer or an irregular surface. Provided the layer is very thin and near transparent over the wavelength range of measurements, its effects on the calculation of the optical constants of the underlying film may be eliminated by considering a two-layer system.

The equations for the reflectance and transmittance of a two-layer system are more complicated than those for a single-layer, but again the functions $(1\pm R)/T$ are much simpler. For the special case where one of the layers is transparent and of known refractive index, we have described how the optical constants of the absorbing film, together with the thicknesses of the transparent and absorbing layers, may be accurately determined from the measured reflectance and transmittance of the system. Although we were concerned primarily with accounting for the surface, the theory developed is quite general and is applicable to any two-layer system where one of the

layers is transparent.

7. 2 ON THE OPTICAL CONSTANTS OF SELENIUM FILMS.

The analyses of the behaviour of the calculated solutions for the optical constants of thin films revealed that Campbell, in his calculation of the optical constants of vitreous selenium films, chose incorrect solutions from those that existed. We therefore recalculated the optical constants of these films from his reflectance and transmittance data. The results obtained for the refractive index of these films are in quantitative agreement with previous work on the bulk material and on sputtered films.

The absorption in the films, although in qualitative agreement with other authors' results in the highly absorbing region, depart from previous results in the low absorption region where the present films exhibit considerable absorption, particularly in the thinner films. As the thickness of the film increased the long wavelength absorption decreased, and the absorption mechanism was attributed to the developing chain structure of the vitreous selenium.

A plot of the absorption coefficient as a function of photon energy was found to consist of two straight lines*, with the change of slope occurring at the energy value of the onset of photoconductivity. The results are consistent with the view that within individual chains or rings carriers are free to move, but to travel to neighbouring chains or rings it is necessary to cross potential barriers.

* see Figure 5.10.

7. 3 ON THE OPTICAL CONSTANTS OF GERMANIUM FILMS.

The wide discrepancies in the published values of the optical constants of germanium films indicated the need for an accurate determination of them. Films with various degrees of crystalline perfection were studied, with amorphous films being studied in greater detail.

The optical constants of films annealed at 650°C, that is polycrystalline and highly oriented films, produced qualitatively similar results to those found for single-crystal germanium. From 0.75eV to 1.1eV the absorption in these films followed the law for indirect transitions, Greater than 1.1eV the absorption followed the law for direct transitions. The main difference between these films and the bulk material is the threshold energies for the onset of indirect and direct transitions, being 0.62eV and 0.81eV respectively for the bulk material, and 0.75eV and 1.1eV for the films.

The optical constants of films deposited on room temperature substrates, that is amorphous films, were in qualitative agreement with the results of Tauc, with the exception of the long-wavelength region beyond the absorption edge. That is, the absorption edge in these films followed the law for indirect transitions from 0.72eV to 1.1eV, and followed the same law but with a change in slope for energies greater than 1.1eV. The results are consistent with the view that the essential features of the band picture for amorphous germanium are basically unaltered from that of crystalline germanium, and that the random structure of the amorphous state removes the conditions for the conservation of momentum, giving rise to an

absorption law similar to indirect transitions.

The long wavelength absorption in the germanium films was found to fall to very small values, in agreement with the photo-emission measurements of Donovan et al.

Polycrystalline films, prepared by deposition onto room temperature substrates with subsequent annealing at 350°C for several hours, produced similar results to the amorphous films, indicating that the size of the randomly oriented crystallites does not have a significant influence on the absorption processes.

The application of Schopper's theory to very thin amorphous films brought the results for these films into near agreement with those of the thicker films. The view that these films consist of long islands is consistent with the kinetics of thin film formation.

Films deposited on substrates at 350°C showed similar properties to the very thin films. The surface of these films was found to be wrinkled in agreement with Sloope and Tiller, but there is a need for further work on the structure of these films before any conclusions can be drawn.

7. 4 FUTURE WORK.

The theory involved in the calculation of the optical constants of thin films from normal incidence reflectance and transmittance measurements was developed in Chapters 3 and 4, and then applied successfully to the determination of n and k of selenium and germanium films. The theory has paved the way for the accurate determination of n and k for thin semiconducting films and work

is already proceeding in this laboratory on the optical constants of silicon and group II-VI semiconductors.

Surface layers and inhomogeneous surfaces have presented problems in the past, but now these can be readily accounted for. It should now be possible to determine accurately the optical constants of thin films of a large number of semiconductors.

APPENDIX A.

PARTIAL DERIVATIVES OF (1±R)/Γ FOR THE SINGLE-LAYER EQUATIONS.

$$\frac{1+R}{\Gamma} = \frac{1}{(n_0+n_2)^2(n_1^2+k_1^2)}\Big[(n_0^2+n_1^2+k_1^2)\{(n_1^2+n_2^2+k_1^2)\cosh 2\alpha_1 + 2n_1n_2\sinh 2\alpha_1\} + (n_0^2-n_1^2-k_1^2)\{(n_1^2-n_2^2+k_1^2)\cos 2\gamma_1 - 2n_2k_1\sin 2\gamma_1\}\Big]$$

$$\frac{1-R}{\Gamma} = \frac{2n_0}{(n_0+n_2)^2(n_1^2+k_1^2)}\Big[n_1\{(n_1^2+n_2^2+k_1^2)\sinh 2\alpha_1 + 2n_1n_2\cosh 2\alpha_1\} + k_1\{(n_1^2-n_2^2+k_1^2)\sin 2\gamma_1 + 2n_2k_1\cos 2\gamma_1\}\Big]$$

$$\frac{\partial\left(\frac{1+R}{\Gamma}\right)}{\partial d_1} = \frac{4\pi}{\lambda(n_0+n_2)^2(n_1^2+k_1^2)}\Big[k_1(n_0^2+n_1^2+k_1^2)\{(n_1^2+n_2^2+k_1^2)\sinh 2\alpha_1 + 2n_1n_2\cosh 2\alpha_1\} - n_1(n_0^2-n_1^2-k_1^2)\{(n_1^2-n_2^2+k_1^2)\sin 2\gamma_1 + 2n_2k_1\cos 2\gamma_1\}\Big]$$

$$\frac{\partial\left(\frac{1+R}{\Gamma}\right)}{\partial n_2} = \frac{2}{(n_1^2+k_1^2)(n_0+n_2)^3}\Big[(n_0^2+n_1^2+k_1^2)\{(n_0n_2-n_1^2-k_1^2)\cosh 2\alpha_1 + n_1(n_0-n_2)\sinh 2\alpha_1\} + (n_0^2-n_1^2-k_1^2)\{k_1(n_2-n_0)\sin 2\gamma_1 - (n_0n_2+n_1^2+k_1^2)\cos 2\gamma_1\}\Big]$$

$$\frac{\partial\left(\frac{1+R}{\Gamma}\right)}{\partial n_1} = \frac{1}{(n_0+n_2)^2(n_1^2+k_1^2)^2}\Big[2n_1\{(n_1^2+k_1^2)^2-n_0^2n_2^2\}\cosh 2\alpha_1 + 2n_2\{(n_1^2+k_1^2)(n_0^2+n_1^2+k_1^2) - 2n_1^2n_0^2\}\sinh 2\alpha_1 + \frac{1}{k}\{4n_1n_2n_0^2k_1^2-(n_1^2+k_1^2)(n_0^2-n_1^2-k_1^2)(n_1^2-n_2^2+k_1^2) \times 2\gamma_1\}\sin 2\gamma_1$$

$$+ 2\{(n_0^2-n_1^2-k_1^2)\{n_1n_2^2-n_2(n_1^2+k_1^2)2\alpha_1\} - n_1(n_1^2+k_1^2)(n_1^2-n_2^2+k_1^2)\}\cos 2\gamma_1\Big) -$$

$$\frac{\partial\left(\frac{1+R}{T}\right)}{\partial k_1} = \frac{1}{(n_0+n_2)^2(n_1^2+k_1^2)^2}\Big(\{(n_1^2+k_1^2)(n_0^2+n_1^2+k_1^2)(n_1^2+n_2^2+k_1^2)\frac{2\gamma_1}{n_1} - 4n_1n_2n_0^2k_1\}\sinh 2\alpha_1$$

$$+ 2\{(2n_2\gamma_1+k_1)(n_1^2+k_1^2)(n_0^2+n_1^2+k_1^2) - n_0^2k_1(n_1^2+n_2^2+k_1^2)\}\cosh 2\alpha_1$$

$$+ 2n_2\{(n_1^2+k_1^2)^2 + n_0^2(k_1^2-n_1^2)\}\sin 2\gamma_1$$

$$+ 2k_1\{n_0^2n_2^2-(n_1^2+k_1^2)^2\}\cos 2\gamma_1\Big)$$

$$\frac{\partial\left(\frac{1-R}{T}\right)}{\partial d_1} = \frac{\cdot 8\pi n_0n_1k_1 \cdots}{\lambda(n_0+n_2)^2(n_1^2+k_1^2)}\Big((n_1^2+n_2^2+k_1^2)\cosh 2\alpha_1$$

$$+ 2n_1n_2\sinh 2\alpha_1 + (n_1^2-n_2^2+k_1^2)\cos 2\gamma_1 - 2n_2k_1\sin 2\gamma_1\Big)$$

$$\frac{\partial\left(\frac{1-R}{T}\right)}{\partial n_2} = \frac{4n_0}{(n_1^2+k_1^2)(n_0+n_2)^3}\Big(n_1^2(n_0-n_2)\cosh 2\alpha_1$$

$$+ n_1(n_0n_2-n_1^2-k_1^2)\sinh 2\alpha_1 - k_1(n_0n_2+n_1^2+k_1^2)\sin 2\gamma_1 + k_1^2(n_0-n_2)\cos 2\gamma_1\Big)$$

$$\frac{\partial\left(\frac{1-R}{T}\right)}{\partial n_1} = \frac{2n_0}{(n_0+n_2)^2(n_1^2+k_1^2)^2}\Big(\{(n_1^2+k_1^2)(n_1^2+n_2^2+k_1^2)$$

$$- 2n_1^2n_2^2\sinh 2\alpha_1 + 4n_1n_2k_1^2\cosh 2\alpha_1$$

$$+ \{(n_1^2+k_1^2)(n_1^2-n_2^2+k_1^2)2\alpha_1 - 4n_1n_2k_1^2\cos 2\gamma_1$$

$$+ 2n_2k_1\{n_1n_2 - 2\alpha_1(n_1^2+k_1^2)\}\sin 2\gamma_1\Big)$$

$$\frac{\partial\left(\frac{1-R}{T}\right)}{\partial k_1} = \frac{2n_0}{(n_0+n_2)^2(n_1^2+k_1^2)^2}\Big(\{(n_1^2+k_1^2)(n_1^2+n_2^2+k_1^2)2\gamma_1$$
$$- 4n_1^2n_2k_1\}\cosh 2\alpha_1 + 2n_1n_2\{(n_1^2+k_1^2)2\gamma_1 - n_2k_1\}\sinh 2\alpha_1$$
$$+ \{(n_1^2+k_1^2)^2 - n_2^2(n_1^2-k_1^2)\}\sin 2\gamma_1 + 4n_2k_1n_1^2\cos 2\gamma_1\Big)$$

APPENDIX B.

DERIVATION OF $\frac{1\pm R}{T}$ AND $\frac{1\pm R^1}{T}$ FROM THE FORMULAE GIVEN BY ALLEN

$$R = \frac{abe^{2\alpha_1}+cde^{-2\alpha_1}+2r\cos 2\gamma_1 + 2\,s\,\sin 2\gamma_1}{bde^{2\alpha_1}+ace^{-2\alpha_1}+2t\cos 2\gamma_1 + 2\,u\,\sin 2\gamma_1}$$

$$R^1 = \frac{cde^{2\alpha_1}+abe^{-2\alpha_1}+2r\cos 2\gamma_1 - 2\,s\,\sin 2\gamma_1}{bde^{2\alpha_1}+ace^{-2\alpha_1}+2t\cos 2\gamma_1 + 2\,u\,\sin 2\gamma_1}$$

$$T = \frac{16n_0n_2(n_1^2+k_1^2)}{bde^{2\alpha_1}+ace^{-2\alpha_1}+2t\cos 2\gamma_1 + 2\,u\,\sin 2\gamma_1}$$

where

$$\begin{matrix} a \\ d \end{matrix} = (n_1 \mp n_0)^2 + k_1^2 \qquad \begin{matrix} b \\ c \end{matrix} = (n_1 \pm n_2)^2 + k_1^2$$

$$\begin{matrix} r \\ t \end{matrix} = (n_0^2+n_2^2)(n_1^2+k_1^2) - (n_1^2+k_1^2)^2 - n_0^2n_2^2 \mp 4n_0n_2k_1^2$$

$$\begin{matrix} s \\ u \end{matrix} = 2k_1(n_2 \mp n_0)(n_1^2+k_1^2 \pm n_0n_2)$$

$$\alpha_1 = 2\pi k_1 d_1/\lambda \qquad \gamma_1 = 2\pi n_1 d_1/\lambda$$

Thus

$$\frac{1\pm R}{T} = \frac{1}{16n_0n_2(n_1^2+k_1^2)}\ F$$

where

$$F = b(d\pm a)e^{2\alpha_1} + c(a\pm d)e^{-2\alpha_1} + 2(t\pm r)\cos 2\gamma_1 + 2(u\pm s)\sin 2\gamma_1$$

$$d\pm a = 2(n_1^2+n_0^2+k_1^2) \text{ or } 4n_0n_1$$

$$t\pm r = 2(n_0^2-n_1^2-k_1^2)(n_1^2+k_1^2-n_2^2) \text{ or } 8n_0n_2k_1^2$$

$$u\pm s = 4n_2k_1(n_1^2+k_1^2-n_0^2) \text{ or } 4n_0k_1(n_1^2+k_1^2-n_2^2)$$

Thus for $\left(\frac{1+R}{T}\right)$

$$F = 2(n_1^2+n_0^2+k_1^2)\{(n_1+n_2)^2 + k_1^2\}e^{2\alpha_1}$$

$$+ 2(n_1^2+n_0^2+k_1^2)\{(n_1-n_2)^2 + k_1^2\}e^{-2\alpha_1}$$

$$+ 4(n_0^2-n_1^2-k_1^2)(n_1^2+k_1^2-n_2^2)\cos 2\gamma_1 + 8n_2k_1(n_1^2+k_1^2-n_0^2)\sin 2\gamma_1$$

$$= 4(n_1^2+n_0^2+k_1^2)\{(n_1^2+n_2^2+k_1^2)\cosh 2\alpha_1 + 2n_1n_2\sinh 2\alpha_1\}$$

$$+ 4(n_0^2-n_1^2-k_1^2)\{(n_1^2-n_2^2+k_1^2)\cos 2\gamma_1 - 2n_2k_1\sin 2\gamma_1\}$$

Hence

$$\frac{1+R}{T} = \frac{1}{4n_0n_2(n_1^2+k_1^2)}\Big\{(n_1^2+n_0^2+k_1^2)\{(n_1^2+n_2^2+k_1^2)\cosh 2\alpha_1 + 2n_1n_2\sinh 2\alpha_1\}$$

$$+ (n_0^2-n_1^2-k_1^2)\{(n_1^2-n_2^2+k_1^2)\cos 2\gamma_1 - 2n_2k_1\sin 2\gamma_1\}\Big\}$$

$$\frac{1-R}{T} = \frac{1}{16n_0n_2(n_1^2+k_1^2)}\Big\{4n_0n_1\{\{(n_1+n_2)^2 + k_1^2\}e^{2\alpha_1} - \{(n_1-n_2)^2 + k_1^2\}e^{-2\alpha_1}\}$$

$$+ 16n_0n_2k_1^2\cos 2\gamma_1 + 8n_0k_1(n_1^2+k_1^2-n_2^2)\sin 2\gamma_1\Big\}$$

$$\frac{1-R}{T} = \frac{1}{2n_2(n_1^2+k_1^2)}\Big\{n_1\{(n_1^2+n_2^2+k_1^2)\sinh 2\alpha_1 + 2n_1n_2\cosh 2\alpha_1\}$$

$$+ k_1\{(n_1^2+k_1^2-n_2^2)\sin 2\gamma_1 + 2n_2k_1\cos 2\gamma_1\}\Big\}$$

Similarly

$$\frac{1\pm R^1}{T} = \frac{1}{16n_0n_2(n_1^2+k_1^2)} \quad G \quad \text{where}$$

$$G = d(b\pm c)e^{2\alpha_1} + a(c\pm b)e^{-2\alpha_1}$$

$$+ 2(t\pm r)\cos 2\gamma_1 + 2(u\mp s)\sin 2\gamma_1$$

$$b\pm c = 2(n_1^2+n_2^2+k_1^2) \quad \text{or} \quad 4n_1n_2$$

Hence for $\frac{1+R^1}{T}$

$$G = 2(n_1^2+n_2^2+k_1^2)\{\{(n_1+n_0)^2 + k_1^2\}e^{2\alpha_1} + \{(n_1-n_0)^2 + k_1^2\}e^{-2\alpha_1}\}$$

$$+ 4(n_0^2-n_1^2-k_1^2)(n_1^2+k_1^2-n_2^2)\cos 2\gamma_1 + 8n_0k_1(n_1^2+k_1^2-n_2^2)\sin 2\gamma_1$$

$$= 4(n_1^2+n_2^2+k_1^2)\{(n_1^2+n_0^2+k_1^2)\cosh 2\alpha_1 + 2n_0n_1\sinh 2\alpha_1\}$$

$$+ 4(n_1^2+k_1^2-n_2^2)\{(n_0^2-n_1^2-k_1^2)\cos 2\gamma_1 + 2n_0k_1\sin 2\gamma_1\}$$

Therefore

$$\frac{1+R^1}{T} = \frac{1}{4n_0n_2(n_1^2+k_1^2)}\Big\{(n_1^2+n_2^2+k_1^2)\{(n_1^2+n_0^2+k_1^2)\cosh 2\alpha_1 + 2n_0n_1\sinh 2\alpha_1\}$$

$$+ (n_1^2+k_1^2-n_2^2)\{(n_0^2-n_1^2-k_1^2)\cos 2\gamma_1 + 2n_0k_1\sin 2\gamma_1\}\Big\}$$

$$\frac{1-R^1}{T} = \frac{1}{16n_0n_2(n_1^2+k_1^2)}\Big\{4n_1n_2\{\{(n_1+n_0)^2 + k_1^2\}e^{2\alpha_1} - \{(n_1-n_0)^2+k_1^2\}e^{-2\alpha_1}\}$$

$$+ 16n_0n_2k_1^2\cos 2\gamma_1 + 8n_2k_1(n_1^2+k_1^2-n_0^2)\sin 2\gamma_1\Big\}$$

$$\frac{1-R^1}{T} = \frac{1}{2n_0(n_1^2+k_1^2)}\Big\{n_1\{(n_1^2+n_0^2+k_1^2)\sinh 2\alpha_1 + 2n_0n_1\cosh 2\alpha_1\}$$

$$+ k_1\{(n_1^2+k_1^2-n_0^2)\sin 2\gamma_1 + 2n_0k_1\cos 2\gamma_1\}\Big\}$$

APPENDIX C.

PARTIAL DERIVATIVES OF (1±R)/Γ FOR THE TWO-LAYER EQUATIONS

SYSTEM 1. ($k_1=k_3=0$)

$$\frac{1-R}{\Gamma} = \frac{2n_0}{(n_0+n_3)^2(n_2^2+k_2^2)}\Big[n_2\{(n_2^2+n_3^2+k_2^2)\sinh 2\alpha_2 + 2n_2n_3\cosh 2\alpha_2\}$$
$$+ k_2\{(n_2^2-n_3^2+k_2^2)\sin 2\gamma_2 + 2n_3k_2\cos 2\gamma_2\}\Big]$$

$$\frac{1+R}{\Gamma} = \frac{1}{4n_1^2(n_2^2+k_2^2)(n_0+n_3)^2}\,F \quad \text{where}$$

$$F = (n_0^2+n_1^2)\Big[2(n_1^2+n_2^2+k_2^2)\{(n_2^2+n_3^2+k_2^2)\cosh 2\alpha_2 + 2n_2n_3\sinh 2\alpha_2\}$$
$$+ 2(n_1^2-n_2^2-k_2^2)\{(n_2^2-n_3^2+k_2^2)\cos 2\gamma_2 - 2n_3k_2\sin 2\gamma_2\}\Big]$$
$$+ (n_0^2-n_1^2)\Big[\{(n_1+n_2)^2 + k_2^2\}\{(n_2^2-n_3^2+k_2^2)\cos 2(\gamma_1+\gamma_2)$$
$$- 2n_3k_2\sin 2(\gamma_1+\gamma_2)\}$$
$$+ \{(n_1-n_2)^2 + k_2^2\}\{(n_2^2-n_3^2+k_2^2)\cos 2(\gamma_1-\gamma_2) + 2n_3k_2\sin 2(\gamma_1-\gamma_2)\}$$
$$+ 2(n_1^2-n_2^2-k_2^2)\cos 2\gamma_1\{(n_2^2+n_3^2+k_2^2)\cosh 2\alpha_2 + 2n_2n_3\sinh 2\alpha_2\}$$
$$+ 4n_1k_2\sin 2\gamma_1\{(n_2^2+n_3^2+k_2^2)\sinh 2\alpha_2 + 2n_2n_3\cosh 2\alpha_2\}\Big]$$

Let $g = 4\pi d_2/\lambda$

$$\frac{\partial\left(\frac{1-R}{\Gamma}\right)}{\partial n_2} = \frac{2n_0}{(n_0+n_3)^2(n_2^2+k_2^2)}\,(A\sinh 2\alpha_2 + B\cosh 2\alpha_2 + C\sin 2\gamma_2 + D\cos 2\gamma_2)$$

where

$$A = n_2^2(n_2^2-n_3^2+k_2^2) + k_2^2(n_2^2+n_3^2+k_2^2)$$

$$B = 4n_2n_3k_2^2$$

$$C = 2n_3k_2\{n_2n_3-2\alpha_2(n_2^2+k_2^2)\}$$

$$D = 2\alpha_2(n_2^2+k_2^2)(n_2^2-n_3^2+k_2^2) - 4n_2n_3k_2^2$$

$$\frac{\partial\left(\frac{1-R}{\Gamma}\right)}{\partial n_2} = \frac{2n_0}{(n_0+n_3)^2(n_2^2+k_2^2)^2}\,(A\sinh 2\alpha_2 + B\cosh 2\alpha_2 + C\sin 2\gamma_2 + D\cos 2\gamma_2)$$

where

$$A = 2n_2n_3\{2\gamma_2(n_2^2+k_2^2) - n_3k_2\}$$

$$B = 2\gamma_2(n_2^2+k_2^2)(n_2^2+n_3^2+k_2^2) - 4n_2^2n_3k_2$$

$$C = n_2^2(n_2^2-n_3^2+k_2^2) + k_2^2(n_2^2+n_3^2+k_2^2)$$

$$D = 4n_2^2n_3k_2$$

$$\frac{\partial\left(\frac{1-R}{\Gamma}\right)}{\partial d_2} = \frac{8\pi n_0n_2k_2}{\lambda(n_0+n_3)^2(n_2^2+k_2^2)}\,(A\sinh 2\alpha_2 + B\cosh 2\alpha_2 + C\sin 2\gamma_2 + D\cos 2\gamma_2)$$

where

$$A = 2n_2n_3$$

$$B = n_2^2+n_3^2+k_2^2$$

$$C = -2n_3k_2$$

$$D = n_2^2-n_3^2+k_2^2$$

$$\frac{\partial\left(\frac{1-R}{\Gamma}\right)}{\partial d_1} = 0$$

$$\frac{\partial\left(\frac{1+R}{\Gamma}\right)}{\partial n_2} = \frac{1}{4n_1^2(n_2^2+k_2^2)(n_0+n_3)^2}\{A\sinh 2\alpha_2 + B\cosh 2\alpha_2$$

$$+ C\sin 2\gamma_2 + D\cos 2\gamma_2 + E\sin 2(\gamma_1+\gamma_2) + F\cos 2(\gamma_1+\gamma_2)$$

$$+ G\sin 2(\gamma_1-\gamma_2) + H\cos 2(\gamma_1-\gamma_2) + J\sin 2\gamma_1 + K\cos 2\gamma_1\}$$

where

$$A = 4n_3(n_0^2+n_1^2)\{k_2^2(n_1^2+k_2^2) - n_2^2(n_1^2-k_2^2)\}$$

$$B = 4n_2(n_0^2+n_1^2)\{(n_2^2+k_2^2)^2 - n_1^2n_3^2\}$$

$$C = 2(n_0^2+n_1^2)\{4n_1^2n_2n_3k_2 - g(n_2^2+k_2^2)(n_1^2-n_2^2-k_2^2)(n_2^2-n_3^2+k_2^2)\}$$

$$D = 4(n_0^2+n_1^2)\left[n_2\{n_1^2n_3^2-(n_2^2+k_2^2)^2\} - n_3k_2g(n_2^2+k_2^2)(n_1^2-n_2^2-k_2^2)\right]$$

$$E = (n_0^2-n_1^2)\left[4n_1n_3k_2(2n_2^2-k_2^2) - g(n_2^2+k_2^2)(n_2^2-n_3^2+k_2^2)\{(n_1+n_2)^2 + k_2^2\}\right]$$

$$F = 2(n_0^2-n_1^2)\left[(n_1+n_2)\{(n_2^2+k_2^2)^2 + n_1n_2n_3^2\} - n_1n_3^2k_2^2 - n_3k_2g(n_2^2+k_2^2)\{(n_1+n_2)^2 + k_2^2\}\right]$$

$$G = (n_0^2-n_1^2)\left[(n_2^2+k_2^2)(n_2^2-n_3^2+k_2^2)\{(n_1-n_2)^2 + k_2^2\}g - 4n_1n_3k_2(n_1n_2-n_2^2+k_2^2)\right]$$

$$H = 2(n_0^2-n_1^2)\left[(n_1-n_2)\{n_1n_2n_3^2-(n_2^2+k_2^2)^2\} + n_1n_3^2k_2^2 - n_3k_2g(n_2^2+k_2^2)\right]$$

$$J = -8n_1n_3k_2(n_0^2-n_1^2)\{n_2n_3\sinh 2\alpha_2 + (n_2^2-k_2^2)\cosh 2\alpha_2\}$$

$$K = -4(n_0^2-n_1^2)\left[n_2\{(n_2^2+k_2^2)^2 + n_1^2n_3^2\}\cosh 2\alpha_2 + n_3\{n_1^2(n_2^2-k_2^2) + k_2^2(n_2^2+k_2^2)\}\sinh 2\alpha_2\right]$$

$$\frac{\partial\left(\frac{J+R}{\Gamma}\right)}{\partial k_2} = \frac{1}{4n_1^2(n_0+n_3)^2(n_2^2+k_2^2)^2}\{A\sinh 2\alpha_2 + B\cosh 2\alpha_2 + C\sin 2\gamma_2 + D\cos 2\gamma_2 + E\sin 2(\gamma_1+\gamma_2) + F\cos 2(\gamma_1+\gamma_2) + G\sin 2(\gamma_1-\gamma_2) + H\cos 2(\gamma_1-\gamma_2) + J\sin 2\gamma_1 + K\cos 2\gamma_1\}$$

where

$$A = 2(n_0^2+n_1^2)\{g(n_2^2+k_2^2)(n_1^2+n_2^2+k_2^2)(n_2^2+n_3^2+k_2^2) - 4n_1^2n_2n_3k_2\}$$

$$B = 4(n_0^2+n_1^2)\{k_2\{(n_2^2+k_2^2)^2-n_1^2n_3^2\} + n_2n_3g(n_2^2+k_2^2)(n_1^2+n_2^2+k_2^2)\}$$

$$C = 4n_3(n_0^2+n_1^2)\{2k_2^2 - (n_2^2-k_2^2)(n_1^2-n_2^2-k_2^2)\}$$

$$D = 4k_2(n_0^2+n_1^2)\{n_1^2n_3^2 - (n_2^2+k_2^2)^2\}$$

$$E = 2n_3(n_0^2-n_1^2)\{(n_1^2+2n_1n_2)(k_2^2-n_2^2) - (n_2^2+k_2^2)^2\}$$

$$F = 2k_2(n_0^2-n_1^2)\left[\{(n_1+n_2)^2+k_2^2\} + (n_2^2+k_2^2)(n_2^2-n_3^2+k_2^2)\right]$$

$$G = 2n_3(n_0^2-n_1^2)\{(n_2^2+k_2^2)^2 + (n_1^2-2n_1n_2)(n_2^2-k_2^2)\}$$

$$H = 2k_2(n_0^2-n_1^2)\{(n_2^2+k_2^2)^2 - n_1n_3^2(2n_2+n_1)\}$$

$$J = 4(n_0^2-n_1^2)\left[n_1k_2g(n_2^2+k_2^2)\{(n_2^2+n_3^2+k_2^2)\cosh 2\alpha_2 + 4n_2n_3\sinh 2\alpha_2\}\right.$$
$$\left. + 2n_1n_2n_3(n_2^2-k_2^2)\cosh 2\alpha_2 + n_1\{(n_2^2+n_3^2+k_2^2)(n_2^2+k_2^2) - 2n_3^2k_2^2\}\sinh 2\alpha_2\right]$$

$$K = 2(n_0^2-n_1^2)\left[g(n_2^2+k_2^2)(n_1^2-n_2^2-k_2^2)\{(n_2^2+n_3^2+k_2^2)\cosh 2\alpha_2 + 2n_2n_3\sinh 2\alpha_2\} - 4n_1^2n_2n_3k_2\sinh 2\alpha_2 - 2k_2\{(n_2^2+k_2^2)^2 + n_1^2n_3^2\}\cosh 2\alpha_2\right]$$

$$\frac{\partial\left(\frac{1+R}{T}\right)}{\partial d_2} = \frac{\pi}{\lambda n_1^2(n_2^2+k_2^2)(n_0+n_3)^2}\{A\sinh 2\alpha_2 + B\cosh 2\alpha_2 + C\sin 2\gamma_2 + D\cos 2\gamma_2$$
$$+ E\sin 2(\gamma_1+\gamma_2) + F\cos 2(\gamma_1+\gamma_2) + G\sin 2(\gamma_1-\gamma_2) + H\cos 2(\gamma_1-\gamma_2)$$
$$+ J\sin 2\gamma_1 + K\cos 2\gamma_1$$

where

$$A = 2k_2(n_0^2+n_1^2)(n_1^2+n_2^2+k_2^2)(n_2^2+n_3^2+k_2^2)$$

$$B = 4n_2n_3k_2(n_0^2+n_1^2)(n_1^2+n_2^2+k_2^2)$$

$$C = -2n_2(n_1^2-n_2^2-k_2^2)(n_0^2+n_1^2)(n_2^2-n_3^2+k_2^2)$$

$$D = -4n_2n_3k_2(n_0^2+n_1^2)(n_1^2-n_2^2-k_2^2)$$

$$E = -n_2(n_0^2-n_1^2)\{(n_1+n_2)^2 + k_2^2\}(n_2^2-n_3^2+k_2^2)$$

$$F = -2n_2n_3k_2(n_0^2-n_1^2)\{(n_1+n_2)^2 + k_2^2\}$$

$$G = n_2(n_0^2-n_1^2)(n_2^2-n_3^2+k_2^2)\{(n_1-n_2)^2 + k_2^2\}$$

$$H = -2n_2n_3k_2(n_0^2-n_1^2)\{(n_1-n_2)^2 + k_2^2\}$$

$$J = 4n_1k_2^2\{(n_2^2+n_3^2+k_2^2)\cosh 2\alpha_2 + 2n_2n_3\sinh 2\alpha_2\}$$

$$K = 2k_2(n_1^2-n_2^2-k_2^2)\{(n_2^2+n_3^2+k_2^2)\sinh 2\alpha_2 + 2n_2n_3\cosh 2\alpha_2\}$$

$$\frac{\partial\left(\frac{1+R}{T}\right)}{\partial d_1} = \frac{\pi(n_0^2-n_1^2)}{\lambda n_1(n_2^2+k_2^2)(n_0+n_3)^2}\{A\sin 2(\gamma_1+\gamma_2) + B\cos 2(\gamma_1+\gamma_2)$$

$$+ C\sin 2(\gamma_1-\gamma_2) + D\cos 2(\gamma_1-\gamma_2) + E\sin 2\gamma_1 + F\cos 2\gamma_1\}$$

where

$$A = -\{(n_1+n_2)^2 + k_2^2\}(n_2^2-n_3^2+k_2^2)$$

$$B = -2n_3k_2\{(n_1+n_2)^2 + k_2^2\}$$

$$C = -(n_2^2-n_3^2+k_2^2)\{(n_1-n_2)^2 + k_2^2\}$$

$$D = 2n_3k_2\{(n_1-n_2)^2 + k_2^2\}$$

$$E = -2(n_1^2-n_2^2-k_2^2)\{(n_2^2+n_3^2+k_2^2)\cosh 2\alpha_2 + 2n_2n_3\sinh 2\alpha_2\}$$

$$F = 4n_1k_2\{(n_2^2+n_3^2+k_2^2)\sinh 2\alpha_2 + 2n_2n_3\cosh 2\alpha_2\}$$

APPENDIX D.

MEASURED REFLECTANCES AND TRANSMITTANCES AND CALCULATED REFRACTIVE AND ABSORPTION INDICES OF VITREOUS SELENIUM FILMS.

FILM SE1.

$d_1 = 40 \pm 10\text{Å}$ $d_2 = 520 \pm 10\text{Å}$

λ(μ)	R	Γ	λ(μ)	R	Γ	λ(μ)	R	Γ
2.000	.101	.904	.750	.353	.651	.520	.413	.406
1.750	.119	.885	.725	.371	.637	.510	.391	.379
1.500	.146	.858	.700	.386	.621	.500	.371	.360
1.250	.184	.818	.675	.401	.604	.490	.353	.342
1.000	.245	.756	.650	.415	.587	.480	.335	.322
.975	.253	.748	.625	.432	.569	.470	.318	.303
.950	.261	.740	.600	.448	.547	.460	.303	.284
.925	.272	.731	.590	.454	.535	.450	.290	.267
.900	.281	.721	.580	.461	.522	.440	.278	.249
.875	.292	.710	.570	.463	.523	.430	.267	.231
.850	.302	.699	.560	.463	.509	.420	.257	.214
.825	.315	.689	.550	.459	.472	.410	.248	.195
.800	.327	.678	.540	.449	.453	.400	.242	.176
.775	.341	.664	.530	.432	.430	.390	.236	.157
						.380	.232	.139

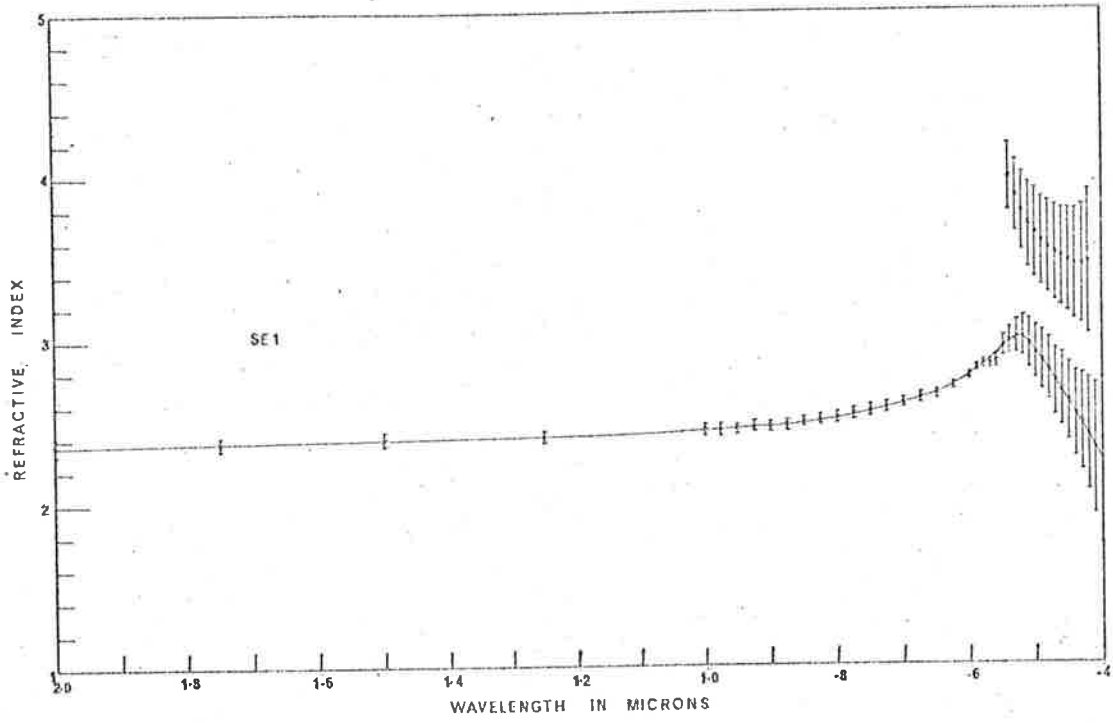
REFRACTIVE INDEX
SE1
WAVELENGTH IN MICRONS

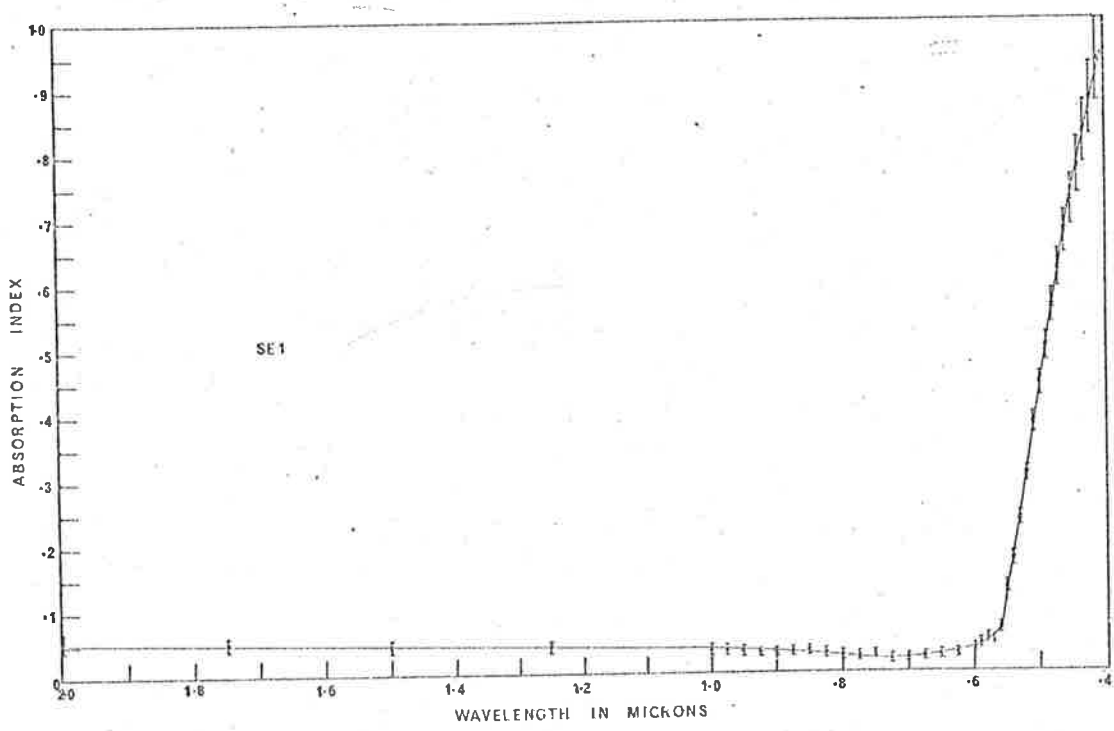
ABSORPTION INDEX
SE1
WAVELENGTH IN MICRONS

FILM SE2.

$d_1 = 125 \pm 10$Å $\qquad$ $d_2 = 682 \pm 10$Å

λ(μ)	R	Γ	λ(μ)	R	Γ	λ(μ)	R	Γ
2.000	.153	.851	.700	.408	.593	.510	.164	.432
1.750	.180	.823	.690	.409	.593	.500	.159	.380
1.500	.215	.788	.680	.409	.593	.490	.159	.334
1.250	.260	.741	.670	.409	.593	.480	.161	.294
1.000	.322	.679	.660	.408	.594	.470	.164	.260
.975	.330	.672	.650	.406	.595	.460	.169	.231
.950	.337	.664	.640	.403	.597	.450	.177	.204
.925	.345	.656	.630	.399	.600	.440	.183	.179
.900	.353	.647	.620	.394	.603	.430	.191	.154
.875	.363	.640	.610	.387	.608	.420	.198	.134
.850	.372	.632	.600	.380	.613	.410	.207	.118
.825	.379	.624	.590	.369	.619	.400	.216	.100
.800	.384	.617	.580	.352	.624	.390	.223	.084
.775	.391	.611	.570	.333	.627	.380	.230	.072
.750	.396	.604	.560	.305	.624	.370	.23¾	.060
.740	.398	.602	.550	.267	.616	.360	.244	.051
.730	.401	.599	.540	.229	.587	.350	.250	.042
.720	.403	.597	.530	.194	.545	.340	.255	.034
.710	.405	.594	.520	.176	.490	.330	.260	.027
						.320	.263	.021

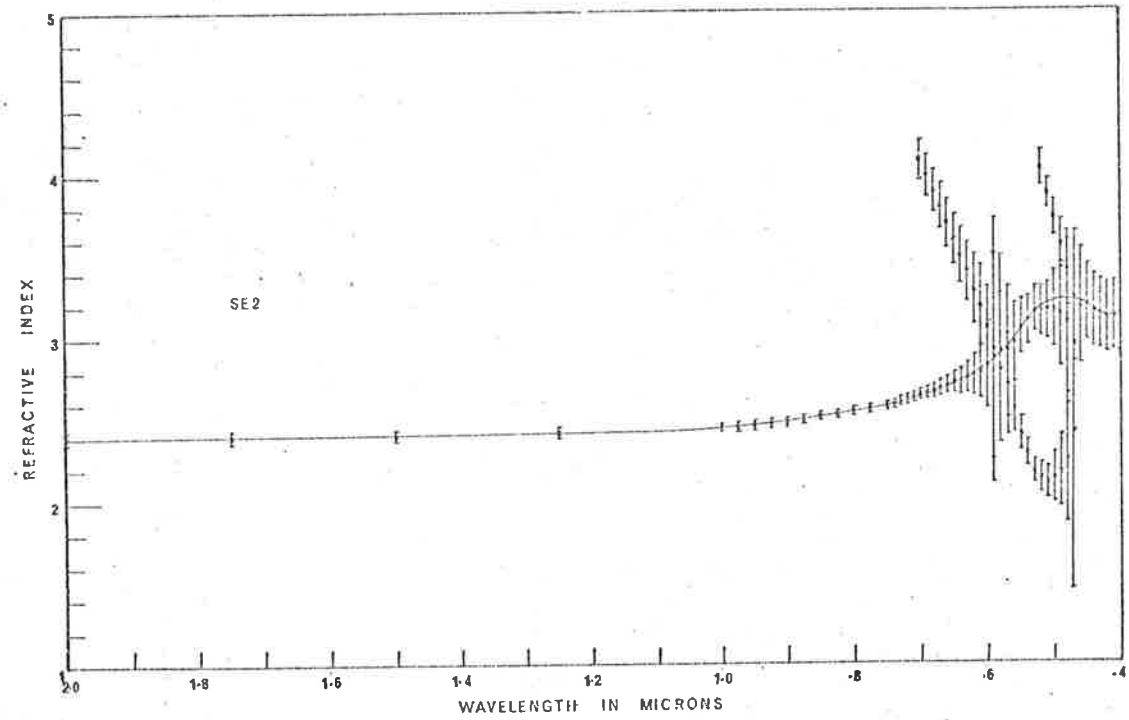
SE2
REFRACTIVE INDEX
5
4
3
2
1
2·0
1·8
1·6
1·4
1·2
1·0
·8
·6
·4
WAVELENGTH IN MICRONS

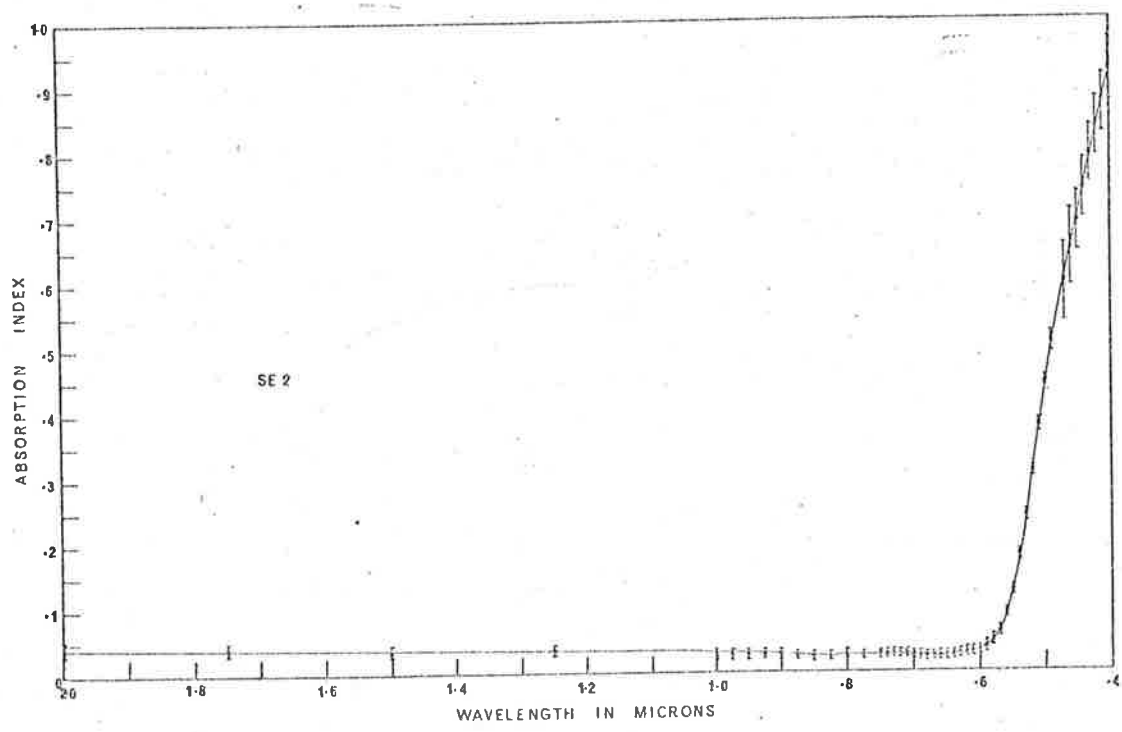
SE 2
ABSORPTION INDEX
1·0
·9
·8
·7
·6
·5
·4
·3
·2
·1
0
2·0
1·8
1·6
1·4
1·2
1·0
·8
·6
·4
WAVELENGTH IN MICRONS

FILM SE3.

$d_1 = 120 \pm 5$Å $\qquad$ $d_2 = 742 \pm 5$Å

λ(μ)	R	Γ	λ(μ)	R	Γ	λ(μ)	R	Γ
2.000	.171	.836	.680	.394	.611	.490	.145	.309
1.750	.200	.806	.670	.391	.614	.480	.157	.265
1.500	.236	.770	.660	.388	.621	.470	.168	.231
1.250	.282	.721	.650	.383	.624	.460	.179	.202
1.000	.341	.664	.640	.376	.632	.450	.190	.176
.975	.349	.658	.630	.366	.641	.440	.199	.152
.950	.354	.651	.620	.355	.650	.430	.210	.131
.925	.362	.643	.610	.342	.660	.420	.219	.113
.900	.369	.637	.600	.328	.669	.410	.228	.097
.875	.375	.631	.590	.308	.680	.400	.235	.081
.850	.382	.624	.575	.270	.698	.390	.241	.069
.825	.387	.621	.560	.220	.701	.380	.247	.057
.800	.390	.616	.550	.179	.682	.370	.251	.048
.775	.394	.610	.540	.146	.640	.360	.256	.040
.750	.396	.607	.530	.128	.574	.350	.260	.033
.725	.397	.606	.520	.120	.498	.340	.262	.028
.700	.398	.608	.510	.125	.423	.330	.264	.023
.690	.397	.609	.500	.135	.362			

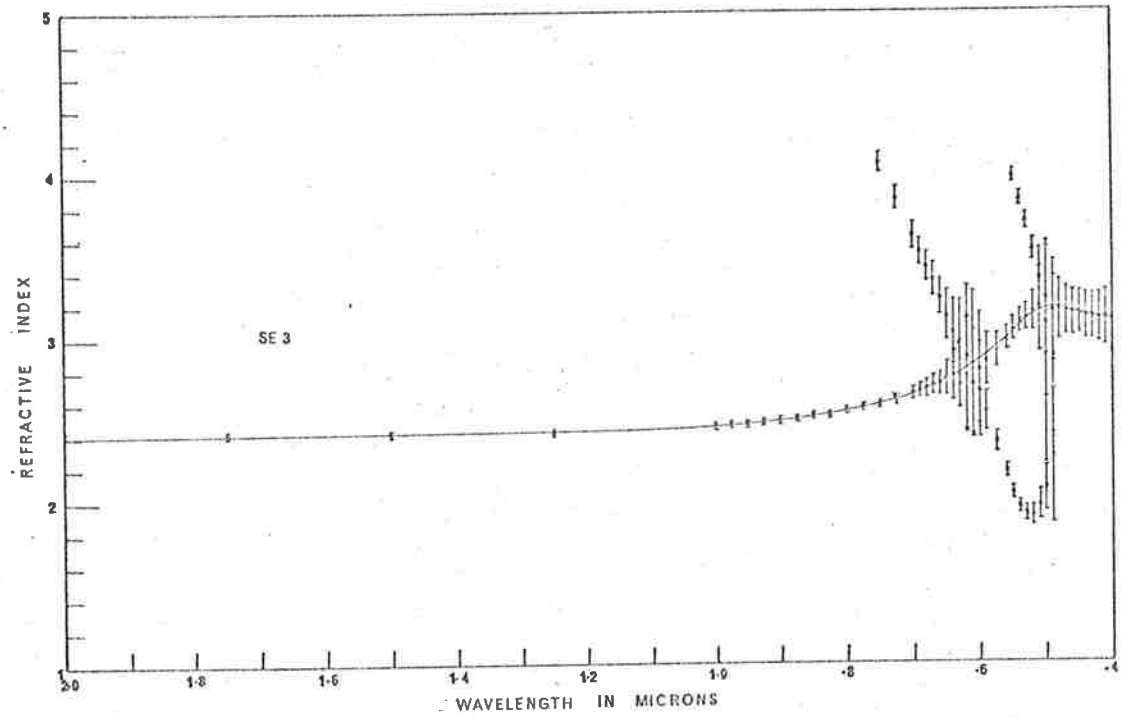
REFRACTIVE INDEX
SE 3
WAVELENGTH IN MICRONS

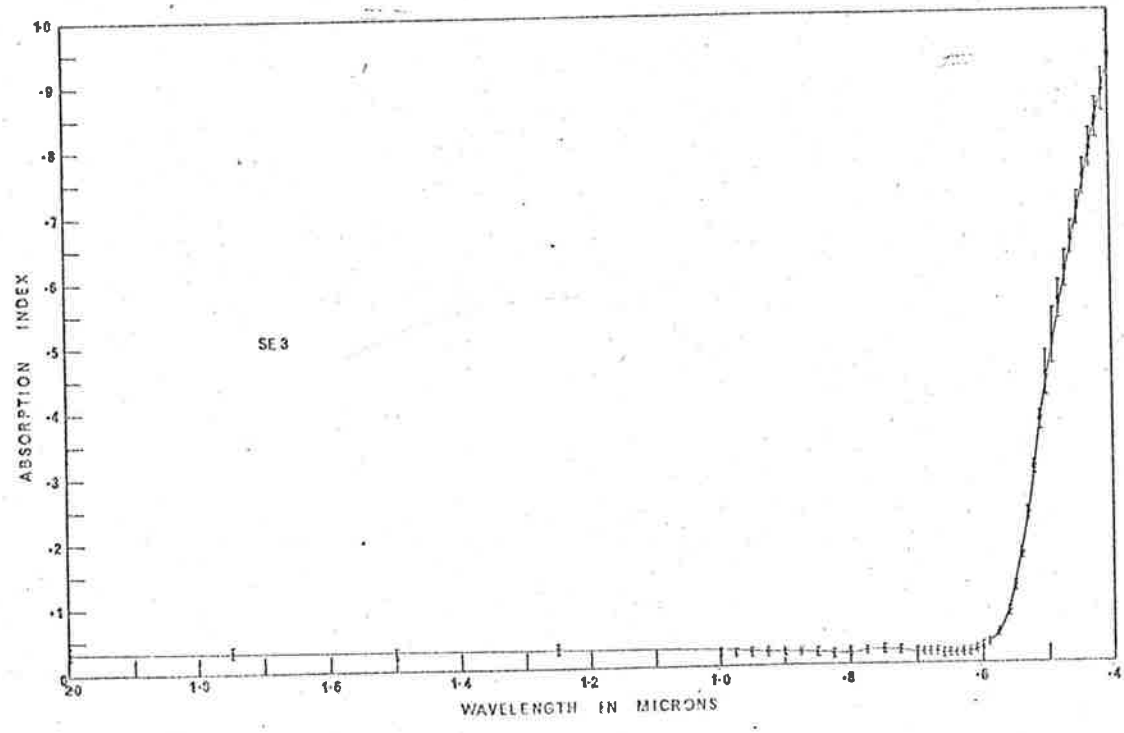
ABSORPTION INDEX
SE 3
WAVELENGTH IN MICRONS

FILM SE4.

$d_1 = 45 \pm 5 \text{Å}$ $d_2 = 930 \pm 5 \text{Å}$

λ(μ)	R	Γ	λ(μ)	R	Γ	λ(μ)	R	Γ
2.500	.181	.842	.825	.382	.630	.590	.083	.911
2.400	.191	.832	.800	.377	.637	.580	.061	.916
2.300	.200	.820	.790	.373	.639	.570	.044	.885
2.250	.203	.814	.780	.371	.643	.560	.043	.853
2.200	.209	.808	.775	.370	.644	.550	.077	.720
2.100	.220	.797	.770	.368	.646	.540	.117	.583
2.000	.231	.778	.760	.363	.650	.530	.151	.474
1.900	.243	.772	.750	.357	.656	.520	.181	.391
1.800	.255	.762	.740	.351	.663	.510	.214	.311
1.750	.262	.756	.730	.345	.669	.500	.231	.240
1.700	.270	.748	.725	.341	.673	.490	.242	.203
1.600	.284	.732	.720	.339	.680	.480	.250	.174
1.500	.300	.716	.710	.328	.689	.470	.256	.153
1.400	.315	.699	.700	.317	.701	.460	.260	.132
1.300	.333	.683	.690	.305	.713	.450	.264	.113
1.250	.341	.676	.680	.294	.728	.440	.267	.096
1.200	.348	.667	.670	.282	.743	.430	.269	.083
1.100	.363	.651	.660	.268	.761	.425	.270	.077
1.000	.379	.633	.650	.243	.783	.420	.269	.071
.975	.381	.629	.640	.222	.801	.410	.269	.061
.950	.383	.627	.630	.200	.824	.400	.269	.051
.925	.387	.624	.625	.189	.836	.390	.268	.043
.900	.388	.625	.620	.174	.848	.380	.265	.037
.875	.387	.624	.610	.142	.870	.370	.263	.031
.850	.384	.625	.600	.109	.890	.360	.260	.024

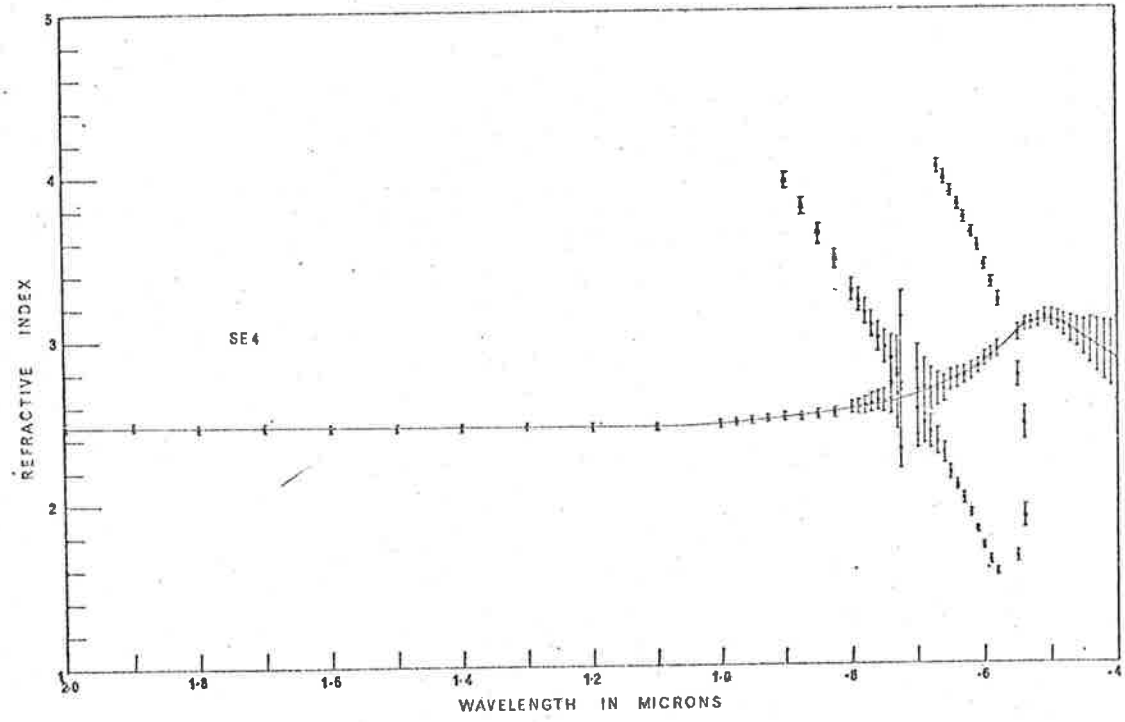
REFRACTIVE INDEX
SE4
WAVELENGTH IN MICRONS

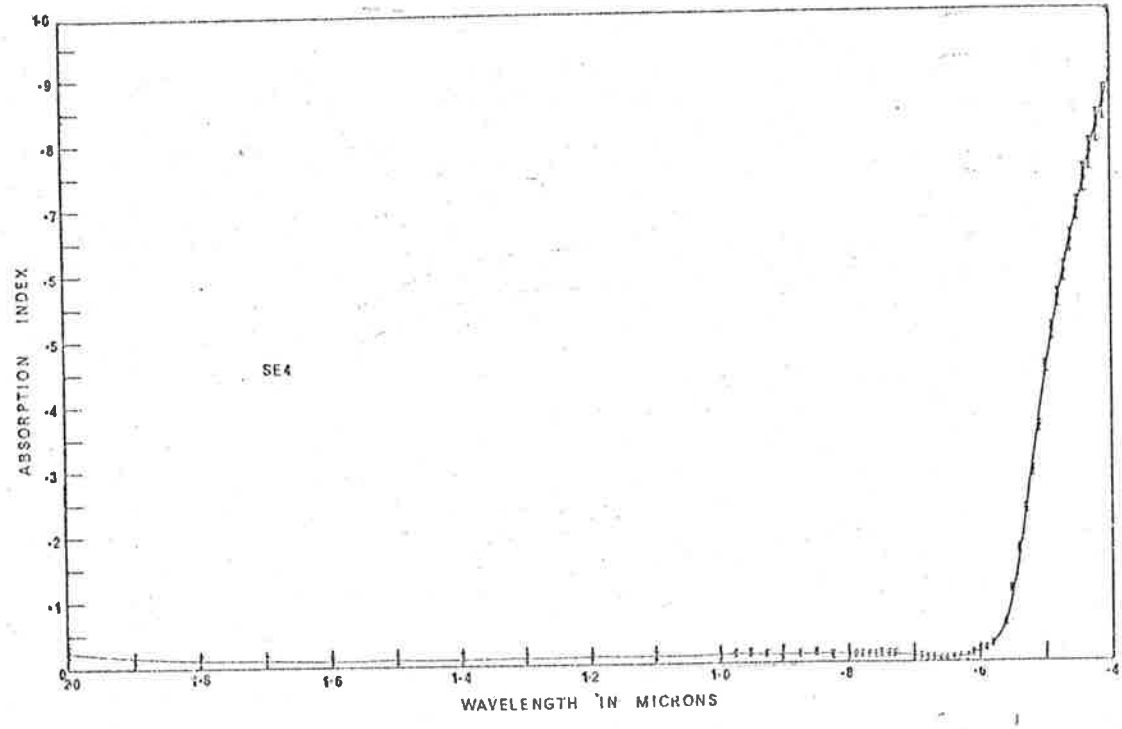
ABSORPTION INDEX
SE4
WAVELENGTH IN MICRONS

FILM SE5.

$d_1 = 45 \pm 5\text{Å}$ $\quad$ $d_2 = 1012 \pm 5\text{Å}$

λ(μ)	R	Γ	λ(μ)	R	Γ	λ(μ)	R	Γ
1.500	.313	.695	.740	.296	.711	.550	.164	.611
1.250	.351	.655	.730	.283	.722	.540	.214	.499
1.000	.378	.628	.720	.272	.734	.530	.253	.394
.975	.379	.628	.710	.258	.751	.520	.274	.314
.950	.379	.628	.700	.244	.766	.510	.287	.252
.925	.379	.628	.690	.228	.783	.500	.293	.207
.900	.376	.632	.680	.210	.803	.490	.294	.173
.875	.373	.638	.670	.189	.824	.480	.295	.145
.850	.367	.644	.660	.166	.841	.470	.294	.124
.840	.363	.648	.650	.143	.862	.460	.293	.108
.830	.360	.651	.640	.119	.887	.450	.291	.090
.820	.356	.654	.630	.094	.910	.440	.288	.078
.810	.352	.659	.620	.073	.929	.430	.284	.065
.800	.346	.664	.610	.055	.948	.420	.282	.054
.790	.339	.671	.600	.042	.958	.410	.278	.045
.780	.331	.678	.590	.039	.944	.400	.274	.036
.770	.323	.686	.580	.046	.902	.390	.271	.029
.760	.314	.693	.570	.068	.838	.380	.267	.023
.750	.308	.702	.560	.106	.746			

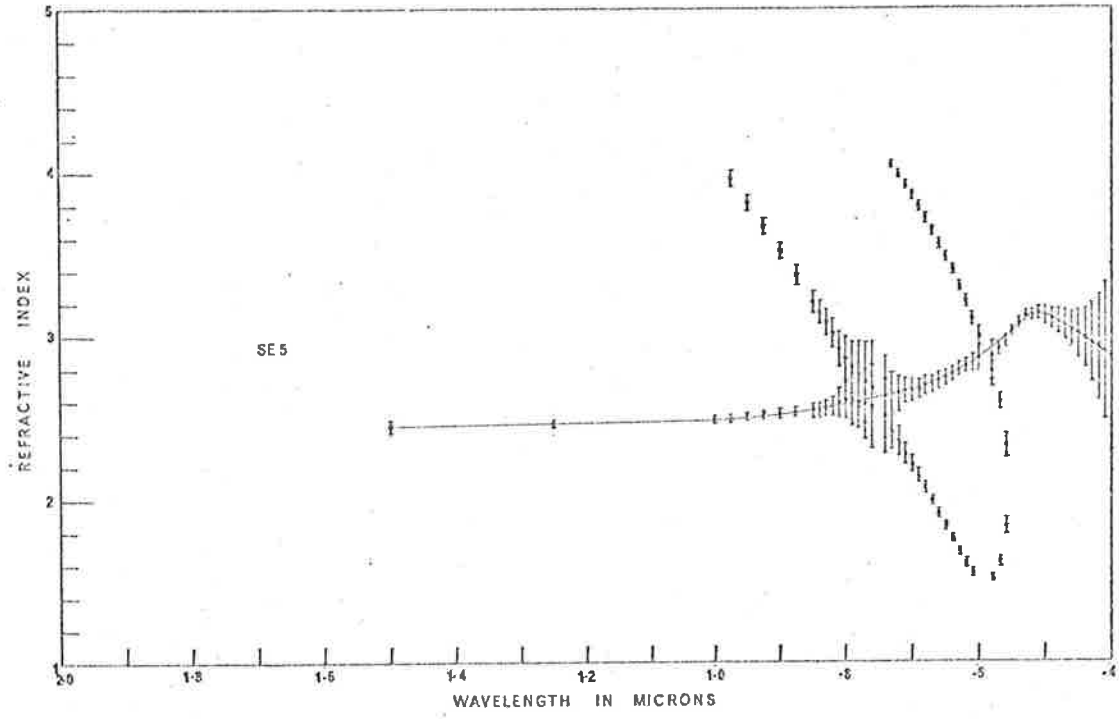
REFRACTIVE INDEX
SE 5
2·0
1·8
1·6
1·4
1·2
1·0
·8
·5
·4
WAVELENGTH IN MICRONS

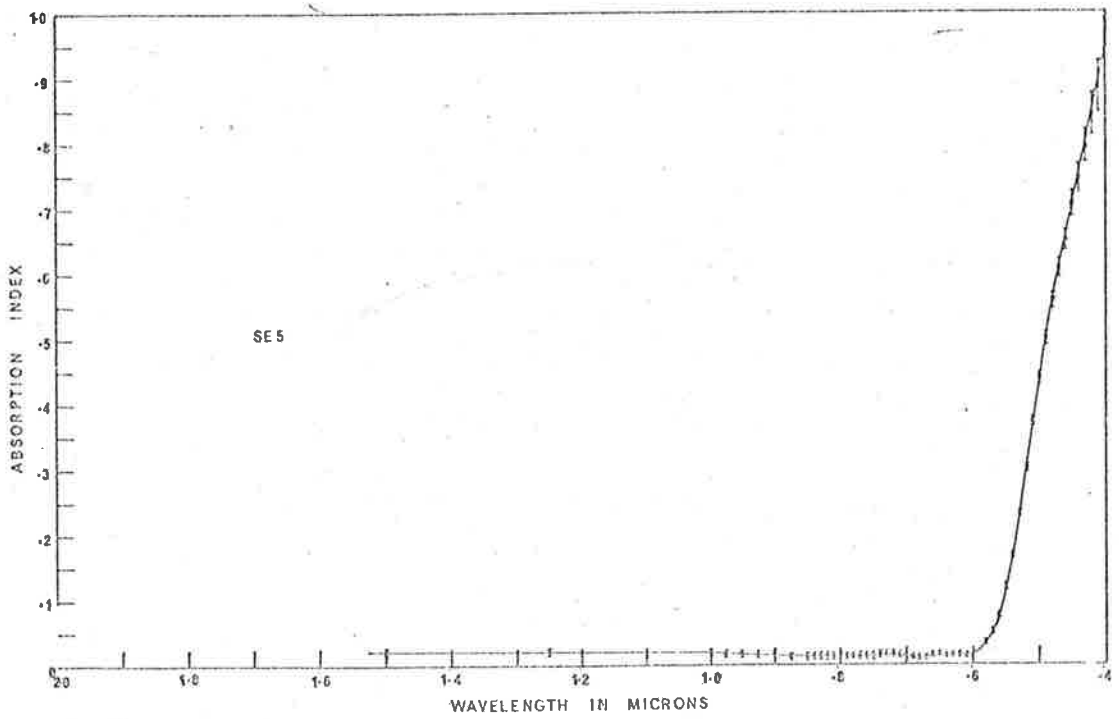
ABSORPTION INDEX
SE 5
2·0
1·8
1·6
1·4
1·2
1·0
·8
·6
·4
WAVELENGTH IN MICRONS

FILM SE6.

$d_1 = 120 \pm 20\text{Å}$ $\quad$ $d_2 = 1600 \pm 40\text{Å}$

λ(μ)	R	Γ	λ(μ)	R	Γ	λ(μ)	R	Γ
2.000	.351	.661	.925	.121	.883	.650	.352	.650
1.950	.353	.658	.900	.092	.914	.640	.381	.624
1.900	.358	.655	.875	.067	.944	.630	.404	.599
1.850	.361	.652	.850	.045	.969	.620	.423	.578
1.800	.364	.649	.840	.039	.978	.610	.437	.558
1.750	.367	.646	.830	.034	.987	.600	.444	.544
1.700	.369	.643	.820	.032	.989	.590	.440	.535
1.650	.370	.642	.810	.031	.990	.580	.423	.529
1.600	.370	.641	.800	.032	.990	.570	.389	.526
1.550	.370	.641	.790	.034	.991	.560	.334	.515
1.500	.367	.642	.780	.040	.982	.550	.258	.490
1.450	.363	.645	.770	.048	.971	.540	.196	.430
1.400	.358	.650	.760	.057	.957	.530	.167	.343
1.350	.353	.655	.750	.072	.936	.520	.169	.252
1.300	.344	.664	.740	.092	.911	.510	.185	.179
1.250	.332	.674	.730	.115	.886	.500	.202	.129
1.200	.316	.688	.720	.142	.861	.490	.217	.093
1.150	.296	.707	.710	.176	.832	.480	.228	.069
1.100	.270	.733	.700	.203	.803	.470	.237	.051
1.050	.238	.767	.690	.233	.777	.460	.243	.041
1.000	.197	.808	.680	.262	.742	.450	.249	.033
.975	.172	.832	.670	.292	.710	.440	.252	.026
.950	.147	.856	.660	.321	.680			

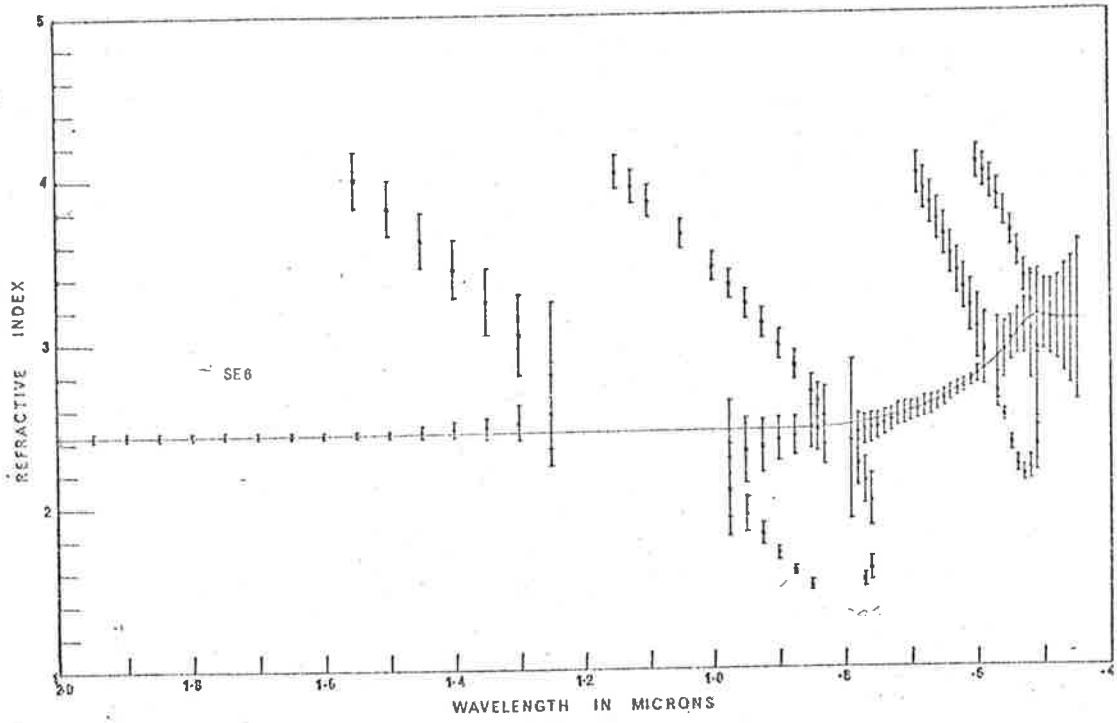
REFRACTIVE INDEX
5
4
3
2
SE6
2·0
1·8
1·6
1·4
1·2
1·0
·8
·6
·4
WAVELENGTH IN MICRONS

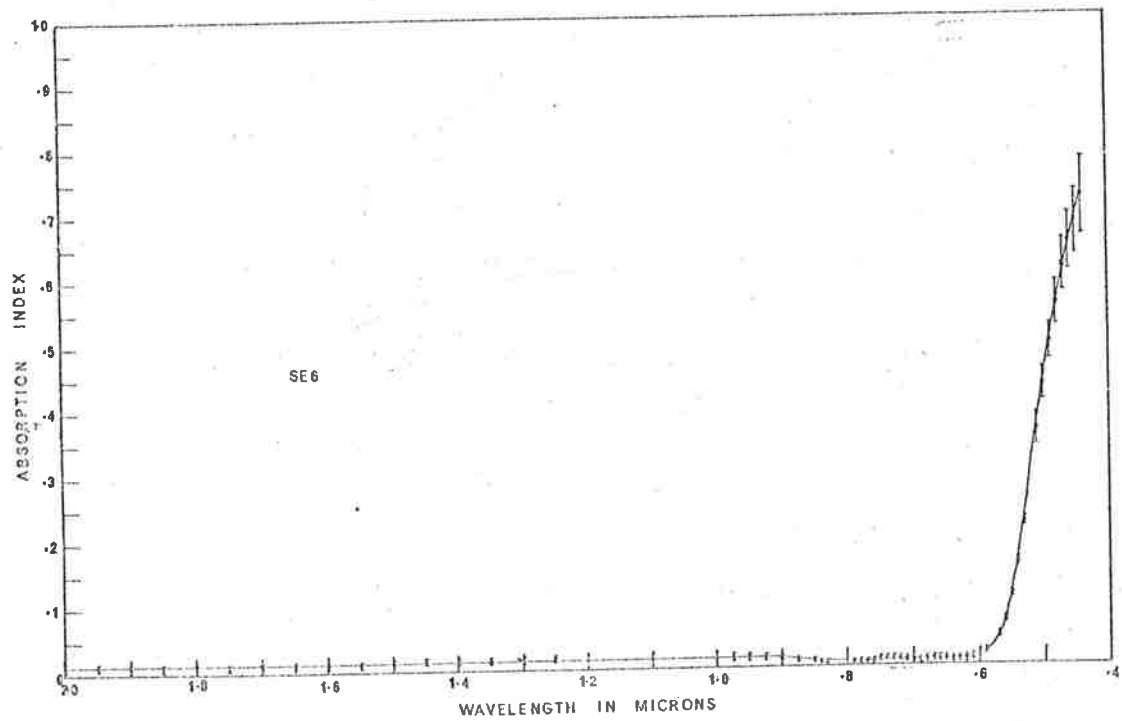
ABSORPTION INDEX
1·0
·9
·8
·7
·6
·5
·4
·3
·2
·1
0
SE6
2·0
1·8
1·6
1·4
1·2
1·0
·8
·6
·4
WAVELENGTH IN MICRONS

FILM SET.

$d_1 = 80 \pm 20$Å $\qquad$ $d_2 = 2500 \pm 50$Å

λ(μ)	R	Γ	λ(μ)	R	Γ	λ(μ)	R	Γ
2.000	.329	.678	.975	.218	.783	.690	.117	.884
1.950	.321	.689	.950	.255	.746	.680	.081	.930
1.900	.310	.697	.925	.292	.707	.670	.049	.966
1.850	.299	.708	.900	.327	.677	.660	.039	.983
1.800	.284	.721	.875	.355	.649	.650	.043	.977
1.750	.268	.736	.850	.377	.627	.640	.071	.935
1.700	.250	.754	.840	.383	.622	.630	.126	.873
1.650	.230	.777	.830	.387	.618	.620	.195	.800
1.600	.208	.800	.820	.390	.614	.610	.270	.717
1.550	.182	.823	.810	.389	.615	.600	.338	.640
1.500	.154	.848	.800	.385	.616	.590	.390	.564
1.450	.123	.878	.790	.378	.622	.580	.416	.504
1.400	.096	.907	.780	.371	.630	.570	.409	.456
1.350	.069	.939	.770	.360	.642	.560	.368	.412
1.300	.046	.970	.760	.347	.657	.550	.298	.368
1.250	.030	.992	.750	.326	.677	.540	.222	.294
1.200	.027	.999	.740	.302	.699	.530	.191	.204
1.150	.036	.986	.730	.273	.729	.520	.199	.126
1.100	.063	.947	.720	.241	.763	.510	.218	.074
1.050	.113	.888	.710	.202	.805	.500	.233	.046
1.000	.180	.820	.700	.157	.843	.490	.241	.031

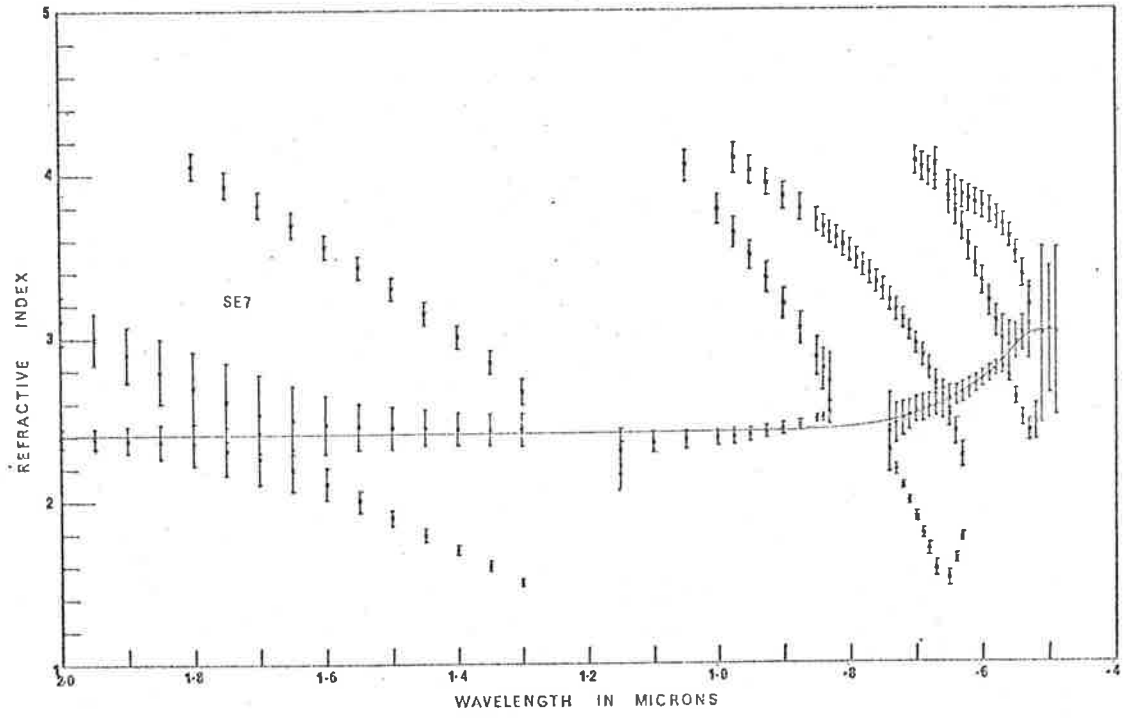
REFRACTIVE INDEX
SE7
WAVELENGTH IN MICRONS

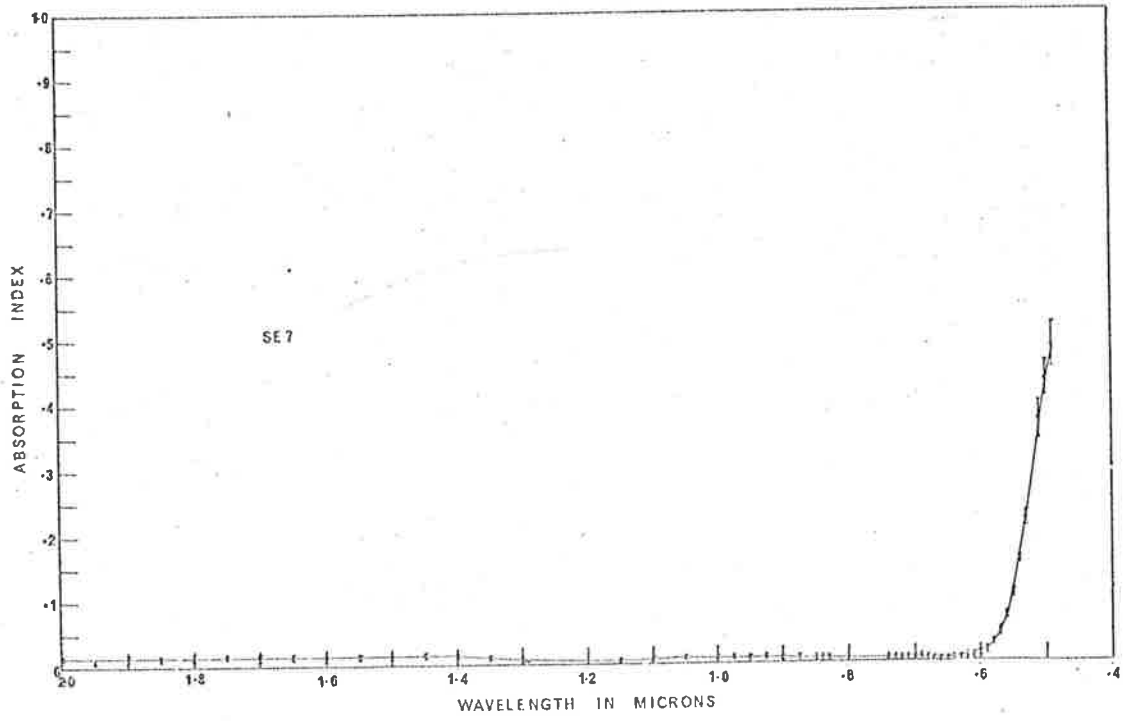
ABSORPTION INDEX
SE7
WAVELENGTH IN MICRONS

FILM SE8.

$d_1 = 120 \pm 20\text{Å}$ $d_2 = 2700 \pm 50\text{Å}$

λ(μ)	R	Γ	λ(μ)	R	Γ	λ(μ)	R	Γ
2.450	.359	.654	1.150	.123	.894	.710	.063	.962
2.400	.350	.663	1.100	.175	.841	.700	.052	.977
2.350	.341	.672	1.050	.236	.772	.690	.050	.980
2.300	.331	.681	1.000	.300	.710	.680	.072	.948
2.250	.321	.690	.975	.327	.683	.670	.103	.908
2.200	.312	.699	.950	.352	.659	.660	.154	.842
2.150	.303	.708	.925	.373	.637	.650	.219	.773
2.100	.294	.716	.900	.384	.622	.640	.272	.712
2.050	.287	.724	.890	.386	.618	.630	.331	.643
2.000	.277	.735	.880	.388	.616	.620	.382	.598
1.950	.269	.748	.870	.389	.616	.610	.418	.542
1.900	.256	.762	.860	.388	.619	.600	.432	.528
1.850	.241	.777	.850	.384	.623	.590	.430	.526
1.800	.228	.791	.840	.378	.624	.580	.374	.528
1.750	.212	.809	.830	.370	.640	.570	.295	.541
1.700	.193	.830	.820	.360	.652	.560	.197	.518
1.650	.173	.850	.810	.344	.671	.550	.138	.416
1.600	.151	.873	.800	.330	.690	.540	.154	.266
1.550	.127	.900	.790	.310	.711	.530	.196	.172
1.500	.101	.926	.780	.284	.734	.520	.228	.120
1.450	.074	.951	.770	.261	.764	.510	.244	.076
1.400	.049	.976	.760	.231	.797	.500	.258	.044
1.350	.032	.987	.750	.191	.836	.490	.260	.037
1.300	.033	.988	.740	.154	.872	.480	.259	.029
1.250	.048	.973	.730	.118	.908	.470	.257	.023
1.200	.080	.937	.720	.088	.938			

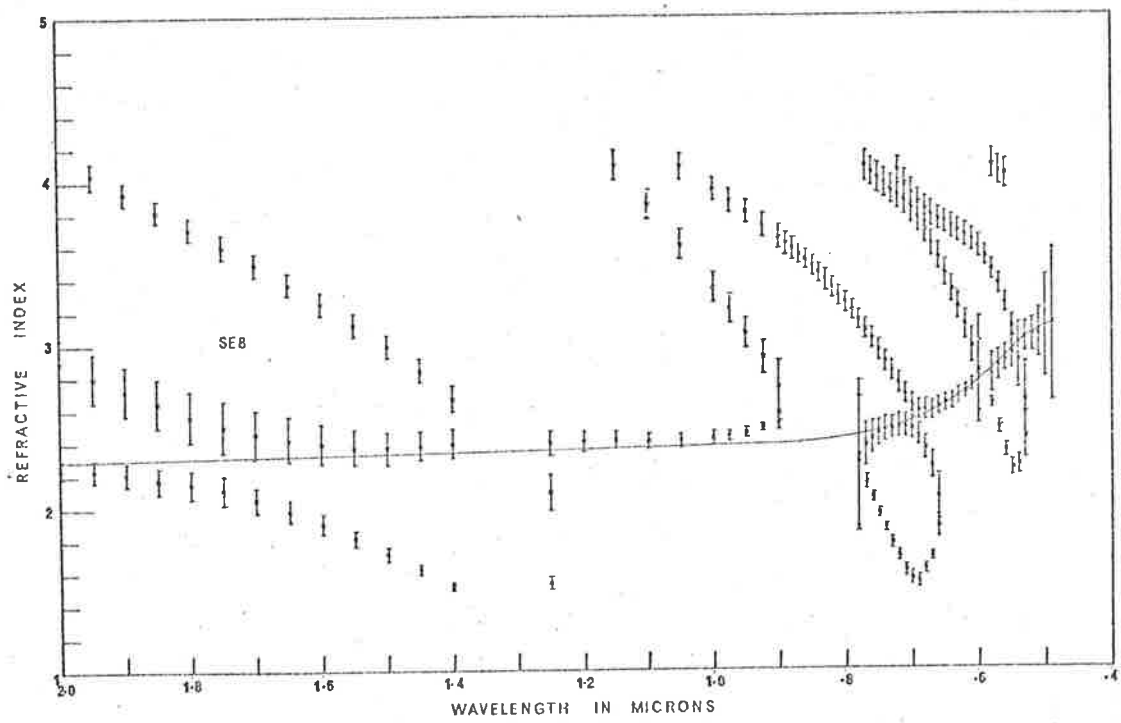
REFRACTIVE INDEX
SE8
WAVELENGTH IN MICRONS

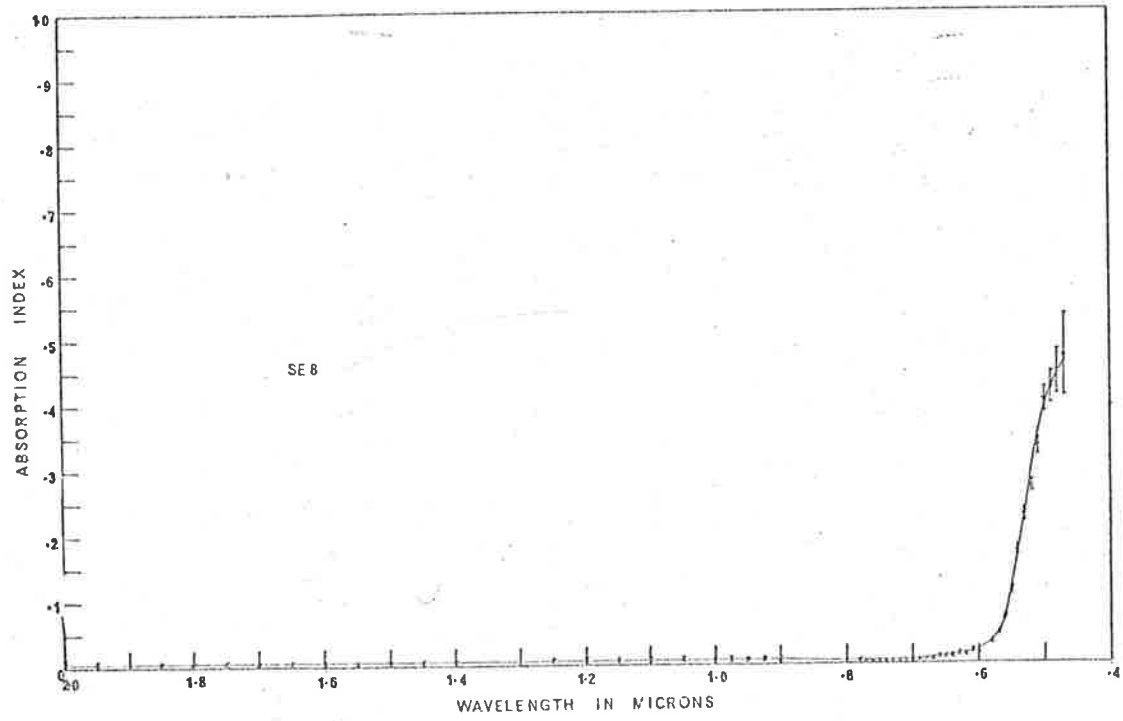
ABSORPTION INDEX
SE8
WAVELENGTH IN MICRONS

APPENDIX E.

MEASURED REFLECTANCES AND TRANSMITTANCES AND CALCULATED REFRACTIVE AND ABSORPTION INDICES OF GERMANIUM FILMS.

FILM GE1.

$d_1 = 5 \pm 3\text{Å}$ $d_2 = 240 \pm 20\text{Å}$

λ(μ)	R	Γ	λ(μ)	R	Γ	λ(μ)	R	Γ
2.02	.147	.875	1.54	.241	.787	1.06	.434	.534
2.01	.148	.875	1.53	.244	.784	1.05	.438	.527
2.00	.150	.874	1.52	.247	.782	1.04	.443	.517
1.99	.152	.872	1.51	.249	.779	1.03	.447	.510
1.98	.153	.871	1.50	.252	.776	1.02	.451	.502
1.97	.154	.869	1.49	.255	.772	1.01	.457	.492
1.96	.155	.868	1.48	.259	.769	1.00	.460	.485
1.95	.156	.867	1.47	.262	.765	.99	.464	.475
1.94	.158	.866	1.46	.265	.762	.98	.469	.466
1.93	.159	.865	1.45	.267	.759	.97	.473	.458
1.92	.160	.863	1.44	.272	.755	.96	.476	.448
1.91	.162	.862	1.43	.274	.751	.95	.482	.440
1.90	.163	.861	1.42	.278	.748	.94	.485	.431
1.89	.166	.859	1.41	.281	.743	.93	.488	.423
1.88	.167	.858	1.40	.285	.740	.92	.491	.414
1.87	.169	.856	1.39	.289	.736	.91	.496	.405
1.86	.170	.855	1.38	.292	.731	.90	.500	.397
1.85	.172	.853	1.37	.297	.727	.89	.502	.388
1.84	.174	.851	1.36	.300	.723	.88	.507	.379
1.83	.175	.850	1.35	.304	.717	.87	.508	.371
1.82	.178	.848	1.34	.308	.713	.86	.512	.360
1.81	.180	.847	1.33	.312	.709	.85	.516	.352
1.80	.182	.845	1.32	.316	.704	.84	.518	.344
1.79	.184	.843	1.31	.320	.699	.83	.523	.332
1.78	.185	.842	1.30	.324	.694	.82	.525	.324
1.77	.187	.839	1.29	.328	.689	.81	.528	.315
1.76	.189	.837	1.28	.332	.684	.80	.531	.306
1.75	.192	.835	1.27	.337	.679	.79	.535	.298
1.74	.194	.833	1.26	.341	.673	.78	.537	.289
1.73	.195	.832	1.25	.345	.667	.77	.539	.281
1.72	.197	.830	1.24	.350	.662	.76	.541	.274
1.71	.199	.828	1.23	.354	.656	.75	.544	.267
1.70	.201	.826	1.22	.359	.650	.74	.547	.259
1.69	.203	.824	1.21	.364	.644	.73	.548	.252
1.68	.206	.822	1.20	.368	.638	.72	.550	.246
1.67	.208	.819	1.19	.372	.631	.71	.551	.238
1.66	.210	.817	1.18	.377	.625	.70	.552	.231
1.65	.213	.815	1.17	.381	.618	.69	.554	.225
1.64	.215	.813	1.16	.386	.611	.68	.555	.217
1.63	.218	.810	1.15	.391	.611	.67	.556	.212
1.62	.220	.808	1.14	.396	.597	.66	.557	.205
1.61	.222	.805	1.13	.400	.590	.65	.557	.199
1.60	.225	.802	1.12	.406	.583	.64	.558	.192
1.59	.227	.800	1.11	.410	.575	.63	.558	.186
1.58	.231	.798	1.10	.415	.567	.62	.558	.180
1.57	.233	.795	1.09	.420	.559	.61	.558	.173
1.56	.235	.792	1.08	.424	.551	.60	.557	.167
1.55	.238	.790	1.07	.429	.543			

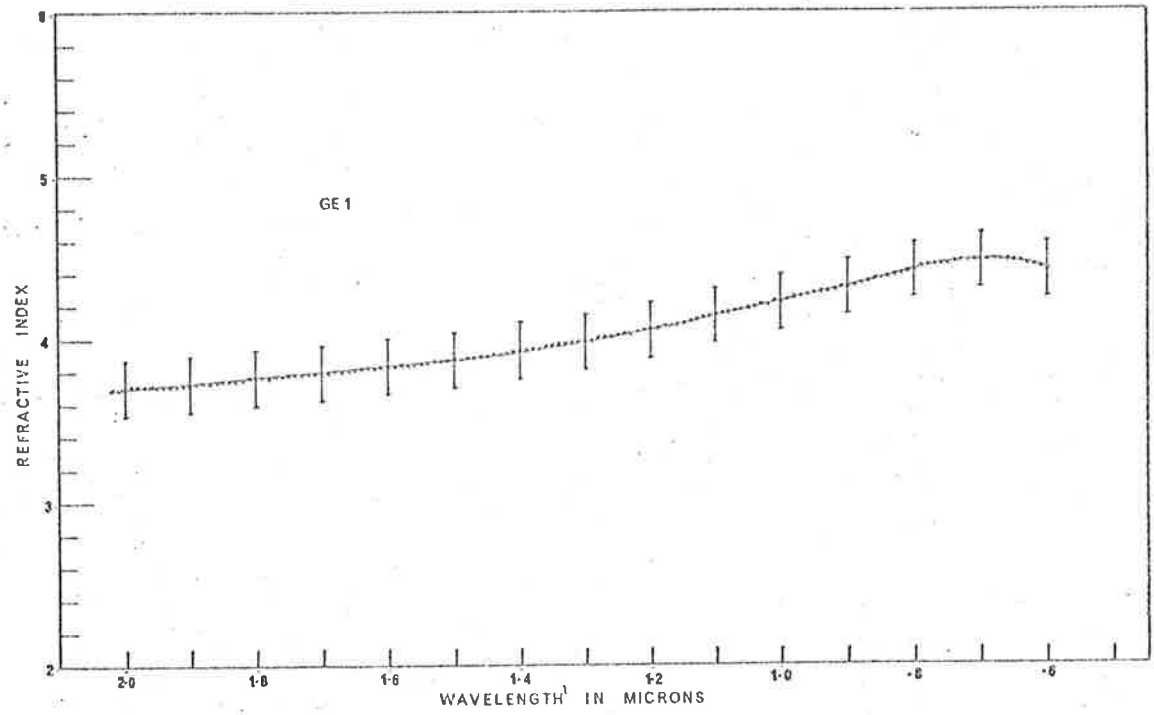
GE 1
REFRACTIVE INDEX
5
4
3
2
2·0
1·8
1·6
1·4
1·2
1·0
·8
·6
WAVELENGTH IN MICRONS

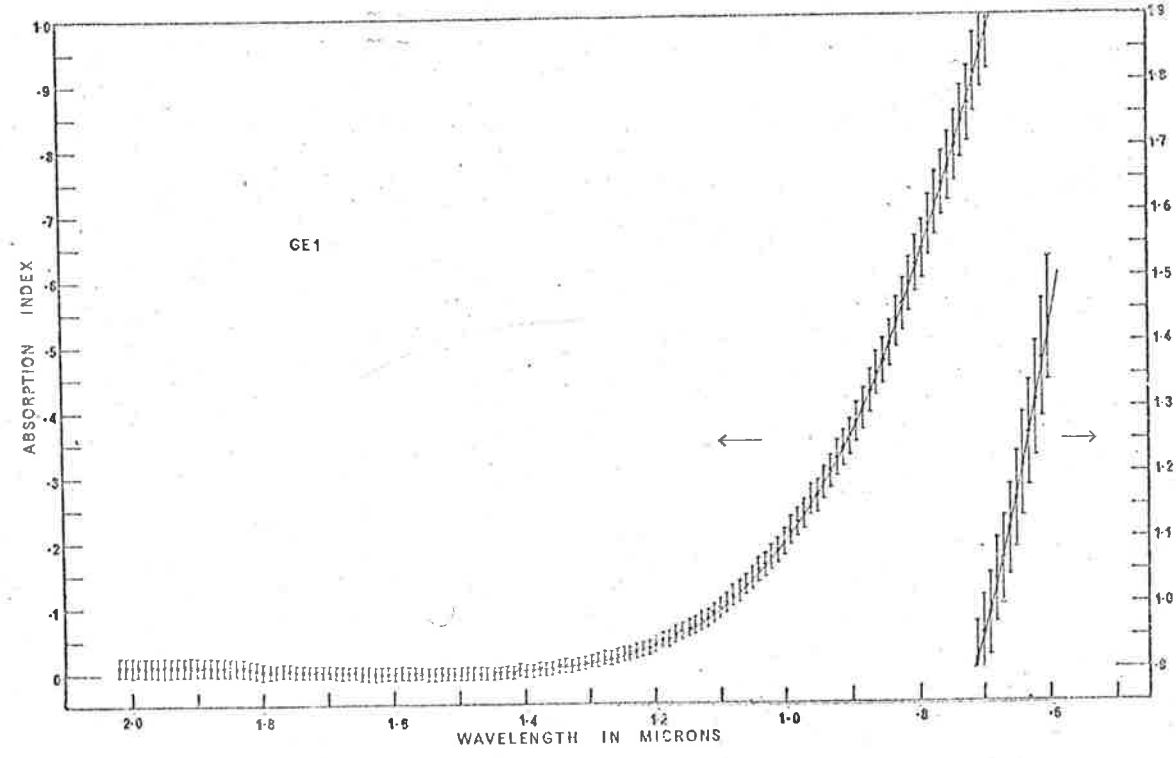
GE 1
ABSORPTION INDEX
1·0
·9
·8
·7
·6
·5
·4
·3
·2
·1
0
2·0
1·8
1·6
1·4
1·2
1·0
·8
·6
WAVELENGTH IN MICRONS

FILM GE2.

$d_1 = 5 \pm 3\text{Å}$ $\qquad$ $d_2 = 250 \pm 20\text{Å}$

λ(μ)	R	Γ	λ(μ)	R	Γ	λ(μ)	R	Γ
2.046	.136	.890	1.588	.209	.820	1.111	.381	.609
2.022	.139	.887	1.566	.215	.815	1.085	.394	.588
1.999	.141	.884	1.542	.221	.808	1.060	.407	.566
1.975	.144	.881	1.519	.227	.802	1.032	.420	.543
1.950	.147	.879	1.494	.233	.796	1.000	.434	.516
1.925	.150	.876	1.470	.240	.789	.973	.446	.492
1.901	.153	.873	1.445	.247	.781	.945	.458	.466
1.877	.156	.869	1.420	.255	.773	.915	.471	.439
1.854	.160	.866	1.395	.262	.764	.886	.481	.413
1.830	.164	.862	1.370	.271	.754	.855	.493	.384
1.806	.168	.859	1.345	.280	.743	.825	.503	.356
1.782	.172	.856	1.320	.290	.733	.795	.513	.327
1.760	.176	.853	1.295	.299	.721	.765	.522	.300
1.734	.180	.848	1.270	.309	.709	.735	.530	.276
1.710	.184	.844	1.245	.320	.695	.705	.536	.254
1.686	.189	.840	1.220	.331	.681	.675	.541	.233
1.661	.194	.835	1.194	.343	.665	.645	.545	.214
1.636	.199	.830	1.166	.355	.647	.615	.546	.197
1.612	.204	.826	1.138	.368	.628	.585	.547	.180

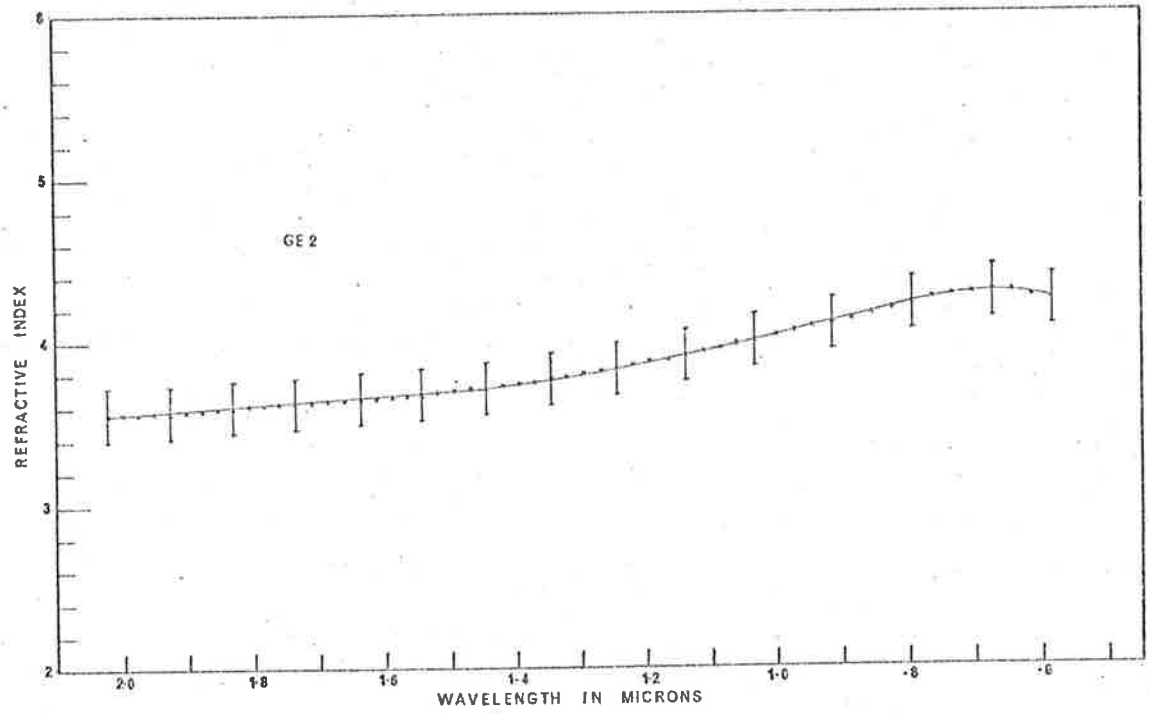
GE 2
REFRACTIVE INDEX
6
5
4
3
2
2·0
1·8
1·6
1·4
1·2
1·0
·8
·6
WAVELENGTH IN MICRONS

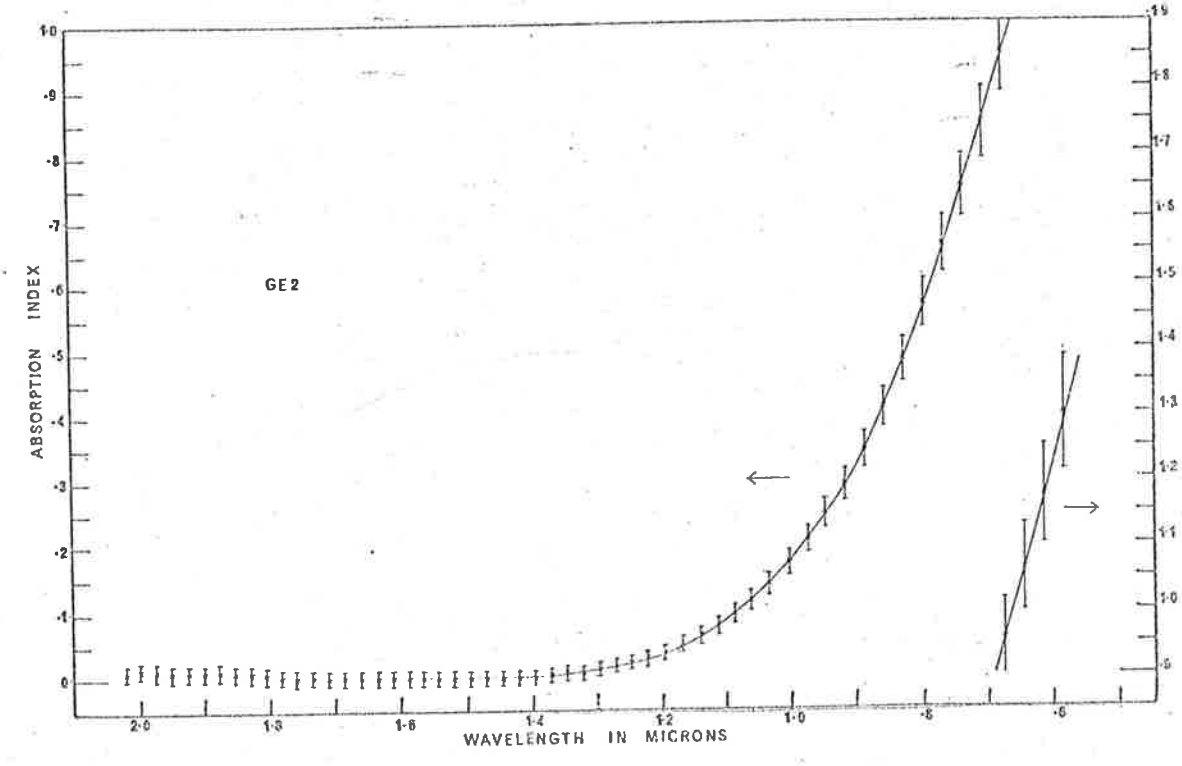
GE 2
ABSORPTION INDEX
1·0
·9
·8
·7
·6
·5
·4
·3
·2
·1
0
2·0
1·8
1·6
1·4
1·2
1·0
·8
·6
1·9
1·8
1·7
1·6
1·5
1·4
1·3
1·2
1·1
1·0
·9
WAVELENGTH IN MICRONS

FILM GE3.

$d_1 = 10 \pm 5\text{Å}$ $d_2 = 500 \pm 20\text{Å}$

λ(μ)	R	Γ	λ(μ)	R	Γ	λ(μ)	R	Γ
2.02	.531	.489	1.57	.653	.366	1.12	.735	.228
2.01	.533	.487	1.56	.656	.363	1.11	.735	.225
2.00	.535	.485	1.55	.659	.360	1.10	.735	.223
1.99	.538	.482	1.54	.662	.357	1.09	.735	.220
1.98	.541	.479	1.53	.665	.354	1.08	.735	.218
1.97	.543	.476	1.52	.662	.352	1.07	.734	.215
1.96	.545	.474	1.51	.670	.348	1.06	.733	.213
1.95	.548	.472	1.50	.672	.345	1.05	.731	.211
1.94	.550	.469	1.49	.675	.342	1.04	.728	.208
1.93	.553	.466	1.48	.677	.340	1.03	.727	.206
1.92	.556	.463	1.47	.679	.336	1.02	.726	.204
1.91	.558	.461	1.46	.682	.333	1.01	.725	.202
1.90	.562	.458	1.45	.684	.330	1.00	.723	.200
1.89	.564	.455	1.44	.687	.326	.99	.721	.197
1.88	.567	.453	1.43	.690	.323	.98	.717	.195
1.87	.569	.450	1.42	.692	.318	.97	.715	.193
1.86	.573	.447	1.41	.694	.315	.96	.711	.191
1.85	.575	.444	1.40	.696	.312	.95	.708	.189
1.84	.577	.442	1.39	.699	.309	.94	.705	.188
1.83	.581	.439	1.38	.701	.305	.93	.702	.186
1.82	.583	.437	1.37	.704	.302	.92	.698	.184
1.81	.587	.434	1.36	.706	.299	.91	.693	.182
1.80	.590	.431	1.35	.708	.296	.90	.687	.179
1.79	.592	.429	1.34	.711	.293	.89	.681	.177
1.78	.594	.426	1.33	.713	.290	.88	.675	.174
1.77	.597	.424	1.32	.715	.286	.87	.669	.172
1.76	.600	.421	1.31	.717	.284	.86	.660	.170
1.75	.603	.418	1.30	.718	.280	.85	.652	.167
1.74	.606	.416	1.29	.720	.278	.84	.641	.165
1.73	.608	.413	1.28	.722	.275	.83	.634	.163
1.72	.611	.410	1.27	.723	.271	.82	.626	.160
1.71	.614	.407	1.26	.725	.268	.81	.615	.157
1.70	.618	.404	1.25	.727	.266	.80	.605	.155
1.69	.620	.402	1.24	.728	.262	.79	.594	.152
1.68	.623	.398	1.23	.729	.260	.78	.584	.149
1.67	.625	.395	1.22	.730	.256	.77	.572	.146
1.66	.628	.392	1.21	.731	.253	.76	.560	.143
1.65	.631	.389	1.20	.732	.250	.75	.550	.140
1.64	.634	.386	1.19	.733	.248	.74	.539	.136
1.63	.637	.383	1.18	.734	.245	.73	.527	.132
1.62	.640	.380	1.17	.734	.242	.72	.516	.129
1.61	.643	.377	1.16	.734	.239	.71	.505	.125
1.60	.646	.374	1.15	.735	.236	.70	.493	.120
1.59	.648	.372	1.14	.736	.234	.69	.482	.115
1.58	.651	.369	1.13	.736	.231	.68	.471	.112

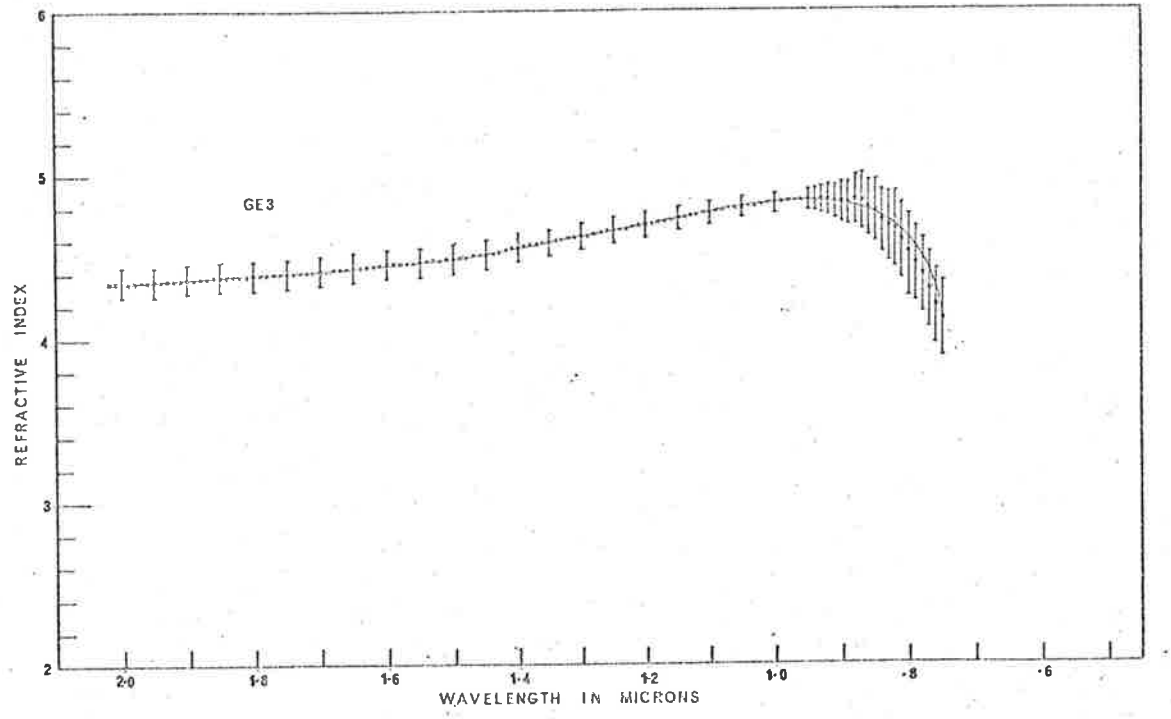
GE3
REFRACTIVE INDEX
6
5
4
3
2
2·0
1·8
1·6
1·4
1·2
1·0
·8
·6
WAVELENGTH IN MICRONS

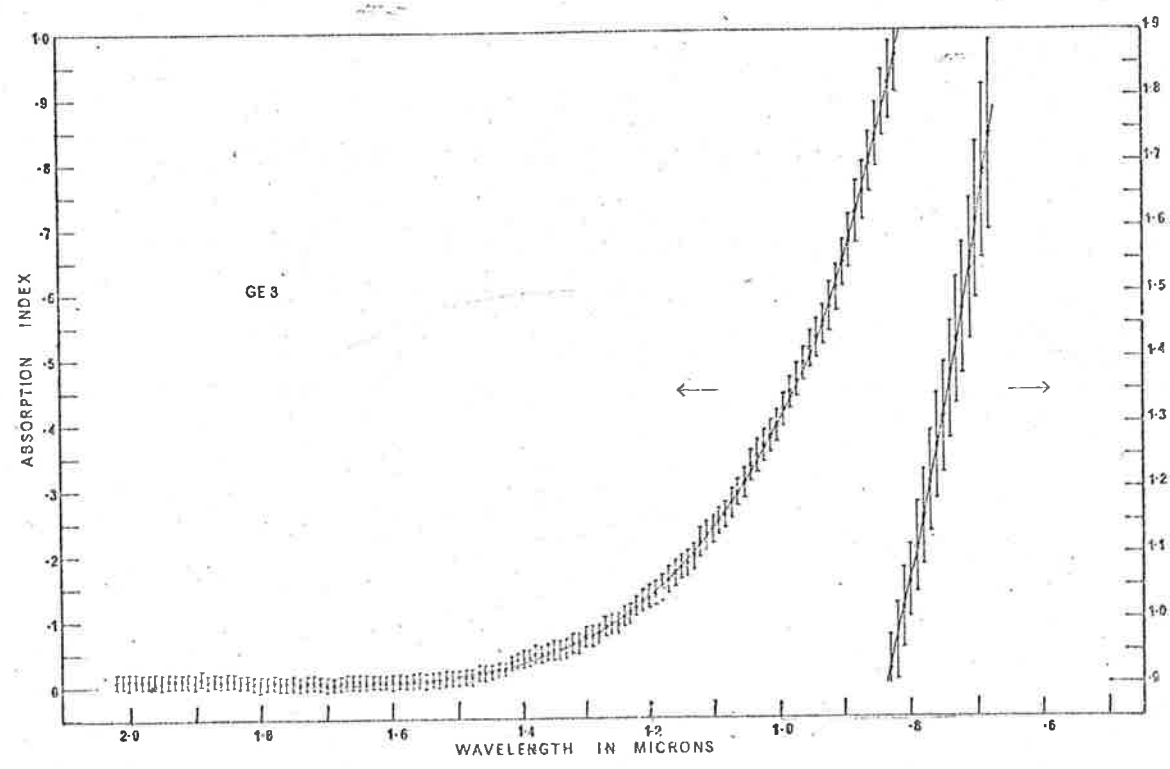
GE 3
ABSORPTION INDEX
1·0
·9
·8
·7
·6
·5
·4
·3
·2
·1
0
1·9
1·8
1·7
1·6
1·5
1·4
1·3
1·2
1·1
1·0
·9
2·0
1·8
1·6
1·4
1·2
1·0
·8
·6
WAVELENGTH IN MICRONS

FILM GE4.

$d_1 = 10 \pm 3\text{Å}$ $\quad\quad$ $d_2 = 997 \pm 3\text{Å}$

λ(μ)	R	Γ	λ(μ)	R	Γ	λ(μ)	R	Γ
2.02	.707	.303	1.57	.724	.281	1.12	.440	.417
2.01	.708	.302	1.56	.723	.281	1.11	.422	.422
2.00	.709	.301	1.55	.723	.281	1.10	.402	.427
1.99	.710	.300	1.54	.722	.282	1.09	.382	.432
1.98	.710	.300	1.53	.721	.282	1.08	.361	.435
1.97	.711	.299	1.52	.720	.283	1.07	.341	.438
1.96	.711	.298	1.51	.719	.283	1.06	.321	.439
1.95	.713	.297	1.50	.718	.284	1.05	.303	.440
1.94	.714	.296	1.49	.716	.285	1.04	.283	.439
1.93	.714	.295	1.48	.715	.286	1.03	.266	.436
1.92	.715	.294	1.47	.714	.286	1.02	.249	.432
1.91	.715	.294	1.46	.712	.287	1.01	.233	.426
1.90	.716	.293	1.45	.710	.289	1.00	.220	.419
1.89	.717	.292	1.44	.708	.290	.99	.209	.411
1.88	.717	.291	1.43	.706	.291	.98	.202	.402
1.87	.718	.290	1.42	.703	.293	.97	.197	.390
1.86	.718	.290	1.41	.701	.294	.96	.196	.377
1.85	.719	.289	1.40	.698	.296	.95	.198	.363
1.84	.719	.288	1.39	.695	.297	.94	.202	.348
1.83	.720	.288	1.38	.691	.300	.93	.210	.332
1.82	.721	.287	1.37	.687	.302	.92	.220	.313
1.81	.721	.287	1.36	.683	.304	.91	.232	.296
1.80	.722	.286	1.35	.679	.307	.90	.244	.278
1.79	.722	.286	1.34	.674	.310	.89	.260	.259
1.78	.723	.285	1.33	.669	.313	.88	.275	.240
1.77	.724	.285	1.32	.664	.316	.87	.292	.220
1.76	.725	.284	1.31	.659	.319	.86	.309	.203
1.75	.725	.284	1.30	.653	.322	.85	.326	.185
1.74	.725	.284	1.29	.647	.325	.84	.343	.167
1.73	.726	.283	1.28	.641	.329	.83	.359	.151
1.72	.726	.283	1.27	.633	.334	.82	.376	.137
1.71	.726	.282	1.26	.625	.338	.81	.390	.122
1.70	.726	.282	1.25	.617	.343	.80	.404	.110
1.69	.727	.281	1.24	.607	.347	.79	.416	.098
1.68	.727	.281	1.23	.598	.353	.78	.427	.088
1.67	.727	.281	1.22	.588	.358	.77	.437	.079
1.66	.727	.281	1.21	.578	.363	.76	.445	.070
1.65	.726	.281	1.20	.565	.369	.75	.452	.061
1.64	.726	.281	1.19	.553	.375	.74	.458	.052
1.63	.726	.280	1.18	.539	.381	.73	.464	.048
1.62	.726	.281	1.17	.524	.387	.72	.468	.040
1.61	.726	.280	1.16	.509	.393	.71	.471	.032
1.60	.726	.281	1.15	.494	.399	.70	.473	.025
1.59	.725	.280	1.14	.478	.405	.69	.474	.021
1.58	.725	.281	1.13	.460	.411			

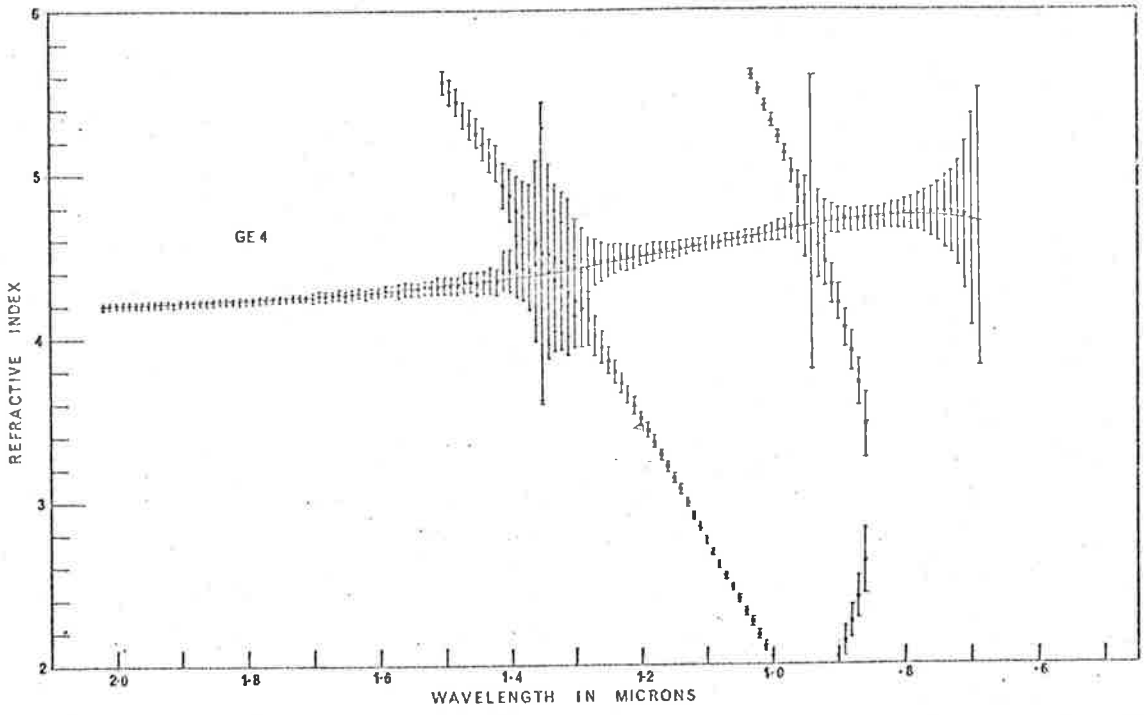
GE 4
REFRACTIVE INDEX
6
5
4
3
2
2·0
1·8
1·6
1·4
1·2
1·0
·8
·6
WAVELENGTH IN MICRONS

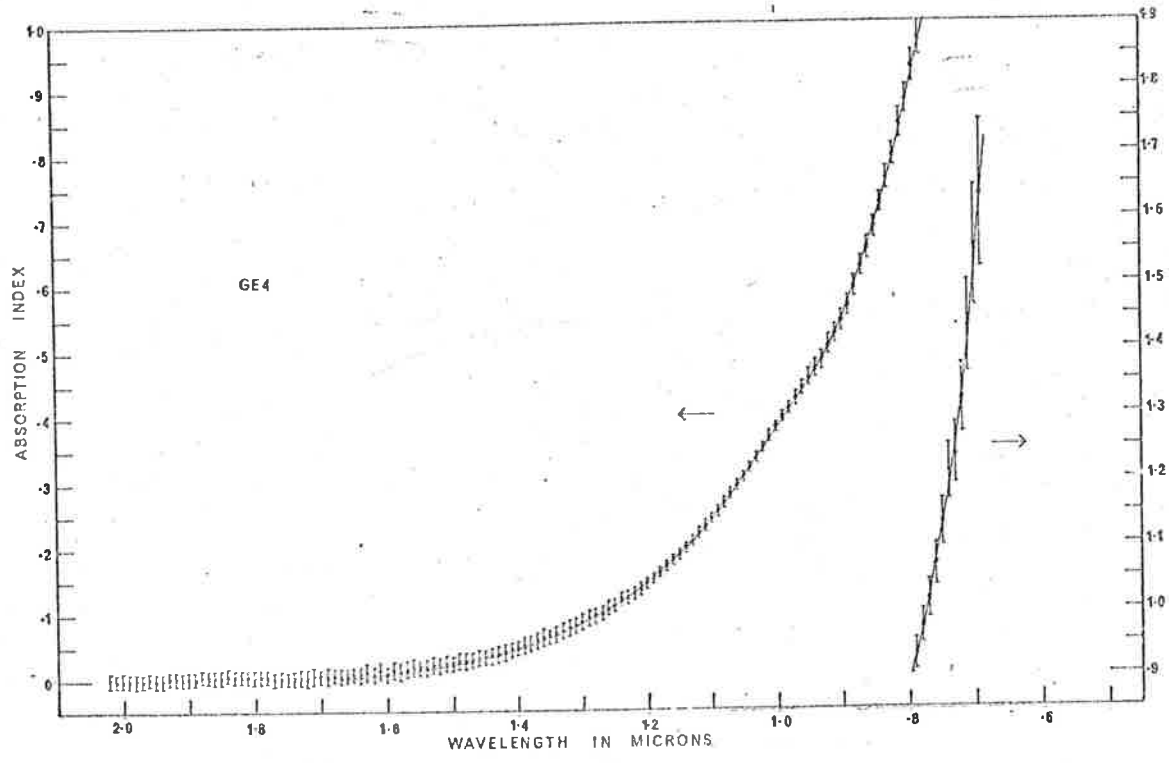
GE4
ABSORPTION INDEX
1·0
·9
·8
·7
·6
·5
·4
·3
·2
·1
0
1·9
1·8
1·7
1·6
1·5
1·4
1·3
1·2
1·1
1·0
·9
2·0
1·8
1·6
1·4
1·2
1·0
·8
·6
WAVELENGTH IN MICRONS

FILM GE5.

$d_1 = 0 \pm 2$ Å $\qquad d_2 = 1098 \pm 10$ Å

λ(μ)	R	Γ	λ(μ)	R	Γ	λ(μ)	R	Γ
2.02	.728	.281	1.60	.719	.288	1.18	.349	.503
2.01	.729	.280	1.59	.717	.290	1.17	.330	.509
2.00	.730	.280	1.58	.715	.291	1.16	.307	.513
1.99	.730	.279	1.57	.714	.293	1.15	.286	.516
1.98	.730	.279	1.56	.712	.295	1.14	.267	.518
1.97	.731	.278	1.55	.710	.297	1.13	.248	.519
1.96	.731	.278	1.54	.707	.298	1.12	.230	.517
1.95	.731	.277	1.53	.705	.301	1.11	.214	.515
1.94	.731	.277	1.52	.703	.303	1.10	.201	.510
1.93	.732	.277	1.51	.700	.305	1.09	.189	.504
1.92	.732	.276	1.50	.696	.307	1.08	.179	.496
1.91	.732	.276	1.49	.693	.310	1.07	.173	.486
1.90	.732	.276	1.48	.690	.313	1.06	.171	.475
1.89	.733	.275	1.47	.686	.316	1.05	.172	.461
1.88	.733	.275	1.46	.681	.319	1.04	.176	.447
1.87	.733	.275	1.45	.677	.322	1.03	.184	.431
1.86	.733	.275	1.44	.672	.326	1.02	.194	.414
1.85	.733	.275	1.43	.665	.332	1.01	.206	.397
1.84	.733	.275	1.42	.659	.336	1.00	.219	.376
1.83	.733	.275	1.41	.653	.340	.99	.234	.358
1.82	.734	.275	1.40	.647	.345	.98	.249	.337
1.81	.733	.275	1.39	.639	.350	.97	.266	.317
1.80	.733	.275	1.38	.632	.355	.96	.283	.296
1.79	.733	.275	1.37	.624	.361	.95	.300	.278
1.78	.734	.276	1.36	.615	.367	.94	.319	.260
1.77	.734	.276	1.35	.606	.373	.93	.336	.241
1.76	.734	.276	1.34	.596	.380	.92	.353	.223
1.75	.733	.276	1.33	.586	.387	.91	.369	.205
1.74	.733	.277	1.32	.576	.394	.90	.385	.189
1.73	.732	.277	1.31	.564	.401	.89	.400	.172
1.72	.731	.278	1.30	.552	.409	.88	.415	.155
1.71	.731	.278	1.29	.539	.417	.87	.429	.140
1.70	.730	.279	1.28	.524	.425	.86	.440	.126
1.69	.730	.279	1.27	.511	.433	.85	.452	.110
1.68	.728	.280	1.26	.496	.441	.84	.462	.098
1.67	.728	.281	1.25	.480	.450	.83	.471	.086
1.66	.727	.282	1.24	.463	.458	.82	.478	.074
1.65	.726	.283	1.23	.446	.466	.81	.484	.064
1.64	.725	.284	1.22	.427	.475	.80	.489	.055
1.63	.724	.285	1.21	.409	.482	.79	.492	.044
1.62	.722	.286	1.20	.389	.490	.78	.495	.039
1.61	.720	.287	1.19	.370	.497	.77	.497	.035
						.76	.497	.027

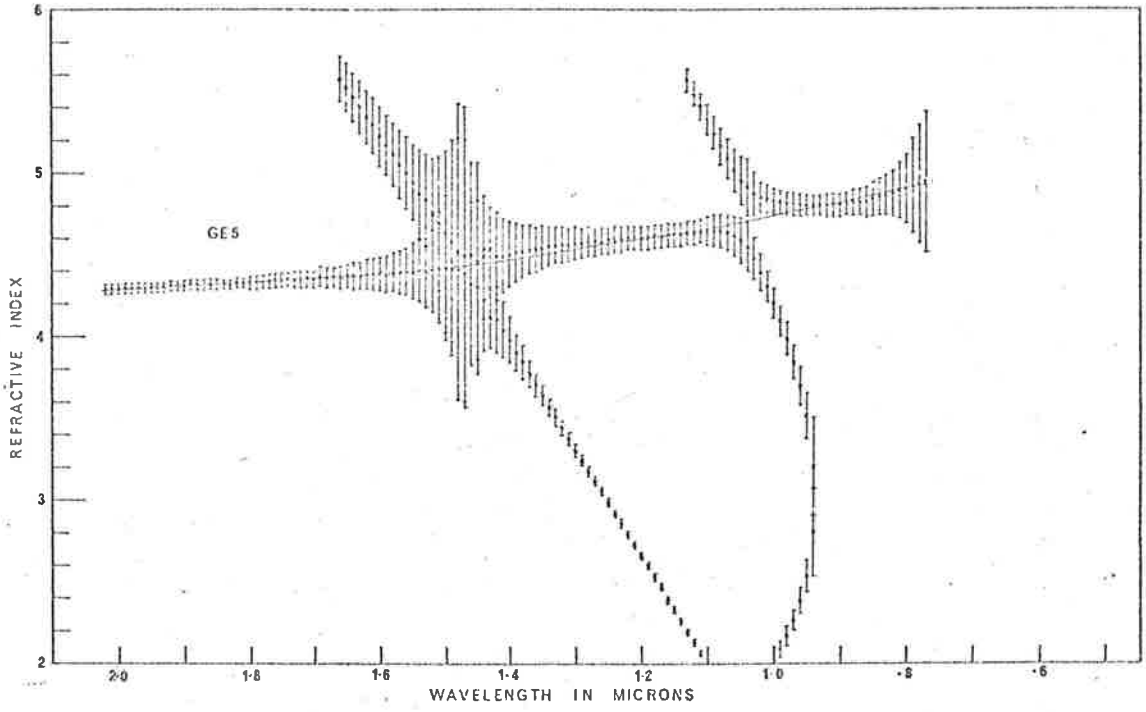
GE5
REFRACTIVE INDEX
6
5
4
3
2
2·0
1·8
1·6
1·4
1·2
1·0
·8
·6
WAVELENGTH IN MICRONS

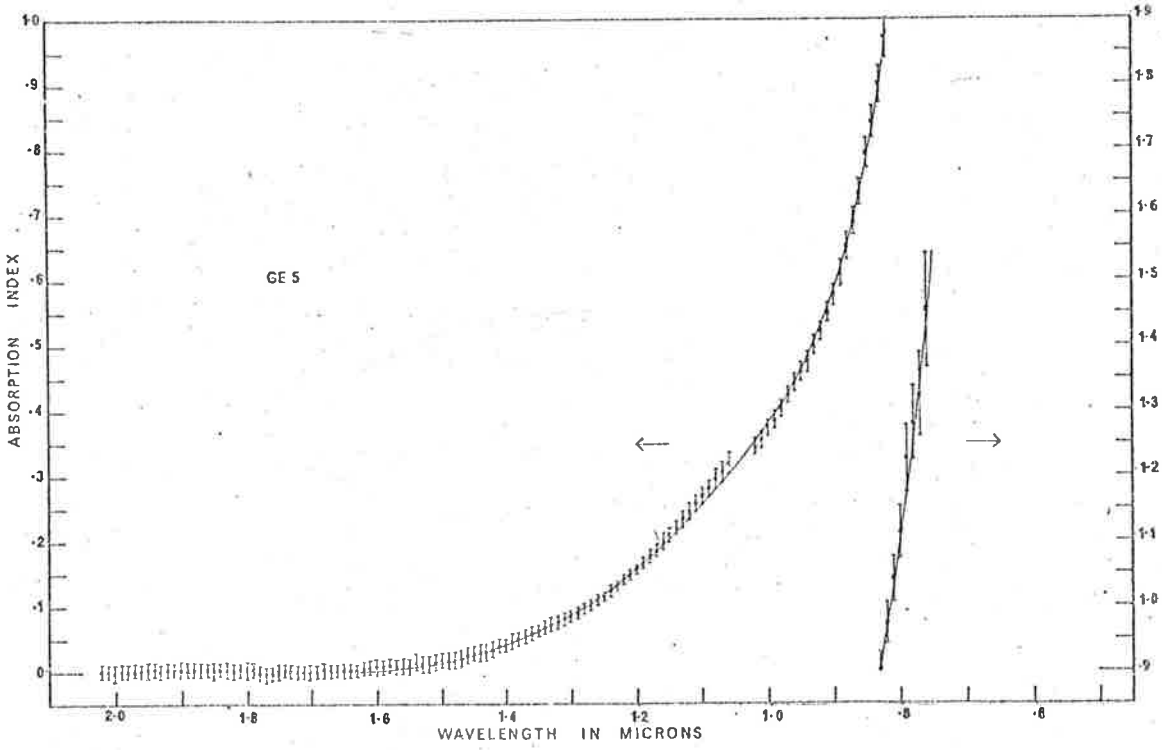
GE 5
ABSORPTION INDEX
1·0
·9
·8
·7
·6
·5
·4
·3
·2
·1
0
1·9
1·8
1·7
1·6
1·5
1·4
1·3
1·2
1·1
1·0
·9
2·0
1·8
1·6
1·4
1·2
1·0
·8
·6
WAVELENGTH IN MICRONS

FILM GE6.

$d_1 = 0 \pm 5$Å $\qquad$ $d_2 = 1130 \pm 5$Å

λ(μ)	R	Γ	λ(μ)	R	Γ	λ(μ)	R	Γ
2.112	.722	.287	1.671	.715	.287	1.220	.391	.486
2.102	.723	.287	1.661	.714	.288	1.210	.370	.495
2.093	.723	.286	1.651	.712	.289	1.200	.350	.503
2.083	.724	.286	1.641	.711	.290	1.189	.329	.510
2.074	.724	.285	1.632	.709	.291	1.178	.309	.516
2.065	.724	.285	1.622	.707	.292	1.166	.289	.521
2.055	.724	.284	1.612	.705	.293	1.155	.266	.525
2.046	.724	.284	1.602	.703	.294	1.144	.247	.527
2.036	.725	.284	1.593	.701	.296	1.133	.228	.528
2.027	.725	.283	1.584	.699	.297	1.122	.210	.526
2.018	.726	.283	1.575	.697	.299	1.111	.195	.523
2.008	.726	.283	1.566	.695	.301	1.101	.181	.517
1.999	.726	.282	1.556	.692	.303	1.091	.170	.510
1.980	.726	.282	1.547	.690	.304	1.080	.163	.499
1.970	.727	.281	1.538	.687	.307	1.070	.160	.487
1.960	.726	.281	1.529	.684	.309	1.060	.161	.472
1.950	.727	.281	1.519	.681	.311	1.049	.166	.455
1.940	.727	.280	1.509	.676	.313	1.038	.174	.437
1.930	.727	.280	1.489	.669	.319	1.026	.187	.416
1.921	.727	.280	1.479	.665	.322	1.013	.201	.395
1.911	.727	.280	1.470	.661	.325	1.000	.218	.374
1.901	.727	.279	1.460	.656	.328	.990	.237	.350
1.891	.727	.279	1.450	.650	.331	.979	.257	.326
1.881	.727	.279	1.440	.645	.335	.968	.277	.303
1.872	.727	.279	1.430	.639	.339	.957	.297	.281
1.863	.728	.279	1.420	.634	.343	.945	.317	.259
1.854	.727	.279	1.410	.628	.347	.931	.338	.238
1.844	.727	.279	1.400	.620	.352	.920	.358	.217
1.835	.727	.279	1.390	.613	.358	.910	.377	.197
1.825	.727	.280	1.380	.605	.363	.899	.394	.180
1.815	.726	.280	1.370	.596	.369	.886	.411	.162
1.806	.726	.280	1.360	.587	.375	.873	.426	.147
1.796	.725	.280	1.350	.578	.382	.860	.441	.132
1.787	.725	.280	1.340	.567	.388	.850	.453	.119
1.778	.724	.281	1.330	.557	.396	.838	.465	.107
1.769	.724	.281	1.320	.546	.402	.825	.474	.096
1.760	.723	.281	1.310	.534	.411	.812	.481	.084
1.749	.722	.282	1.300	.521	.418	.800	.488	.075
1.739	.721	.282	1.290	.508	.426	.789	.491	.066
1.729	.721	.283	1.280	.494	.434	.778	.493	.058
1.719	.720	.283	1.270	.479	.443	.765	.493	.053
1.710	.719	.284	1.260	.464	.451	.752	.492	.048
1.700	.718	.284	1.250	.446	.460	.740	.490	.047
1.691	.717	.285	1.240	.428	.469	.729	.487	.037
1.681	.716	.286	1.230	.409	.478	.718	.482	.028

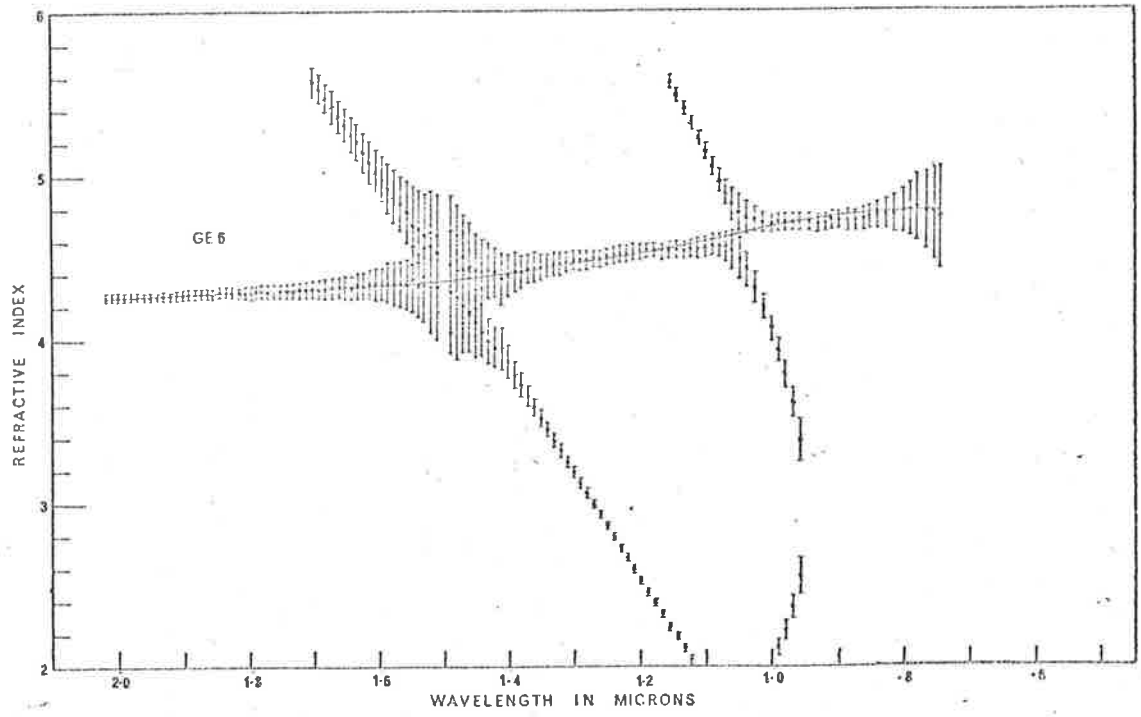
GE 6
REFRACTIVE INDEX
6
5
4
3
2
2·0
1·8
1·6
1·4
1·2
1·0
·8
·6
WAVELENGTH IN MICRONS

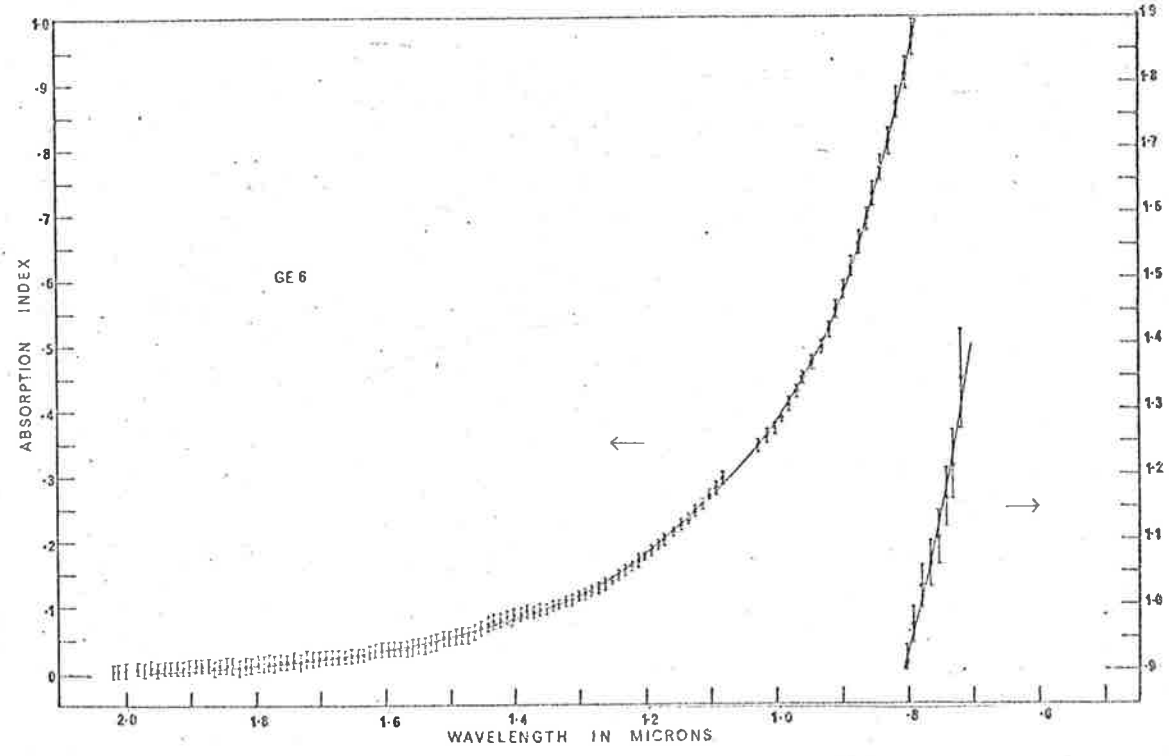
GE 6
ABSORPTION INDEX
1·0
·9
·8
·7
·6
·5
·4
·3
·2
·1
0
1·9
1·8
1·7
1·6
1·5
1·4
1·3
1·2
1·1
1·0
·9
2·0
1·8
1·6
1·4
1·2
1·0
·8
·6
WAVELENGTH IN MICRONS

FILM GE7.

$d_1 = 0 \pm 5$Å $\qquad$ $d_2 = 1425 \pm 20$Å

λ(μ)	R	T	λ(μ)	R	T	λ(μ)	R	T
2.02	.707	.303	1.59	.528	.465	1.16	.310	.468
2.01	.706	.304	1.58	.517	.474	1.15	.331	.443
2.00	.704	.305	1.57	.507	.483	1.14	.353	.419
1.99	.703	.307	1.56	.496	.493	1.13	.374	.395
1.98	.702	.308	1.55	.484	.503	1.12	.395	.370
1.97	.700	.309	1.54	.471	.514	1.11	.415	.348
1.96	.698	.311	1.53	.458	.525	1.10	.434	.327
1.95	.696	.312	1.52	.445	.537	1.09	.451	.307
1.94	.694	.314	1.51	.430	.549	1.08	.467	.289
1.93	.692	.315	1.50	.415	.561	1.07	.483	.271
1.92	.691	.317	1.49	.400	.573	1.06	.497	.254
1.91	.688	.319	1.48	.384	.586	1.05	.510	.239
1.90	.687	.321	1.47	.366	.599	1.04	.521	.225
1.89	.685	.324	1.46	.349	.612	1.03	.532	.211
1.88	.681	.325	1.45	.333	.625	1.02	.540	.200
1.87	.679	.328	1.44	.314	.639	1.01	.548	.188
1.86	.676	.331	1.43	.295	.652	1.00	.554	.178
1.85	.673	.333	1.42	.277	.666	.99	.559	.168
1.84	.670	.336	1.41	.258	.678	.98	.563	.159
1.83	.667	.339	1.40	.239	.690	.97	.566	.151
1.82	.665	.342	1.39	.219	.702	.96	.567	.143
1.81	.661	.345	1.38	.201	.712	.95	.568	.136
1.80	.658	.348	1.37	.182	.723	.94	.567	.129
1.79	.654	.352	1.36	.163	.729	.93	.565	.123
1.78	.650	.355	1.35	.147	.736	.92	.563	.117
1.77	.646	.358	1.34	.132	.740	.91	.559	.111
1.76	.643	.362	1.33	.119	.742	.90	.553	.106
1.75	.639	.366	1.32	.108	.741	.89	.548	.101
1.74	.634	.370	1.31	.100	.739	.88	.542	.096
1.73	.628	.374	1.30	.095	.734	.87	.535	.092
1.72	.624	.379	1.29	.094	.727	.86	.522	.087
1.71	.618	.383	1.28	.097	.718	.85	.513	.082
1.70	.613	.389	1.27	.103	.706	.84	.503	.077
1.69	.607	.394	1.26	.113	.691	.83	.491	.072
1.68	.601	.400	1.25	.127	.675	.82	.479	.065
1.67	.594	.406	1.24	.143	.656	.81	.467	.061
1.66	.588	.412	1.23	.158	.637	.80	.457	.057
1.65	.580	.418	1.22	.179	.616	.79	.447	.051
1.64	.572	.425	1.21	.199	.593	.78	.439	.047
1.63	.565	.433	1.20	.219	.569	.77	.432	.042
1.62	.556	.440	1.19	.242	.543	.76	.426	.039
1.61	.547	.448	1.18	.265	.518	.75	.422	.037
1.60	.538	.457	1.17	.286	.494	.74	.418	.032

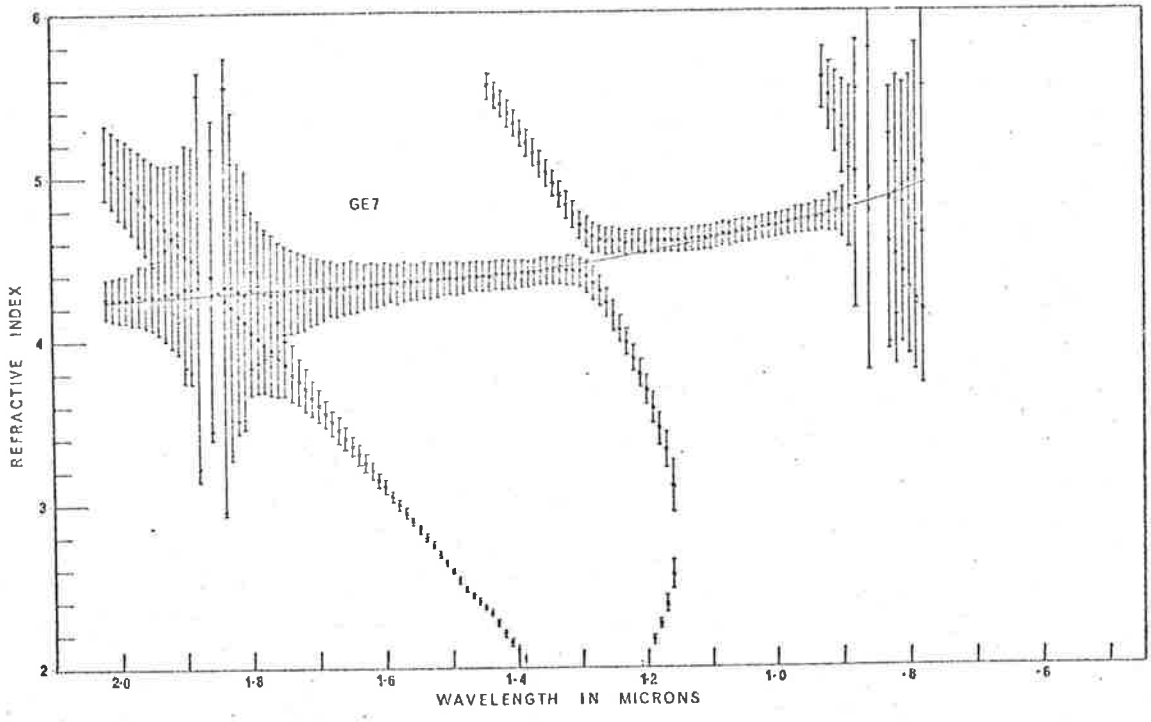
GE7
REFRACTIVE INDEX
6
5
4
3
2
2·0
1·8
1·6
1·4
1·2
1·0
·8
·6
WAVELENGTH IN MICRONS

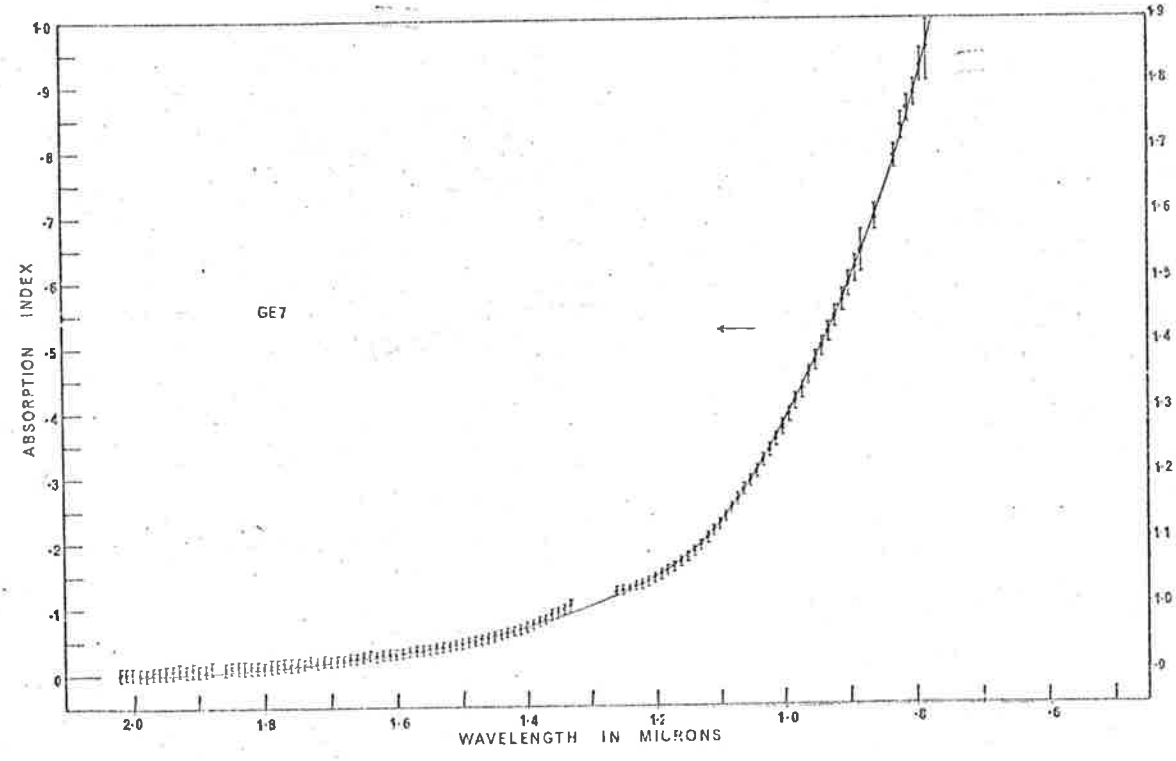
GE7
ABSORPTION INDEX
1·0
·9
·8
·7
·6
·5
·4
·3
·2
·1
0
1·9
1·8
1·7
1·6
1·5
1·4
1·3
1·2
1·1
1·0
·9
2·0
1·8
1·6
1·4
1·2
1·0
·8
·6
WAVELENGTH IN MICRONS

FILM GE8.

$d_1 = 10 \pm 5$ Å $\qquad$ $d_2 = 1750 \pm 20$ Å

λ(μ)	R	Γ	λ(μ)	R	Γ	λ(μ)	R	Γ
2.02	.561	.451	1.63	.070	.881	1.24	.633	.269
2.01	.554	.458	1.62	.059	.888	1.23	.640	.258
2.00	.547	.464	1.61	.050	.891	1.22	.647	.247
1.99	.540	.471	1.60	.043	.893	1.21	.653	.238
1.98	.533	.478	1.59	.039	.892	1.20	.657	.229
1.97	.525	.486	1.58	.037	.889	1.19	.661	.221
1.96	.517	.494	1.57	.038	.885	1.18	.664	.213
1.95	.508	.502	1.56	.046	.879	1.17	.665	.206
1.94	.499	.510	1.55	.056	.870	1.16	.665	.200
1.93	.489	.519	1.54	.070	.860	1.15	.665	.194
1.92	.479	.528	1.53	.084	.848	1.14	.663	.188
1.91	.469	.539	1.52	.099	.835	1.13	.660	.184
1.90	.457	.549	1.51	.118	.820	1.12	.655	.179
1.89	.447	.560	1.50	.137	.802	1.11	.651	.175
1.88	.435	.570	1.49	.157	.784	1.10	.644	.172
1.87	.424	.583	1.48	.176	.763	1.09	.636	.169
1.86	.411	.594	1.47	.199	.742	1.08	.627	.166
1.85	.399	.607	1.46	.220	.717	1.07	.616	.163
1.84	.385	.621	1.45	.243	.694	1.06	.604	.160
1.83	.372	.633	1.44	.267	.668	1.05	.590	.158
1.82	.358	.646	1.43	.290	.646	1.04	.575	.156
1.81	.345	.658	1.42	.317	.620	1.03	.559	.153
1.80	.330	.672	1.41	.341	.595	1.02	.543	.150
1.79	.317	.648	1.40	.366	.569	1.01	.525	.148
1.78	.301	.698	1.39	.390	.544	1.00	.504	.144
1.77	.286	.713	1.38	.413	.519	.99	.486	.141
1.76	.271	.726	1.37	.436	.495	.98	.467	.137
1.75	.256	.741	1.36	.458	.472	.97	.445	.131
1.74	.240	.754	1.35	.478	.450	.96	.428	.125
1.73	.224	.769	1.34	.499	.429	.95	.409	.119
1.72	.207	.782	1.33	.516	.409	.94	.394	.111
1.71	.192	.796	1.32	.532	.391	.93	.380	.103
1.70	.176	.813	1.31	.548	.372	.92	.366	.095
1.69	.158	.826	1.30	.564	.355	.91	.358	.082
1.68	.143	.837	1.29	.577	.338	.90	.352	.070
1.67	.127	.849	1.28	.591	.323	.89	.350	.061
1.66	.112	.859	1.27	.603	.309	.88	.350	.047
1.65	.097	.869	1.26	.613	.295	.87	.353	.040
1.64	.083	.877	1.25	.623	.282			

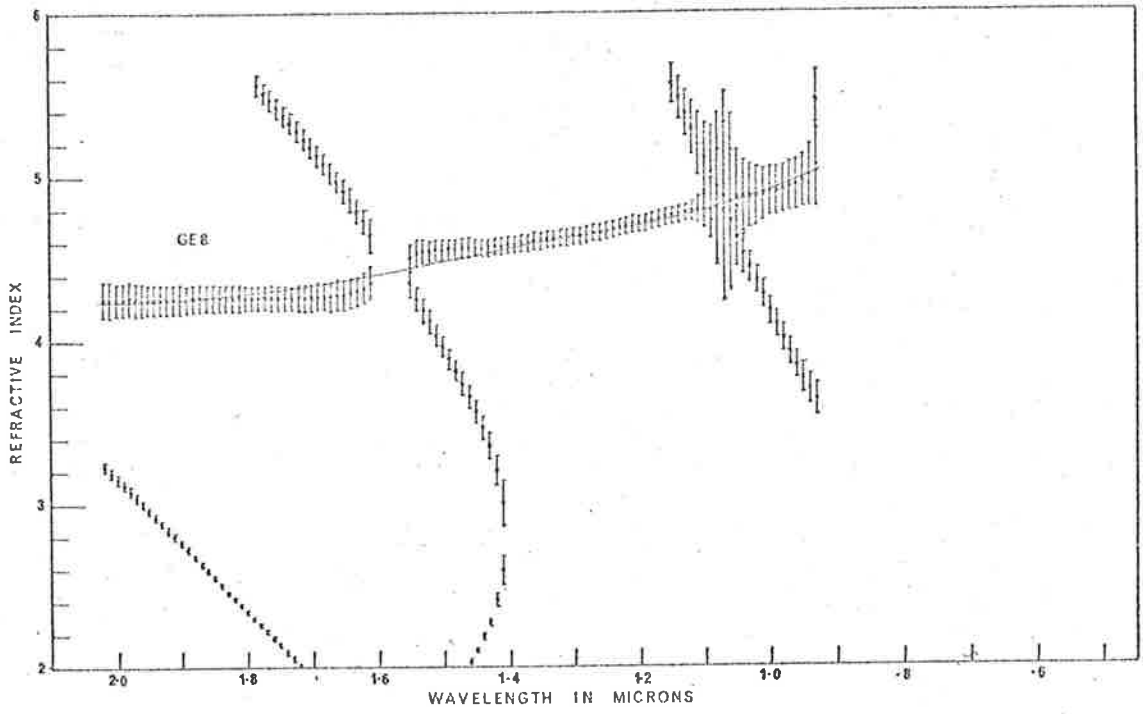
GE 8
REFRACTIVE INDEX
WAVELENGTH IN MICRONS

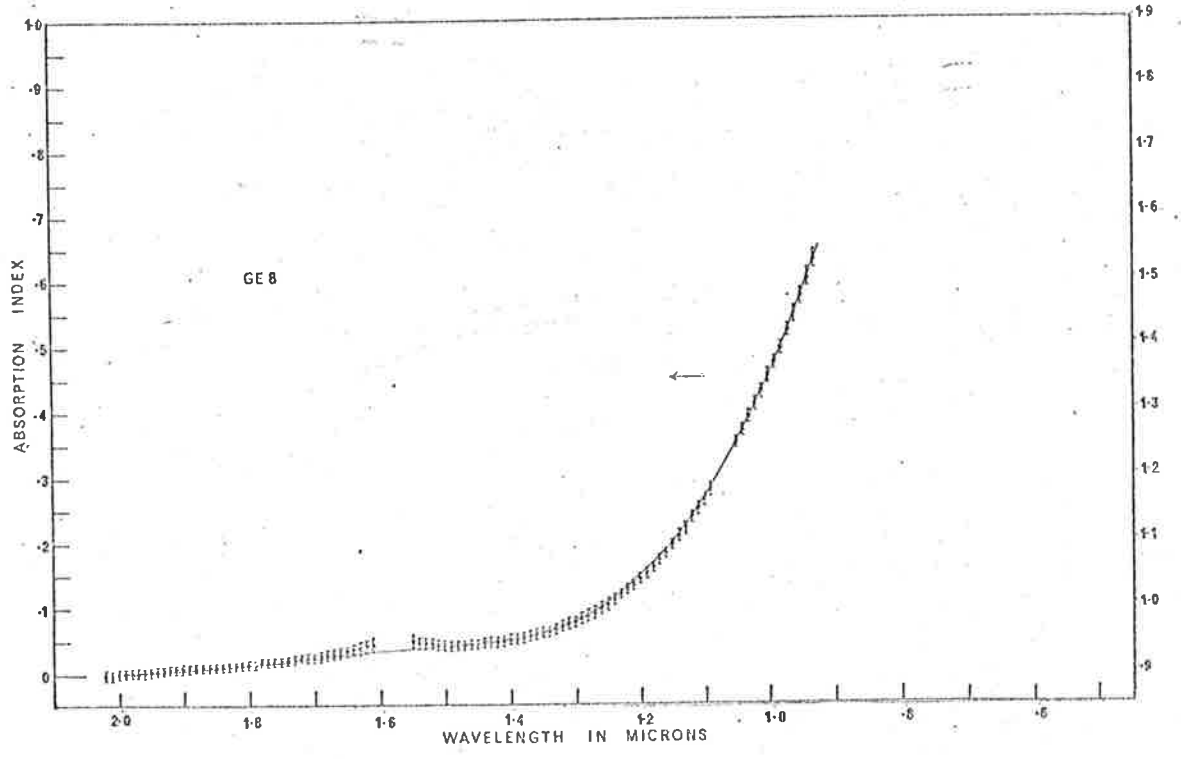
GE 8
ABSORPTION INDEX
WAVELENGTH IN MICRONS

FILM GE9.

$d_1 = 0 \pm 5$ Å $\qquad$ $d_2 = 915 \pm 40$ Å

λ(μ)	R	T	λ(μ)	R	T	λ(μ)	R	T
2.02	.714	.293	1.59	.747	.262	1.16	.606	.358
2.01	.715	.292	1.58	.747	.262	1.15	.593	.365
2.00	.717	.291	1.57	.747	.262	1.14	.580	.372
1.99	.718	.290	1.56	.747	.262	1.13	.563	.380
1.98	.719	.289	1.55	.747	.262	1.12	.547	.387
1.97	.720	.288	1.54	.747	.262	1.11	.529	.394
1.96	.721	.287	1.53	.747	.262	1.10	.512	.402
1.95	.722	.286	1.52	.747	.262	1.09	.492	.409
1.94	.723	.285	1.51	.747	.262	1.08	.472	.417
1.93	.724	.284	1.50	.746	.262	1.07	.451	.423
1.92	.725	.283	1.49	.746	.262	1.06	.430	.429
1.91	.726	.282	1.48	.746	.263	1.05	.409	.434
1.90	.727	.281	1.47	.745	.263	1.04	.385	.439
1.89	.728	.280	1.46	.744	.264	1.03	.363	.441
1.88	.729	.279	1.45	.743	.264	1.02	.336	.444
1.87	.730	.278	1.44	.742	.265	1.01	.315	.444
1.86	.730	.277	1.43	.741	.266	1.00	.296	.443
1.85	.731	.276	1.42	.740	.267	.99	.276	.439
1.84	.732	.276	1.41	.739	.268	.98	.259	.434
1.83	.733	.275	1.40	.737	.269	.97	.245	.427
1.82	.734	.274	1.39	.735	.270	.96	.232	.418
1.81	.735	.273	1.38	.733	.272	.95	.223	.409
1.80	.736	.273	1.37	.731	.273	.94	.219	.393
1.79	.737	.272	1.36	.729	.275	.93	.217	.379
1.78	.737	.271	1.35	.727	.277	.92	.219	.361
1.77	.738	.271	1.34	.724	.279	.91	.224	.345
1.76	.739	.270	1.33	.721	.281	.90	.232	.325
1.75	.739	.270	1.32	.718	.283	.89	.243	.306
1.74	.740	.269	1.31	.714	.286	.88	.257	.286
1.73	.740	.268	1.30	.711	.289	.87	.272	.263
1.72	.741	.267	1.29	.707	.292	.86	.290	.242
1.71	.742	.267	1.28	.703	.295	.85	.307	.218
1.70	.743	.266	1.27	.698	.298	.84	.325	.196
1.69	.743	.266	1.26	.693	.302	.83	.344	.175
1.68	.744	.265	1.25	.687	.306	.82	.362	.154
1.67	.744	.265	1.24	.681	.311	.81	.380	.134
1.66	.745	.264	1.23	.674	.317	.80	.395	.117
1.65	.745	.264	1.22	.667	.322	.79	.410	.100
1.64	.746	.263	1.21	.659	.327	.78	.423	.084
1.63	.746	.263	1.20	.650	.333	.77	.435	.070
1.62	.746	.263	1.19	.641	.338	.76	.445	.060
1.61	.747	.262	1.18	.630	.345	.75	.454	.048
1.60	.747	.262	1.17	.617	.351	.74	.461	.040

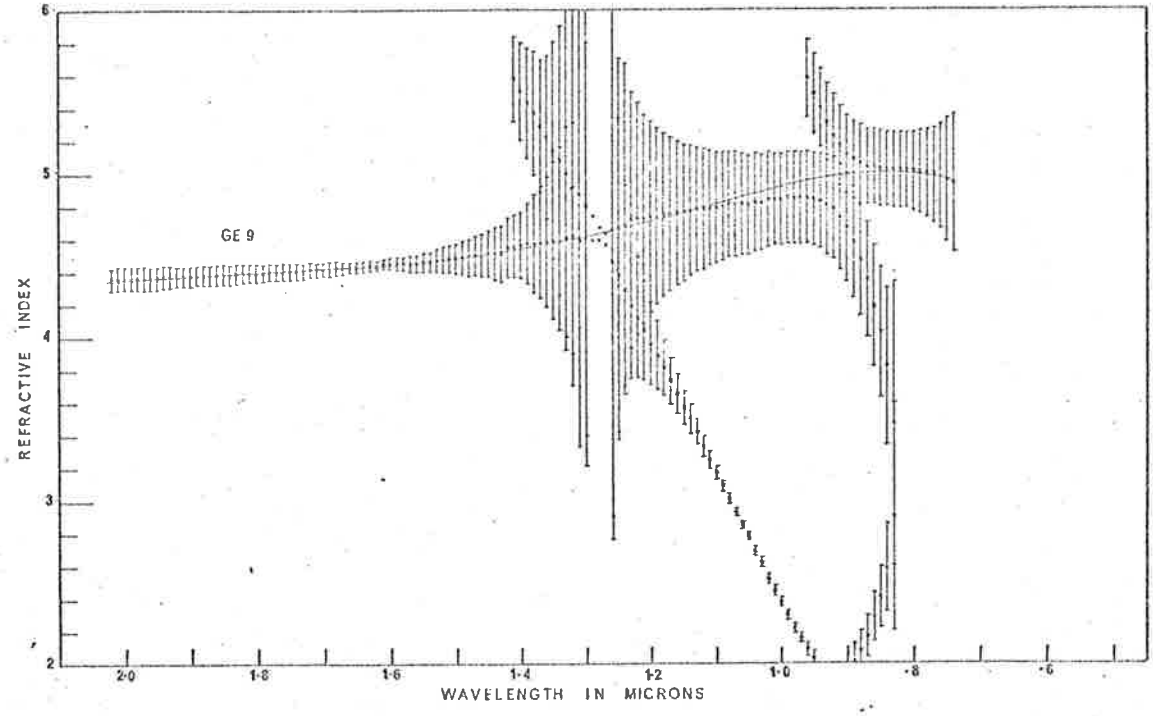
GE 9
REFRACTIVE INDEX
WAVELENGTH IN MICRONS

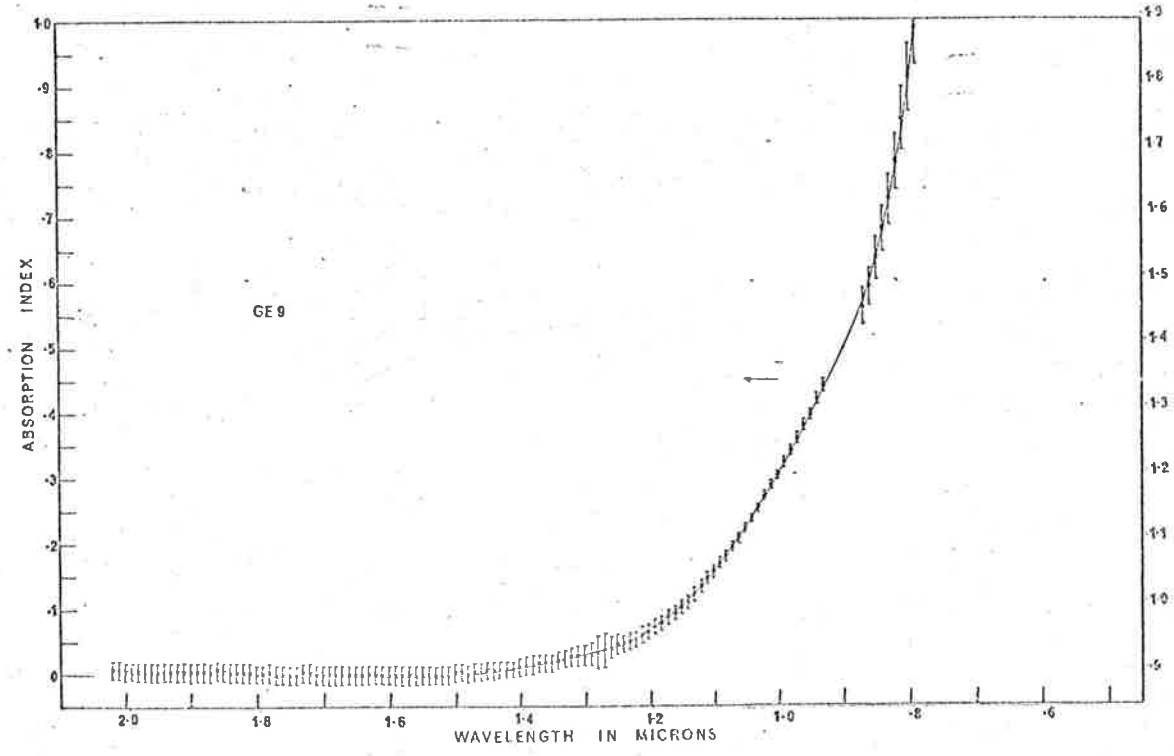
GE 9
ABSORPTION INDEX
WAVELENGTH IN MICRONS

FILM GE10.

$d_1 = 155 \pm 5$ Å $\qquad d_2 = 715 \pm 5$ Å

λ(μ)	R	Γ	λ(μ)	R	Γ	λ(μ)	R	Γ
2.02	.624	.389	1.54	.702	.305	1.06	.669	.278
2.01	.626	.388	1.53	.703	.303	1.05	.666	.279
2.00	.627	.386	1.52	.704	.302	1.04	.662	.281
1.99	.629	.384	1.51	.705	.300	1.03	.655	.283
1.98	.631	.382	1.50	.706	.299	1.02	.649	.284
1.97	.632	.380	1.49	.706	.297	1.01	.643	.286
1.96	.634	.379	1.48	.707	.296	1.00	.638	.289
1.95	.637	.377	1.47	.709	.294	.99	.631	.291
1.94	.639	.375	1.46	.709	.293	.98	.622	.294
1.93	.640	.373	1.45	.710	.291	.97	.613	.297
1.92	.642	.371	1.44	.710	.290	.96	.604	.300
1.91	.643	.370	1.43	.711	.289	.95	.595	.303
1.90	.645	.368	1.42	.711	.287	.94	.585	.306
1.89	.647	.366	1.41	.712	.286	.93	.574	.311
1.88	.649	.364	1.40	.712	.285	.92	.563	.315
1.87	.650	.362	1.39	.712	.283	.91	.549	.319
1.86	.653	.360	1.38	.712	.282	.90	.536	.324
1.85	.654	.359	1.37	.713	.281	.89	.520	.329
1.84	.656	.357	1.36	.713	.280	.88	.504	.334
1.83	.658	.355	1.35	.714	.279	.87	.484	.340
1.82	.661	.353	1.34	.714	.278	.86	.463	.346
1.81	.662	.351	1.33	.714	.277	.85	.442	.351
1.80	.664	.350	1.32	.714	.277	.84	.421	.358
1.79	.666	.348	1.31	.714	.276	.83	.397	.363
1.78	.668	.346	1.30	.714	.276	.82	.369	.369
1.77	.669	.345	1.29	.713	.275	.81	.343	.373
1.76	.671	.343	1.28	.713	.274	.80	.317	.377
1.75	.673	.341	1.27	.713	.274	.79	.291	.379
1.74	.674	.340	1.26	.712	.273	.78	.266	.378
1.73	.676	.338	1.25	.712	.273	.77	.244	.376
1.72	.678	.336	1.24	.711	.272	.76	.225	.370
1.71	.679	.334	1.23	.710	.272	.75	.211	.363
1.70	.680	.332	1.22	.709	.272	.74	.201	.352
1.69	.681	.331	1.21	.707	.271	.73	.198	.337
1.68	.683	.329	1.20	.706	.271	.72	.201	.320
1.67	.686	.327	1.19	.705	.271	.71	.212	.300
1.66	.687	.325	1.18	.703	.271	.70	.227	.277
1.65	.689	.324	1.17	.702	.271	.69	.250	.252
1.64	.690	.322	1.16	.700	.271	.68	.277	.226
1.63	.691	.320	1.15	.699	.271	.67	.305	.200
1.62	.693	.318	1.14	.696	.271	.66	.335	.174
1.61	.695	.317	1.13	.694	.272	.65	.365	.150
1.60	.695	.315	1.12	.692	.272	.64	.394	.125
1.59	.696	.313	1.11	.689	.273	.63	.419	.103
1.58	.698	.311	1.10	.686	.274	.62	.441	.082
1.57	.699	.310	1.09	.681	.275	.61	.459	.067
1.56	.700	.308	1.08	.679	.276	.60	.471	.048
1.55	.701	.306	1.07	.675	.277			

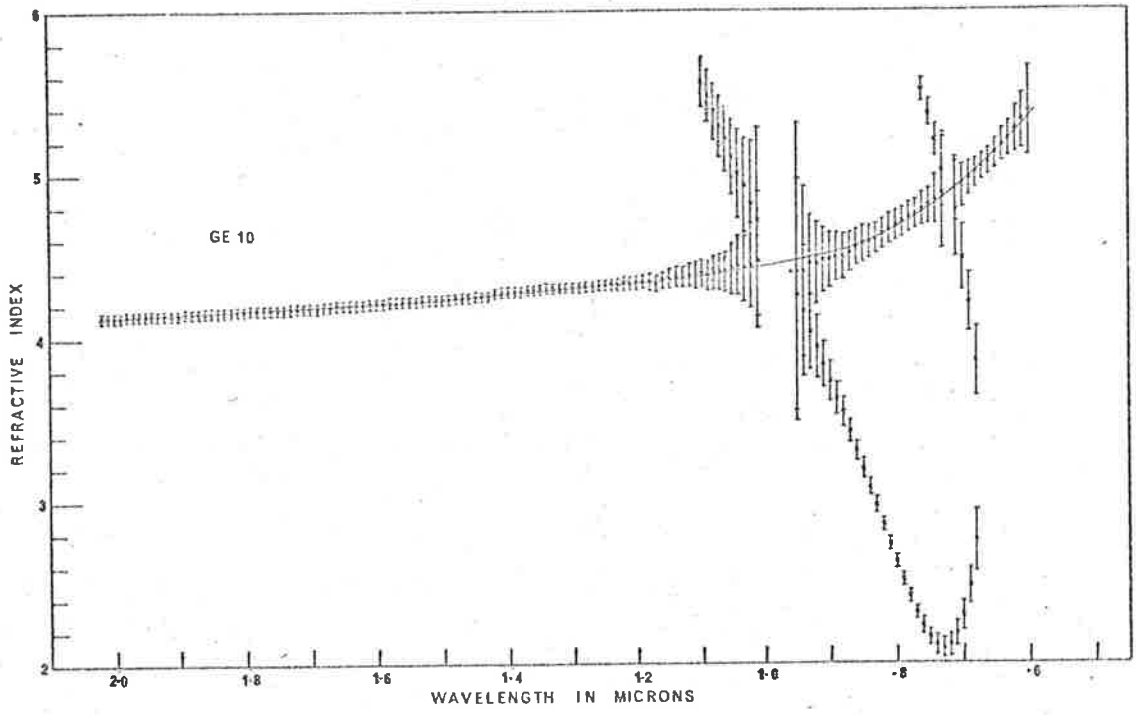
GE 10
REFRACTIVE INDEX
WAVELENGTH IN MICRONS

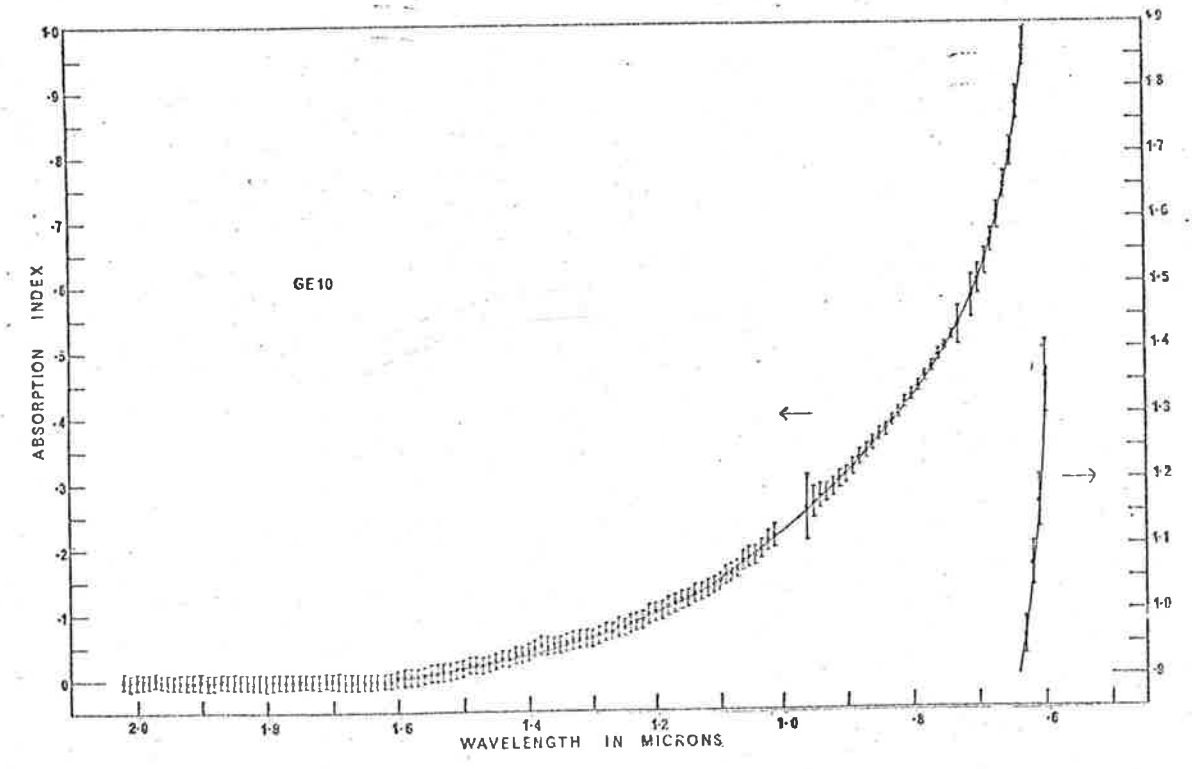
GE10
ABSORPTION INDEX
WAVELENGTH IN MICRONS

FILM GE11.

$d_1 = 100 \pm 5$ Å $\qquad$ $d_2 = 855 \pm 5$ Å

λ(μ)	R	Γ	λ(μ)	R	Γ	λ(μ)	R	Γ
2.02	.574	.440	1.54	.647	.363	1.06	.589	.347
2.01	.576	.438	1.53	.647	.362	1.05	.583	.348
2.00	.578	.437	1.52	.648	.361	1.04	.578	.350
1.99	.579	.435	1.51	.649	.359	1.03	.570	.352
1.98	.582	.433	1.50	.649	.358	1.02	.562	.354
1.97	.583	.432	1.49	.650	.356	1.01	.554	.356
1.96	.585	.430	1.48	.650	.355	1.00	.545	.358
1.95	.587	.428	1.47	.651	.354	.99	.535	.361
1.94	.589	.426	1.46	.651	.352	.98	.524	.363
1.93	.590	.425	1.45	.651	.351	.97	.514	.366
1.92	.592	.423	1.44	.651	.350	.96	.502	.369
1.91	.593	.422	1.43	.651	.349	.95	.490	.372
1.90	.595	.420	1.42	.651	.348	.94	.476	.375
1.89	.596	.418	1.41	.651	.347	.93	.462	.378
1.88	.597	.417	1.40	.651	.346	.92	.444	.382
1.87	.599	.415	1.39	.651	.345	.91	.429	.385
1.86	.601	.414	1.38	.651	.344	.90	.412	.388
1.85	.602	.412	1.37	.650	.343	.89	.394	.391
1.84	.604	.411	1.36	.650	.343	.88	.371	.393
1.83	.605	.409	1.35	.650	.343	.87	.352	.395
1.82	.608	.408	1.34	.650	.342	.86	.329	.397
1.81	.609	.406	1.33	.650	.341	.85	.304	.396
1.80	.611	.405	1.32	.650	.341	.84	.281	.397
1.79	.613	.403	1.31	.650	.340	.83	.260	.394
1.78	.615	.402	1.30	.649	.340	.82	.237	.390
1.77	.616	.400	1.29	.649	.339	.81	.219	.385
1.76	.618	.398	1.28	.648	.339	.80	.205	.377
1.75	.620	.397	1.27	.648	.338	.79	.196	.367
1.74	.621	.395	1.26	.647	.338	.78	.191	.354
1.73	.623	.394	1.25	.646	.338	.77	.190	.340
1.72	.625	.392	1.24	.645	.337	.76	.194	.324
1.71	.627	.390	1.23	.644	.337	.75	.203	.307
1.70	.629	.389	1.22	.643	.337	.74	.215	.287
1.69	.630	.387	1.21	.640	.337	.73	.230	.269
1.68	.632	.386	1.20	.638	.337	.72	.248	.249
1.67	.633	.384	1.19	.637	.337	.71	.269	.230
1.66	.634	.382	1.18	.635	.337	.70	.292	.209
1.65	.635	.381	1.17	.633	.337	.69	.317	.188
1.64	.636	.379	1.16	.630	.338	.68	.341	.169
1.63	.638	.377	1.15	.628	.338	.67	.365	.151
1.62	.639	.376	1.14	.623	.339	.66	.387	.133
1.61	.640	.374	1.13	.621	.339	.65	.407	.115
1.60	.642	.373	1.12	.617	.340	.64	.424	.096
1.59	.643	.371	1.11	.614	.340	.63	.439	.081
1.58	.644	.369	1.10	.609	.342	.62	.447	.058
1.57	.644	.368	1.09	.604	.343	.61	.451	.041
1.56	.645	.366	1.08	.599	.344	.60	.448	.021
1.55	.646	.365	1.07	.594	.345			

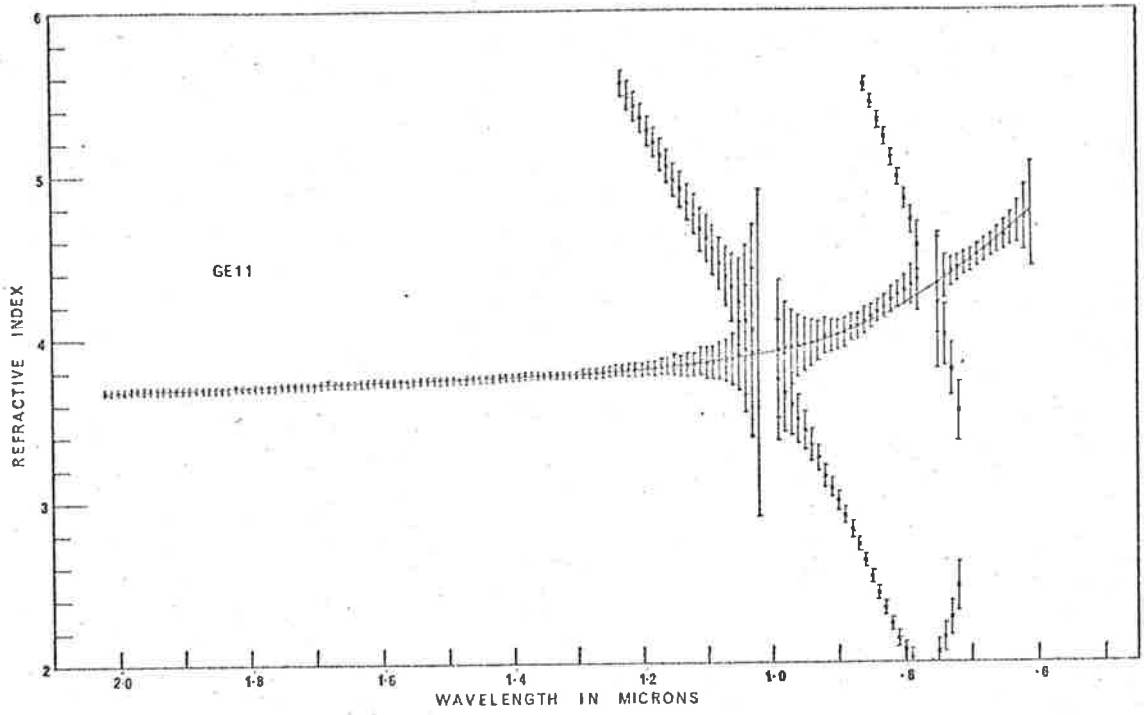
GE11
REFRACTIVE INDEX
6
5
4
3
2
2·0
1·8
1·6
1·4
1·2
1·0
·8
·6
WAVELENGTH IN MICRONS

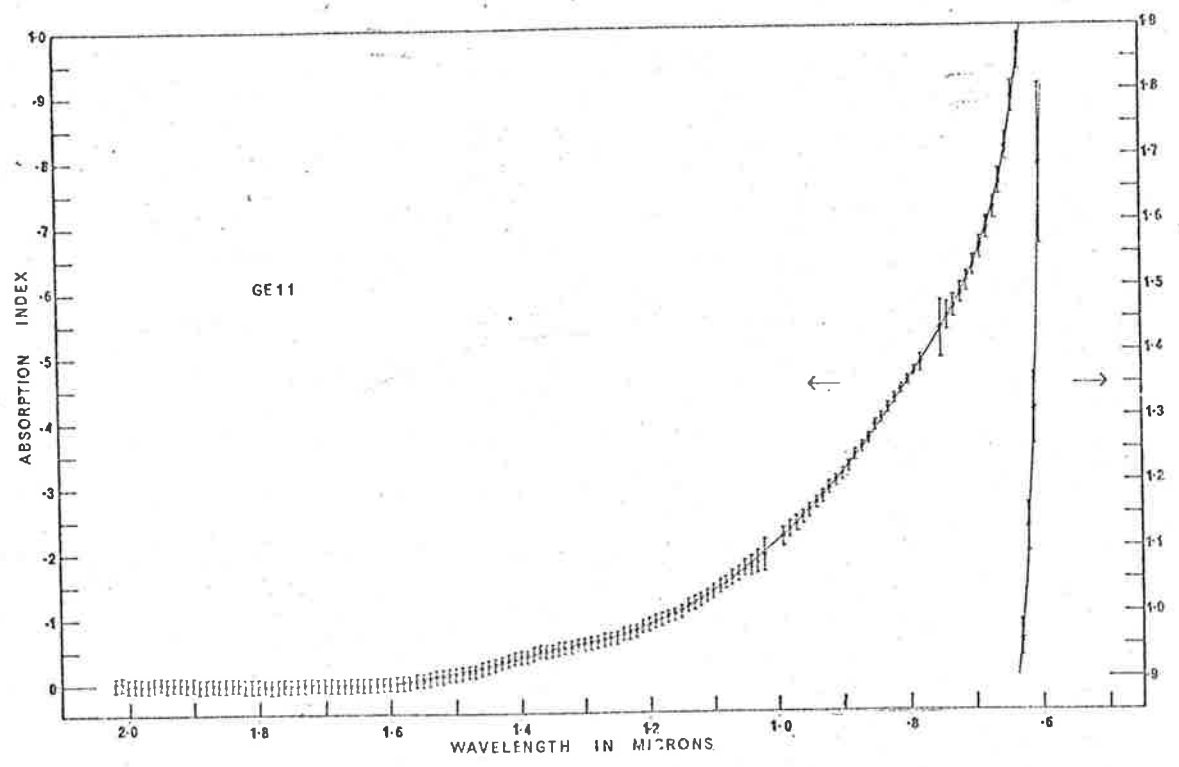
GE11
ABSORPTION INDEX
1·0
·9
·8
·7
·6
·5
·4
·3
·2
·1
0
1·9
1·8
1·7
1·6
1·5
1·4
1·3
1·2
1·1
1·0
·9
2·0
1·8
1·6
1·4
1·2
1·0
·8
·6
WAVELENGTH IN MICRONS

FILM GE12.

$d_1 = 0 \pm 5$Å $\qquad$ $d_2 = 1072 \pm 10$Å

λ(μ)	R	Γ	λ(μ)	R	Γ	λ(μ)	R	Γ
2.02	.676	.335	1.56	.691	.310	1.10	.386	.439
2.01	.678	.334	1.55	.689	.311	1.09	.368	.442
2.00	.679	.333	1.54	.688	.311	1.08	.352	.445
1.99	.681	.332	1.53	.686	.312	1.07	.334	.447
1.98	.682	.331	1.52	.685	.312	1.06	.317	.448
1.97	.682	.330	1.51	.683	.312	1.05	.301	.450
1.96	.684	.329	1.50	.681	.313	1.04	.285	.449
1.95	.684	.328	1.49	.680	.314	1.03	.269	.450
1.94	.685	.327	1.48	.678	.315	1.02	.253	.448
1.93	.686	.326	1.47	.675	.316	1.01	.241	.445
1.92	.686	.325	1.46	.673	.317	1.00	.227	.441
1.91	.688	.324	1.45	.671	.318	.99	.215	.438
1.90	.688	.323	1.44	.668	.319	.98	.204	.433
1.89	.689	.322	1.43	.665	.321	.97	.195	.428
1.88	.690	.322	1.42	.662	.322	.96	.188	.421
1.87	.691	.321	1.41	.659	.324	.95	.182	.414
1.86	.692	.320	1.40	.655	.326	.94	.179	.406
1.85	.692	.320	1.39	.651	.328	.93	.177	.397
1.84	.693	.319	1.38	.647	.330	.92	.178	.388
1.83	.693	.318	1.37	.643	.332	.91	.180	.377
1.82	.693	.317	1.36	.639	.335	.90	.185	.366
1.81	.694	.317	1.35	.634	.338	.89	.192	.354
1.80	.695	.316	1.34	.629	.341	.88	.201	.341
1.79	.696	.316	1.33	.625	.343	.87	.212	.328
1.78	.696	.315	1.32	.620	.346	.86	.225	.315
1.77	.697	.314	1.31	.614	.349	.85	.240	.301
1.76	.697	.314	1.30	.608	.352	.84	.255	.287
1.75	.697	.314	1.29	.602	.356	.83	.273	.271
1.74	.697	.313	1.28	.595	.360	.82	.292	.256
1.73	.698	.312	1.27	.588	.363	.81	.310	.241
1.72	.698	.312	1.26	.580	.367	.80	.329	.225
1.71	.698	.312	1.25	.572	.371	.79	.346	.210
1.70	.698	.311	1.24	.562	.375	.78	.364	.195
1.69	.698	.311	1.23	.554	.379	.77	.380	.180
1.68	.698	.310	1.22	.545	.384	.76	.395	.166
1.67	.697	.310	1.21	.534	.388	.75	.408	.153
1.66	.697	.310	1.20	.523	.393	.74	.419	.139
1.65	.697	.310	1.19	.512	.398	.73	.428	.125
1.64	.696	.310	1.18	.499	.403	.72	.434	.113
1.63	.696	.309	1.17	.488	.408	.71	.438	.099
1.62	.695	.309	1.16	.474	.413	.70	.439	.086
1.61	.695	.309	1.15	.461	.417	.69	.439	.072
1.60	.694	.309	1.14	.446	.422	.68	.437	.061
1.59	.693	.309	1.13	.433	.426	.67	.435	.046
1.58	.692	.310	1.12	.418	.431	.66	.431	.034
1.57	.691	.310	1.11	.401	.435			

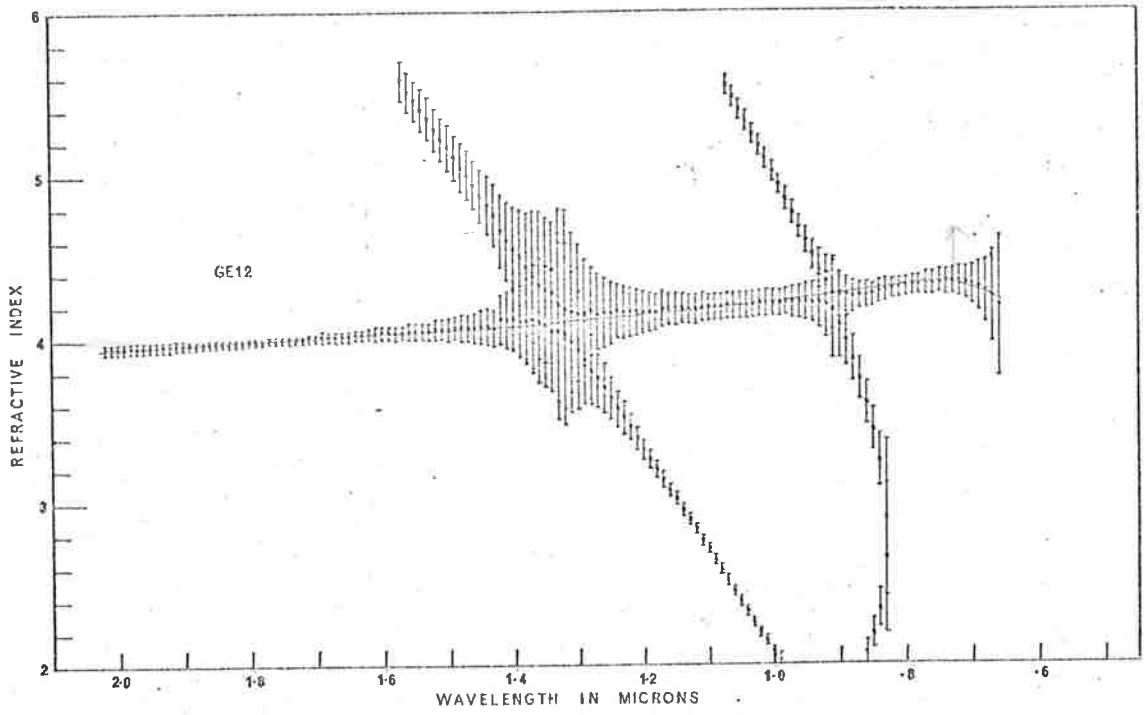
GE12
REFRACTIVE INDEX
6
5
4
3
2
2·0
1·8
1·6
1·4
1·2
1·0
·8
·6
WAVELENGTH IN MICRONS

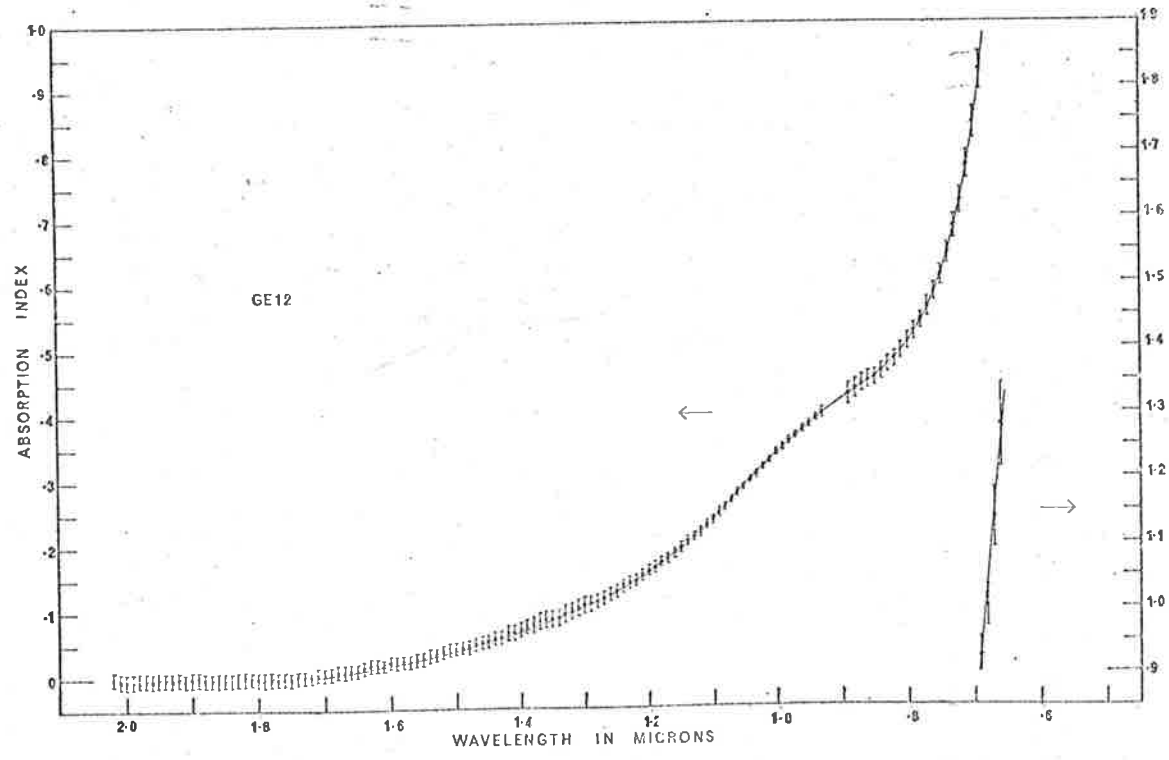
GE12
ABSORPTION INDEX
1·0
·9
·8
·7
·6
·5
·4
·3
·2
·1
0
1·9
1·8
1·7
1·6
1·5
1·4
1·3
1·2
1·1
1·0
·9
2·0
1·8
1·6
1·4
1·2
1·0
·8
·6
WAVELENGTH IN MICRONS

REFERENCES.

ABELES F., Progress in Optics, Vol.2, North Holland Publishing Co., 1963.

BENNETT J.M., J. Opt. Soc. Amer., 54, 5, 612, 1964.

BENNETT H.E., KOEHLER W.F., J. Opt. Soc. Amer., 50, 1, 1, 1960.

BOUSQUET P., Ann. Physique, 7, 163, 1957.

BRATTAIN W. H., BRIGGS H. B., Phys. Rev. 75, 11, 1705, 1949.

CAMPBELL R.D., Proc. Inst. Radio and Elec. Eng. Aust., 28, 4, 102, 1967.

CAMPBELL R.D., Ph.D. Thesis, University of Adelaide, 1968, (Unpublished).

CARDONA M., HARBEKE G., J. App. Phys., 34, 4, 813, 1963.

COHEN A.J., SMITH H.L., J. Phys. Chem. Solids, 7, 4, 301, 1958.

DASH W.C., Phys. Rev., 96, 822, 1954.

DASH W.C., NEWMAN R., Phys. Rev., 99, 1151, 1955.

DONOVAN J.M., ASHLEY E.J., J. Opt. Soc. Amer., 54, 9, 1141, 1964.

DONOVAN T.M., SPICER W.E., BENNETT J.M., Phys. Rev. Letters, 22, 1058, 1969.

DOWD J.J., Proc. Phys. Soc. (London), B64, 783, 1951.

GARINO - CANINA V., C.R. Acad. Sci. (Paris), 247, 5, 593, 1958.

GARINO - CANINA V., C.R. Acad. Sci. (Paris), 248, 10, 1488, 1959.

GEBBIE H.A., Ph.D. Thesis, Reading, 1952 (Unpublished).

GOODWIN R.D., Ph.D. Thesis, University of Adelaide, to be submitted.

GRANT P.M., PAUL W., J. App. Phys., 37, 8, 3110, 1964.

GUBANOV A.I., "Quantum Theory of Amorphous Conductors", Consultants Bureau, New York, 1965.

HEAVENS O.S., "Optical Properties of Thin Solid Films", Butterworths, London, 1955.

HENZLER M., Surface Science, 24, 209, 1971.

HERMAN F., Phys. Rev., 93, 1214, 1954.

HERMAN F., Phys. Rev., 95, 847, 1954.

HERMAN F., J. Electronics, 1, 103, 1955.

HERMAN F., Proc. Inst. Radio Engrs., 43, 1703, 1955.

JOHNSON J.E., Vacuum Microbalance Techniques, 4, 81, 1965.

KOEHLER W.F., ODENCRANTZ F.K., WHITE W.C., J. Opt. Soc. Amer., 49, 109, 1959.

KREBS H., SCHULTZE - GEBHARDT F., Acta Cryst., 8, 412, 1955.

KUHN H., WILSON B.A., Proc. Phys. Soc. (London), B63, 745, 1950.

KUROV G.A., SEMILETOV S.A., PINSKER Z.G., Soviet Phys.-Cryst., 2, 53, 1957.

KUROV G.A., VASILEV V.D., KOSAGANOVA M.G., Soviet Phys. Solid State, 3, 2571, 1962.

KUROV G.A., VASILEV V.D., KOSAGANOVA M.G., Soviet Phys.-Cryst., 7, 625, 1963.

LUKES F., Czech. J. Phys., 10, 59, 1960.

McCOY D.G., Ph.D. Thesis, University of Adelaide, 1966, (Unpublished).

MACDONALD R.J., Proc. Inst. Radio and Elec. Eng. Aust., 28, 4, 104, 1967.

MAYER H., Optik dunner Schichten, 1, 168, 1950.

MOOSER E., PEARSON W.B., Canad. J. Phys., 34, 1369, 1956.

MOOSER E., PEARSON W.B., J. Electronics, p.629, 1956.

MOOSER E., PEARSON W.B., J. Chem. Phys., 7, 65, 1958.

MOOSER E., PEARSON W.B., Prog. in Semiconductors., 5, 103, 1960.

MOSS T.S., "Optical Properties of Semiconductors", Butterworths, London, 1959.

NATIONAL PHYSICAL LABORATORY, "Modern Computing Methods", H.M. Stationery Office, London, 1961.

NILSSON P.O., J. App. Optics, 7, 435, 1968.

PAPAZIAN H., J. App. Phys., 27, 1253, 1956.

POTTER R.F., Phys. Rev., 150, 2, 562, 1964.

ROUARD P., J. Opt. Soc. Amer., 46, 370, 1956.

ROUARD P., BOUSQUET P., Progress in Optics, Vol.4,
North Holland Publishing Co., 1965.

SCHOPPER H., Z. Physik, 130, 565, 1951.

SCHOPPER H., Z. Physik, 131, 215, 1952.

SCHOPPER H., Z. Physik, 132, 146, 1952.

SEIMSEN K.J., FENTON E.W., Phys. Rev., 161, 632, 1967.

SLOOPE B.W., TILLER C.O., J. App. Phys., 33, 12, 3458, 1962.

SMITH R.A. "Semiconductors", Cambridge University Press, 1959.

SMITH R.A., "Wave Mechanics of Crystalline Solids",
Chapman and Hall, London, 1961.

TAUC J., Phys. Non-Cryst. Solids, Proc. Int. Conf., Delft, p.606, 1964.

TAUC J., Prog. in Semiconductors, 9, 87, 1965.

TAUC J., Proc. Int. Conf. Semic., Kyoto., J. Phys. Soc. Japan,
Vol.21, Suppl., p.123, 1966.

TAUC J., "Optical Properties of Solids", edited by F. Abeles,
North Holland Publishing Co., Amsterdam, 1970.

TOLANSKY S., "Surface Microtopography", Longmans, London, 1960.

TOMLIN S.G., Brit. J. App. Phys. (J. Phys. D), 2, 1, 1667, 1968.

TOMLIN S.G., To Be Published.

WALES J., LOVITT G.J., HILL R.A., Thin Solid Films, 1, 137, 1967.

WARD J., Private Communication, 1971.

WOOD R.W., Phil. Mag., 3, 607, 1902.